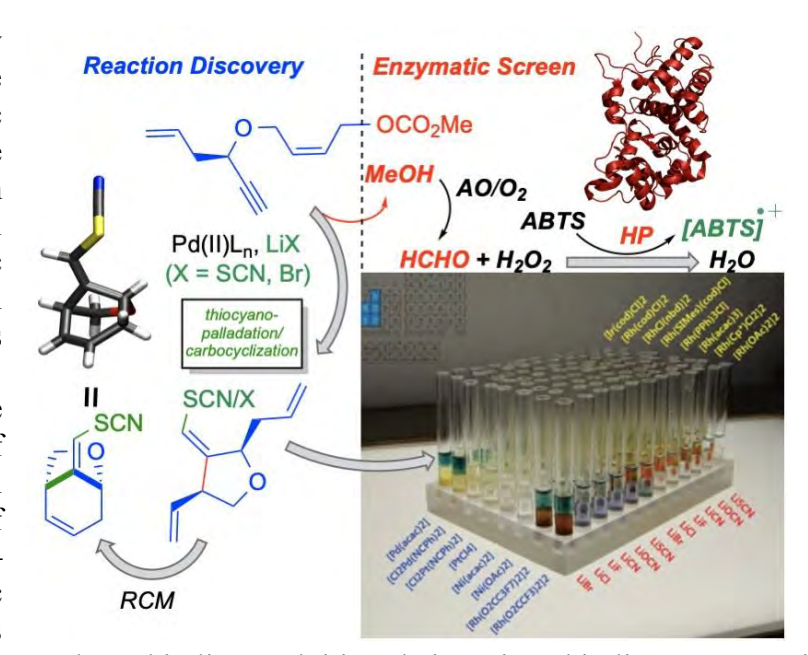
Biomacromolecule-Assisted Screening for Reaction Discovery and Catalyst Optimization

Stephany M. Ramos De Dios, Virendra K. Tiwari, Christopher D. McCune, Ranjeet A. Dhokale, David B. Berkowitz*

Reaction discovery **Abstract:** and catalyst screening lie at the synthetic heart of organic chemistry. And while there are efforts at de novo catalyst design computation/artificial using intelligence; at its core, synthetic chemistry is an experimental science. This review overviews biomacromolecule-assisted screening methods and the follow-on elaboration of chemistry so discovered. All three types of biomacromolecules discussedenzymes, antibodies, and nucleic acids-have used been



'sensors' to provide a readout on product chirality exploiting their native chirality. Enzymatic sensing methods yield both UV-spectrophotometric and visible, colorimetric readouts. Antibody sensors provide direct fluorescent readout upon analyte binding in some cases, or provide for cat-ELISA (Enzyme-Linked ImmunoSorbent Assay)-type readouts. DNA biomacromolecule-assisted screening allows for templation to facilitate reaction discovery, driving bimolecular reactions into a pseudo-unimolecular format. Also, the ability to use DNA-encoded libraries permits the barcoding of reactants. All three types of biomacromolecule-based screens afford high sensitivity and selectivity. Among the chemical transformations discovered by enzymatic screening methods Ni(0)-mediated asymmetric are the first allvlic amination. and new thiocyanopalladation/carbocyclization transformation in which both C-SCN and C-C bonds are fashioned sequentially. Cat-ELISA screening has identified new classes of sydnone-alkyne cycloadditions and DNA-encoded screening has been exploited to uncover interesting oxidative Pd-mediated amido-alkyne/alkene coupling reactions.

- 1. Introduction
- 2. Direct Enzymatic Screening Methods
 - 2.1. Enzymatic Methods Providing Relative Rate Readout
 - 2.1.1. UV-Vis Readout Using Alcohol Dehydrogenase/Aldehyde Dehydrogenase Reporting Enzymes (In Situ Enzymatic Screening ISES)
 - 2.1.1.1. Initial Screening Hit: Ni(0)-Mediated Allylic Amination
 - 2.1.1.2. Hit Elaboration: Ni-Catalyzed Allylic Substitution
 - 2.1.2. Colorimetric Readout Using Alcohol Oxidase/Peroxidase Reporting Enzymes
 - 2.1.2.1. Initial Screening Hit: Bromorhodiation/Carbocyclization Reaction
 - 2.1.2.2. Hit Elaboration: Transition Metal-Catalyzed Halometalation Enyne Cyclization
 - 2.1.2.3. Initial Screening Hit: Thiocyanopalladation/Carbocyclization Reaction
 - 2.1.2.4. Hit Elaboration: Toward O-, N-, S-Heterocycles with Control of Relative Stereochemistry
 - 2.2. Enzymatic Methods Providing Readout on Enantiopreference/Enantiomeric Excess
 - 2.2.1. In Situ Enzymatic Screening (ISES)-Readout on Relative Rate and Enantioselectivity
 - 2.2.1.1. Double Cuvette Screening
 - 2.2.1.2. Cassette Format
 - 2.2.1.2.1. Initial Screening Hit: β-Pinene-Derived Chiral Salen Ligand with Potential for Asymmetric Catalysis
 - 2.2.1.2.2. Hit Elaboration: Application to the Enantioselective Synthesis of the Linearifolin and Zaluzanin A Cores
 - 2.2.1.3 Mini-ISES Configuration
 - 2.2.1.3.1. Initial Screening Hit: Synthesis of the β-D-(Carba)fructopyranose-1,2-Diamine-Derived Chiral Salen Ligand with Potential for Asymmetric Catalysis
 - 2.2.2. Post-Work-Up Readout on Conversion and Enantioselectivity
 - 2.2.2.1. Initial Screening Hit: Enantioselective *O*-Acyl Cyanohydrin Formation
 - 2.2.2.2. Hit Elaboration: Transition Metal-Based, Lewis Acid-Promoted *O*-Acyl Cyanohydrin Formation
 - 2.2.3. Post-Work-Up Readout on Enantioselectivity (Reporting Enzyme Turnover)
 - 2.2.4. Post-Work-Up Readout on Enantioselectivity (Reporting Enzyme Inhibition)
- 3. Hybrid Antibody-Enzymatic Screening Methods
 - 3.1. Immunoassay Screening for Reaction Discovery
 - 3.1.1. Reaction Discovery Using a Sandwich Immunoassay
 - 3.1.2. Discovery of Chemoselective and Biocompatible Reactions Using Immunoassay Screening
 - 3.1.2.1. Initial Screening Hit: Sydnone-Alkyne Cycloaddition Reaction

- 3.1.2.1.1. Hit Elaboration: Cu-Catalyzed Iminosydnone-Alkyne Cycloaddition Reaction
- 3.1.2.1.2. Hit Elaboration: Strain-Promoted Sydnone-Alkyne Cycloaddition Reaction
- 3.1.2.1.3. Hit Elaboration: Ir-Catalyzed Azide-Alkyne Cycloaddition-Reaction to Access Diverse Triazoles.
- 3.1.2.2. Initial Screening Hit: Pyridine Ylide-Nitrile Cyclo-Condensation Reaction
- 3.2. Immunoassay Screening for Enantioselective Catalysts
 - 3.2.1. High-Throughput Screening of Enantioselective Catalyst by Immunoassay-Two Competitive Cat-ELISAs
- 4. Single Antibody-Based Screening Methods
 - 4.1. A Remarkable Antibody-Based Optical Sensor: Stilbenoid Ligand-Antibody Co-Crystal Structure Provides Insight into Tryptophan Fluorescence Mechanism.
 - 4.2. Discovery of Antibody Showing Enantioselective Fluorescence with Stilbenoid Analytes
 - 4.3. Chiral Sensing with the Blue Fluorescent Antibody for Enantioselective Metal-Salen-Catalyzed Epoxide Opening
 - 4.4. Application of Blue-Fluorescent Antibody to Chiral PTC Library Screening for Asymmetric Unnatural Amino Acid Synthesis
- 5. Nucleic Acid-Based Screening Methods
 - 5.1. DNA-Templated Methods
 - 5.1.1. Proof of Principle for Specific DNA-Encoded Reaction Pairs
 - 5.1.1.1. Reaction Scope with DNA-Templated Platform
 - 5.1.2. Reaction Discovery Enabled by DNA-Templated Synthesis via Disulfide Cleavage Selection and DNA Microarray Readout
 - 5.1.2.1. Initial Hit: Macrocyclization via Pd-Mediated, Oxidative Amido-alkyne/ Alkene Coupling Reaction
 - 5.1.2.1.1. Hit Elaboration: Other Macrolide Formation
 - 5.1.2.1.2. Hit Elaboration: Six-Endo-Dig Cyclization Reactions
 - 5.1.2.1.3. Hit Elaboration: Five-Endo and Exo-Dig Cyclization Reactions
 - 5.1.2.1.4. Hit Elaboration: Intermolecular Amido-alkyne/Alkene Coupling Reactions
 - 5.1.3. Novel DNA Architectures for DNA-Templation
 - 5.1.3.1. Use of a Double-Templated DNA Ternary Complex with Selection by Photocleavable Linker and PAGE Readout
 - 5.1.3.2. Exploration of Double-Helix-Templation with Intervening Elongator (E10) or Loop (Ω 5) Sequences with Selection by Sulfone Cleavage and MALDI-MS Product Identification
 - 5.1.3.3. Hairpin Formation via DNA-Templation with Selection via Disulfide Cleavage and Hairpin-Promoted PCR Readout
 - 5.1.3.3.1 Reaction Scope with DNA-Templated Platform

5.2. DNA-Ligation-Based Methods

- 5.2.1. Proof of Principle: Platform for High-Throughput Screening of DNA-Encoded Catalyst Libraries in Organic Solvents via Biotin-Avidin Selection and DNA Sequencing Readout
- 5.2.2. Reaction Discovery by Hybridization-Independent DNA-Encoded Reactants with Disulfide Cleavage Selection and DNA Microarray Readout
 - 5.2.2.1. Application to Au(III)-Catalyzed Friedel-Crafts-Like Indole Alkylation
 - 5.2.2.2. Application to Visible-Light-Induced Azide Reduction
- 5.3. DNA-Based Method for Enantioselectivity Readout
 - 5.3.1. Enantioselectivity Readout Using Enantiomeric DNA Aptamers

6. Conclusion

Author Information

Corresponding Author

ORCID

Notes

Authors

Biographies

Acknowledgments

References

1. INTRODUCTION

The scientific community has benefited significantly from both deliberate and more spontaneous catalyst screening resulting in the discovery of valuable new transformations, with success here spurring on continued development of enabling screening methodologies. Advances in transition metal catalysis have dramatically influenced the field of synthetic organic chemistry. In fact, 90% of all commercial chemical processes involve using one or more steps mediated by a metal, organo-or enzyme catalyst.² Classic examples of reactions of practical import in the area of asymmetric catalysis are exemplified in the 2001 Nobel Prize in Chemistry to W. S. Knowles, ³ K. B. Sharpless⁴ and R. Noyori. Knowles contribution relates to the stereoselective Monsanto L-DOPA process that avails itself of transition metal complex-mediated asymmetric hydrogenation^{6,7} that revolutionized the production of L-DOPA, chemistry that has had enormous practical impact as L-DOPA/carbidopa combination is still the regimen of choice for the treatment of Parkinson's disease. More recent work by Merck process chemists also utilized asymmetric hydrogenation to access Sitagliptin (JanuviaTM).⁸ Interestingly, the Sitagliptin process has been further developed, and the second-generation route now utilizes an enzymatic reductive amination with a highly engineered transaminase; whereby catalyst screening, once again, played a huge role. 9 Both the asymmetric hydrogenation route and the enzymatic transamination route to Sitagliptin were recognized with the Presidential Green Chemistry Challenge awards in 2006 and 2010, respectively, illustrating the value of both transition metal catalysis and biocatalysis in stereocontrolled process chemistry and the central role of catalyst screening in both pursuits. A much more recent example from the Merck process group involves the biocatalytic cascade-based synthesis of Islatravir in which nine biocatalytic steps are employed, of which five involve evolved enzymes, achievable only with advances in biocatalyst screening.¹⁰

Of course, Sharpless and co-workers have uncovered several different transformations-(i) the titanium-tartrate-guided asymmetric allylic epoxidation, ¹¹ (ii) the cinchona alkaloid-mediated asymmetric dihydroxylation ¹² and (iii) the Cu-mediated azide-alkyne cyclocondensation of the Huisgen variety, ^{13,14} all of great importance in synthesis, medicinal chemistry at chemical biology, and all developed by a decidedly empirical approach. In the case of the azide-alkyne cyclocondensation, subsequent examination of broader chemical and catalyst space led to the development of the Ru-mediated variant by Fokin, ^{15,16} providing access to the complementary 1,5-triazoles and to the use of strain-promoted variants by Bertozzi¹⁷⁻²⁰ that obviate the need for the transition metal entirely, for appropriate systems. This is a notable example of how a new reaction modality discovered in a highly empirical fashion has spawned important follow-on chemistry, chemistry that has truly revolutionized chemical biology.

These examples highlight the empirical and iterative nature of the reaction discovery, catalyst development, and optimization endeavors in both academic settings and in process chemistry laboratory settings. That being said, there is increasing interest in computational approaches to catalyst design, from DFT-based calculations^{21,22} of putative transition states, to machine-learning²³ and iterative principal component analysis.²⁴ And rational design endeavors will likely continue to grow, enabled by advancements in computing power and an ever-expanding knowledge base of known catalytic transformations. Yet, at least with the current state of the art, and given the nature of catalysis and the variables inherent in catalytic processes, development must ultimately still rely on extensive experimental screening.²⁵⁻³⁰ At the opposite extreme, the groups of Hartwig^{30,31} and MacMillan³² have recognized the role that almost untargeted screening can play in providing an entrée into fundamentally new elements of reactivity space or as yet unexplored reaction manifolds; a process that the latter calls 'accelerated serendipity.'

In fact, many reaction discovery campaigns involve both approaches, combining intuition and a sense of reactivity with an element of screening and optimization. To effectively enable the discovery of new reactions or catalysts, a screening method must be selected that provides an accurate and rapid method to identify successful reactions. Thus, there has been great interest in the development of new screening methods to better equip those developing and optimizing new reactions in the academic and industrial process chemistry communities to uncover new and exciting transformations.

In the past two decades, the community has responded with the active exploration of a broad array of strategies, encompassing a panoply of analytical techniques for the screening of catalytic chemistry. In thinking about these approaches, key variables include convenience, validity of the method/perturbation of the system, generality of the method, information content of the readout, and potential to enhance throughput. The approaches taken include the measurement of heats of reaction for both exotherms and endotherms by way of IR thermography, pioneered by Maier, Reetz and Morken.³³⁻³⁶ The use of mass spectrometry, ESI-MS (electrospray ionization MS, particularly Pfaltz, Reetz and Finn)³⁷⁻⁴² and SAMDI-MS (self-assembled monolayer matrix-assisted laser desorption/ionization MS, particularly Mrksich)⁴³⁻⁴⁸ and SALDI-MS (semiconductor-assisted MALDI; Xiong and Nie)⁴⁹ for readout allows for the establishment of product identity and, in favorable cases, also catalyst enantioselectivity, by taking advantage of microscopic reversibility, for example, and examining how catalyst stereochemistry 'matches' with each of the two potential enantiomeric products of a targeted transformation. ³⁷⁻⁴⁰ There have also been complementary methods developed with tags identifiable by IR⁵⁰ or NMR.⁵¹ The use of optical tools comprises screens resulting in visual colorimetric output, 52-56 and those that take advantage of chromophores that fluorescence⁵⁷⁻⁶² or communicate with one another via Förster resonance energy transfer (FRET). 63,64 Other methods particularly focused on enantioselectivity readout include a number based upon chiroptical methods (CD/ORD – particularly Mikami, Ding, Anslyn, Wolf)⁶⁵⁻⁶⁸ and those that take advantage of sensor arrays and utilize indicator displacement assays (IDA; particularly Anslyn). 66,69-72 And particularly in the area of heterogeneous catalysis. Senkan and coworkers have demonstrated the innovative use of laser-induced (multi)photonbased ionization methods to expedite catalyst screening. 73,74

A number of reviews of catalyst screening methods have appeared in recent years, 75-78 including a particularly thorough review by Glorius and coworkers, ¹ that complements and updates earlier overviews. 79-82 There is also a nice set of reviews that focus on chiroptical methods to establish enantioselectivity by Anslyn and coworkers. 66,83,84 Finally, there are excellent recent reports describing the development of reaction miniaturization to the nanomole scale and high throughput experimentation (HTE) in the pharmaceutical process sector, 85,86 and the need for appropriate and compatible screening methods to support such approaches. None of these reviews focuses on biomacromolecule-assisted screening methods. And while there are focused discussions of our own in situ enzymatic screening (ISES) method, 87 of the use of antibody-based sandwich assays for reaction discovery⁸⁸ and of the use of DNA-encoded libraries for selection^{89,90} and of nucleic acid arrays for chiral recognition, 91 an overview of the entire field of biomacromolecule-assisted screening has not yet appeared. It is, therefore, the goal of this review to provide the reader with a comprehensive view of biomacromolecule-assisted screening methods, with a particular emphasis on the most interesting catalytic chemistry that has been uncovered through such approaches how these new reaction modalities have been optimized and developed, and how they have spawned follow-on chemistry and, in this way, nucleated new directions in synthetic and catalytic chemistry.

Why Use Biomacromolecules as Sensors to Assist in Reaction Discovery/Catalyst Screening?

Biomacromolecules have evolved naturally through Darwinian selection for biological function that leads to the survival of the fittest, and that biological function includes molecular recognition and catalysis. For example, humans have evolved an immune response to protect against xenobiotics whereby the combinatorial system built into immunoglobulin system allows for vital macromolecular antibodies to be constructed in response to the foreign antigen. The levels of molecular recognition achieved, in terms of both specificity and binding affinity, are remarkable. This observation served to launch the field of catalytic antibodies and has clearly motivated the use of antibodies for reaction discovery and catalyst optimization, launching the newer pursuit of cat-ELISA, as will be discussed herein. Nature has also evolved enzymes as catalytic proteins designed to control nearly all metabolic steps. Of course, both antibodies and enzymes have the ability to achieve chiral recognition. Indeed, synthetic chemists have taken advantage of the high sensitivity afforded by protein-based sensing methods and high enantioselectivity afforded by chiral protein binding pockets. In addition to being able to raise an antibody to an unnatural reaction product of interest, the rapidly expanding field of directed enzyme evolution means that a synthetic chemist can produce a *de novo* sensor for an unnatural reaction based upon either an antibody or an enzyme, depending on the analyte and the screening goals. Reflecting on all of this, it must be said, that underlying the work in our own group and that in other research groups who utilize proteins to report on organic reactivity is the evolutionarilyguided notion that proteins, both antibodies and enzymes, are perhaps ideally suited biomacromolecules for the recognition of small molecule antigens. We and others have taken that principle from Nature to exploit these biomacromolecules as reporting sensors for the catalyst discovery enterprise.

Parallel to the work with protein biomacromolecules--antibodies and enzymes--as sensors for reaction analysis and catalyst optimization, there has been a complementary and creative use of nucleic acid biomacromolecules as tools for reaction discovery. That nucleic acids are ideally suited to fold into three dimensional structures capable of molecular recognition and catalysis for such purposes is also motivated by considerations of evolutionary biology. Namely, there is considerable evidence to support the idea that RNA was the earliest biomacromolecule in support of life in a so-called the "RNA world,"92 wherein RNA essentially fulfilled all the three functions of the central dogma of molecular biology. This is where RNA is the repository of encoded information, as we see in RNA retroviruses today such as SARS-CoV-2 and HIV. RNA is, of course, the message, and is responsible for forming the amide bond in protein synthesis catalyzed by the ribosome, itself very much a sophisticated rRNA ribozyme with associated mRNA and tRNA partners. Therefore, the early enzymes were likely all RNA, with molecular recognition and catalysis components. Indeed, current technology allows us to artificially evolve synthetic-RNAs to recognize small molecule analytes. For example, the SELEX (Systematic Evolution of Ligands by Exponential Enrichment) technology for aptamer selection developed by Tuerk and Gold, 93 and Ellington and Szostak 94 serves as a biomimetic protocol for directed evolution. Using this approach, one can select for single-stranded RNA or DNA-aptamers with high binding affinity for the target analyte through iterative rounds of selection. 95

The natural encoding function of nucleic acids offers additional opportunities in the use of these biomacromolecules in service of reaction discovery. DNA-based screening methods take advantage of the genetic code as a natural bar-coding mechanism for *encoding* candidate reactants and for *templating* these to probe for new reactivities in a pairwise fashion. To screen for multiple such reactant combinations in a single vessel, one needs an effective way to pull down successful

reactions by having the bond-making process distinguish the DNA-tags from the productive reactant pairs from all others. DNA templation allows for two sets of substrates to react with each other at high effective molarity, with the DNA-guided reaction effectively becoming an intramolecular one, while DNA-encoding allows the successful reaction pairs to be decoded. As DNA has naturally evolved to replicate itself through the templation process and to encode genetic information, these principles naturally follow from biology.

2. DIRECT ENZYMATIC SCREENING METHODS

Biocatalysis has taken on ever increasing importance for pharmaceutical process groups, ⁹⁶⁻⁹⁹ including the design of enzyme cascades ^{10,100-123} to mediate key steps in building ever more complex molecular frameworks. ^{9,10,96,124} Biocatalysis is becoming more and more versatile and high-throughput assay systems have rendered directed evolution approaches more practical. Modern protein engineering methods allow for the combination of directed evolution approaches with in silico design of biocatalysts to enhance properties such as stability, substrate specificity and enantioselectivity. The research groups of Bornscheuer, ¹²⁵⁻¹³² Turner and Flitsch, ¹³³⁻¹³⁷ Lutz, ¹³⁸⁻¹⁴⁰ Reymond, ¹⁴¹⁻¹⁴⁵ and Reetz ^{34,36,50,51,58,82,146-149} in particular have contributed significantly to the development of creative and often parallel screening methods for enzyme engineering and directed evolution.

Biocatalyst work and enzymatic screening design have inspired the use of enzymes to study organometallic transformations in a high-throughput manner. Enzymes in screening methods take advantage of the ability of these biomacromolecules to fold into well-defined three-dimensional structures that are, of course, themselves chiral and capable of recognizing chirality in small molecule ligands/analytes and often also of performing catalytic turnover of these. This screening method utilizes enzyme catalysis with an associated chromophore, often a catalytically active cofactor, that provides for a UV-vis signal upon turnover, that can be monitored with a spectrophotometer or with the naked eye.

2.1. Enzymatic Methods Providing Relative Rate Readout

2.1.1. UV-Vis Readout Using Alcohol Dehydrogenase/Aldehyde Dehydrogenase Reporting Enzymes (In Situ Enzymatic Screening – ISES)

The Berkowitz group has been interested in exploring new chemical transformation space and ligand development with the assistance of enzymes as screening tools due to their ability to provide spectroscopic signatures without the need to install chromogenic labels. The initial approach was to examine enzymes with associated cofactors that could provide a spectroscopic signal upon processing a product or byproduct of the organic/organometallic reaction under screening. Such an approach would, in principle, allow for the continuous UV/vis-monitoring of reaction without the need to take aliquots, quench the reaction, or inject samples into a separate instrument. This method has been termed "in situ enzymatic screening," or ISES.

The first iteration of ISES was to study the transition metal-mediated intramolecular allylic amination of an allylic carbonate to give a protected α -vinylglycinol product (**Figure 1**). ¹⁵⁰ Mechanistically, the low valent transition metal complex presumably forms a π -allyl intermediate by oxidative addition into the allylic carbonate substrate, thus displacing an ethyl carbonate leaving group. It is the free ethyl carbonate that this enzymatic screen monitors. This screening approach is designed to run the reaction in a biphasic system, in which the organic reaction takes place in the organic layer (THF:toluene:hexane (2:1:1) – upper layer here) and the reporting enzyme

chemistry takes place in the aqueous buffer layer. When ran in a biphasic system, the ethyl carbonate leaving group is expected to decarboxylate into carbon dioxide and ethoxide, the latter rapidly protonating to ethanol at the aqueous interface. The ethanol byproduct then diffuses into the aqueous layer, where two reporting enzymes are positioned to monitor its formation. Yeast alcohol dehydrogenase (YADH) converts ethanol to acetaldehyde, which is then oxidized to acetate via a yeast aldehyde dehydrogenase (YAIDH) (Figure 1A). The first enzymatic step

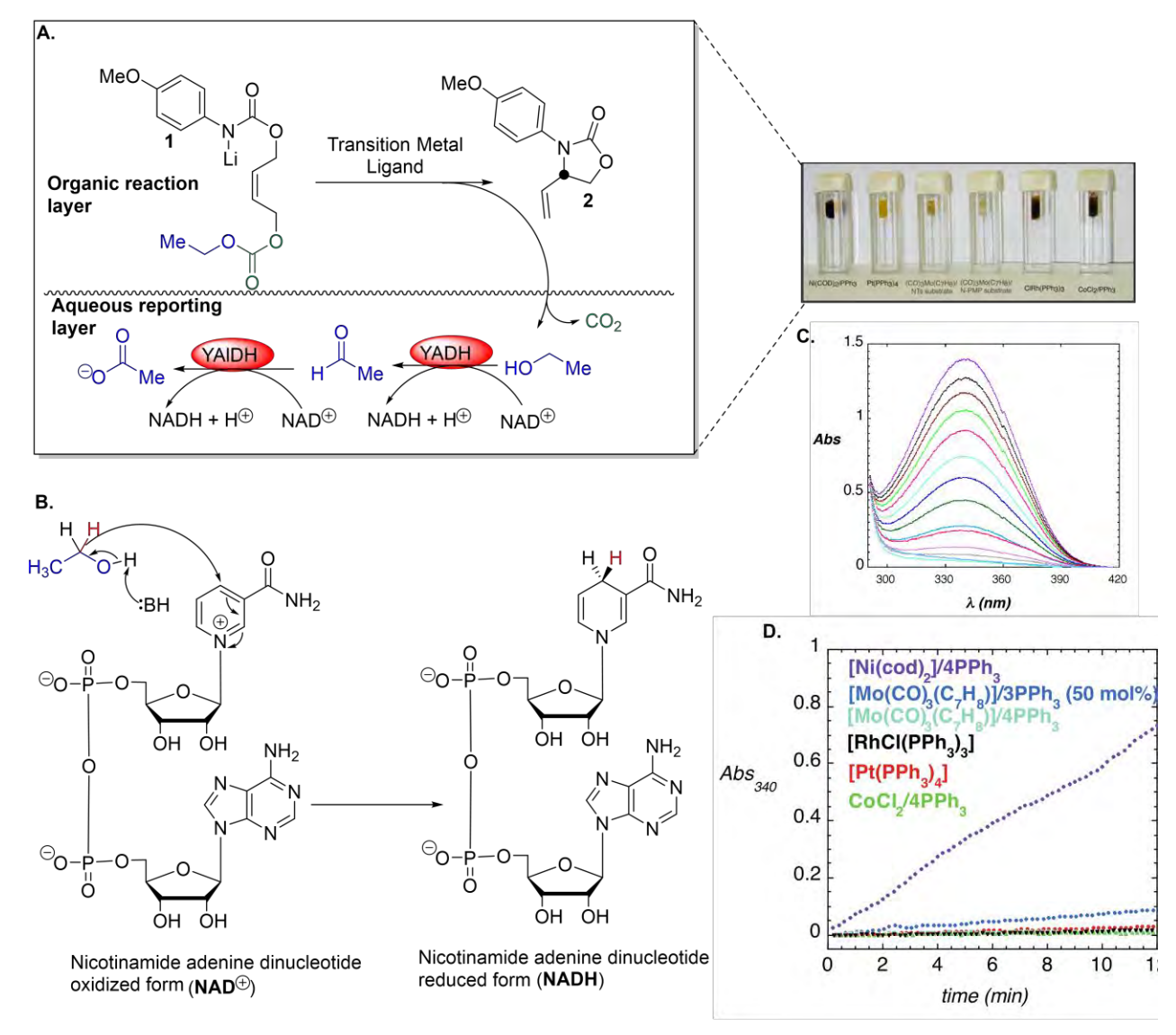


Figure 1. In situ enzymatic screening (ISES). A. Targeting a transition metal-mediated intramolecular allylic amination route into α-vinylglycinol as assayed via ISES. Experiments were conducted in a cuvette array with an organic upper layer featuring transition metal/ligand catalyst candidates with a lower, aqueous reporting layer that includes yeast alcohol dehydrogenase (YADH), yeast aldehyde dehydrogenase (YAIDH) and the cofactor NAD⁺ with NADH formation providing the assay readout. B. Two electron reduction of NAD+ to NADH leading to the formation of the 1,4-dihydronicotinamide chromophore with λ_{max} at 340 nm. C. UV/vis spectral scans of the reporting layer taken at two-minute intervals showing the formation of NADH. D. Relative rate readout by UV absorption at 340 nm. Figure adapted with permission from ref 150. Copyright © 2002 Wiley-VCH. Panel (A) cuvette image, (C), and (D) reprinted with permission from ref 87. Copyright © 2017 John Wiley & Sons, Inc.

NAD+-oxidation of ethanol to acetaldehyde--is endergonic (@ pH 7.7, Δ G' = + 4.6 kcal mol⁻¹), ¹⁵¹ whereas the second enzymatic step-oxidation of acetaldehyde to acetic acid and its ionization to

acetate is highly exergonic (pH 7.7, $\Delta G' = -15.6$ kcal mol⁻¹) driving the overall reporting reaction forward. Each enzymatic oxidation delivers a hydride equivalent to C-4 of the nicotinamide ring, producing the 1,4-dihydronicotinamide ring of the NADH cofactor (**Figure 1B**). As can be seen in **Figure 1D**, this chromophore has an absorption maximum and 340 nm and easily monitored in a UV spectrophotometer as it forms, on the fly, in the ISES experiment. (**Figure 1C**). For each turnover, two molecules of NADH are generated; when run in parallel cuvettes with an automated cell changer, this UV-vis-based screening method can be used to rank a set of catalytic combinations in parallel. Proof of principle of this ISES approach was demonstrated with a catalyst discovery screen under Ar atmosphere to allow for the sampling of even highly air-sensitive metals, such as Ni(0) catalyst candidates (**Figure 1D**).

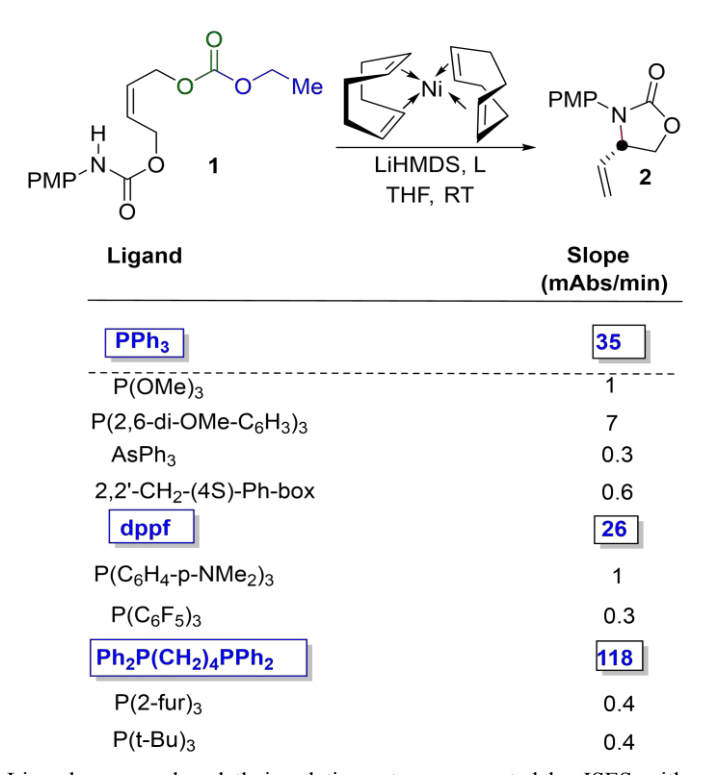
2.1.1.1. Initial Screening Hit: Ni(0)-Mediated Allylic Amination

Typically, each ISES-subproject in the Berkowitz group is motivated both by a screening goal; e.g. demonstrating proof of principle of a new enzymatic assay, and a synthetic goal. In the case of the reaction being targeted in **Figure 1**, the screen is for a transition metal-mediated intramolecular allylic amination-based entry into the α -vinylglycine scaffold. The Berkowitz group has had a longstanding interest in developing methodology for the synthesis of β , γ -unsaturated amino acids as potential mechanism-based inhibitors (MBIs) of PLP-dependent enzymes. Through these efforts, it has been seen that absolute stereochemistry is important,

but approaches to the control of stereochemistry in synthesizing these compounds were *stoichiometric* in chirality largely. So, several important synthetic goals have emerged: (i) to develop new *catalytic* routes into these scaffolds; (ii) to do so with control of stereochemistry and (iii) if possible to move away from precious metals in so doing.

To be more specific, the parent member of the family vinylglycine, produced naturally by mushrooms, and a demonstrated mechanism-based inhibitor of ACC (1amino-1-cyclopropane carboxylate) synthase. 167 The Berkowitz group had previously developed stereocontrolled synthesis of L-αvinylglycine from L-homoserine. 168 The group has also developed synthesize chemistry to higher, 'quaternary' α-vinylic amino acids that bear the same α-vinyl MBI-trigger, but

Table 1. Ligands Screening



Ligands screened and their relative rates as reported by ISES with $Ni(cod)_2$ for intramolecular allylic amination reaction.

also contain the characteristic AA side chain, 153,154,157,159,160,166 as well as quaternary, α -(1'-fluoro)vinyl AAs 152 and α -(2'Z-fluoro)vinyl AAs, 165,166 and demonstrated the ability of such β , γ -

unsaturated AAs to inactivate their cognate, PLP-dependent AA decarboxylase (AADC) enzymes. The group had also shown that α -vinyl AAs serve as useful precursors to interesting α -oxiranyl AAs, ¹⁵⁸ as well as α -chlorovinyl and α -bromovinyl AAs. ¹⁵⁶

Trost and coworkers had demonstrated a Pd-based asymmetric allylic amination entry into α -vinylglycine. This cemented our interest in screening for earth-abundant transition metal variants of such chemistry. So, the Berkowitz group chose to screen for non-Pd-based catalytic metal-ligand combinations for this transformation. With this synthetic goal in mind, the group demonstrated the first enzymatic screening method for the intramolecular allylic amination reaction of the allylic carbonate 1 as a model substrate (**Figure 1**). The ISES method was used to screen a combination of transition metals and ligands, ultimately identifying the successful Ni(0) metal/phosphine ligand combination to efficiently yield vinyl oxazolidinone 2.

With this method, six reactions were screened in parallel, and relative kinetic data were collected for a 10-minute window (**Figure 1 D**). Based on the NADH formation for the different transition metal-catalyzed reactions; one can identify catalyst/ligand combinations with promise for the targeted reaction (**Figure 1D**). Of the initial non-Pd transition metals screened for the test substrate, the combination of Ni(cod)₂ and phosphine ligation gave the most promising initial rate

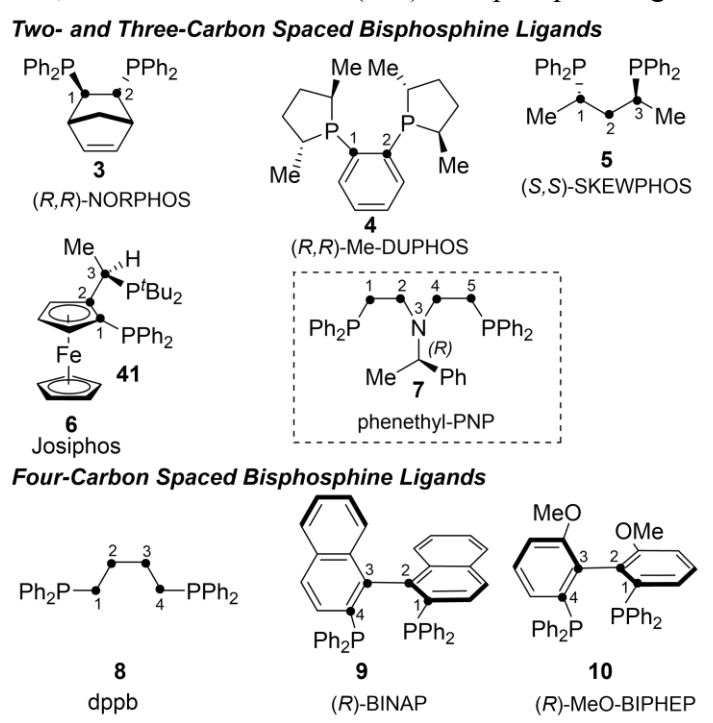


Figure 2. Bidentate bisphosphine ligands with two, three and four carbon spacing and NPN tridentate ligand examined for asymmetric, Ni(0)-mediated asymmetric allylic amination.

(Figure 1D). To probe for a correlation between the rate of cofactor reduction in the reporting layer and reaction turnover in the organic layer, Berkowitz group examined relative product formation rates independently by an NMR-based time point assay by drawing aliquots from the upper organic layer with time. A comparable relative rate pattern was seen for product formation in the organic layer and rate of reduction of cofactor in the aqueous, reporting layer.

ISES identified Ni(0) as a promising earth-abundant transition metal catalyst for the targeted reaction. This initial result inspired the team to screen a range of phosphine ligands with the Ni(0) pre-catalyst. Electronrich phosphine ligands such as

PPh₃, dppf [bis(diphenylphosphino)ferrocene] and dppb [1,4-bis(diphenylphosphino)butane] emerged as effective ligands with Ni(0) for this transformation (**Table 1**). As it turned out, the combination Ni(cod)₂ and bidentate phosphine ligands proved to be optimal, with resulting in the fastest turnover (**Table 1**). In fact, the ISES ligand screening results suggest that the use of a Ni(0) pre-catalyst with bidentate phosphine ligands possessing a four-carbon spacer results in the most dramatic ligand-accelerated catalysis. This result further guided the group to screen chiral, electron-rich bidentate phosphine ligands and identify several that give significant asymmetric

induction. These include chiral bidentate phosphine ligands such as Josiphos (6), as well as BINAP (9) and methoxy-BIPHEP (10) with three- and four-carbon spacing, respectively, that mediate the first reported examples of Ni(0)-mediated asymmetric allylic amination as is described in more detail below. 172,173

2.1.1.2. Hit Elaboration: Ni-Catalyzed Allylic Substitution

Based upon the observation that bidentate phosphine ligands promote this Ni(0)-mediated allylic amination chemistry, the group expanded its ligand screen across a broader range of PP, PN, NN, and PNP-ligands (**Figure 2**) under ISES conditions. This screening led to the identification of N,N-bis(2-diphenylphosphinoethyl)alkylamine (PNP) **7** as the fastest ligand for this transformation. Unfortunately, ligand **7** showed no discernable enantio-discrimination for product **2** (chiral HPLC). The group also expanded its screen to include the Vigabatrin-leading substrate **12**, in addition to the α -vinylglycine-leading substrate **1**. This reaction was further screened against the Ni(0)-catalyst with a variety of two-four carbon spaced bidentate phosphine ligands (**Figure 2**). Among the ligands screened, Josiphos (**6**) and BINAP (**9**) gave notable initial rates and both ligands showed the potential for asymmetric induction in this transformation (chiral HPLC).

Scheme 1. Ni(0)-Catalyzed Asymmetric Intramolecular Allylic Amination Reaction

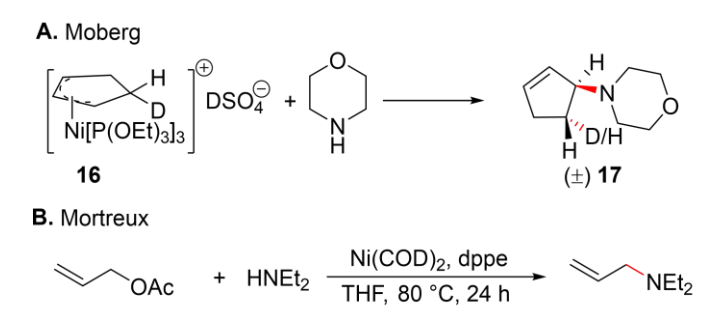
A. Formal Ni(0)-catalyzed asymmetric allylic amination entry into S-Vigabatrin substrate

B. Ni(0)-mediated asymmetric route into L- α -vinylglycine.

These chiral ligands were examined under flask conditions for the asymmetric synthesis of lactam 12, a known intermediate toward the anti-epilepsy drug Vigabatrin 13 (Scheme 1). The three-carbon-spaced Josiphos-type ligand 6 gave the highest ee (74%) but low yield and the two-carbon-spaced centrally chiral ligand DUPHOS gave excellent yield with 66% ee (Scheme 1A). For the asymmetric synthesis of vinyl oxazolidinone 2 under flask conditions the Josiphos ligand 6 gave 82% ee with moderate yield. The four-carbon-spaced ligand (R)-MeO-BIPHEP, possessing axial chirality, gave the product in 88% yield with 75% ee, which could be enriched up to 97% ee by a single recrystallization (Scheme 1B). The enantio-enriched vinyl oxazolidinone has been carried forward through further functional group manipulation and deprotection to achieve a Ni(0)-mediated asymmetric entry into (L)- α -vinylglycine 15 (Scheme 1B).

In the past decade or so, Ni-catalyzed chemistry has really come to the fore in organotransition metal chemistry. Motivated by our own ISES-based discovery in this area (vide supra), in this section of the review, we will mostly focus on Ni-catalyzed allylic substitution reactions since 2004. The pioneering reports on transition metal-mediated allylic substitution appeared from Tsuji¹⁷⁰ and Trost¹⁷⁴ initially with Pd(0) and phosphine ligands or with Pd(II) and in situ generation of Pd(0). This Tsuji-Trost chemistry originated with malonate nucleophiles and simple symmetrical allylic acetate or carbonate electrophiles and has evolved into a versatile transformation accommodating a wide range of nucleophiles, including heteroatom-centered nucleophiles, and a significant array of unsymmetrical allylic systems as electrophiles. Pdmediated allylic substitution has become a staple reaction in organic synthesis and has been method developments over five decades and remained an attractive method in organic chemistry. 175,176 In the past few decades, the asymmetric Pd(0)-mediated version of this reaction, featuring a stable of viable, primarily phosphine-based chiral ligands has been established across a considerable range of nucleophiles and electrophiles. 177-181 And while Pd has been front and center in allylic substitution chemistry, several other late transition metal catalysts have been found useful depending upon the allylic system and nucleophile. 182,183 Our focus here is on asymmetric transition metal-mediated allylic amination, a transformation that has been most thoroughly explored with Pd, ^{177,180,184} Ir, ^{182,183} Rh and ¹⁸⁵⁻¹⁸⁷ Ru. ¹⁸⁸⁻¹⁹¹ The Ni-mediated asymmetric variant of this transformation has arisen from earlier ISES studies described above. 172,173

Scheme 2. Early Ni-Catalyzed Allylic Amination Reactions Using Amines as Soft Nucleophiles



Nickel-Catalyzed Allylic Substitution – Precedents and Early Leads

To our knowledge, the earliest reports of Ni-catalysis for allylic substitution 192 emanated from the groups of Tolman 193 and Yamamoto 194,195 who reported on the formation of π -allyl Ni-complexes. In a key breakthrough, Hiyama and coworkers demonstrated that, under Ni-catalysis, a hard nucleophile such as a Grignard reagent could undergo

asymmetric allylic substitution reaction by utilizing chiral a NiCl₂(S,S-Chiraphos) precatalyst. ¹⁹⁶

Following upon this observation, the groups of Consiglio^{197,198}, RajanBabu,¹⁹⁹ and Hoveda^{200,201} reported Ni-mediated allylic substitution reactions with Grignard reagents as the nucleophilic species. Interestingly, these reports were focused largely on hard nucleophiles. However, Ni-

Scheme 3. Ni(0)-Catalyzed Allylic Amination Reactions Upon Allylic Alcohols

catalysts have been well-studied less allylic for with substitution nucleophiles. soft There are a few precedents found in literature in this context in which an amine has been used as soft

nucleophile for Ni-catalyzed allylic amination reactions. Moberg put forward key work in this space in 1980, 202 reporting on the formation of a cyclic π -allyl-Ni complex **16** and its treatment with morpholine to give racemic N-substitution product **17** (**Scheme 2A**). These early experiments involved stoichiometric Ni chemistry. Later, Mortreux co-workers, 203 described the first, simple catalytic examples of this Ni chemistry with diethylamine as nucleophile and allyl acetate/carbonate as the electrophile (**Scheme 2B**).

The targeted transition metal-mediated intramolecular amination reaction described above as a platform to explore ISES was chosen by the Berkowitz group because it would provide a streamlined route into α -vinylglycine, a target of great interest to the group. As it turned out, the

promising results seen with Ni(0) as catalyst and the rate acceleration seen with bidentate phosphine ligands by ISES, set the stage for the discovery of the first catalytic, asymmetric allylic amination with Ni reported by Maiti and Berkowitz in 2004.¹⁷² To this day, this remains the key precedent for exploiting earth-abundant Ni for asymmetric allylic amination reaction.204

These observations derived from key ISES-

Scheme 4. Ni-Catalyzed Allylic Amination Reaction Using Ni(II) as Pre-Catalyst With In Situ Reduction to Ni(0) Using Zn(0)

screening results in 2004 appear to have stimulated work elsewhere on Ni(0)-mediated allylic substitution chemistry. In 2015, the Mashima group described the amination of allylic alcohols using a Ni(0) catalyst to give products **19** and **23** (**Scheme 3**). In this report, the use of "Bu₄NOAc as an additive improved catalytic turnover significantly. Based on mechanistic studies, the authors proposed the reaction proceeds *via* a pentacoordinate neutral allyl-Ni complex **20**, in contrast to the usual tetracoordinate cationic allyl-Ni-complex.

More recently, in an interesting development, the Sweeney research group reported a

Scheme 5. Ni(0)-Catalyzed Allylation of Active Methylene Substrates

related allylic amination transformation, utilizing an airstable Ni(II) pre-catalyst in the presence of an equimolar amount of Zn (Scheme 4).²⁰⁶ The Zn(0) presumably reduces the Ni(II) to Ni(0) in situ, with the Ni(0)dppf complex then oxidatively adding into the allyl alcohol substrate to produce an π -allyl intermediate Ni complex. The reaction works well with primary, the

secondary, and phthalimide-based nitrogen nucleophiles. The authors also demonstrated that such an N-allylation reaction could be conducted with triacetyluridine acting as a functionalized uracilbased imide nucleophile. The desired N-allylated triacetyluridine product **29** was obtained in good yield. These results from both the Mashima and the Sweeney groups also serve to very nicely validate our initial finding in the early ISES screens that the combination of Ni(0) catalyst and electron-rich bidentate phosphine ligands works very well for Ni(0)-mediated allylic amination chemistry. ^{150,172,173}

Nickel-Catalyzed Allylic Substitution by Carbon Nucleophiles

In 2016, Bonin and co-workers reported the Ni(0)-catalyzed alkylation of allylic alcohols

Scheme 6. Ni(0)-Catalyzed Selective Mono-Allylation of Active Methylene Substrate Using Ni(II) Pre-Catalyst

methylene using active compounds soft nucleophiles. These authors also utilized the same sort of ligandmetal combination discovered in our 2004 work, namely pairing the Ni(0) precatalyst with the dppb ligand, a bis-phosphine ligand with a four carbon spacer (Scheme 5).²⁰⁷ In this work, it was found that one could drive the chemistry to bis-alkylation by using an excess of allylic alcohol. The same research group also demonstrated an

alternative catalytic approach in which a Ni(II) precatalyst was reduced in situ by zinc metal to the active Ni(0) species. Interestingly, by switching the ligand to dppf with the Ni(II)/Zn combination, the Sweeney group was able to achieve selective mono-allylation of active methylene nucleophiles with either allyl alcohols or allyl amines as the allylic electrophile (**Scheme 6**). ²⁰⁸

Scheme 7. Ni-Catalyzed Allylation of Diarylmethanes

A. Ni-catalyzed allylation of di(pyridin-2-yl)methane. **B.** Stereo-probe demonstrating overall retention of configuration, presumably via a double displacement mechanism.

Walsh and coworkers reported the study of diarylmethanes as pronucleophiles for catalyzed allylic substitution whereby range of lithiated diarylmethanes were employed Cas nucleophiles. In this report, the authors screened 178 chiral ligands the for asymmetric allylic alkylation reaction whereby Josiphos-type ligand 41, a bidentate phosphine with three-carbon spacing, gave the most promising results under DYKAT (dynamic kinetic asymmetric transformation)

conditions.²⁰⁹ This is another interesting example that follows directly from the initial ISES-based Ni(0) chemistry reported by the Berkowitz group in 2004. There too the combination of Ni(0) and Josiphos, proved to be a promising combination for asymmetric allylic substitution

Scheme 8. Ni(0)-Catalyzed Asymmetric Allylic Alkylation to form All Carbon Quaternary Center

A. Using allylic alcohols as an allylic precursor. **B.** Using allylic amine as an allylic precursor.

chemistry.^{172,173} Under optimized conditions here, the allylation of **39** produced the **42** in 92% yield and 91% *ee* (**Scheme 7A**).

The palladium-catalyzed allylic substitution reaction with soft nucleophiles is known to follow a double inversion mechanism, whereas hard nucleophiles give a single inversion product. To confirm whether this reaction follows a soft or hard nucleophile mechanism, the authors performed a stereo-probed control reaction on substrate 43 with chiral Josiphos ligand 54 and achiral dppf ligand, where it was observed that both ligands give racemic cis 44 product. These results suggest that the reaction follows a double inversion path, and the lithiated diarylmethane behaves as a soft nucleophile. Interestingly, the control reaction with the Josiphos ligand also suggests that the transformation on 43 is fully substrate-controlled.

In 2006, Mashima and coworkers described a Ni-catalyzed asymmetric allylic substitution

Scheme 9. Nickel-Catalyzed Asymmetric Allylic Alkylation Reaction to Construct Homoallylic All Carbon Quaternary Centers in Lactone/Lactam Scaffolds

reaction on allylic alcohols, wherein β-keto-ester enolates serve as soft nucleophiles. This protocol uses a combination of Ni(COD)₂ pre-catalyst with a four-carbon spaced chiral bidentate S-H₈-BINAP ligand (47), and to install an all carbon quaternary center (Scheme 8A) with high enantiomeric excess and in excellent yield.²¹⁰ The same research group 2020 demonstrated another Nicatalyzed asymmetric allylic alkylation reaction on allylic amines, using another fourcarbon spaced and electronbidentate rich chiral bisphosphine ligand 53 to set

another quaternary center (**Scheme 8B**) 211 shown in product **47**. Based on mechanistic investigations, the authors propose that the β -keto ester is deprotonated by the allylic amine nitrogen, thereby also generating an allylic ammonium species facilitating C-N bond cleavage to

Scheme 10. Use of Ni-Based Tandem Catalysis for the Asymmetric Synthesis of 1.3 Dinitriles

deliver the π -allyl-Ni intermediate. Nucleophilic substitution by the β -keto ester enolate then yields 47 in high yield and enantiomeric excess. In both reports by Mashima and co-workers showed bisphosphine ligands with a four-carbon spacing play a considerable role in the Nicatalyzed asymmetric transformation. This harks back to the earlier Berkowitz group observations on the importance of four-carbon spaced bidentate phosphine ligands for the Ni-catalyzed allylic amination reaction (e.g., see **Scheme 1A**). 172,173

Recently Stoltz and co-workers reported another nice example of Ni-catalyzed asymmetric allylic alkylation utilizing β -keto-lactam/lactone enolate nucleophiles and the (R)-P-PHOS **56** ligand. Once again, four-carbon spacing is seen in this chiral bidentate phosphine ligand with this approach

Scheme 11. Stereospecific Ni-Catalyzed Allylic Substitution with Aryl Borinates

 efficiently setting chirality in homoallylic all-carbon quaternary centers in the substituted lactone/lactam product(s) 57 (Scheme 9).212 A range of linear and branched allylic

alcohols have been investigated as allylic substrate platforms this reaction. Interestingly, the reaction yields exclusively linear products, indicating that the nucleophile preferably attacks the less hindered carbon in the presumptive intermediate Ni- π -allylic complex. This is another elegant study that further points to the value of examining four-carbon spaced bisphosphine ligands possessing axial chirality for such Ni(0)-chemistry. In 2020, the Fang group demonstrated a one-pot approach to the Ni(0)-catalyzed 1,3-dicyanation of allylic alcohols via allylic cyanation followed by hydrocyanation, yielding product(s) **66 (Scheme 10)**.

In the context of Ni-catalyzed allylic substitution chemistry, there have been a number of interesting allylic arylation demonstrated. For example, using ate complexes derived from aryl boroxines and borinates as the nucleophile, $Trost^{214}$ and Kobayashi²¹⁵⁻²¹⁹ have developed effective allylic substitution chemistry upon allylic amine and carbonate substrates. Uemura and co-workers reported an asymmetric version of this reaction in 2002, albeit with modest enantiomeric excess. Recently, the Watson group described a stereospecific Ni-catalyzed allylic substitution reactions upon allylic pivalates, using arylboroxine-derived ate complexes as nucleophiles. The authors propose that the reaction proceeds via a π -allyl-Ni(II) intermediate with inversion of absolute stereochemistry to deliver 1,3-diaryl product 73 in good yield and high enantiomeric excess (Scheme 11).

2.1.2 Colorimetric Readout Using Alcohol Oxidase/Peroxidase Reporting Enzymes

While the initial approach to in situ enzymatic screening (ISES) developed in the Berkowitz group relied upon the observation of NADH formation by UV/vis spectrophotometry and led to a set of remarkably information-rich screens with information on relative rate, enantioselectivity and substrate selectivity, as will be discussed in Section 2.2, 221-223 the group also took a parallel interest in developing variants of ISES that provide for a visible light read-out. The first iteration of visible, colorimetric ISES takes its inspiration from ELISA (Enzyme-Linked ImmunoSorbent

Assay) technology that finds such wide spread use in clinical chemistry type assay, exploiting the ability of peroxidase enzymes to be linked to redox dyes that provide the experimentalist with a visible readout. This approach allows for the biphasic reaction system to be read by the naked eye in place of a UV/vis spectrophotometer, allowing for higher throughput.

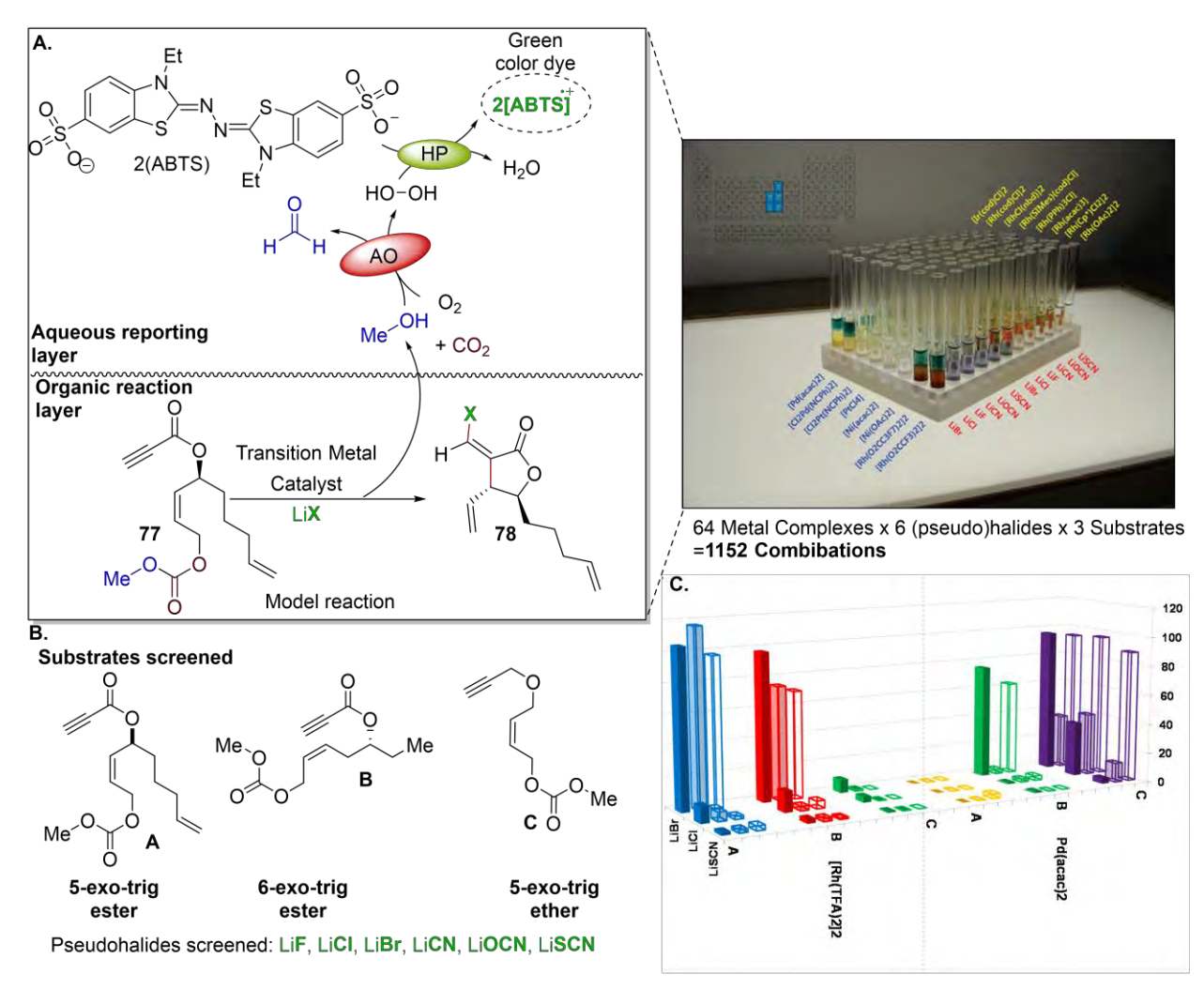


Figure 3. Colorimetric ISES. A. Schematic layout of the in-situ screen for transition metal-mediated halometalation/carbocyclization transformations with alcohol oxidase (AO) and horseradish peroxidase (HP) as reporting enzymes, yielding 2,2-azino-bis(3-ethylbenzothiazoline-6-sulfone) (ABTS.+) radical cation as a visible read-out signal. The layout of the assay consisting of a 96-well format for each substrate, featuring candidate TM catalyst/(pseudo)halide combinations. 96-well image reprinted with permission from ref 224. Copyright © 2011 Wiley-VCH. B. Structures of the three substrates screened (5-exo-trig ester, 6-exo-trig ester, and 5-exo-trig ether). Each was screened against 6 pseudohalides and 64 metal complexes to give 1152 reaction combinations. C. More quantitative view obtained by UV/vis spectrophotometry for selected catalyst/(pseudo)halide candidate combinations for substrates A, B, and C, respectively (relative rates in mAbs₄₀₅ min⁻¹).

Each ISES iteration has both a screening goal and a synthetic goal. For this first visual, colorimetric ISES demonstration, the screen was directed in a rather exploratory fashion for the discovery of new formal (pseudo)halometalation/carbocyclization transformations, inspired by the pioneering work of Lu and Ma on Pd(II)-catalyzed acetoxymetallation/carbocyclization on appropriate allylic enyne substrates. This type of transformation was seen as providing a potentially streamlined entry into the core of sesquiterpenoid natural products of the xanthanolide family. The substrates selected for this screen contain a terminal alkyne positioned to allow for

transition metal coordination, followed by addition of a halide (or pseudohalide) into the alkyne. The intermediate (pseudo)halovinyl-metal species thereby obtained would then be positioned to undergo migratory insertion into a pendant allylic carbonate, forming a 5- or 6-ring in this cyclization step, followed by β -elimination of the metal and carbonate leaving group to complete the catalytic cycle.

With each turnover of the (pseudo)halometalation/carbocyclization substrate, a methyl carbonate leaving group is released and visualized through an ISES-reporting enzyme pathway. The assay is run in a biphasic system with a lower organic layer containing the reaction of interest and an upper aqueous reporting layer. The released methyl carbonate group diffuses into the aqueous layer and undergoes decarboxylation to provide one molecule of carbon dioxide and one molecule of methanol for successful reactions (Figure 3A). Methanol is converted to formaldehyde by the reporting enzyme, alcohol oxidase (AO), with molecular oxygen serving as the oxidant, producing hydrogen peroxide as byproduct. Upon production, H₂O₂ acts as a substrate for the second reporting enzyme, horseradish peroxidase (HP), and undergoes reduction to H₂O. A variety of dyes are known to serve as a terminal reducing agent with HP enzyme. We chose to use the colorless 2,2-azino-bis(3-ethyl-benzothiazoline-6-sulfone) (ABTS) dye here as it is known to be readily oxidized to ABTS.⁺ radical cation (single electron oxidation), with each H₂O₂ reduction producing two equivalents of this chromophore. The ABTS⁺ radical cation appears as a jungle green species with a broad absorption window at 405-414 nm and a large extinction coefficient. Thus, successful substrate turnover presents a green color in the aqueous reporting phase, while unproductive conditions result in colorless wells.

In the case at hand, 64 transition metal complexes were crossed with 6 candidate (pseudo)halides across three different cyclization substrates (**Figure 3B**). The assay was performed in a 96-test tube rack to give a total of 1152 combinations under a week. Two instances of particularly novel reactivity arose from this wide-ranging screen. **Figure 3** summarizes these with the first being a perfluorinated Rh(II)-pre-catalyst-promoted carbocyclization initiated by lithium bromide addition into the alkyne. This bromorhodiation/carbocyclization transformation was found to work well across all substrates screened, including the 5-exo-trig ester and ether substrates, as well as the 6-exo-trig ester substrate. The second discovery of this screen is the new thiocyanopalladation carbocyclization transformation catalyzed by Pd(II), wherein the pseudohalide, LiSCN, is found to support this type of Pd(II)-mediated chemistry. This transformation was seen exclusively with the 5-exo-trig *ether* substrate, presumably due to competing conjugate addition of the thiocyanate anion with the α,β -unsaturated *ester* substrates. This work constitutes the first reported example of such a transformation highlighting the potential for using ISES for reaction discovery. The substrates are substrated of such a transformation highlighting the potential for using ISES for reaction discovery.

Given novelty potential high value the and ofthe new thiocyanopalladation/carbocyclization transformation arising from colorimetric ISES screen, the Berkowitz group next set out to optimize this reaction, again taking advantage of this new reporting system. 224,229 Initial probing of this transformation indicated the need for elevated temperature conditions to reproducibly achieve high conversion. However, this condition presented the limitation that the reporting enzymes used for this screen are not thermophilic enzymes and thus have limited activity at elevated temperatures. A modified screen was utilized to address this limitation. The new design involves measuring the amount of methanol produced at early time points which correlates with reaction efficiency. The organic layer is loaded and subjected to the reaction temperature for 10-15 minutes and then allowed to cool down to room temperature. Then the enzymatic reporting layer is layered above the organic reaction layer in the well and the color is developed. As before, the intensity of the green color produced correlates with the relative rate of substrate turnover (Figure 4A). 229

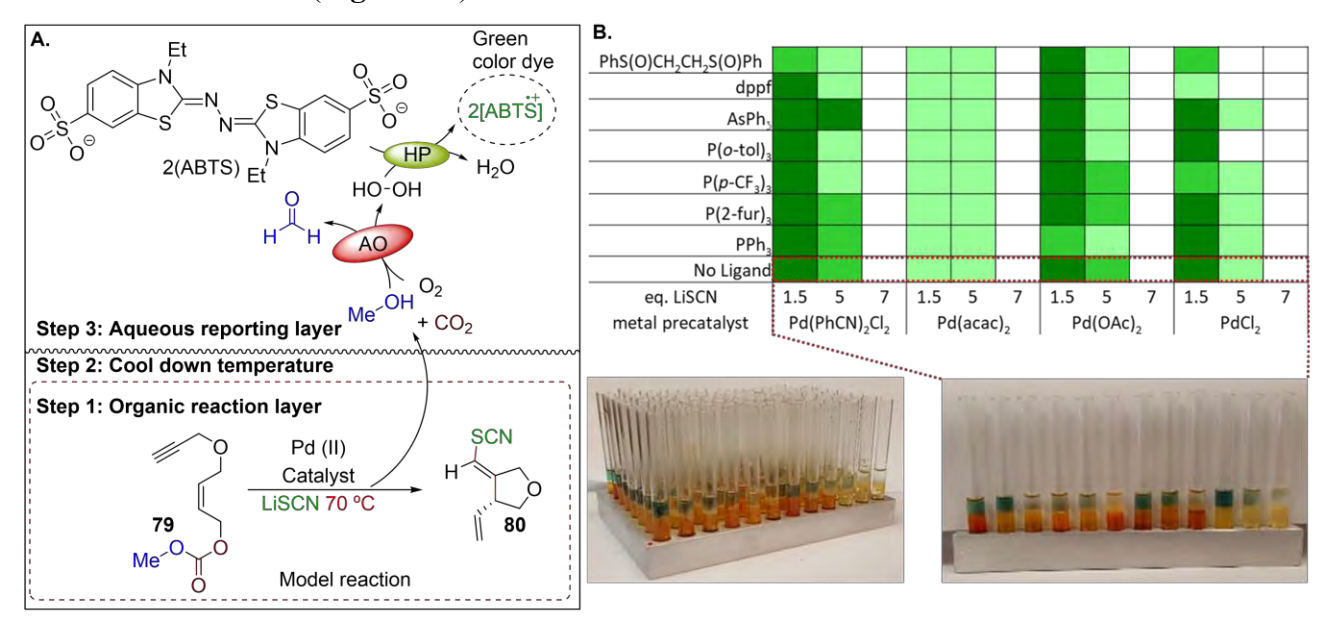


Figure 4. Colorimetric adapted-enzymatic screen at elevated temperature by a three-step assay **A**. Assay for the optimization of the thiocyanopalladation/carbocyclization transformation discovered in the original 1152 combination screen with alcohol oxidase (AO) and horseradish peroxidase (HP) as reporting enzymes. The optimization here is also in a 96- tube format in an aluminum plate heated to 70 °C (aluminum plate; sand bath). The read-out of the assay arises from the formation of the 2,2-azino-bis(3-ethyl-benzothiazoline-6-sulfone) (ABTS.⁺) radical cation producing a jungle green color. **B**. Relative rates are characterized by the intensity of the ABTS.⁺ dye signal (three shades of green depicted). **Panel B (table and 96-tube images) republished with permission from ref 229. Copyright 2017 Royal Society of Chemistry under CC BY-NC 3.0 (https://creativecommons.org/licenses/by-nc/3.0/).**

For these optimization studies, LiSCN was retained as the nucleophile and was screened against Pd(II) catalyst candidates, including Pd(PhCN)₂Cl₂, Pd(acac)₂, Pd(OAc)₂, and PdCl₂ with a set of predominantly phosphine ligands examined for their influence on reaction rate (**Figure 4B**). Most efficient reaction conditions were established by intensity of the ABTS radical cation readout, and this is depicted schematically with a three-shaded intensity scale (**Figure 4B**). This larger screen was performed in a machined aluminum 96-well plate containing narrow bore glass culture tubes for each reaction. The 96-well tray was heated by placing the fully loaded plate in a sand bath for 15 minutes, followed by developing the plate with the screening enzyme layer, as described. The screen identified Pd(PhCN)₂Cl₂ as the best catalyst with Pd(OAc)₂ also displaying good reactivity. Unfortunately, the limited ligand screen did not reveal any kinetic benefit in this transformation, though more screening is clearly necessary here before dismissing the potential

for ligand-accelerated catalysis. The optimized conditions established from this enzymatic screening procedure call for 2.5 mol% of Pd(PhCN)₂Cl₂ at 70 °C with 1.5 eq of LiSCN as the nucleophile.²²⁹

2.1.2.1. Initial Screening Hit: Bromorhodiation/Carbocyclization Reaction

As discussed, colorimetric ISES allows the experimentalist to identify reaction hits by naked eye, and, in the initial 'proof of principle' run published by the Berkowitz group, 1152 combinations were screened expeditiously, leading to the discovery of the bromorhodiation/carbocyclization

Scheme 12. Rhodium-Catalyzed Bromocarbocyclization Reaction

A. Rhodium-catalyzed bromocarbocyclization of an allyl propiolate ester for the synthesis of transdisubstituted bromomethylene lactone **95. B.** Entry into the 5,7-fused terpenoid natural product cores of ixerin and xanthatin, respectively.

reaction. This transformation uses Rh(II)perfluorocarboxylates as precatalysts and LiBr as a nucleophile (and possibly reducing agent, as Rh(I), generated in situ, may be the actual catalytic form) and results in the concomitant formation of C-Br and C-C bonds, leading to highly functionalized δ - and γ -lactone products such as **82** that feature an exocyclic double bond (**Scheme 12A**)²²⁴ In the literature, Rh(II)-chemistry is well documented for carbene and nitrene insertion reactions, all the more reason to suspect that an in situ-generated Rh(I)perfluorocarboxylate may be needed to initiate the chemistry. This bromorhodiation/carbocyclization allows for rapid and

Scheme 13. Pd-Catalyzed Enyne Cyclization With an Intramolecular Halogen Shift for the Synthesis of α-Halomethylene-γ-Butyrolactones

stereocontrolled entry into the 5,7-fused core of the terpenoid natural products ixerin Y and (-)-xanthatin (**Scheme 12**).

In the case at hand, the absolute stereochemistry is set by using an (S)-Alpine borane reduction of

alkynone intermediate to give **85**. The new rhodium-mediated halometalation/carbocyclization reaction then controls the relative stereochemistry, giving access to the enantiomerically enriched 1,2-trans product **87**. The vinylic substituent generated in the carbocyclization is then fused with

Scheme 14. Palladium-Catalyzed Enyne Cyclization Examples

A. Pd-catalyzed halocarbocyclization. **B.** Pd-catalyzed acetoxypalladation/carbocyclization **C.** Pd-catalyzed acetoxypalladation/carbocyclization followed by oxidative cyclopropane formation.

97

the pendant alkene in substrate using Grubbs **RCM** chemistry to give 5,7fused bicyclic bromoexomethylene β-The lactone 88. exocyclic bromomethylene functionality featured in core structure 88 can further functionalized by TMcatalyzed crosscoupling reactions or nucleophilic addition/elimination chemistry providing library for greater diversification. as desired. Berkowitz and co-workers have further expanded the

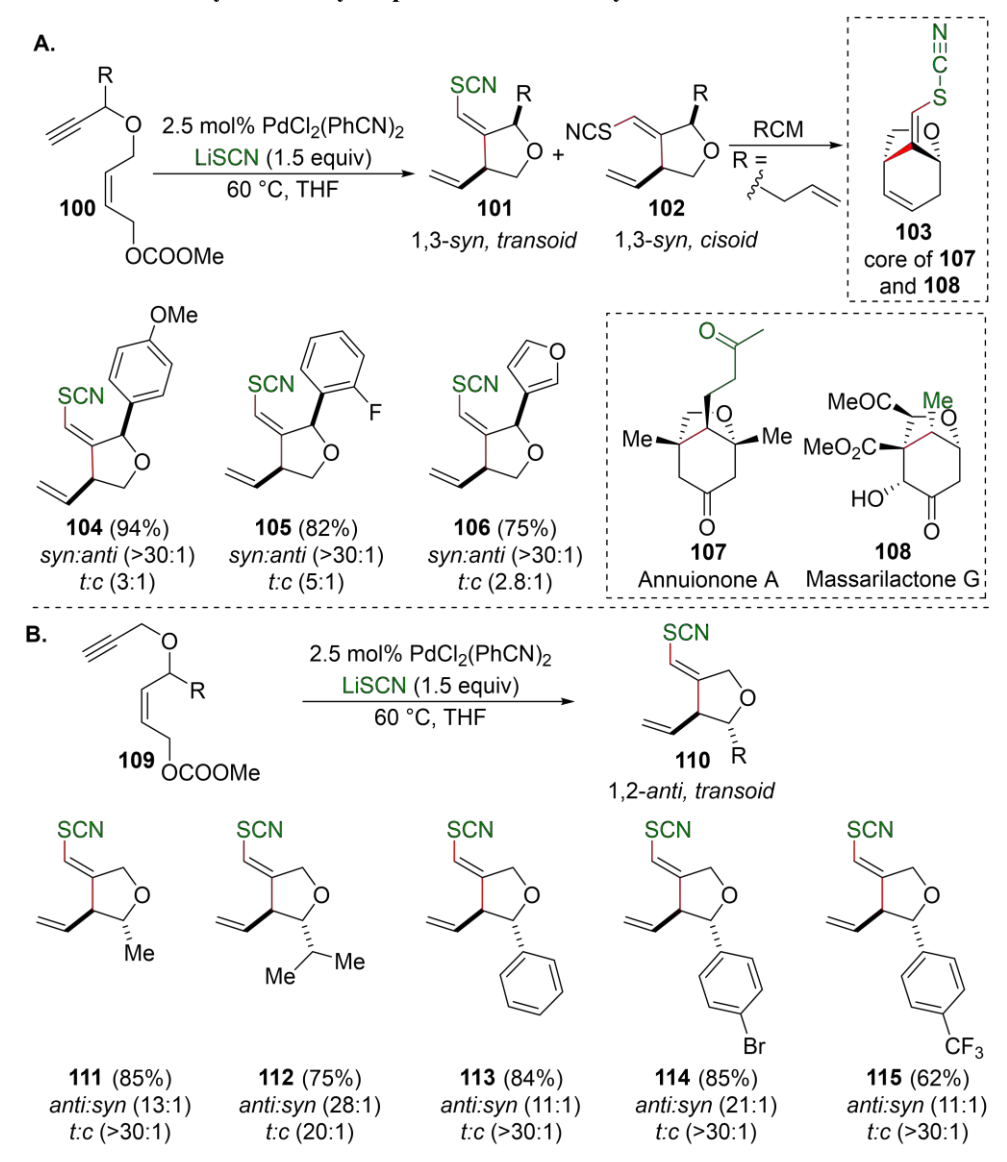
scope of this bromorhodiation/carbocyclization transformation to include 6-ring formation and combine with a new variant of the Jacobsen hydrolytic kinetic resolution to access the cores of the terpenoid natural products linearifolin, and zaluzanin (See section 2.2.1.2.2).²³⁰

(±) 99 (79%)

When one surveys the literature for related chemistries, one finds instances in which halogen²³¹⁻²³³ and acetate^{225,234,235} have been employed as nucleophiles, for alkyne additions, in which Pd²³³⁻²³⁵ or Rh^{232,236-238} catalysts activate the alkyne. For example, Zhang and co-workers reported the Rh(I)-catalyzed cycloisomerization of 1,6-enynes. In this reaction, Rh(I)-catalyzed C-C bond formation is followed by an intramolecular halogen shift to produce α -halomethylene- γ -butyrolactones (**Scheme 13**).²³² Mechanistic studies suggest that the intramolecular halogen shift proceeds through the intermediacy of a π -allyl rhodium complex.²³⁸ As alluded to in the introduction to this section, there is some direct precedent for the Pd- and Rh-mediated

nucleopalladation of alkynes particularly from the pioneering work of the Ma and Lu groups leading into γ -butyrolactone products. ^{226-228,233,239-246} (**Scheme 14A**). Lu and co-workers have provided a number of examples of the acetoxy-palladation/carbocyclization reaction (**Scheme 14B**) following on their earliest reports of this type of chemistry in the 1990s. ²³⁴ The reaction appears to proceed via acetoxypalladation of the alkyne, followed by 5-endo trig-cyclization to

Scheme 15. Pd-Catalyzed Thiocyanopalladation/Carbocyclization Reaction



Scheme 15 A. Pd-catalyzed thiocyanopalladation/carbocyclizations upon allyl propargyl ether substrates bearing a propargyl substituent (high 1,3-syn stereoinduction). **B.** Related Pd-catalyzed thiocyanopalladation/carbocyclizations with substrates bearing allylic substituents (high 1,2-anti relative stereochemistry).

give intermediate 95, which undergoes β -elimination to release product 96 (Scheme 14B).²³⁴ In 2007, Sanford and co-workers took this method one step further in which the acetoxypalladation

Scheme 16. Plausible Mechanism

A. Plausible mechanism for 1,3-syn stereoinduction "(propargylic substituent present)"

B. Plausible mechanism for 1,2-anti stereoinduction "(allylic substituent present)"

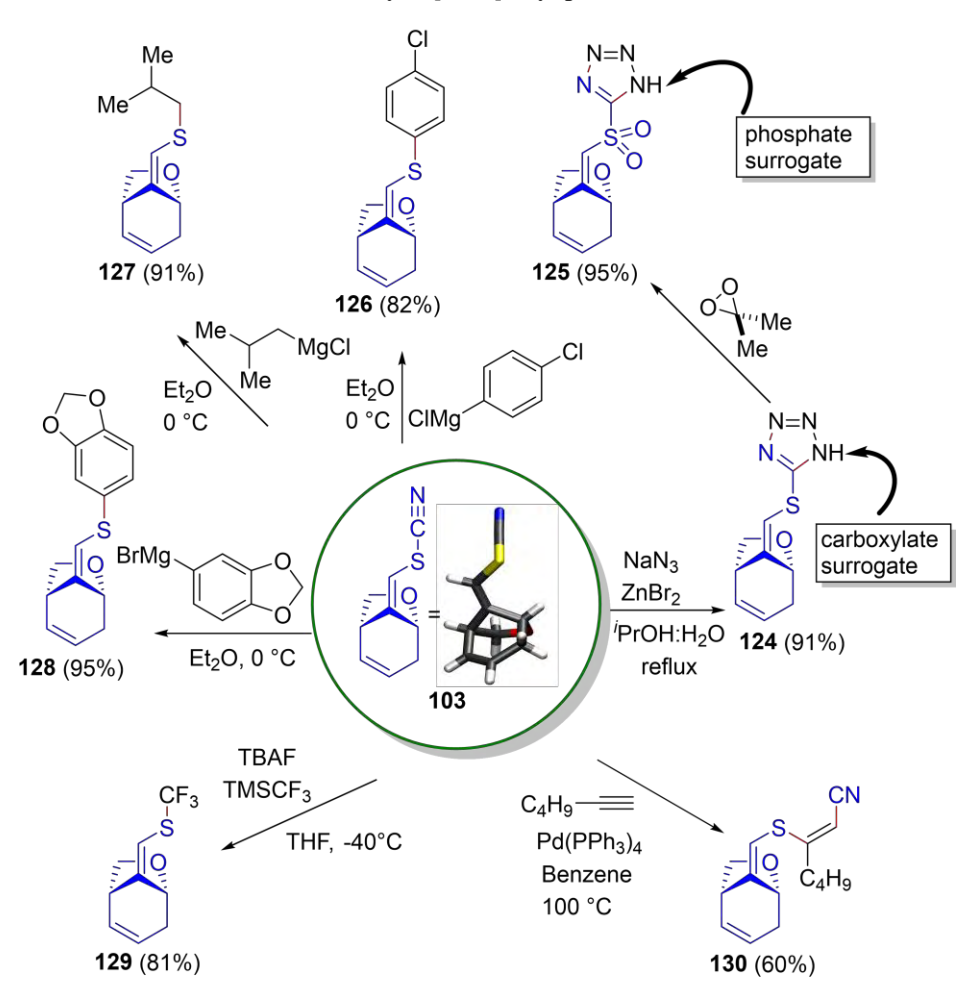
A. Plausible mechanism for 1,3-syn stereoinduction in the thiocyanopalladation/carbocyclization reaction with a propargylic substituent present. **B.** Plausible mechanism for 1,2-anti stereoinduction with an allylic substituent present.

followed on 97 bv cyclization gives intermediate 111 that can be intercepted with a strong oxidant such as bis(acetoxy)iodobenzene to generate a Pd(IV) complex. Interestingly, this Pd(IV) complex undergoes functionalization to give fused bicyclic product 99 (Scheme 14C). 235 Against the backdrop of these precedents, the inclusion of lithium thiocyanate as pseudohalide in the broad (pseudo)halometallation/ carbocyclization screen chosen for the original colorimetric ISES study in the Berkowitz group was truly fortuitous. In examining the hits gleaned from the 1152 catalyst/ nucleophile/ substrate envne combinations screened (Figure 3), the most exciting and novel discovery made was that the first ever observation of a TMmediated

thiocyanometalation/carbocyclization reaction.
This result is particularly noteworthy when one considers that anionic sulfur-containing functionalities, in general, and thiocyanate in particular, had been known as catalytic

poisons, for transition metal-mediated chemistry.²⁴⁷ Perhaps related to this, in the optimization process, it was found that lower concentrations of LiSCN (1.5 equiv.) are optimal, giving clean Pd-catalyzed C-SCN and C-C bond formation in a single transformation (**Scheme 15**). The transformation shows selectivity favoring a transoid alkene geometry, suggestive of external attack by thiocyanate anion upon a TM-coordinated alkyne. The Berkowitz group examined the reaction scope and stereoselectivity of this transformation, with substituents at the propargylic position

Scheme 17. Exploiting the New Thiocyanopalladation/Carbocyclization Transformation for DOS of Bicyclo[3.2.1]octyl product Core 103.



inducing 1,3-syn relative stereochemistry in the carbocyclization 101/102 (Scheme 15A) and with allylic substituents giving predominantly 1,2antistereochemistry in the cyclization products 110 15B).²³¹ (Scheme Both stereochemical outcomes are consistent with models for migratory insertion proceeding out of the least hindered rotational conformer, to minimize steric in strain this transition state, as discussed more detail below.

selectively

The new thiocyanopalladation/carbocyclization transformation has been applied in the synthesis of 103, the core of the natural products of annuionone A (107) and massarilactone G (108) (Scheme 15A). The transformation proceeds with both high geometric preference (transoid:cisoid = 7:1) and impressive diastereoselectivity (1,3-syn:anti >30:1). The high level of stereochemical control is consistent with the proposed mechanism. As illustrated in Scheme 16, initial Pd(II)-coordination to the 1,6-enyne is expected to be followed by anti-thiocyanopalladation of the alkyne give a (thiocyano)vinylpalladium intermediate 116/120 (Scheme 16). Subsequently, migratory insertion would close the 5-membered ring and β -elimination of the elements of Pd-OCO₂Me would give product 101 and regenerate the L₂PdX₂ catalyst. Where the cyclization substrate

possesses a propargylic substituent, 1,3-syn stereoinduction is expected based on a consideration of rotamers 117 and 118 at the migratory insertion step. The 118-rotamer possesses an unfavorable 1,3-diaxial-type interaction between the pendant alkene and the hydrogen (Scheme 16A). When this is rotated to relieve strain, and the vinyl group projects out in a pseudo-equatorial fashion with respect to the five-ring envelope formed in the migratory insertion step. This pathway predicts 1,3-syn product formation (Scheme 16A).²³¹

In the case of a substrate bearing an allylic substituent, similarly, two distinct rotamers 121/122 can be considered at the migratory insertion step whereby 1,2-syn rotamer 122 is expected to experience destabilizing allylic strain. The 1,2-anti rotamer 121, on the other hand, is expected to be relatively free from strain and lead to selective formation of the 1,2-anti diastereoisomer (Scheme 16B) upon migratory insertion.

The thiocyanate functional group has real significance in chemical biology as a bioorthogonal spectroscopic probe, with the potential to provide information on site-specific structure and dynamics. The SCN infrared chromophore is in an isolated spectroscopic window which allows it to be probed in complex environments, including in enzyme active sites, with high precision. Moreover, the vibrational absorption spectrum of the SCN functionality is exquisitely sensitive to the local environment, allowing one use the vibrational Stark effect (VSE) to estimate the active site dielectric with probe molecules bearing this group, or by installing the SCN itself. 248-256 functionality into the active site The beauty thiocyanopalladation/carbocyclization transformation is that it readily allows for the installation of this functionality onto natural product-like scaffolds, potentially enabling the construction of myriad VSE probe molecules.

In fact, the Berkowitz group has demonstrated the utility of the ISES-discovered thiocyanopalladation/carbocyclization for the construction of natural product cores and of diversity-oriented synthetic libraries. For example, they have utilized this new transformation to provide a stereocontrolled entry into the oxabicyclo[3.2.1]octyl core (103) of the natural products annuionone A and massarilactone G bearing a vinyl thiocyanate functionality (Scheme 17). The synthetic utility of vinylic thiocyanate moiety for diversity-oriented synthesis (DOS) was then exploited, creating a constellation of compounds with a functionally diverse, decorated oxabicyclo[3.2.1]octyl core as a natural product-inspired DOS library of value for screening

Scheme 18. Copper-Catalyzed Trifluoromethylthiocyanation of Olefins

TMSSCN, DMSO, rt

131

132

5 mol% Cu(CH₃CN)₄PF₆

TMSSCN, DMSO, rt

(±) 133

(±) 135 (70%)

30:1 dr

136 (76%)

30:1 dr

R SCN

CF₃

R SCN

CF₃

TMSSCN, DMSO, rt

(±) 137 (24%)

30:1 dr

against biological targets. 257-262

The versatility of the thiocyanate functional group for chemical diversification is highlighted in Scheme 17, whereby one can (i) 'split' the bond S-CN when utilizing Grignard reagents or a CF₃anion equivalent

(Ruppert reagent) to displace cyanide, (ii) perform a formal azide cycloaddition across the cyano moiety of the S-CN group, or (iii) add the elements of S-CN across an alkyne under Pd-mediated conditions.

To put this new ISES-discovered transformation in context, most of the reported protocols for constructing C-SCN bonds are either oxidative thiocyanation²⁶³⁻²⁶⁶ reactions or electrochemical^{267,268} oxidative thiocyanation reactions. The Liu group in 2015 reported a coppercatalyzed

Scheme 19. Copper-Catalyzed Aminothiocyanation Reaction

A. Stoichiometric use of copper acetate for aminothiocyanation. **B.** Catalytic variant with K₂S₂O₈ as terminal oxidant.

trifluoromethylthiocyanation of alkenes using TMS-SCN as the SCN equivalent and the Togni reagent as the CF₃ source (**Scheme 18**).²⁶⁹ In 2018, the Li group described the coppermediated aminohalogenation/ aminothiocyanation of vinylic hydrazones.²⁷⁰ In this report, the authors investigated a wide range of nucleophiles found to be compatible with the reactants including NaN3, NaI, NaBr, and NaSCN. Copper was utilized stoichiometric in amounts, but in the case of the KSCN nucleophile low reaction vields were seen, limiting the practicality of this transformation. Following on this result, in 2019, Zhu and coworkers developed the first

copper-catalyzed domino cyclization/thiocyanation of β , γ -vinylic hydrazones to afford the SCN-appended pryrazolenes in good yield (**Scheme 19**).²⁷¹

2.2. Enzymatic Methods for Determining Enantiomeric Excess

2.2.1. In Situ Enzymatic Screening (ISES)- Readout on Relative Rate and Enantioselectivity

With the desire to establish a more information-rich enzymatic screening assay, the Berkowitz group next worked to develop a system that provides both a relative rate and an enantioselectivity readout.²²¹ This new ISES iteration seeks to take advantage of enzyme chirality, utilizing the enzyme(s) to not only amplify a signal and translate it into a UV/visible signal, but also to report out on the enantiomeric composition of the product. In this case, reporting enzymes are used to report directly on the formation a chiral product rather than upon release of a leaving group. While the latter approach could be used to discern enantioselectivity of a catalyst being screened by running the reaction in an enantiomer competition mode, enzymatic interrogation of the chiral product itself would be more direct and would not require having access to both enantiomers of the product or educt to conduct the screen. For this to work optimally, it became apparent that utilizing two distinct reporting enzymes with different enantioselectivities for the chiral product would be ideal. This is because there are two unknowns in such a screen, total product being generated at time t and the R:S ratio of that product. To provide an estimate of both relative rate and enantioselectivity of a chiral catalyst being screened, having two reporting enzymes report with disparate enantioselectivities interrogating the same product stream, in parallel, would supply the two equations needed to solve for these two unknowns. As is shown below, one can then use

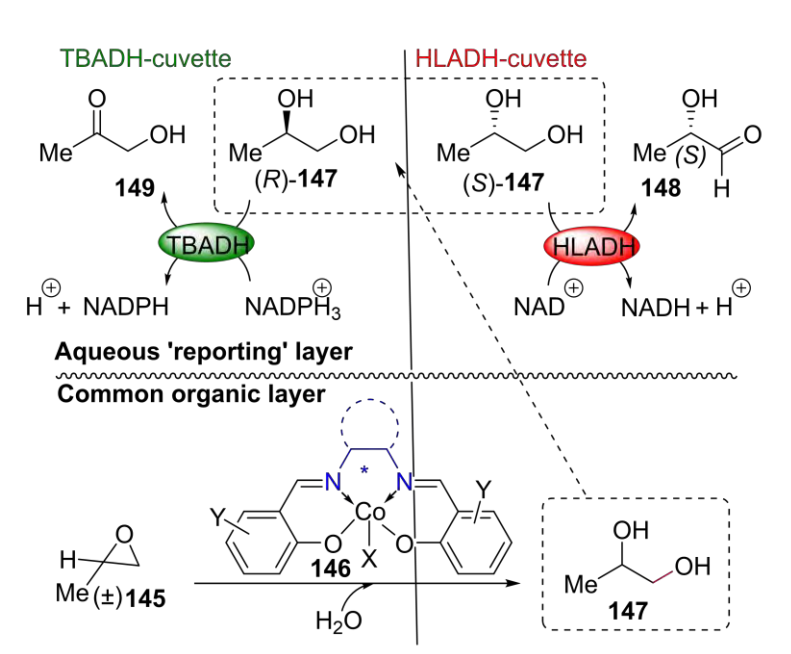
the two disparate outputs from the same product stream to mathematically solve for the estimated *R*:*S* selectivity of the chiral catalyst or ligand being screened.

The Berkowitz group chose to use the hydrolytic kinetic resolution (HKR) of terminal epoxides as a platform for proof of principle of this 'double-cuvette-ISES' (vide infra). The chiral

$$\frac{[R]}{[S]} = \frac{\left[\frac{Sel_{E_2}}{Sel_{E1}} (v_{E2} - v_{E1})\right]}{Sel_{E_2}(v_{E2} - v_{E1})}$$

Figure 5. Equation giving the enantiomeric ratio in the product as a function of the ISES reporting rates from the two disparate reporting enzymes.

Co(III)- or Cr(III)-salen-mediated HKR is one of the most important and practical enantioselective transformations available and was developed by Eric Jacobsen and coworkers. The so-called 'Jacobsen catalyst' utilizes the Co(III)-complex with the salen ligand derived from trans-1,2-cyclohexanediamine and a 3',5'-di-tert-butylsalicylaldehyde as the chiral catalyst for the kinetic resolution of a range of terminal epoxides. As will be described in more detail below, while the screening goal here was to demonstrate the ability of this dual reporting enzyme approach to provide an information-rich (relative rate and ee) screen, the synthetic goal was to utilize this platform to identify new chiral salen frameworks with potential for use in asymmetric catalysis.



Scheme 20. Double Cuvette-ISES. General layout for the screen of the HKR of (\pm) -propylene oxide with chiral Co(III)-salen catalyst candidates. Each of the paired reporting cuvettes contains a common lower organic layer but contains a different reporting enzyme in the upper layer, either *Thermoanaerobium brockii* dehydrogenase (TBADH) or horse liver dehydrogenase (HLADH), with preferences for R- and S-1,2-propanediol, respectively.

The idea behind the HKR is that a racemic terminal epoxide substrate can, in principle, be kinetically resolved by a catalyst through the selective hydrolysis of one enantiomer over the other. In a hypothetically 'perfect' kinetic resolution 50% of the epoxide would be retained as a single enantiomer while the remaining 50% of the epoxide would be converted to the diol with opposite stereochemistry. For such a kinetic resolution, in general, catalyst or ligand enantioselectivity is most often delineated by the S-value or E value which is defined as the ratio of rate constant for the R-selective reaction divided by the rate for the S-selective constant reaction. A synthetically useful HKR catalyst would

conversions that approach 50% and above 90% *ee* for both the product 1,2-diol and the remaining epoxide. This result would coincide with an E value of approximately 50.

The readout of the ISES-assay developed to this HKR screen involves the use of dehydrogenase reporting enzymes, exploiting the UV chromophore in their nicotinamide-based redox cofactors.

Reporting rates are measured by observing the formation of NAD(P)H in real time at 340 nm (ϵ_{340} = 6.22 mM⁻¹ cm⁻¹) with enzymes that show significantly different enantio-preferences for the reaction product. The selectivity can be predicted according to the equation shown in **Figure 5** ²²¹ The *R* to *S*-selectivity ratio is determined as a function of both the observed rates (ν_{E1} and ν_{E2}) from each of the reporting enzymes (*E*1 and *E*2) as a function of the inherent enantioselectivities for these reporting enzymes for the *R*-diol over the *S*-diol (Sel_{E1} and Sel_{E2}). As will be explained in greater detail in the following sections, based upon this concept, the Berkowitz group developed several iterations of this dual-reporting enzyme variant of the ISES method, being labeled sequentially as 'double cuvette-,'²²¹ 'cassette-,'²²³ and 'mini'- ISES.²²²

2.2.1.1 Double Cuvette Screening

Table 2.

	CHO Bu—OH Bu	сно он _{tBu}	СНО	СНО	СНО Н ОН е	BnO CHO OH	Me CHO
Me NH ₂ 150	+56 +72 6.9	+68 +75 10	8	+75 +81 12	+47 [†] +28 2.1	\$	§
NH ₂ 151	-97 -93 -37	-73 -75 -9.4	ş	-15 -54 -3.7	+4 -41 -2.6	\$	-41 [#] -71 -5.9
NH ₂ 152	+48 +55 4.8	+70 +57 4.1	§	-54 -30 1.9	§	§	1
NH ₂ 153 NH ₂	+77 +76 9.5	+91 +59 5.1	§	1	+43 [#] +14 1.3	+57 +51 3.6	ş
154 NH ₂ NH ₂	+87 +66 6.4	+65 +68 7.6	§	+9 +11 1.3	+35 -5 -1.1	§	§
Me 155 NH ₂ Me Me	177	+70 [*] +42 [*] 2.6	§	1	1	1	1
Me 156 NH ₂ NH ₂ NH ₂	-33 [*] -64 [*] -4.7	-28 [*] -40 [*] -2.5	§	§	+87 (+85)* +81 (+83)* 11 13	§	1

Double Cuvette-ISES (as depicted in **Scheme 20**. Each box provides HKR data for the Co(III)-salen acetate derived from the indicated salen. Presented are the % ee of the 1,2-propanediol product ["+" for (S) and "-" for (R)] as estimated by double cuvette-ISES (indigo) and as observed by chiral HPLC (black). Where available, observed catalyst E values are also provided (enclosed boxes). The cuvette experiments are run in a bilayer of pH 8.6 buffer over 7.2 M epoxide in CHCl₃, containing 0.25 mol % catalyst, for 15-35 min. "Inherent" catalyst ee values are judged by running the HKR in neat propylene oxide, containing 0.55 equiv of H₂O, also at 0.25 mol% catalyst. § These catalysts gave ISES signals < 20 mAbs min⁻¹ over 35 min. † This catalyst was tested at 0.05 mol%, as it was especially fast. #The catalysts derived from **151g** and **153e** displayed ISES rates of 14.9 and 18.1 mAbs min⁻¹, respectively, in the HLADH cuvette, over 35 min. Difficulty was encountered in synthesizing appreciable quantities of these salens. *The 3,5-dinitrobenzoate counterion was employed for these Co(III) catalysts.

In the initial roll-out of double cuvette-ISES, the Berkowitz group screened a library of new Co(III)-salen catalyst candidates for their efficacy in mediating the HKR of propylene oxide (**Scheme 20**). The HKR of (\pm)-propylene oxide would preferentially yield one enantiomer of the product, either R- or S-1,2 propanediol 147. These two antipodal products are recognized by two enzymes with different enantioselectivities. The assay set-up involves a biphasic system with a lower organic reaction layer and an upper aqueous reporting layer. Note that it has been found useful to include chlorinated co-solvents to ensure that the organic layer is the more dense and therefore constitutes the lower layer. This, in turn, has the advantage of preventing any particulate matter (could give false positive reading via light scattering) that might form at the aqueous-organic interface from crossing the light path of the spectrophotometer beam which passes directly through the upper aqueous layer here. The diols produced from the HKR reaction partition into the aqueous, enzymatic sensing layer where they can be oxidized. This use of two enzymes with complementary enantioselectivities in parallel cuvettes allows for the efficient monitoring of the R-(147) and S-1,2-propanediol (147) HKR products.

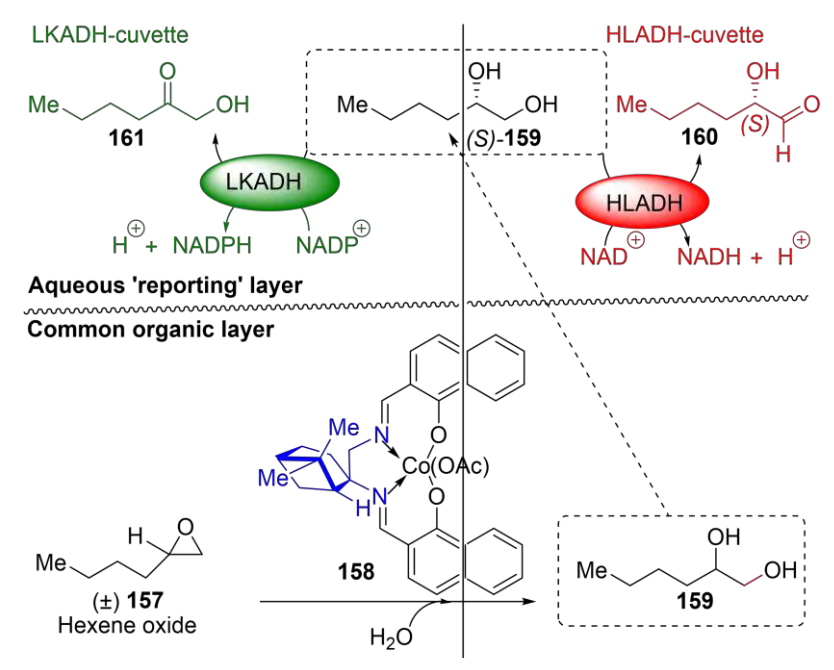
As illustrated in **Scheme 20**, for the HKR of (\pm)-propylene oxide, the Berkowitz group found that *Thermoanaerobium brockii* alcohol dehydrogenase (TBADH) and horse liver alcohol dehydrogenase (HLADH) provide complementary selectivity for the 1,2-propanediol HKR product. Under standard conditions, the TBADH enzyme oxidizes the *R*-1,2-propanediol eight times faster than the *S*-propanediol, and HLADH exhibits a three-fold preference for the *S*-propanediol. Therefore, if the same catalyst is run in two ISES cuvettes, one with the TBADH reporting enzyme and the other with the HLADH reporting enzyme, a comparison of the UV rates at 340 nm from the NADPH and NADH formed, respectively, allows the experimentalist to estimate the enantioselectivity of the catalyst being screened.

This method is substantially faster than derivatizing the products with a chromophore and subjecting these to chiral HPLC analysis for examination of enantiomeric purity. The Berkowitz group found that double cuvette-ISES provides a quite useful screen for catalyst success across a range of non-C₂-symmetric salen ligands being evaluated for their potential utility in asymmetric synthesis (Table 2). Among the most promising hits from the screen is the salen derived from the condensation of two equivalents 1-hydroxy-2-napthtaldehyde with the β-pinene-derived diamine (150d). Another highlight of the screen is the notable stereoselectivity observed with the salen formed from the β-D-fructopyranose-derived diamine 156 and 3',5'-diiodo- salicylaldehyde (156e). Particularly interesting here is that this catalyst is considerably more selective than the analogous catalyst constructed from the same diamine (156) and the canonical 3',5'-di-tert-butylsalicylaldehyde (156a). Moreover, 156e and 156a exhibit opposite enantioselectivities (Table 2). This constitutes a non-intuitive 'enantioswitch' whereby changing the sterics in the achiral salicylaldehyde sector of the catalyst leads to inverted catalyst enantioselectivity, even while holding the chiral diamine sector fixed.²²¹ This observation warrants further examination across a broader range of substrates and transformations for this new salen family. In thinking about this result, it must also be remembered that the projection of chiral space into the Co(III)-salenmediated HKR transition state is complex as the reaction is known to involve two molecules of Co(III)-salen-catalyst, one presumably electrophilically activating the epoxide by coordination and the other delivering the hydroxide nucleophile to the terminal carbon of the epoxide²⁷³.

2.2.1.2 Cassette Format

The Berkowitz group next developed a new iteration of ISES that would increase information content of the screen by allowing the investigator to screen chiral catalyst candidates for both enantioselectivity and relative rate across two different substrates, in parallel. This variant of ISES

Scheme 21. Cassette-ISES



For each Co(III)-salen catalyst candidate, in addition to screening for the HKR of (\pm) -propylene oxide, two new cuvettes were added to screen for a second substrate, (\pm) -hexene oxide. Each new cuvette contains a specific reporting enzyme, with HLADH again showing modest S-selectivity and Lactobacillus kefir alcohol dehydrogenase (LKADH) showing high S selectivity These enzymes lead to the formation of NADH and NADPH respectively.

is termed 'cassette-ISES' and once again utilized the

Co(III)-salen-mediated HKR as a platform to develop proof of principle for the highly informationrich screen.²²³ To actualize this new cassette-ISES platform a second HKR substrate, (±)-hexene oxide (157), was added alongside the original (±)-propylene oxide substrate. The two substrates would each require two cuvettes charged with two distinct reporting enzymes exhibiting significantly different

enantioselectivities for the product. To actualize this cassette-ISES, the authors needed to find two reporting enzymes for the 1,2 hexanediol (159) product (HKR of hexene

oxide) to use in tandem with the TBADH (R-selective) and HLADH (S-selective) enzymes employed for the 1,2 propanediol product as described above ((HKR of propylene oxide). In this case, the authors demonstrated that they could use two different S-selective reporting enzymes, but with significantly distinct levels of enantioselectivity illustrating the point that the paired ISES reporting enzymes need not have opposite enantiomeric preferences. In fact, for 1,2-hexanediol, the chosen reporting enzymes were horse liver alcohol dehydrogenase (HLADH) with modest S-selectivity ($k_S/k_R \sim 2.2$) and $Lactobacillus\ kefir$ alcohol dehydrogenase (LKADH) with remarkably high S-selectivity ($k_S/k_R \sim 20$). As is illustrated in **Scheme 21**, the enzymatic chemistry and spectroscopic readout for this assay is similar to the previous screen; with LKADH generating an NADPH signal and HLADH leading to an NADH signal.

The proof of principle of this cassette-ISES was demonstrated with Co(III)-salen catalysts derived from an array of salens generated by pairing substituted salicylaldehydes with chiral 1,2-diamines derived from amino acids and terpenes, to probe new chiral space (**Table 3**). The highlight of the screen was the result with catalyst **158**, bearing the β -pinene-derived salen ligand (**158**) with this catalyst displaying the highest (*S*) selectivity.²²³ of note, the β -pinene-derived chiral diamine needed to construct this promising salen ligand is available in a mere two steps from β -pinene itself with the key step being the Mn^{III}-mediated alkene diazidation from the pioneering work Snider and coworkers.²⁷⁴

Table 3.

	CHO TBu OH TBu	СНО	сно Сно	он сно	e O O
Me NH ₂ NH ₂ 150	56(S) 93(S) 72(S) 80(S) 6.9(S) 12(S)	47(S) 36(S) 28(S) 53(S) 2.1(S) 4.6(S)	** 56(S) 71(S) 6.8(S)	75(S) 94(S) 81(S) 76(S) 12(S) 13(S)	** §
NH ₂	87(S) 64(S) 66(S) 67(S) 6.4(S) 5.8(S)	35(S) § 5(R) 1.1(R)	** §	9(S) 17(S) 11(S) 0 1.3(S) 1(S)	** §
NH ₂ NH ₂ 162	81(R) 96(R) 74(R) 72(R) 9.2(R) 7.0(R)	8(R) 29(R) 12(R) 5(R) 1.3(R) 1.1(R)	** §	8(R) 27(R) 20(R) 21(R) 1.5(R) 1.7(R)	** §
NH ₂ NH ₂ (R)-153	77(R) 84(R) 82(R) 86(R) 15(R) 15(R)	22(R) § 5(R) 1.4(R)	** §	31(R) 18(R) 14(R) 22(R) 1.3(R) 1.6(R)	** §

Cassette-ISES results for the HKR with Co(III)-salen acetate catalysts derived from this 5x4 salen/baen ligand library. Within a box, the entries (top to bottom) represent the ISES-estimated ee values, the observed ee values (flask conditions: neat, RT), and the calculated E value. Black (left) and blue (right) columns designate results with propylene oxide and hexene oxide, respectively. ** and & denote slow catalysts showing enzymatic reporting rates of <15 mAbs min⁻¹ for propylene oxide and hexene oxide, respectively.

2.2.1.2.1. Initial Screening Hit: β-Pinene-Derived Chiral Salen Ligand with Potential for Asymmetric Catalysis

As described above, the dual cuvette- and cassette-ISES approaches developed by the Berkowitz group were utilized to probe chiral ligand space with a focus on the important salen ligand class. New combinations of substituted salicylaldehydes and non-C₂-symmetric chiral 1,2-diamines were probed in search of promising chiral scaffolds, with the ultimate goal of identifying new 'privileged' chiral elements. The notion of 'privileged' scaffolds is not without controversy but has been used in medicinal chemistry where certain heterocycles, for example, appear to be particularly well suited for protein binding, while also retaining the ability to be transported effectively, presumably relating to binding to serum albumin, say. In an entirely different sector of the chemical enterprise the notion of 'privileged chiral ligands' has been discussed, whereby one observes that certain chiral elements have been demonstrated to impart a useful chiral bias to a catalytic center, across more than one reaction type, usually upon coordination to a metal.^{275,276} It has been argued that for catalysis, privileged scaffolds with C₂-symmetry, are particularly useful as these systems limit number of chiral approaches to the catalytic center. A notable example would be the axially chiral BINAP system developed by Noyori, a vital component of the 2001

Nobel prize in chemistry. Building on examples such as this, many others have developed chiral ligands with C₂-symmetry. A₁2,277-311 This, of course, includes the parent Jacobsen-salen ligand arising from the *trans*-1,2-diaminocyclohexane and 3',5'-di-*tert*-butylsalicylaldehyde relevant to the HKR chemistry discussed here but useful for many other asymmetric transformations as well. However, this same chiral element has been used in non-C₂-symmetric applications as well. For example, in the process of building an asymmetric Strecker catalyst to generate a more enzymelike system, Jacobsen and Sigman very effectively incorporated this *trans*-1,2-diaminocyclohexane motif into a chiral thiourea. This work, along with the impressive performance of non-C₂-symmetric chiral elements such as the cinchona alkaloids, inspired the Berkowitz group to explore non C₂-symmetric salens for the HKR reaction, as has been described. In what follows, we describe one such catalyst that has proven particularly versatile for target-directed synthesis.

2.2.1.2.2 Hit Elaboration: Application to the Enantioselective Synthesis of the Linearifolin Zaluzanin A Cores

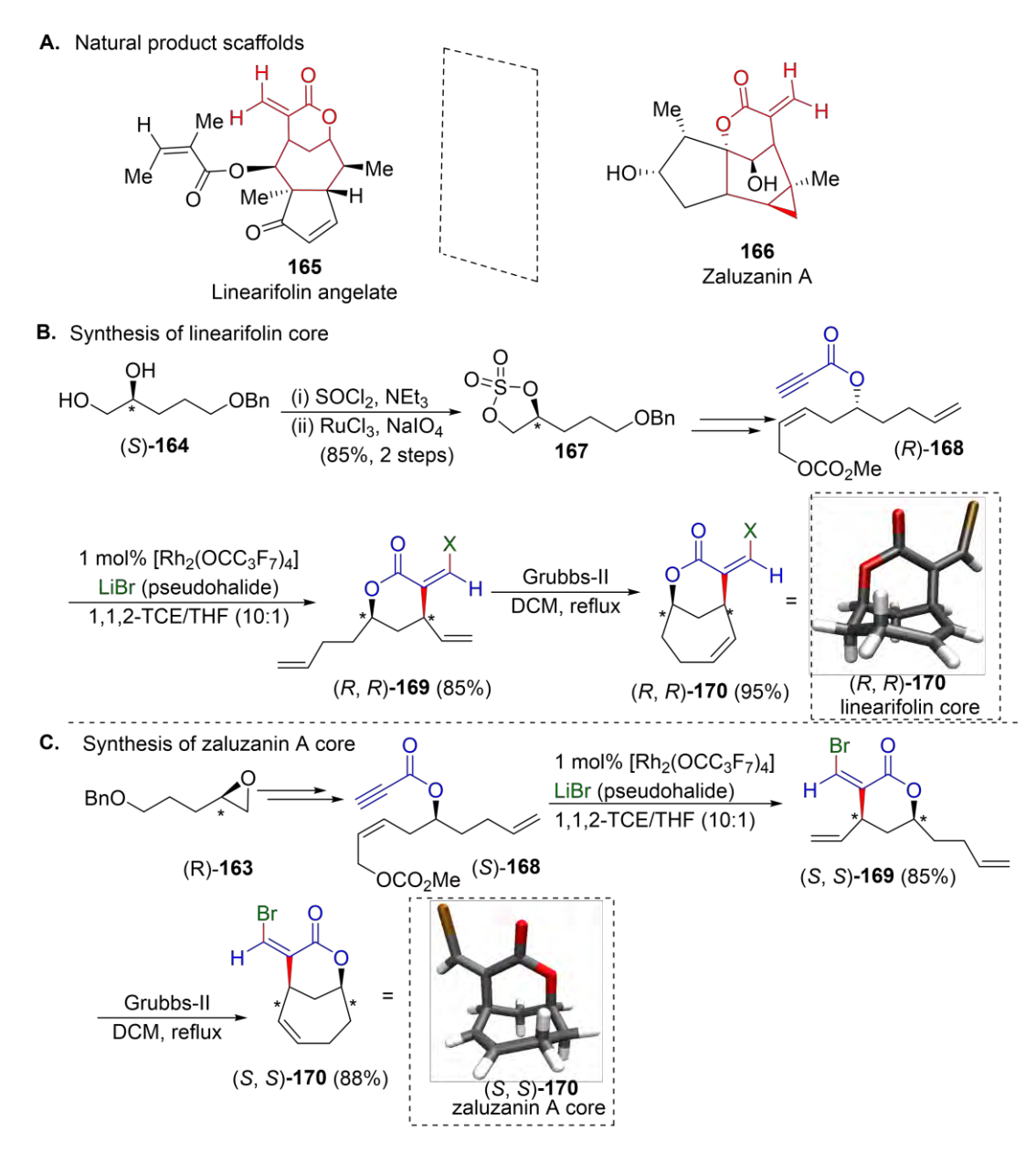
The chiral 1,2-diamines selected for the construction of non-C₂-symmetric salens for these dual enzyme ISES-variants are derived from the chiral pool and are based on amino acids, terpenes, and carbohydrates. The new salen derived from the β -pinene-based diamine²⁷⁴ and 1-hydroxy-2-naphthaldehyde (**150d**, **Table 3**) proved to be 'matched' to the 5-benzyloxy-1,2-pentene oxide HKR substrate. As is illustrated in **Scheme 22**, the kinetic resolution of this terminal epoxide with the Co(III)-salen catalyst (**158**), derived from salen **150d** produced a 47% yield of each component with the *R*-epoxide obtained in 92% *ee* and the *S*-1,2-diol (**164**) produced in 97% *ee*.^{221,223} In this case, each antipode could be used as a key building block for the construction of a natural product core. Namely, the Berkowitz group was able to exploit this effective HKR to take the essentially enantiomeric products forward for the syntheses of the pseudo-enantiomeric cores of sesquiterpenoid natural products linearifolin and zaluzanin A.²³⁰

Scheme 22. HKR Entry into Pseudo-Enantiomeric Building Blocks for Natural Product Core Synthesis.

This synthetic foray into this natural product class proved to be an ideal showcase for both this new salen ligand that arose out of cassette-ISES screening, but also for the novel bromorhodiation/carbocyclization transformation uncovered by colorimetric-ISES (*vide supra*, **Figure 3** and **Scheme 12**).²²⁴ The synthetic approach into these two sesquiterpene lactone cores, for linearifolin and zaluzanin A is illustrated in **Scheme 23A**.²³⁰ The exocyclic bromomethylene functionality that is appended to these cores as a result of the bromorhodiation/carbocyclization chemistry may have real advantages for chemical biology. Namely, there has been considerable previous work directed at the synthesis of this class of sesquiterpene lactones³²⁴⁻³²⁸ as the external exocyclic olefin may be a key determinant in observed NFKB-inhibition in the family. NFKB (nuclear factor kappa-light-chain-enhancer of activated B cells), an important transcription factor

associated with the immune response and NFKB signaling, has been associated with cancer and autoimmune disease. Thus, there is great interest in small molecules that inhibit NFKB-signaling in chemical biology and medicinal chemistry circles. This inhibition is believed to occur via an active-site cysteine capture where Merfort developed a QSAR (Quantitative Structure-Activity Relationship) model for the inhibition/anticancer activity in these systems. 329,330

Scheme 23 Application of Bromorhodiation/Carbocyclization for the Synthesis of Natural Product Core



A. Natural product scaffolds for linearifolin and zaluzanin A. **B.** Convergent assembly from the HKR-derived cyclic sulfate using the bromorhodiation/carbocyclization and RCM as key steps into the linearifolin core. **C.** Convergent assembly of the enantiomeric zaluzanin A core by a similar route from the corresponding HKR-derived epoxide.

As is shown in **Schemes 22 and 23**, the nearly perfect kinetic resolution of 5-benzyloxy-1,2-pentene oxide (E value \sim 180!) provides direct access to the *R*-epoxide building block **163** for the zaluzanin A core and the *S*-1,2-diol building block **164** for the linearifolin core. The latter is

converted to the cyclic sulfate engendering this antipodal building block with 'epoxide-like' reactivity. The antipodal cyclic sulfate and epoxide so generated are then progressed through parallel synthetic pathways to produce the mirror image natural product cores (**Scheme 23B & C**). First, the 1,2 electrophile is opened and the resultant hydroxyl is silylated and the alkyne is subsequently converted to the *cis*-alkene via a Lindlar-type hydrogenation. The distal benzyl ether is then reductively deprotected, oxidized to the corresponding aldehyde under Swern conditions, and subsequently converted to a terminal methylene via Wittig chemistry. Functional group interchange to install the carbonate ester, followed by Mitsunobu-based installation of the propiolate ester substrate then gives the substrates *R*-168/S-168 (**Scheme 23B & C**), setting the stage for the key bromorhodiation/carbocyclization. Treatment of these substrates with the Rh(II)-perfluorocarboxylate/LiBr combination described in the original colorimentric-ISES report yields the desired lactone *R*, *R*-169/S, *S*-169. The pendant vinyl group on this compound is set up for a Grubbs-type ring-closing metathesis reaction to form the natural product core in each enantiomeric series *R*, *R*-170/S, *S*-170.

2.2.1.3 Mini-ISES Configuration

Another iteration of ISES was developed by the Berkowitz group, with the dual goals of reducing the amount of catalyst/ligand needed and increasing throughput in the UV/vis assay. The approach was inspired by the move to high throughput experimentation (HTE), in general, in process chemistry, and particularly motivated by an excellent report from the Merck process group highlighting the utility of microscale screening. Reprevious ISES screens were completed with a biphasic system in a 1 mL quartz cuvette, while this new iteration designated 'mini-ISES' takes advantage of the quartz multimicrocell developed by Shimadzu (*vide infra*) and requires only a 110 μ L total volume. In fact, the organic reaction layer comprises only 20 μ L, which dramatically reduces the amount of catalyst needed to effectively screen new combinations as the previous iteration of ISES utilized a 300 μ L organic reaction layer.

In this study, the team expanded the suite of reporting enzymes for both propylene oxide and hexene oxide to include several ketoreductase (KRED) enzymes--many of these said to be recombinant--from Codexis. As is illustrated in **Figure 6**, this mini-ISES version of the cassette-ISEE format described above retains the *R*-selective *Thermoanaerobium brockii* alcohol dehydrogenase (TBADH) and utilizes the complementary *S*-selective KRED 23 for the 1,2-propanediol product.²²² The assay uses the *S*-selective KRED 107 and the complementary *R*-selective KRED 119 for the 1,2-hexanediol product.²²² The screen is performed with a quartz micromulticell, a single quartz cell containing 16 parallel wells, with just over 100 uL per well and a 1 cm path length (see **Figure 6C**). This allows for an information-rich screen with four catalyst candidates to be screened concurrently, each across two different substrates. Thus, one obtains information on relative rate, enantioselectivity and substrate scope, in parallel.

Proof of principle was demonstrated by screening a library of salen candidates focused upon carbohydrate-derived chirality. Specifically, the Berkowitz group set out to further study the promising D-fructopyranose-derived 1,2-diamine-based salen ligands uncovered in the original double-cuvette ISES study (**Section 2.2.1.1**). There is an apparent 'enantioswitch' seen when pairing the β-D-fructopyranose-derived diamine with the 3',5'-di-tert-butylsalicylaldehyde (modestly *R*-selective) versus with the 3',5'-di-iodo-salicylaldehyde (significantly *S*-selective). To rule out that this might be due to anomerization of the 1,2-diamine, the Berkowitz group constructed the carbocylic analogue of D-fructopyranosyl-1,2-diamine in both pseudo-anomeric forms. ^{221,222} When crossed with four salicylaldehydes, this resulted in the targeted 4x4 array of novel salen ligands delineated in **Table 4**. The 16 unique salen scaffolds were converted to the

corresponding Co(III) catalyst and examined for the HKR of both propylene oxide and hexene oxide, under the new 'mini-ISES' screening conditions. For comparison, the results were examined in parallel to traditional flask conditions. The ISES readout for this assay, similar to the previous screen, is based on the formation of the reduced nicotinamide cofactor (NADPH/NADH) in the reporting layer and the corresponding increase in absorbance at 340 nm monitored by UV/vis spectroscopy (Scheme 20). As can be seen in Figure 6B, even though the volumes have been dramatically decreased for this variant of ISES, the micromulticell preserves the full 1 cm pathlength. The UV/vis traces obtained are well-behaved and the corresponding *ee* estimates

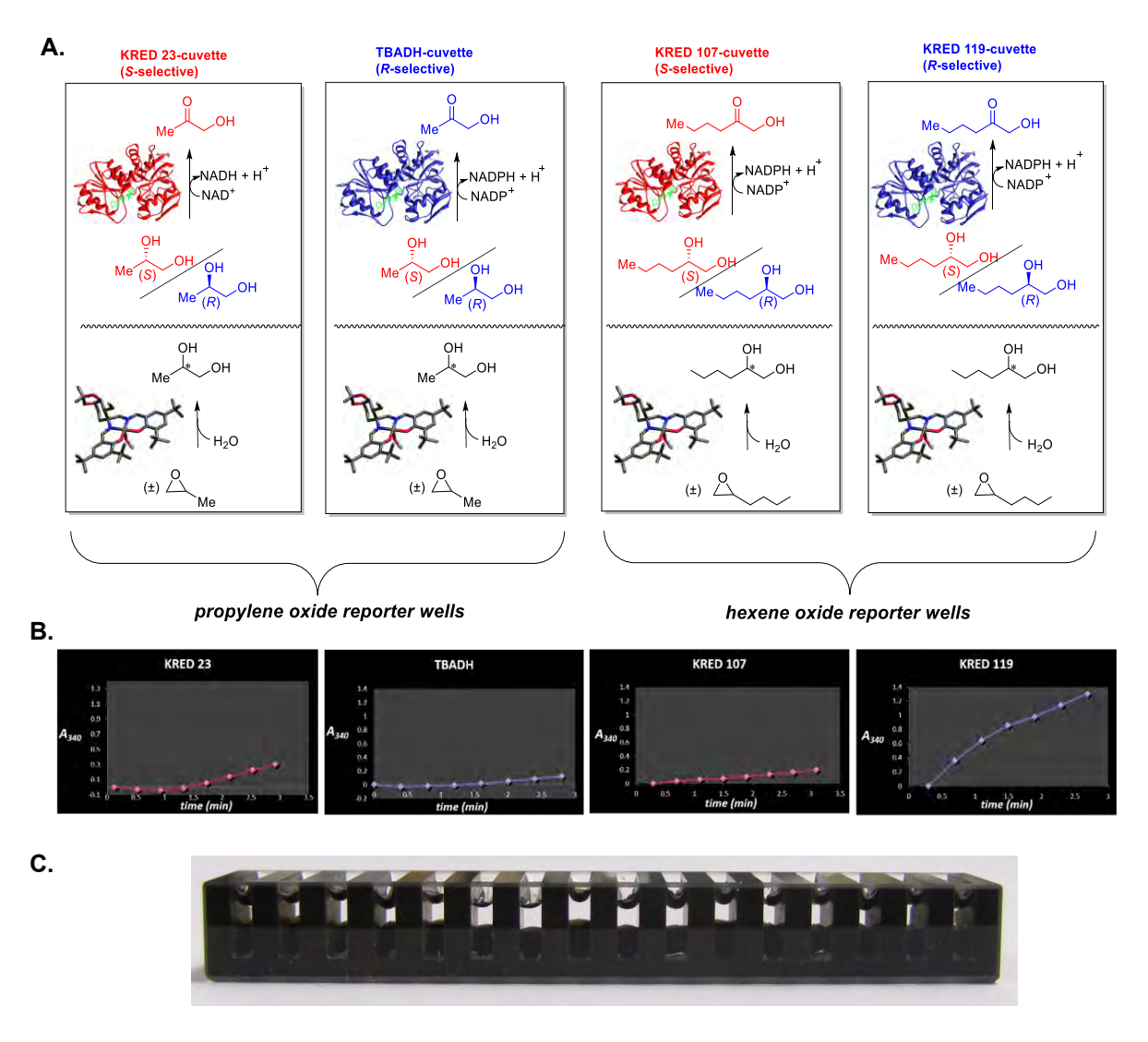


Figure 6. Mini-ISES = Miniaturized Cassette-ISES. A. General layout for an HKR screen of the (±)-propylene oxide and (±)-hexene oxide substrates, respectively with chiral Co(III)-salen catalyst candidates. Each substrate is screened with two distinct reporting enzymes with complementary stereoselectivities; KRED 23 and KRED 107 have S-selectivity for 1,2-propanediol and 1,2-hexanediol oxidation, respectively. In contrast, Thermoanaerobium brockii alcohol dehydrogenase (TBADH) and KRED 119 display R-selectivity toward 1,2-propanediol and 1,2-hexanediol oxidation, respectively. Panel A adopted with permission from ref 222. Copyright © 2015 The Authors under CC-BY-NC 4.0 (https://creativecommons.org/licenses/by-nc/4.0/). B. Output of the assay showing increasing absorbance at 340 nm associated with the formation of NADH/NADPH C. 16-well micromulticell used for ISES. Panel B and C republished with permission from ref 222. Copyright © 2015 The Authors under CC-BY-NC 4.0 (https://creativecommons.org/licenses/by-nc/4.0/).

derived from these ISES-rates prove to be quite accurate predictors of both sense and magnitude

Table 4. Targeted (Carba)Fructopyranose Salen

	CHO tBu tBu a		CHO OH tBu b		СНО		СНО	
Me NH ₂ NH ₂ Me Me NH ₂ 156	[77(+)] 69(+) 6.2(+)	[64(+)] 45(+) 4.0(+)	[70(+)] 42(+) 2.6(+)	[67(+)] 40(+) 2.4(+)	1		§ # 25(+) 1.7(+)	
	[33(-)] 64(-) 4.7(-)	# 52(-) 4.2(-)	[28(-)] 40(-) 2.5(-)	[31(-)] 36(-) 2.4(-)	[85(+)] 83(+) 13(+)	[77(+)] 85(+) 28(+)	§	§
Me O NH ₂ NH ₂ Me 171	[53(-)] 37(-) 2.3(-)	[23(-)] 29(-) 2.0(-)	[76(-)] 75(-) 8.2(-)	[40(-)] 45(-) 3.5(-)	[91(-)] 85(-) 17(-)	[42(-)] 63(-) 5.0(-)	[78(-)] 61(-) 4.3(-)	[59(-)] 55(-) 3.8(-)
Me O NH ₂ NH ₂ 172	[39(-)] 28(-) 1.9(-)	# 30(-) 2.1(-)	[67(-)] 48(-) 3.4(-)	[50(-)] 53(-) 3.4(-)	[94(+)] 93(+) 44(+)	[77(+)] 92(+) 104(+)	§	[13(-)] 34(-) 2.2(-)

Overview of ISES results across 4 (pseudo)carbohydrate-derived-1,2-diamines and 4 salicylaldehydes. The results presented in blue are for data obtained with hexene oxide while result in black were obtained with propylene oxide as substrate. Entries shown from top to bottom are respectively: ISES-estimated ee, observed ee under flask conditions, and the calculated E value [S(+)] and [S(+)] and [S(+)] are catalysts gave negilible ISES rates; § Thsee catalysts gave a <2% conversion after 72 h.

of enantioselectivity (see **Table 4** and the comparison with *ee* values observed under flask conditions).

To establish proof of principle of the mini-ISES method, the Berkowitz group screened the catalyst candidates for their performance in the HKR of propylene oxide and hexene oxide, in parallel, with the chiral 1,2-diol products being monitored by KRED reporting enzymes as shown in **Figure 6**. The research team validated the accuracy and efficiency of the ISES screening method by comparing the sense and magnitude of Co(III)-salen enantioselectivity to those measured by

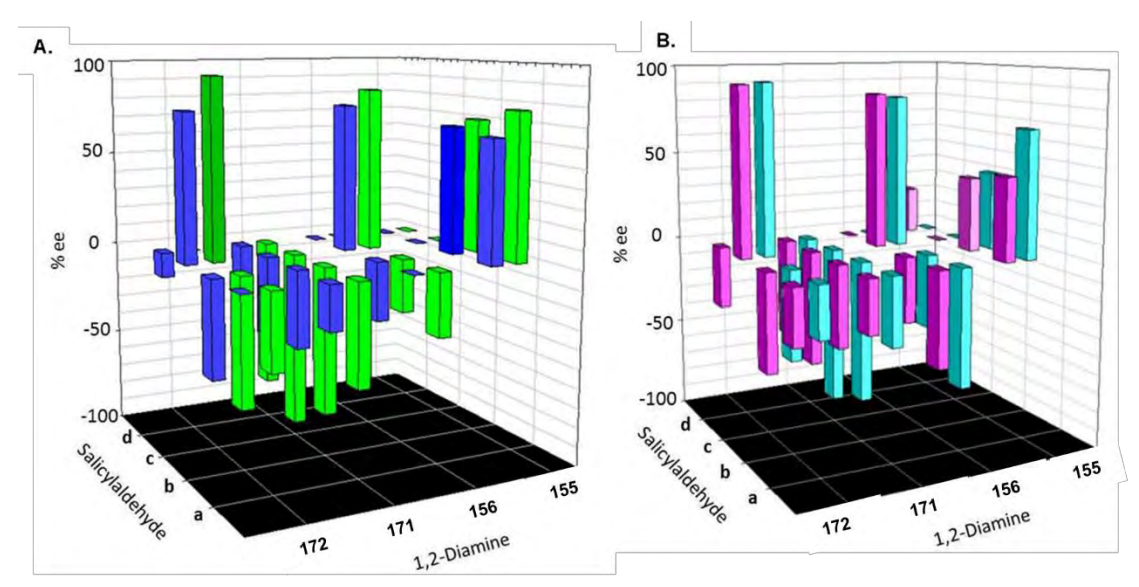


Figure 7. Three-dimensional bar graph of ISES screening of enantioselectivity of the Co-salen HKR catalysts, **A.** 3D graph presenting the ee outcome from the ISES screen **B.** For comparison, ee outcome of the same reactions under typical 'RB flask reaction conditions' as determined by chiral HPLC. Note: positive deflection = *S*-selective; negative deflection = *R*-selective; blue, pink = HKR of hexene oxide; green, aqua = HKR of propylene oxide. **Figure adopted with permission from ref 222.** Copyright © 2015 The Authors under CC-BY-NC 4.0 (https://creativecommons.org/licenses/by-nc/4.0/).

chiral HPLC under typical 'RB flask conditions.' A three-dimensional (3D) bar graph of this comparison is shown in **Figure 7**, in which each salen ligand is represented by the combination of

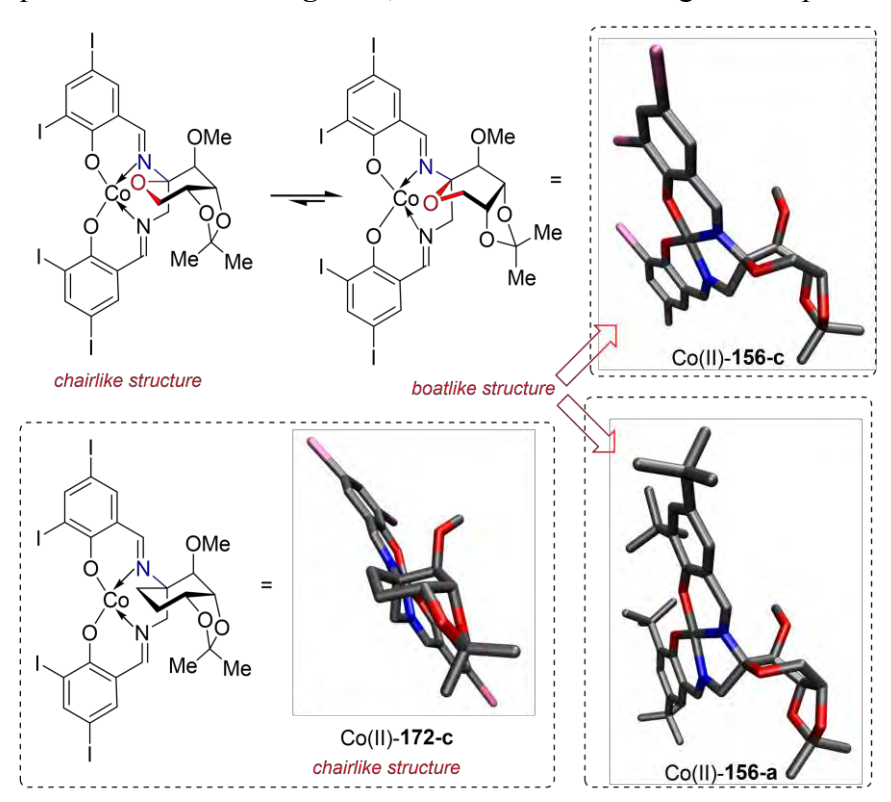


Figure 8. X-ray crystal structure of Co(II)-salen complexes.

salicylaldehyde (two equivalents-z-axisprojecting backward) and chiral 1,2-diamine (one equivalent-xaxis-projecting horizontally). This comparative study demonstrates that mini-ISES is a useful method for reading out catalyst enantioselectivity and substrate scope (i.e. HKR of propylene oxide and hexene oxide screened, parallel) even with these small volumes (~ 20 mL reaction volume) highlighting information the content and value of the technique. From a

salen ligand design point of view, the so-called 'enantioswitch' was preserved in the carbocyclic series, indicating that the shift from *R*- to *S*-selectivity observed in the β-D-(carba) fructopyranosyl-1,2-diamine series is due the change in salicylaldehyde alone (not anomerization). The most promising salen ligand seen in this study is **172c**, the pairing of the new β-D-(carba) fructopyranosyl-,1,2-diamine (**171**) with 3',5'-diiodo-salicylaldehyde. *The Co(III)-172c* catalyst shows high *S*-product selectivity with *E* values in the range of 44-100 for the HKR substrates screened here and maintains high *S*-selectivity when evaluated on other terminal epoxides. Crystal structures of the carbocyclic Co(II)-**172c** catalyst show it to have a chair-like structure in contrast to the boat-like structures seen by X-ray crystallography for the oxacycles in the Co(II)-**156a** and Co(II)-**156c** (see Figure 8) revealing an unexpected fringe benefit of moving to the carbocyclic pseudo-carbohydrate scaffold. 222

2.2.1.3.1. Initial Screening Hit: Synthesis of the β-D-(Carba)Fructopyranose-1,2-Diamine-Derived Chiral Salen Ligand with Potential for Asymmetric Catalysis

As just described, the carbocyclic β-D-(carba)fructopyranosyl-1,2-diamine scaffold, when combined with two equivalents of 3',5'-diiodo-salicylaldehyde, leads to a new salen scaffold with an interesting three-dimensional structure and with great promise in asymmetric catalysis. As has

Scheme 24. Entry into the β -D-(Oxa)Fructopyranose-1,2-Diamine-Derived Salen Skeleton Derived from D-Fructose

been alluded to in the discussion, the synthesis of carbocyclic analogue of D-fructose was motivated by promising initial results with 1,2-diamine derived from the native oxacyclic D-

Scheme 25. Entry into the D-(Carba)Fructopyranose-1,2-Diamine-Derived Salen Skeleton

A. Synthesis of intermediate 188 from quinic acid

B. Synthesis of intermediate 189 from methyl α -D-mannopyranoside

C. Synthesis of carbofructanose diamine from common intermediate 187

A. Route from quinic acid to the common intermediate **189**. **B.** Second generation route from methyl α -D-mannopyranoside to **189**. **C.** Common final stage of the synthesis involving a key Snider-type diazidation step.

fructopyranose system. The notion of constructing salens bearing this chiral scaffold was

motivated to no small extent by the success that Shi and coworkers had seen with a protected D-fructopyranose scaffold carrying a dioxirane functionality for asymmetric epoxidation chemistry. Of course, building the 1,2-diamine instead and constructing salen ligands around this core would create an entirely new three dimensional projection of that chirality and would allow one to wrap that extended D-fructopyranosyl-4,5-acetonide core around a metal center!

The synthesis for the parent oxacyclic D-fructopyranose derived diamines is presented in Scheme 24.²²⁴ The 1,2:4,5-bis-acetonide was formed in a 75% yield by acid-catalyzed ketal formation with acetone and dimethoxypropane. Following this, the C-3 hydroxyl group was methylated with MeI, providing the fully alkylated pyranose form 174 in 95% yield. A TMSOTfmediated anomeric azidation was performed next to afford a 1:4 anomeric mixture of azido alcohols 175/176 in 90% yield, with the β-anomer being favored. The free hydroxyl of 175/176 was then subjected to triflic anhydride and pyridine, and the resulting triflate was treated with sodium azide to obtain the diazide anomers 177/178 (1:4) in 94% yield over the two steps. The hydrogenation of diazides 177/178 with a PtO₂ catalyst at 4 atm of hydrogen afforded the desired chiral diamine 179/180 elements in 98% yield with a 1:9 anomeric ratio in favor of the β anomer. Separation of these anomers is not possible as they are in dynamic equilibrium. To overcome this, these diastereomeric diamines are captured directly in bis-imine salen linkages, and the resulting stable anomeric salen structures are separated chromatographically. Upon treatment with Co(OAc)₂, these salens are easily metalated to the Co(II) pre-catalyst form, suitable for storage or recrystallization. The active cobalt(III) catalyst is then formed by air oxidation in the presence of acetic acid or 1,3-dinitrobenzoic acid, as desired.

The carbocyclic analogue of the above D-fructopyranose catalyst was synthesized via two distinct routes. The first generation route (Scheme 25A) begins from (-) quinic acid 183,334 and utilizes the diazidation chemistry developed by the Snider group that was also employed for the B-pinene-derived diamine. 274 In this case, a 1:3 ratio in favor of the α-anomer **186** is obtained. To obtain this intermediate 177/178, (-) quinic acid is first protected as an acetal of cyclohexanone under acidic conditions and further promoting the lactonization of the quaternary carboxylate to afford 184. Cleavage of the lactone followed by PCC oxidation of the secondary alcohol with subsequent β-elimination generate a vinyl ester 185 in good yields. The sodium borohydride reduction of carbonyl group of 185 occurs in 82% yield, and an acetonide 186 is then formed between this new hydroxyl and its adjacent alcohol following the deprotection of the cyclohexyl acetal. Barton deoxygenation is performed on 186 and reaction yielded 90% product, followed by a bis-methyl Grignard attack on the ester, forming an exocyclic tertiary alcohol in 80 % yield. The tertiary alcohol undergoes dihydroxylation with osmium, and the resultant secondary alcohol 187 is selectively methylated with MeI to achieve 188. This gives two free hydroxyl groups readily cleaved by Pb(OAc)₄ to form the key cyclohexanone intermediate **189** in 95% yield. This ketone species directly overlaps with the second-generation synthesis described below.

The fructopyranose diamines 179/180 were synthesized from D-fructose (173) as delineated in Scheme 24. The second-generation synthesis (Scheme 25B) 224 intersects with the quinic acid route at compound 189 but starts from readily available methyl α –D-mannopyranoside 190. An Appel reaction to form the primary iodide on C-6 is followed by acetonide formation across C-2 and C-3, affording 191 in 78% yield over the two steps. The remaining hydroxyl group on 191 is methylated cleanly, followed by base-mediated E2-elimination putting in place an enol acetal. This sets up an efficient Ferrier-type carbocyclization under Pd(OAc)₂ catalysis, presumably via the mechanism shown. The resultant alcohol (192) is mesylated, leading to β -

elimination in the same pot. Hydrogenation of the resultant α,β -unsaturated ketone over Pearlman's catalyst gives the common intermediate **189**. Wittig methylenation of this ketone proceeds smoothly (80%), giving the exocyclic olefin needed for Snider diazidination (**Scheme 25C**). This reaction proceeds in an 80% yield and favors the α -pseudoanomer in a 3:1 ratio. Then hydrogenation with palladium on carbon provides the targeted α -and β -carbofructopyranosyl-1,2-diamines (**179/180**) in a 92% yield.

The ISES results with these salen catalysts show that the bulky salicylaldehydes believed to be critical for the outstanding success of the Jacobsen salen are detrimental to the selectivity for the non- C_2 -symmetric diamines described in the screen. Generally, the β -stereoisomer is more selective than the α - for both the parent oxacyclic and the newly reported carbocyclic scaffolds. In all cases, it appears the 3,5-diiodosalicylaldehyde is the better matched partner for these chiral diamines than its bulkier t-butyl or extended naphthyl counterparts. As noted above, crystallography reveals that carbocyclic fructopyranose analogues lead to a switch from the boatlike carbohydrate structure to the chair-like carbocycle, an interesting and likely important twist.

2.2.2. Post-Work-Up Readout on Conversion and Enantioselectivity

Parallel to the emergence of the In Situ Enzymatic Screening (ISES) method being developed in the Berkowitz group, ^{87,172,173,221,224} ^{222,223} the Seto group³³⁵⁻³³⁷ reported the Enzymatic Method for Determining the enantiomeric excess (EMDee) method for analyzing enantiomeric excess of a reaction product enzymatically. Much like ISES, EMDee circumvents the need for time-consuming analysis as HPLC on chiral stationary phases. Like ISES, in EMDee, an enzyme selectively catalyzes a reporting reaction with a preference for one enantiomer of the product allowing the measurement of enantiomeric excess by a UV- or fluorescence-based plate reader in 96- or 384-well format assay. The EMDee method is generally conducted post-work-up, under more controlled conditions than ISES, and can be a quite accurate estimate of ee, particularly as this is often done in a single phase, albeit upon work-up rather than in real time.

The initial EMDee description by Seto was followed by work from Moberg, Hult, and coworkers who reported a more information-rich EMDee variant in which both enantioselectivity and conversion can be captured with a combination of three enzymes.³³⁸ The reaction of interest here is the titanium salen-catalyzed cyano-acetylation of benzaldehyde that requires dual Lewisacid/base catalysis to provide the expected product without the formation of byproducts (Scheme 26).³³⁹ The enzymatic screen starts by monitoring unreacted benzaldehyde with horse liver ADH (HLADH) to form benzyl alcohol, leading to a decrease in absorbance at 340 nm as NADH is consumed, easily monitored with a UV/vis spectrophotometer. In this variant of EMDee, lipase enzymes serve to provide enantioselectivity; these enzymes are coupled with an alcohol dehydrogenase carrying a nicotinamide chromophore, for actual readout. For example, Candida antarctica lipase B (CALB) selectively hydrolyzes the S-enantiomer of the acetyl cyanohydrin to release benzaldehyde which can then be quantitated with HLADH. Similarly, the (R)-enantiomer of the acetyl cyanohydrin is cleaved with pig liver esterase (PLE) to again release benzaldehyde for quantitation with HLADH. The three HLADH-readouts provide complementary information: step 1 involves HLADH-reduction of remaining benzaldehyde and so gives overall conversion. Steps 2 and 3 then provide the amount of each enantiomer present in the product, thereby allowing for the determination of the enantiomeric excess of product for each of the reaction conditions screened. This method is very thorough and accurate but is post work-up and rather step-intensive.

2.2.2.1. Initial Screening Hit: Enantioselective *O*-Acyl Cyanohydrin Formation

Scheme 26. Enantioselective Cleavage of O-Acetyl Cyanohydrin **Product(s) with Lipase Enzymes**

Step 1: Unreacted benzaldehyde analysis:

Step 2: (S)-O-Acetyl cyanohydrin analysis:

Step 3: (R)-O-Acetyl cyanohydrin analysis:

A. Enantioselective cyanation of aldehyde using acetyl cyanide and cyanoformate as cyanide sources under dual Lewis-acid/base activation. B. Enzymatic screen for enantiomeric excess determination of O-acetylated cyanohydrins by analyzing; Step 1: unreacted benzaldehyde with horse liver alcohol dehydrogenase (HLADH) alone, Step 2: (S)-O-acetylated cyanohydrin with Candida antarctica lipase B (CALB); then HLADH and Step 3. (R)-Oacetylated cyanohydrin with pig liver esterase (PLE), then HDLADH. Readout is the decrease in absorbance at 340 nm as NADH is consumed.

Enantiomerically enriched cvanohydrins and their functionalized derivatives are useful precursors for synthesis of biologically active molecules^{340,341} and serve as building blocks for industrial synthesis of pesticides.³⁴² This sort of chemistry finds precedent in a very early report of the addition of benzoyl cyanide to an aldehyde in the presence of base, yielding an O-benzoyl cyanohydrin as reaction product.³⁴³ And while there are a number of other literature reports of direct acyl cyanide additions to aldehydes in the absence of catalyst, 344-346 recent focus for this transformation has been on catalysis by acids, bases³⁴⁶⁻³⁵⁰nucleophiles, ^{351,352}

and Lewis acids. 339,350,353-358

In important development, the Moberg group described the asymmetric formal addition of acetyl cyanide to a prochiral carbonyl center to give a chiral Oacylated cyanohydrin product (Scheme 27A).³⁵⁵ The reaction is promoted by a combination of titanium salen dimer (S,S)-196 and a Lewis-base. In this report, the authors screened a range of bases. triethylamine and the titanium salen combination giving the results. Control experiments suggest that the amine base is necessary for reaction initiation

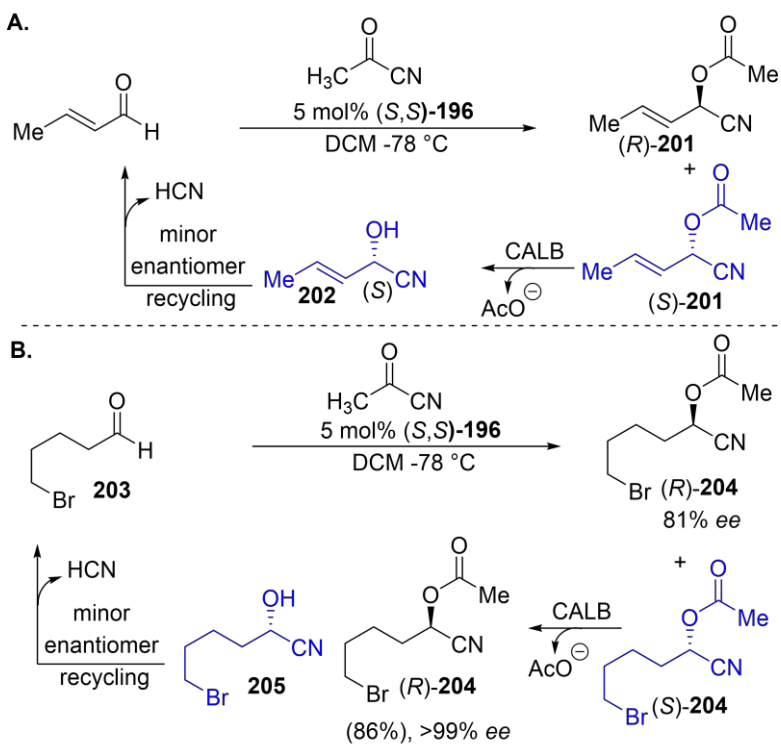
nucleophilic addition into the acyl cyanide, with the chiral titanium-salen Lewis-acid catalyst directing the enantioselective addition of the cyanide thereby released into the carbonyl center. Later, the same group demonstrated that the product ee could be improved and the minor

Scheme 27. Chiral Lewis-Acid/Base Catalyzed Asymmetric Addition of Acetyl cyanide on Aldehydes

enantiomer recycled, at the same time, by adding a lipase step, following acyl cyanide formation. Similar to the by approach taken the Berkowitz group, this is an example of a 'reporting enzyme' being repurposed as a chiral (co)catalyst asymmetric synthesis. As was noted above for the EMDee screen, the CALB enzyme is preferentially known to hydrolyze the S-enantiomer of O-acyl the cvanohydrin,

leaving behind almost exclusively the *R*-enantiomer of *O*-acylated cyanohydrin product **(Scheme 28A)**. ^{359,360} In 2012, Moberg and coworkers extended the combination of chiral salen-mediated aldehyde

Scheme 28. Minor Enantiomer Recycling



A. Inclusion of a subsequent enzymatic step to improve ee and recycle the minor enantiomer. **B.** Asymmetric synthesis of O-acetyl ω -bromocyanohydrins using this catalytic combination.

(215) analogous in 2015 (Scheme 29 III). 363

cyanoacylation/lipase 'product polishing' to the synthesis of enantioenriched *O*-acyl ω -bromocyanohydrins (**Scheme 28B**). 127

2.2.2.2. Hit Elaboration: Transition Metal-Based, Lewis Acid-Promoted OAcyl Cyanohydrin Formation

Based on their own seminal work, the Moberg group further demonstrated minor enantiomer recycling concept by using combination of chiral Lewisacid/enzyme for the synthesis of 4-amino-2(5H)-furanones (208) in 2013 (Scheme 29 (S)-propanolol (212), and (R)-pronethalol in 2014 (Scheme 29 $II)^{362}$ synthesis of β₃-adrenergic receptor agonist solabegron

Scheme 29. Application of Minor Enantiomer Recycling for the Synthesis of 4-Amino-2(5H)-Furanones, (R)-Pronethalol and Solabegron

2.2.3. Post-Work-Up Readout on Enantioselectivity (Reporting Enzyme Turnover)

As mentioned at the outset of this section, the EMDee method developed by Seto and coworkers aided the experimentalist in screening for asymmetric catalysis without the need for chiral HPLC. 336,337 The EMDee method was applied to the asymmetric addition of diethylzinc to benzaldehyde under the aegis of chiral oxazolidine ligands **217/218** (**Scheme 30**). $^{364-368}$ To establish ee, the resulting 1-phenylpropanol product **216** is oxidized by the (S)-selective aromatic alcohol dehydrogenase from *Thermoanaerobium sp.* (TsADH) to produce phenyl ethyl ketone. The rate of this reaction is monitored by observing the production of NADPH at 340 nm. Conveniently, (S)-**216** is a good substrate for this enzyme where the (R)-antipode is an inhibitor.

By monitoring the rate of this enzymatic reaction, the authors can rather accurately determine the

Scheme 30. Enzymatic Method for Determining the Enantiomeric Excess (EMDee) Applied to a Chiral Catalyst Promoted ZnEt₂ Addition into Benzaldehyde

ee achieved for the chiral ligands being screened. Α complimentary (R)selective alcohol dehydrogenase from Lactobacillus kefir can be used to quantify the amount of (R)-product. This general idea was expanded later include two screening enzymes from outset to quantify the optical purity of chiral alcohols by Li and coworkers.369

Seto and

coworkers further expanded the scope of the EMDee method with regards to (i) reaction product being screened, (ii) the type of reporting enzyme used, and (iii) the nature of the readout. They set out to demonstrate an enzymatic readout for the enantiomeric composition of allylic acetates reactions using a lipase. The α -methylcinnamyl acetate 219 was chosen as a test analyte, such compounds are both products of interest for kinetic resolutions and common substrates for transition metal-mediated allylic substitution reactions. *Pseudomonas cepacia* lipase (PcL) was

Scheme 31. EMDee Applied to Mixtures of Allylic Acetates Based on Model Reaction Products

discovered to selectively cleave only the (R)-acetate (219) while the (S)-enantiomer is simply a spectator in the reaction, being neither a substrate nor inhibitor. The rate of the lipase-catalyzed reaction correlates to the amount of (R)-acetate produced in a reaction of interest. The PcL-reporting enzyme produces one molecule of acetic acid with each turnover of the (R)-amethylcinnamyl acetate. Acetic acid production is read by UV-vis spectroscopy utilizing a p-nitrophenolate anion indicator ($\lambda_{max} \sim 405$ nm). One observes the decrease in absorbance at 405 nm (and the fading of the yellow indicator color) as acetic acid is produced and neutralizes the p-nitrophenolate anion indicator (**Scheme 31**).

This assay was conducted across 88 samples of α -methylcinnamyl acetate of different enantiomeric compositions in a 96-well format using a UV-vis plate reader to demonstrate that reporting rates observed correlate with ee of the sample. This beta-test of the assay was performed

Scheme 32. EMDee PcL Analysis of an Array of Allylic Alcohols by Chiral DMAP and Acetic Anhydride

on crude reaction mixtures obtained from DMAP-mediated acetylation of the corresponding alcohol samples. In this way, the authors were mimicking a reaction set derived from kinetic

resolution experiments on (\pm) - α -methylcinnamyl alcohol utilizing chiral DMAP-type acylating reagents, say, of the sort developed by Fu and coworkers²⁸¹ (**Scheme 32**). Seto and coworkers also demonstrated that this lipase shows high (*R*)-enantioselectivity across a diverse array of arylsubstituted and fused bicyclic secondary alcohols of synthetic interest, highlighting the versatility of the approach.

2.2.4 Post-Work-Up Readout on Enantioselectivity (Reporting Enzyme Inhibition)

The Seto group next turned the tables on the EMDee method and asked the question, "If reporting

Scheme 33. EMDee Applied to a Chiral Mixture of Enantiomeric Sulfoxides Produced from the Ti(IV)-Tartrate-Promoted Thioether Oxidation

Unknown mixture of ŌΘ `Me Ti(O-*i-*Pr)₄, H₂O, 4 Å MS (S)-223 PhC(CH₃)₂)O₂H, DCM -20 °C,18h $Ki = 33 \mu M$ R=Me, Et; Bn, i-Pr, n-Bu Reaction crude filter through a silica plug ee of sulfoxide are estimated monitor rate of NADH formation at HLADH by a calibration curve 340 nm by a 96-well plate reader NAD^{\oplus}

These chiral sulfoxides act as inhibitors of horse liver alcohol dehydrogenase (HLADH). Mixtures rich in (S)-sulfoxide inhibit well and present a slow initial rate whereas those rich in (R)-sulfoxide show markedly lower levels of HLADH inhibition. This allows one to establish a calibration curve between sulfoxide enantiopurity and reporting rate. The readout of the assay is the formation of NADH at 340 nm by UV/vis absorbance in 96-well plate format.

enzymes be used in a positive sense to read out a product by catalyzing its catalytic turnover, leading to a visible or UVsignal, cannot enzymes read an analyte also in a negative sense, if that analyte were to selectively inhibit catalytic activity?"

After all, just as one can see enantioselection in substrate binding and catalytic processing, one might also expect to see enantioselection in inhibitor binding and efficacy.³³⁵ As a reporting enzyme here, the Seto group utilized the well-studied HLADH enzyme that also served Moberg and Hult so well (*vide supra*). As a test-bed synthetic reaction, they selected the classical asymmetric oxidation of sulfides to sulfoxides by titanium tartrate catalysts reported by Kagan and coworkers.³⁷⁰

The default reporting reaction here is the HLADH-catalyzed oxidation of ethanol to acetaldehyde whereby the HLADH enzyme exhibits enantioselective inhibition by chiral aryl methyl sulfoxides. Specifically the p-toyl methyl sulfoxide enantiomers 223 display uncompetitive inhibition whereby the (S)-enantiomer acts as a potent inhibitor with a Ki of 33 \pm 3 μ M and the (R)-enantiomer displays much more modest inhibition with a Ki of 656 \pm 66 μ M (Scheme 33). This allows the experimentalist to use the initial rate observed for the HLADH-catalyzed oxidation of ethanol to acetaldehyde to measure the ee of chiral sulfoxide inhibitor present. This assay requires that one set a fixed total sulfoxide inhibitor concentration to cleanly correlate observed Michaelis-Menten steady state rate with ee of the sulfoxide added. By first establishing a calibration curve studying the rate of acetaldehyde formation from ethanol with different mixtures of sulfoxide enantiomers, the authors show that they can then estimate the ee of a sulfoxide sample of unknown ee. For proof of principle, several catalysts featuring tartrate esters coordinated to a Ti(IV) center were screened with results approaching 90% ee for the diethyl tartrate-based catalyst, the classical Sharpless catalyst for asymmetric epoxidation of allylic alcohols.

3. HYBRID ANTIBODY-ENZYMATIC SCREENING METHODS

3.1. Immunoassay Screening for Reaction Discovery

High-throughput immunoassays have recently emerged as alternative biomacromolecular tools for screening and reporting on novel synthetic strategies. To be sure, in clinical settings, immunoassays have become a widely used analytical tool due to their specificity, rapid output and cost-effectiveness.³⁷¹ In chemistry research laboratory settings, hybrid antibody-enzymatic screening approach have evolved based on this clinical technology. These approaches utilize a competitive enzyme immunoassay (EIA) to interrogate a library of reactions. This method requires a highly specific binding affinity of a monoclonal antibody (mAbs) and a hapten derived from a small molecule of interest. 372 Detection is made possible with a label attached to either the antibody or hapten.³⁷² This method requires utilization of the hybridoma technology, discovered by Georges Kohler, Cesar Milstein, and coworkers, to identify monoclonal antibodies (mAbs) with high binding affinities to the molecule of interest. 88,373,374 Specifically, hybridoma cell lines that express a large amount of one specific mAb are used. These cell lines are formed by the fusion of B cells with an immortal myeloma cell line lacking the hypoxanthine-guanine-phosphoribosyltransferase (HGPRT) gene. A general procedure for antibody development requires that a species of interest be immunized against a specific epitope located on an antigen to generate B-lymphocytes and enable fusion with the myeloma cell line. Cell cultures are then screened for the specific antibody activity desired.³⁷⁵ Notably, the binding and/or catalytic activity for the antibody of interest is dependent on the design of the hapten used in the immunization.³⁷⁶

Inspired by ELISA (Enzyme-Linked ImmunoSorbent Assay) technology, 373 377,378 reaction screening methods employing enzyme-linked antibodies have recently been reported. Linked to a solid support, the substrate to be screened is subjected to various antibody-binding stages, eventually leading to immuno-catalysts. An early iteration of this method is illustrated in **Figure** 9 in which the small molecule of interest is bound to a microtiter plate, and the reaction being screened is catalysis of a simple p-nitrophenyl ester. Upon hydrolysis, an antibody raised against the free carboxylate is added to the plate, allowing it to bind to the hydrolysis product. As in the ELISA technique, a second antibody, fused to a peroxidase enzyme is then bound to the productbinding antibody. This is followed by the addition of hydrogen peroxide (peroxidase substrate) and a dye cofactor. Here, the redox-sensitive dye, ABTS, is employed and reports on the Conveniently, peroxidase activity can be visualized in real-time by peroxidase activity. monitoring the absorbance at 690 nm associated with the ABTS radical cation oxidation product, two equivalents of which are generated in the peroxidase-mediated redox reaction (Figure 9B). 373 Monitoring the intensity of the absorbance at 690 nm provides valuable information on the effectiveness of the esterase catalyst(s) being screened. As proof of principle, the hybridoma

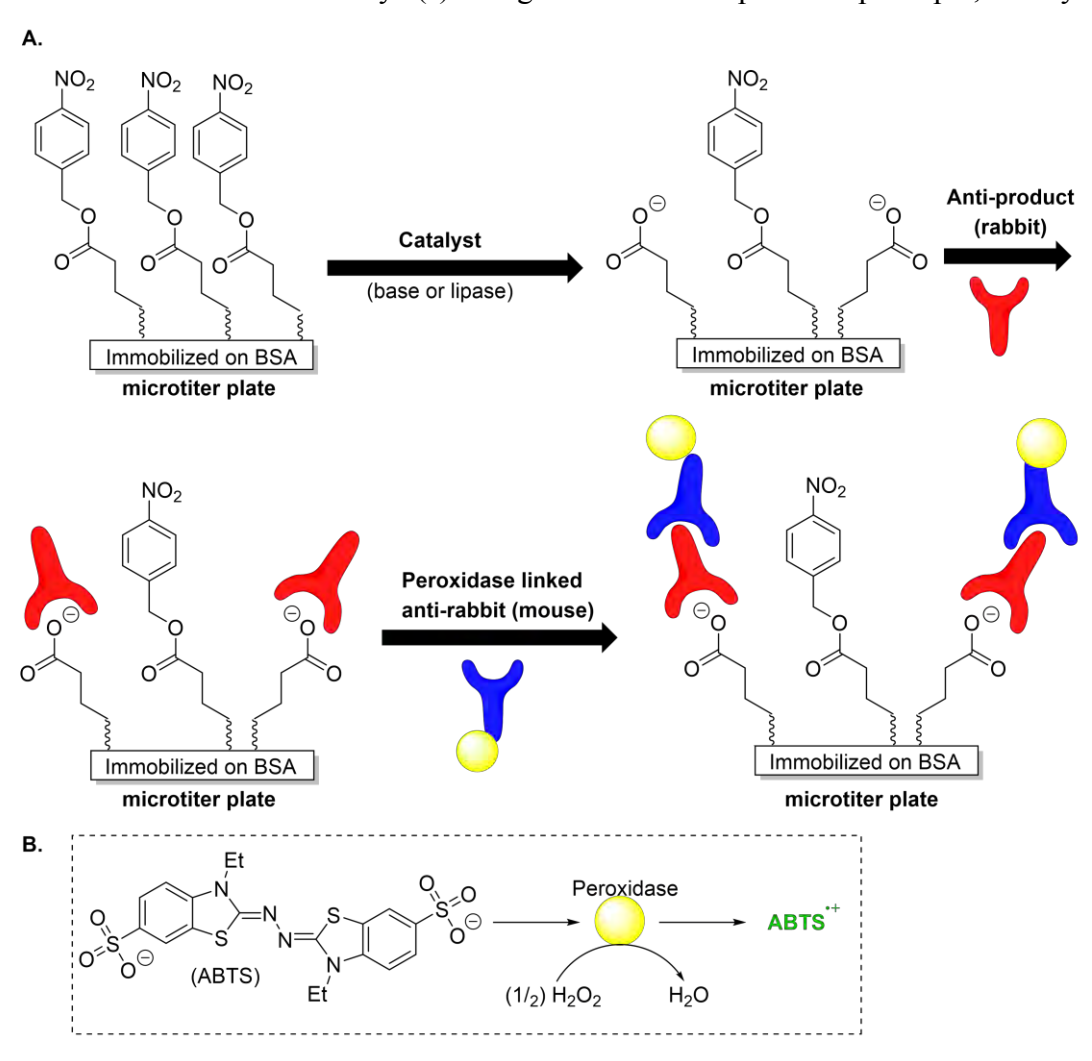


Figure 9 A. ELISA inspired screen to optimize catalytic antibody ester hydrolysis catalysts. **B.** Peroxidase assay.

clones were raised against a phosphonate TS analog and amide substrate to study the cleavage of the corresponding *p*-nitrobenzyl ester. While this screen successfully uncovered catalytic antibodies for the ester hydrolysis reaction of interest, this antibody-based screen is specific for the reaction of interest.³⁷³ In order to apply this method across different reaction pathways, new specific antibodies must be raised in order to bind to a different product of interest. Importantly, this screen demonstrates proof of principle for utilizing an antibody-based screening approach, albeit here for a simple ester hydrolysis (**Figure 9**).

3.1.1. Reaction Discovery Using a Sandwich Immunoassay

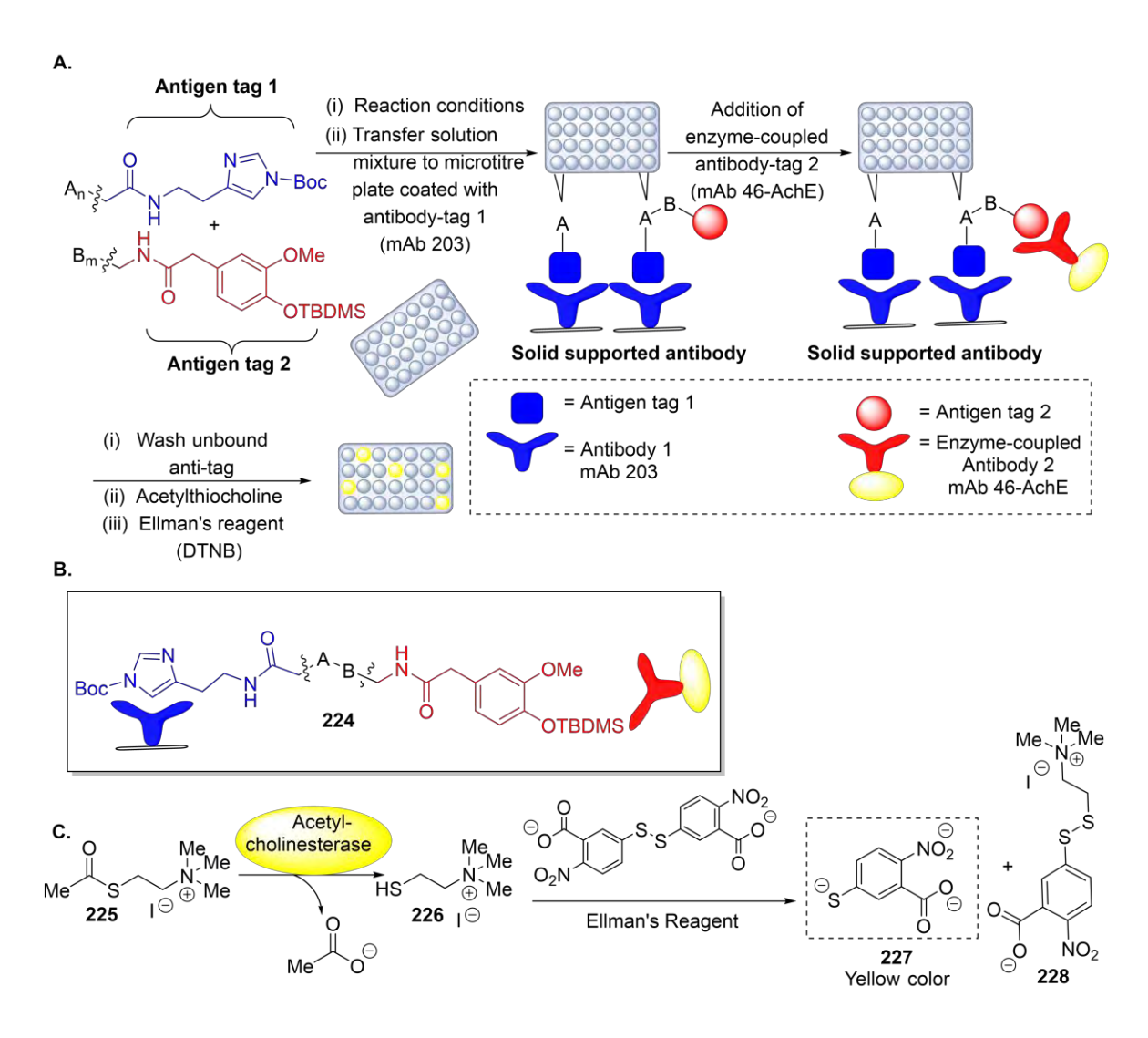


Figure 10. Approach for sandwich immunoassay-based reaction discovery. **A.** General procedure for parallel reaction study and high-throughput screening. The bond formation product shows a yellow color and absorb at 415 nm. **B.** Antibodies interaction with hapten, where blue represents antibody 1 (mAb 203)-antigen tag 1 complex and red/yellow represents enzyme-coupled antibody 2 (mAb 42-AchE) complex. **C.** Reaction for the detection of bond formation product involving an enzymatic step with acetylcholinesterase followed by the disulfide reaction with Ellman's reagent (DTNB). The product of this last reaction can be monitor at 412 nm and presents a yellow color.

Taran and coworkers developed an enzyme immunoassay platform "sandwich"-type assay to study intermolecular reactions. ³⁷⁹⁻³⁸¹ Generally, sandwich immunoassays involve two specific monoclonal antibodies (mAbs) which bind to the epitope recognition site. One of the monoclonal

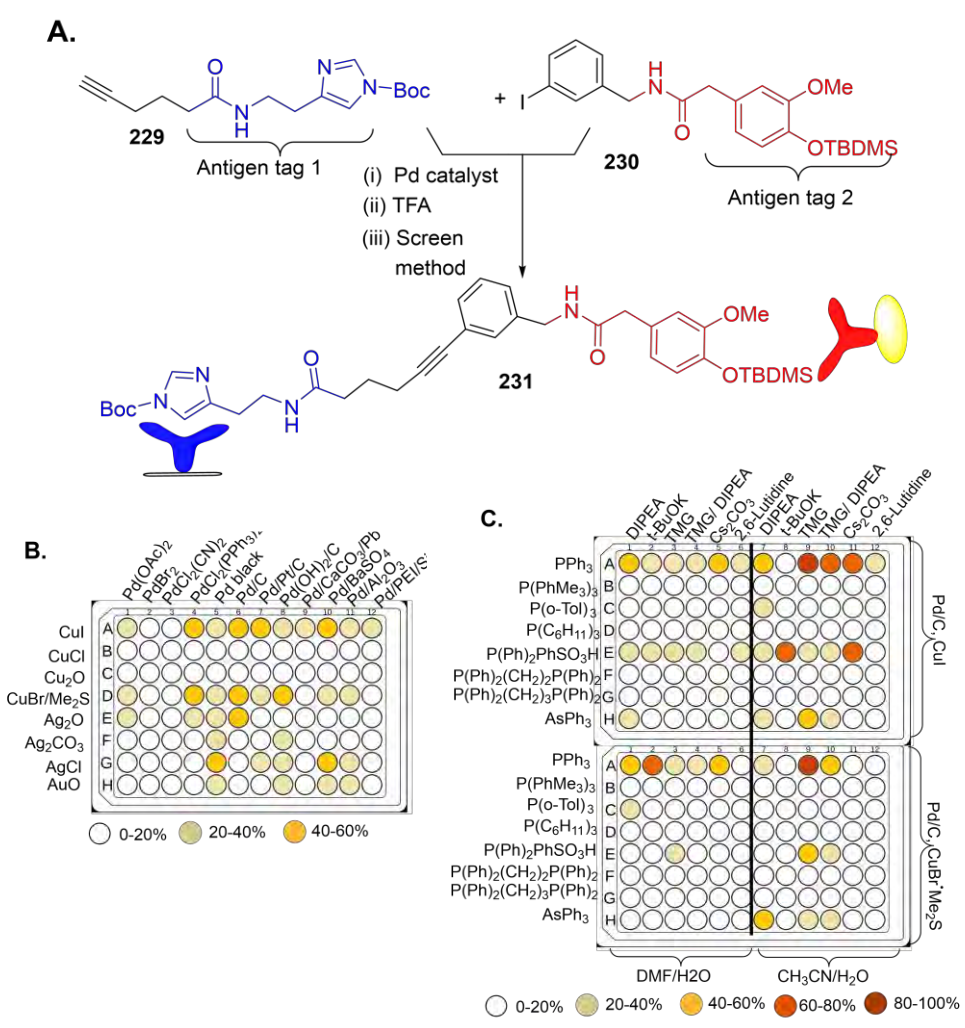


Figure 11. Catalyst screening through sandwich immunoassay screen. **A.** Sonogashira cross-coupling reaction studied between alkyne and aryl iodide. **B.** Reaction screen were performed in a 96-well plate format with 3% of Pd and co-catalyst (10% (w/W)) at 80 °C in DMF/H₂O (95:5) for 20 h. **C.** Reaction screen was performed in a 96-well plate format with 3% of Pd and co-catalyst (10% (w/W)) at 80 °C in DMF/H₂O or CH₃CN/H₂O (95:5) for 20 h.

antibodies is coated onto a solid surface and bound to the epitope of a specific antigen. The second antibody, bound to an enzyme, facilitates the assay detection (**Figure 10**). ³⁷⁹ As mentioned previously, the hapten design is essential for this type of technique. In this case, the hapten is chemically synthesized, known as hapten H3, and then covalently bound to a carrier protein, known as the keyhole limpet hemocyanin (KLH) for immunization of mice. This process will lead to an immune response in the form of antibody production. Further testing of the hapten-specific antibodies will determine which candidate is ideal and contains an efficient binding affinity for the reaction scaffold of interest. This sandwich immunoassay technique, modified to study covalent bond forming reactions, consisted of substrates A and B outfitted with functional groups which can be easily tagged with specific haptens (**Figure 10A**). ³⁷⁹ The tags for this method were a *tert*-butyloxycarbonyl (Boc)- protected imidazole and a *tert*-butyldimethylsilyl (TBDMS)-protected

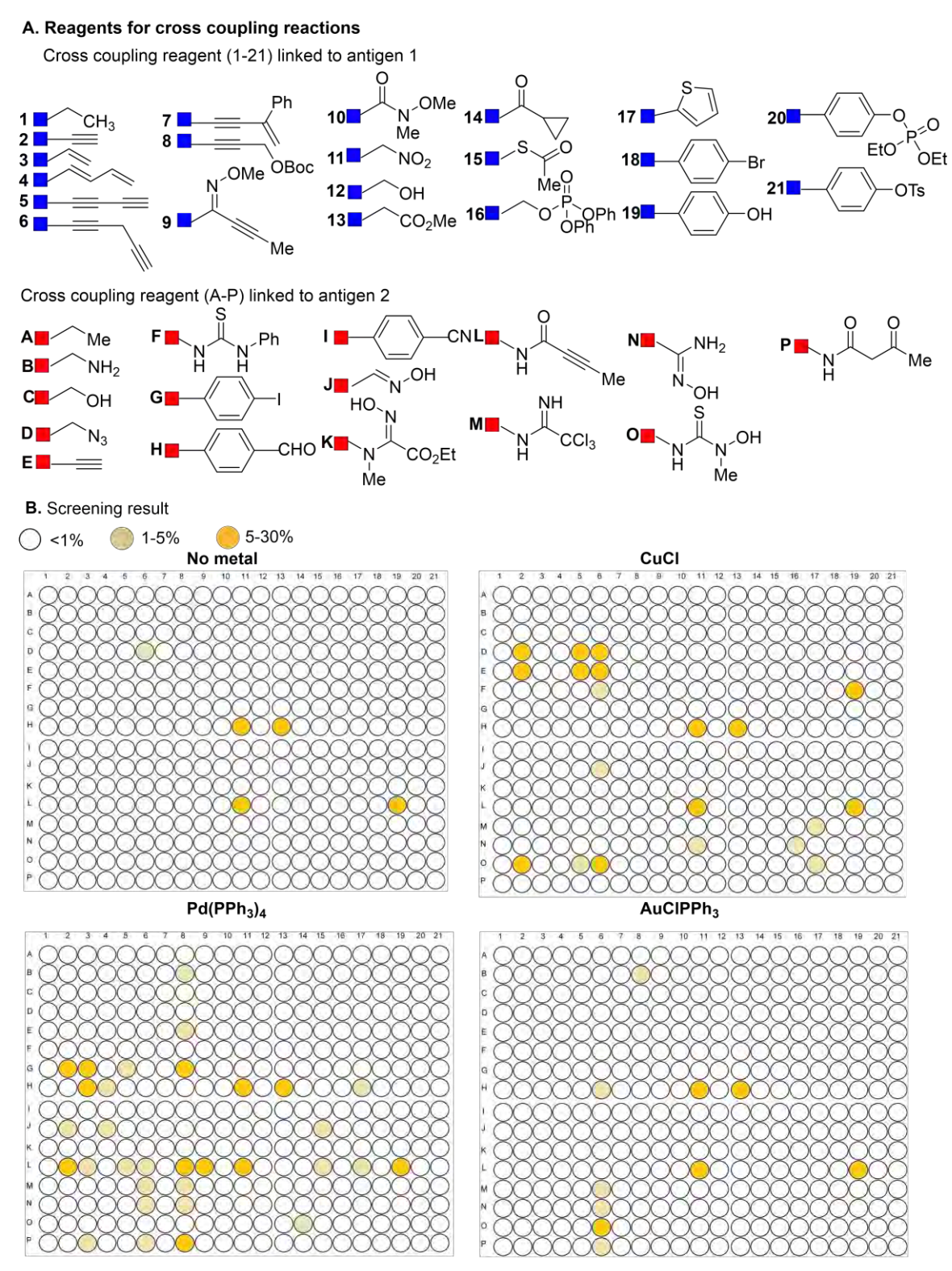
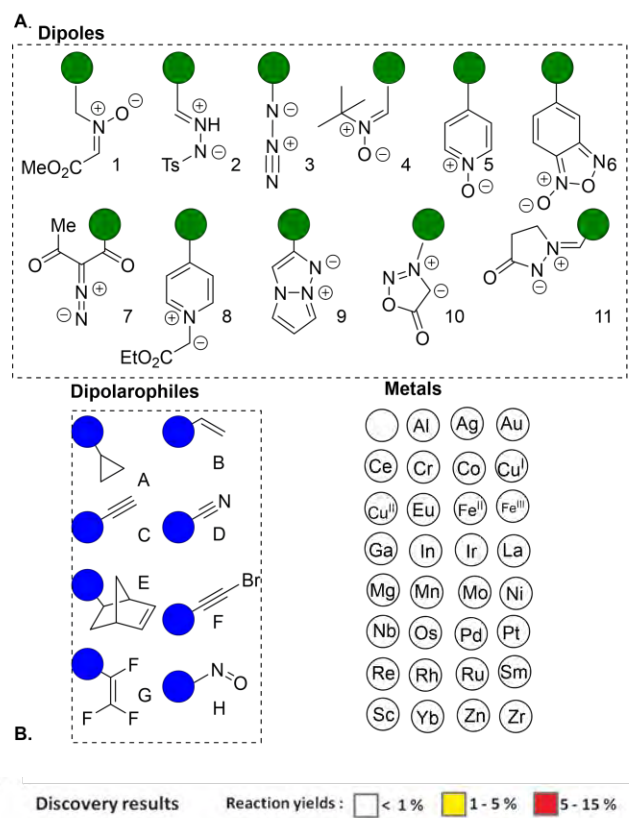


Figure 12. Reaction discovery through sandwich immunoassay screen. **A.** Cross coupling reagents. **B.** Screening results. The reactions were performed with 5mM of substrates, 10mM of triethylamine (TEA), 5 mM of transition-metal in the selected cases and 40 uL of dimethylacetamide (DMA) solvent. The reaction showing product were analyzed by LC/MS.

guaiacol derivative, respectively.379 Substrate A, linked to a hapten specific to the antibody, is

coated to the solid surface. Substrate B is bound to the hapten specific to the enzymecoupled antibody. Once the substrates have been subjected to the covalent bond forming reaction between A and B, the reaction mixture is further washed to remove any unbound antibodies. The Ab-linked enzyme, acetylcholinesterase, reacts with the sensing substrate. acetylthiocholine, to form thiocholine. Coupling this product to Ellman's reagent, 5,5'-dithiobis-(2nitrobenzoic acid), produces the thiolate anion of 5-mercapto-2-nitrobenzoic acid which can be quantified by measuring the absorbance at 412 nm³⁷⁹ (Figure 10C). In this way, only the reaction substrates undergoing the targeted bond formation will bring the enzyme-coupled antibody complex coated to the solid surface, allowing this method to give an estimate of reaction yield using a calibration curve from the doubletagged standard product.³⁷⁹

Taran and coworkers first applied this screening method to study a Sonogashira cross-coupling reaction under heterogeneous catalysis conditions (Figure 11).³⁷⁹ The screen was performed in a 96-well plate configured with a palladium (Pd)-based catalyst for the transformation between an alkyne and aryl iodide (Figure 11A). Various palladium sources and eight cocatalysts including copper, silver, and gold were screened. auenched (trifluoroacetic acid = TFA), and subjected to the sandwich immunoassay in 96-well microtiter plate format (Figure 10 and 11A & B). The screen reported the highest yields of 40-60% for Pd/C combined with CuI or CuBr·Me₂S, as confirmed by HPLC analysis (Figure 11B).³⁷⁹ These initial conditions were further optimized by studying these two catalyst combinations with various ligands, base, and solvent to generate 192 reaction combinations (Figure 11C). Optimization efforts improved overall reaction yields (80-



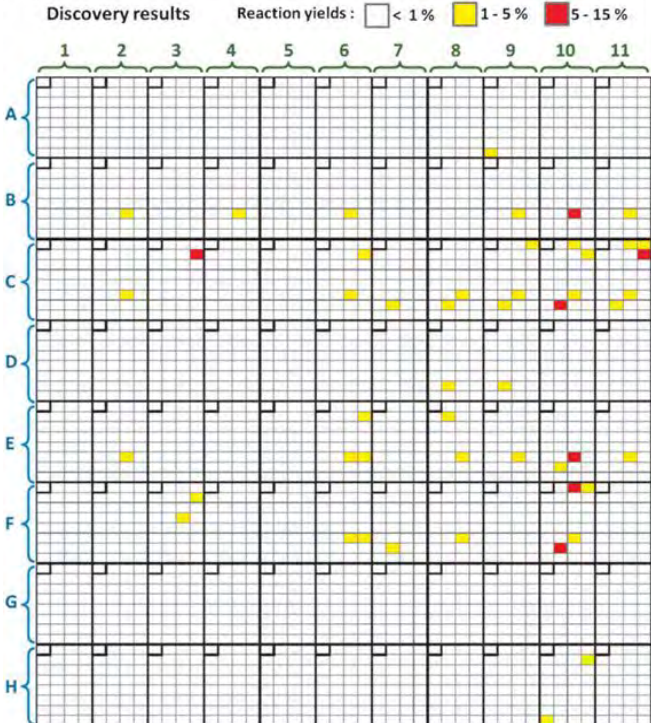


Figure 13. Reaction discovery through immunoassay screening. **A.** Substrates combination of 11 tagged dipoles, 8 tagged dipolarophiles reactants and 31 metals. **B.** Screening result. **Panel B republished with permission from ref 381. Copyright** © **2013 Wiley-VCH.**

100%). The screen successfully identified the metal/ligand combinations consisting of either

Pd/C/CuI or $Pd/C/CuBr \cdot Me_2S$ with PPh_3/TMG (methyl-1-thio- β -D-galactopyranoside) as the best reaction conditions. ³⁷⁹

25-50% 5-25% 50-100% New active combinations L & M salts Optimization Solvents & B 8 h 24 h Nucleophiles Chemo Electrophiles Proteins Sugars Cell Culture Cell Lysate

Table 5. Optimization of Reaction Discovery Through Immunoassay Screening Substrates

Table republished with permission from ref 381. Copyright © 2013 Wiley-VCH.

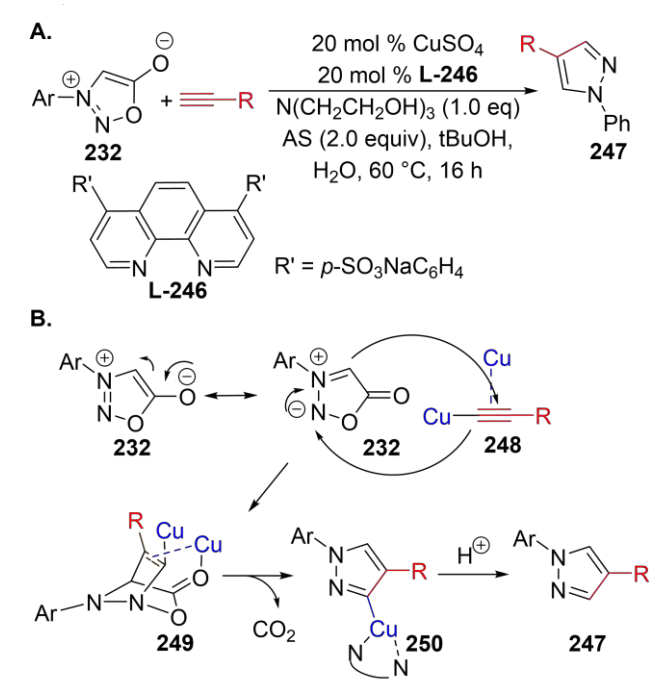
In 2012, Taran and coworkers once again used a sandwich-based immunoassay to rapidly screen a diverse reaction discovery effort. Here, an array of 21 different functional groups linked to antigen 1 were screened against 16 different functional groups linked to antigen 2.³⁸⁰ As illustrated in **Figure 12**, substrate functionality included hydroxyl, nitro, amino, alkenyl, monoand bis-alkynyl, azido, formyl, keto, cyano, N-hydroxy thiourea, alkynyl oxime, and amidoxime, among others.³⁸⁰ Transition metals including Cu, Pd, Au, and Ru were introduced to the screen in stoichiometric quantity. As proof of concept, over the course of 2-days, this high-throughput assay enabled 1,344 different reaction combinations to be screened in parallel. (**Figure 12B**).³⁸⁰ The screen reported hits involving 57 different Cu-, Pd-, and Au-mediated coupling reaction products, with yields ranging between 5-30%. Upon further analysis by LC/MS, it was concluded that products formed by a variety of well-known reactions including Henry, Knoevenagel, and Michael reaction, Cu-catalyzed alkyne-azide cycloaddition, alkyne-alkyne dimerization, Pd-catalyzed Sonogashira and, Pd-catalyzed Heck reaction (**Figure 12**).³⁸⁰ Perhaps the most exciting chemistry discovered from the screen was the copper-mediated coupling of phenols and thioureas leading to an isourea product and the coupling of alkynes with *N*-hydroxy-thioureas leading to thiazoles.³⁸⁰

In later work, the sandwich immunoassay screen further assisted in the discovery of novel chemoselective and biocompatible [3+2] cycloaddition reactions.³⁸¹ Here, 11 tagged dipoles and 8 dipolarophiles were introduced to different "click"-type reactions conditions mediated by different TM catalysts (**Figure 13**).³⁸¹ To demonstrate the high-throughput of this method, the use of a 96-well plate enabled 2,816 reaction combinations to be screened in parallel. Noteworthy, this iteration led to the discovery of a Cu-catalyzed sydnone-alkyne cycloaddition via decarboxylative retro-cycloaddition, affording a pyrazole product (**Scheme 34**). The product hits from the screen were further evaluated in aqueous buffer alongside common biomolecules such as proteins, sugars, nucleic acids, cell culture, cell lysate, and plasma to further examine their biocompatibility (**Table 5**).³⁸¹ Here, it was discovered that pyrazoles formed under Cu-catalyzed syndone-alkyne cycloaddition (CuSAC) revealed to be a biocompatible transformation.³⁸¹ While further optimization may be warranted, this application showcases the potential role of the Cu-catalyzed syndone-alkyne cycloaddition to evolve in the world of bioconjugation, where bioorthogonality plays a vital role.^{382,383}

Scheme 34. Reaction Hits Found Through the Immunoassay Screen

A. Cu (I)-catalyzed click reaction. **B.** Rh (I)-catalyzed 1,3-dipolar cycloaddition. **C.** Ir (I)-catalyzed reactions of azides with bromoalkynes. **D.** Pd (II)-catalyzed dehydrogenative Heck reaction.

Scheme 35. Cu(I)-Catalyzed [3+2] Cycloaddition



A. Cu(I)-phenanthroline complex gives 1,4 -pyrazoles under milder conditions. **B.** Mechanism of copper acetylene and sydnone **232** *via* [3+2] cycloaddition.

Sydnone-Alkyne Cycloaddition Reaction

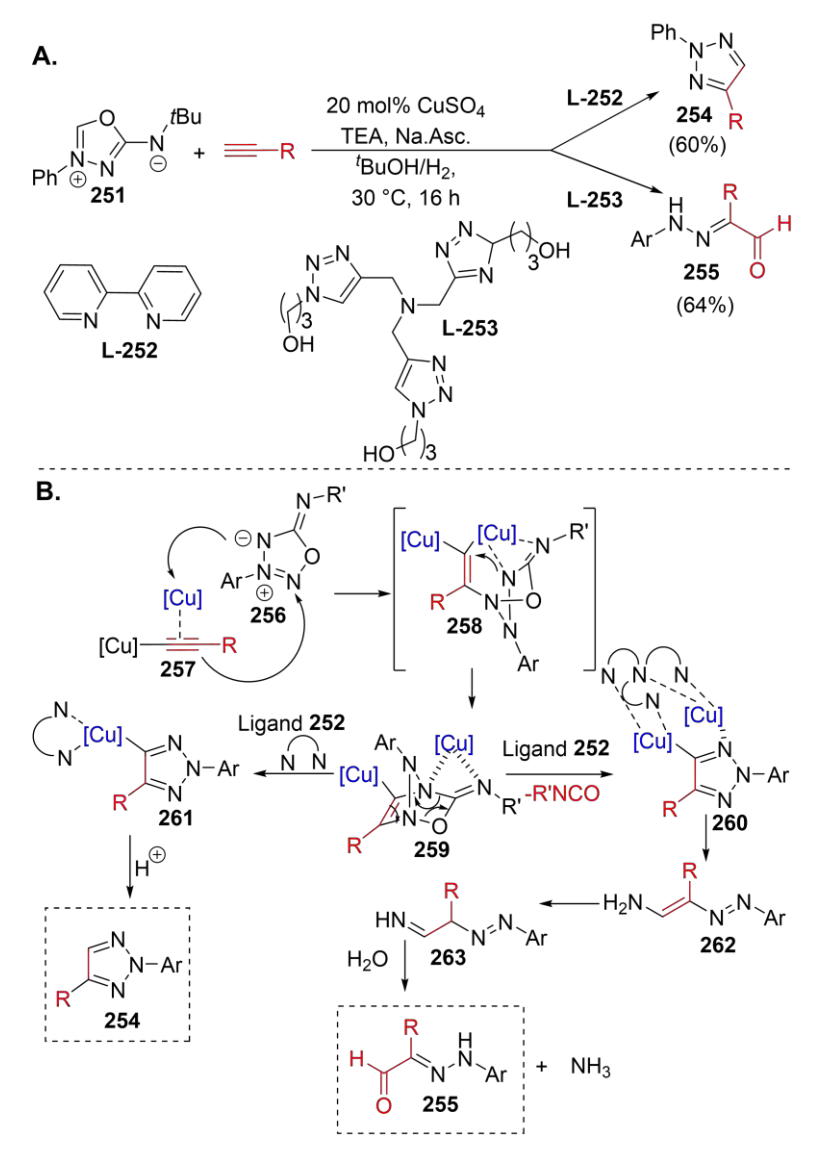
Notably, Taran and co-workers have provided an excellent review highlighting their efforts in combinatorial catalysis guided by enzyme-assisted immunoassays greater detail.88 It is expected that sandwich immunoassay methods will continue to be an important tool for reaction discovery and optimization. The sandwich immunoassay has the advantage of being highly sensitive and selective. Furthermore, this assay does not require a workup, thus can be high throughput with 1000+ reaction combinations being screened in a single day without the need for robotics.

3.1.2. Discovery of Chemoselective and Biocompatible Reactions Using Immunoassay Screening

3.1.2.1. Initial Screening Hit:

The Taran group, through their pioneering work in high-throughput immunoassay screening,

Scheme 36. Cu(I)-Catalyzed Reaction of Aza-Iminosydnone Diels-Alder Reaction



A. Cu(I)-catalyzed reaction of aza-iminosydnone with terminal alkynes. **B.** Plausible mechanism of copper acetylene and sydnone through a retro Diels-Alder reaction

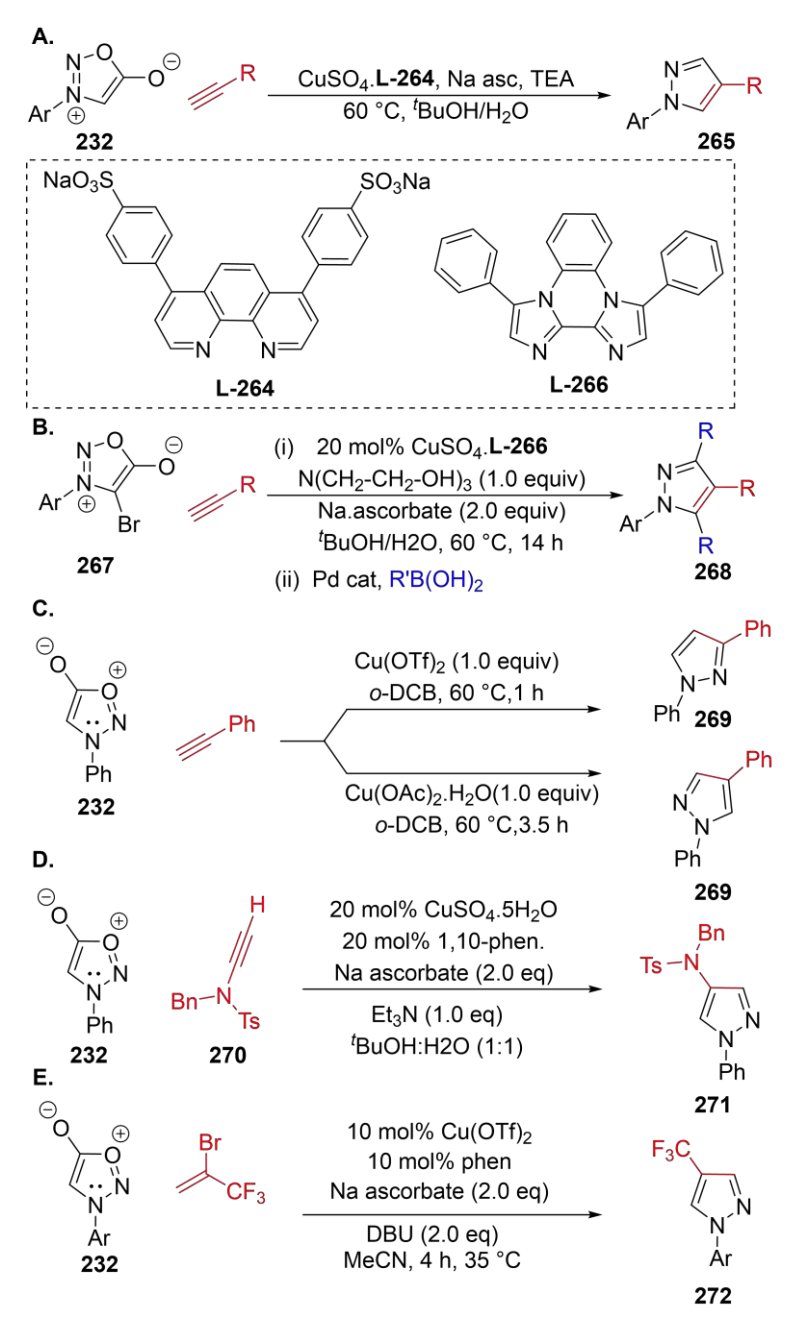
discovered a novel reaction involving [3+2] cycloaddition chemistry.^{381,384} The highthroughput immunoassay screening conducted was using 11 tagged dipoles, 8 tagged dipolarophile reactants, and 31 various metals. Using 96-well plates to run reactions in parallel, 2816 total reactions were screened in two days (Figure 13). During this screen, 51 cycloaddition reactions showed positive results. Of these, 9 hits were well-known reactions. The other 42 where novel reactions discovered by the high-throughput immunoassay screen. These further hits were optimized under different reaction conditions varying metals. ligands, solvents, nucleophiles (amine, thiol, acid, etc.) or electrophiles (Michael acceptor. bromoalkane, aldehyde, etc.), and under different biological conditions. From this screen, four of the reactions showed greater than 50% yield: (I) a Cu(I)-catalyzed 'click' reaction (Scheme 34A), (II) a Rh(I)-catalyzed 1.3-dipolar cycloaddition (Scheme 34B), (III) Ir(I)-catalyzed reactions

of azides 238 with bromoalkynes 239 in the presence of the iridium dimer [Ir(cod)Cl]₂ (Scheme 34C), and (IV) the Pd(II)-catalyzed dehydrogenative Heck reaction between 232 and olefins (Scheme 34D).

3.1.2.1.1. Hit Elaboration: Cu-Catalyzed Iminosydnone-Alkyne Cycloaddition Reaction

At this point, the Cu(I)-catalyzed 'click' reaction (**Scheme 34A**) proved to be the most efficient, chemoselective, and bioorthogonal of the 2816 reactions compared to the other three hits. The modified Huisgen cycloaddition, dubbed 'click' chemistry by K. B. Sharpless led to a flurry of activity in the Cu(I)-catalyzed azide-alkyne cycloaddition space globally, because of the broad

Scheme 37. Hit Elaboration of Cu-Catalyzed Sydnone-Alkyne Cycloaddition Reaction (CuSAC)



A. One-pot conversion of arylglycines to 1,4-pyrazole products via a nitrosylation/cyclization sequence. **B.** Synthesis of 1,4-disubstituted pyrazoles, followed by Suzuki coupling leading to polyfunctionalized 1,4,5-pyrazoles. **C.** Regioselective Cu-promoted SAC: Cu(OTf)₂ yields 1,3-disubstituted pyrazoles and Cu(OAc)₂ yields 1,4-isomers products. **D.** Synthesis of substituted aminopyrazoles products from ynamides. **E.** Synthesis of 4-(trifluoromethyl)-substituted pyrazole products from 2-bromo-3,3,3-trifluoropropene.

utility of this chemistry in organic synthesis, materials science, biotechnology. 13,14,385 In this context, the innovation introduced in Cu (I)catalyzed 'click' reaction by Taran further elevates the significance and breadth of this chemistry. exclusive regioselectivity with Cu(I)phenanthroline complex gives 1,4 pyrazoles under milder conditions (Scheme 35). The reaction result can be to previous literature compared methods, which involve harsh reaction conditions and further involve low regioselectivity. The reaction scope was further investigated on a battery of functional groups present on either the sydnone alkyne substrate. or Mechanistic studies have support the formation of bicyclic intermediate 249 from copper acetylene 248 and sydnone 232 via [3+2] cycloaddition (Scheme **35B).** Liberation of CO₂ from **249**, followed by protonation of intermediate 250 would provide the expected pyrazole **247**.

In 2018, the Taran group explored the reactivity of azaiminosydnone with 251 terminal alkynes in the presence of a copper catalyst (Scheme 36).³⁸⁶ The selective formation of the products 254 and 255 was dictated by the choice of ligands. bipyridine ligand, (L-252),provided triazole 254 whereas ligand 253 delivered product 255 (Scheme **36A**). Mechanistically, the bicyclic intermediate 259 is likely formed by coordinating the N-4 atom of the azaiminosydnone to the acetylide-copper center (Scheme 36B). From this intermediate, two different paths could occur, depending on the ligand choice; 259 undergoes a retro Diels-Alder reaction leading to intermediate 261

followed by protonation providing 254 in the presence of L-252. However, the tetradentate ligand

would coordinate two Cu atoms providing intermediate **260**, which would generate product **255** under further decomposition (Scheme **36B**). ³⁸⁶

The Cu-catalyzed sydnone-alkyne cycloaddition reaction (CuSAC) has profound practical benefits including broad substrate tolerance and high regioselectivity, but it requires prior preparation of sydnone substrates. Taran and coworkers expanded the potential of the CuSAC reaction using a one-pot protocol yielding sydnone crude products that can be directly applied to the CuSAC without the need for further purification.³⁸⁷ The expeditious use of readily available arylglycines as starting material for the conversion of the nitrosylation product followed by cyclization in the presence of TFAA leads to crude sydnone in one pot (Scheme 37A). In the same pot, the construction of 1,4-pyrazoles via CuSAC is attained in decent yield (Scheme 37A).³⁸⁷ The scope of this one-pot procedure was then investigated on numerous electron-rich or electron-poor N-aryl sydnones which, successfully contributed in this transformation. Despite the involvement of multi-precursors in one-pot, the 1,4-pyrazole was the only product formed with no trace of a 1,3-regioisomer detected (Scheme 37A).³⁸⁷

The Taran group unraveled the limitation of CuSAC to synthesize 1,4-disubstituted pyrazoles by exploring the 4-position substitution pattern on the mesoionic sydnone ring (**Scheme 37B**). The series of C-4-substituted (Cl, Br, I, Ph, CF₃, CN, etc.) sydnones were screened for effective cyclization with the standard, phenylbutyne. The highest yielding results were observed for Cl and Br substituted sydnones, although with less regioselectivity. The optimization for exclusive 1,4-regioisomer was observed using the 10-phenanthroline derived **L-264** ligand. The one-pot procedure starting from bromination, followed by CuSAC, adds an advantage to this methodology. Further polyfunctionalized 1,4,5-pyrazoles were elegantly afforded via Suzuki cross-coupling. ³⁸⁸

The regioselectivity in CuSAC has always been a challenge, requiring proper ligand and catalyst selection. In 2015, Harrity and co-workers reported a new finding that highlights the importance of the Cu-promoter, e.g. Cu(OTf)₂ or Cu(OAc)₂, for regioselectivity (**Scheme 37C**). The Cu(OTf)₂ promoter provides 1,3-disubstituted pyrazoles, whereas Cu(OAc)₂ produces the corresponding 1,4-isomers. Both experimental and theoretical studies reveal that Cu(OTf)₂ promotes the cycloaddition of sydnones and alkynes through a Lewis acid-assisted activation of the mesoionic compound. In contrast, Cu(OAc)₂ undergoes in situ reduction to CuI by Glaser-coupling of the alkyne, and the cycloaddition proceeds by a Cu(I) acetylide, leading to pyrazoles with complementary regiochemistry.

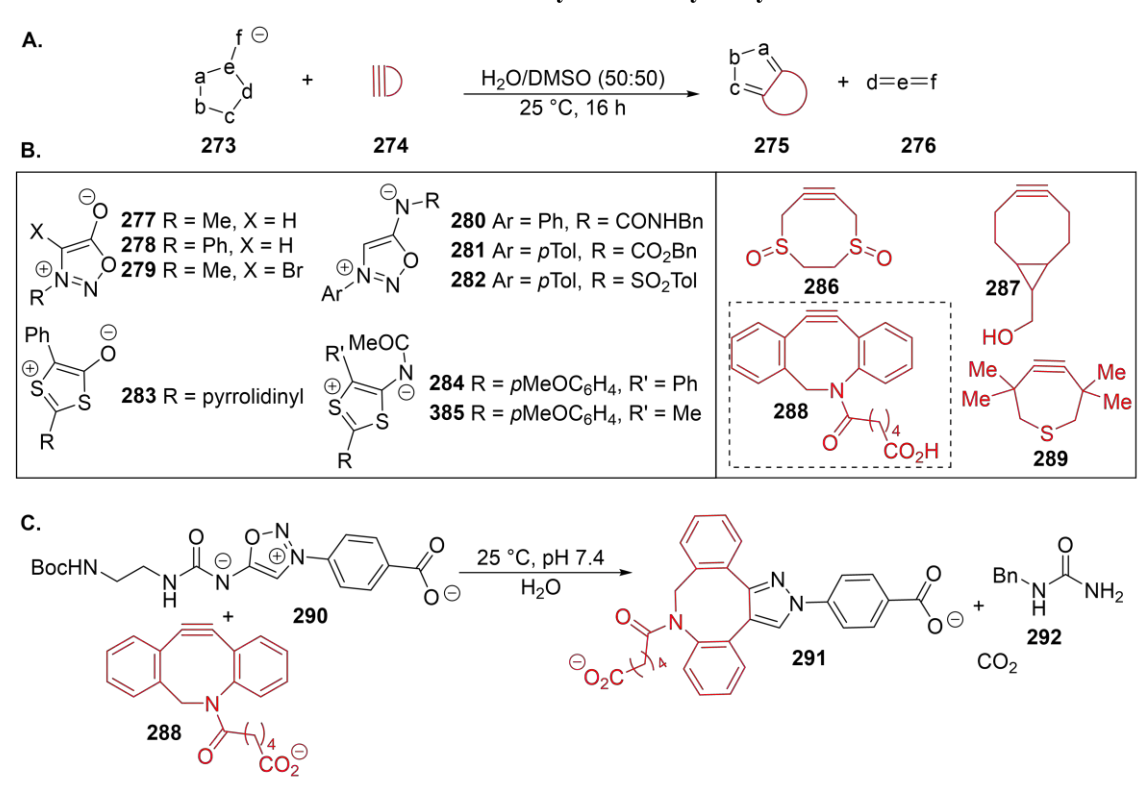
In 2017, Brase and coworkers reported on CuSAC by substituting for the alkyne reactant with an ynamide, delivering substituted aminopyrazoles (Scheme 37D).³⁹⁰ However, the suitability of ynamides for this protocol was compromised due to the high reactivity and susceptibility of these functionalities to hydrolysis in the presence of the various Cu-complexes. Similar to the Taran methodology, this protocol proved to be efficient for CuSAC chemistry involving terminal ynamides but appears to much more limited for internal ynamide substrates.

Weng and coworkers reported a more general and practical approach for synthesizing 4-trifluoromethylated pyrazoles with 2-bromo-3,3,3-trifluoropropene as the key synthetic building blocks for the CuSAC chemistry (**Scheme 37E**).³⁹¹ Notably, the trifluoromethylated pyrazole scaffold is found in drugs such as Celecoxib,³⁹² penthiopyrad,³⁹³ and Razaxaban,³⁹⁴ which demonstrates the diverse biological activity and agrochemical importance of this compound class.

3.1.2.1.2. Hit Elaboration: Strain-Promoted Sydnone-Alkyne Cycloaddition Reaction

A novel biorthogonal 'click' reaction involving strained alkynes and iminosydnones was reported by Taran and coworkers (**Scheme 38A**).³⁹⁵ In total, 25 different mesoionic compounds and 4 different strained alkynes were reacted in H₂O-DMSO and screened using LC-MS (**Scheme 37B**). Iminosydnones **280-282** and strained alkyne combinations proved to be best suited for this 'click' reaction, providing pyrazole products (**Scheme 38A & B**). From this, sydnone **290** was further investigated with alkyne **287** and **288** (**Scheme 38C**) and later used for the trans-tagging of proteins under physiological conditions.³⁹⁵

Scheme 38. Hit Elaboration of Strain-Promoted Sydnone-Alkyne Cycloaddition Reaction



A. General scheme of the biorthogonal 'click' reaction of strained alkynes and mesoionic compounds. **B.** Structures of mesoionic compounds screened in the study **C.** Best iminosydnones reacted with strained alkynes.

3.1.2.1.3. Hit Elaboration: Ir-Catalyzed Azide-Alkyne Cycloaddition-Scope and Limitations to Access Diverse Triazoles.

An iridium-catalyzed cycloaddition reaction between azides and 1-bromoalkynes has been discovered using a high throughput screening approach by Taran and co-workers. Further investigation of this approach also led to a single regioisomer, 1,5-disubstituted 4-bromo-1,2,3-triazoles, in the presence of [Ir(cod)Cl]₂ (Scheme 39A). Earlier work by Fokin and coworkers

Scheme 39 Ir-Catalyzed Azide-Bromoalkyne Cycloaddition Reaction

triazoles. 396 Mechanistic studies on the iridium-catalyzed cycloaddition reaction support a pathway

Scheme 40. Ir-Catalyzed Azide-Thioalkyne Cycloaddition-Reaction

A. SR'
$$2 \text{ mol}\% [\text{Ir}(\text{cod})\text{Cl}]_2$$
 $\text{DCM}, N_2, \text{rt}, \text{overnight}$ R'S 300 R SR' SOO R'S 300 R'S R'S

reported on a copper-catalyzed cycloaddition involving azides and iodoalkynes, furnishing the 5-iodo-triazoles.¹⁴ Here, a rutheniumcatalyzed process involving the cycloaddition between azides and internal alkynes, leads to 1,4,5-trisubstituted triazoles. 14 The limitation of Fokin's protocol is that it relies on electronically unsymmetrical alkynes donors to gain exclusive regioselectivity. 14 limitation has been unraveled by Taran and co-workers describing the formation of 1,5-4-bromotriazoles disubstituted using [Ir(cod)Cl]₂ and aromatic and aliphatic bromoalkynes.³⁸¹

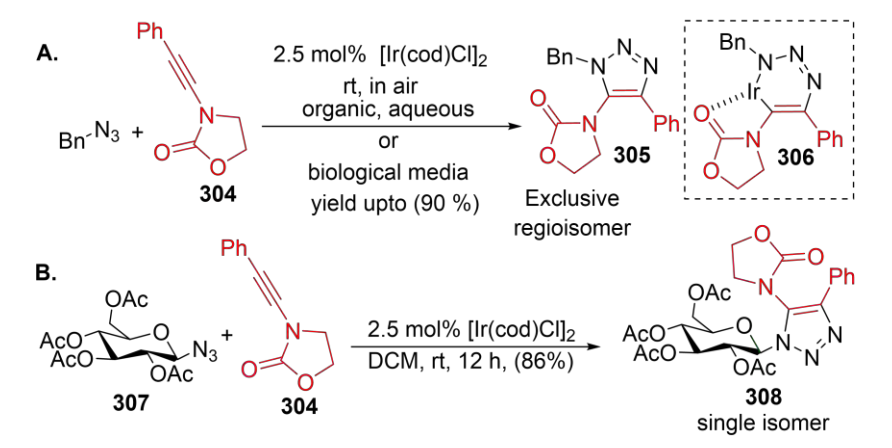
The scope of the azide/bromoalkyne cycloaddition mediated by [Ir(cod)OMe]₂, was examined. The transformation was found to yield a diverse array of 4-bromo-1,5triazoles in reasonable to excellent vield **39A**).³⁹⁶ (Scheme Furthermore, functionalization 1,5-disubstituted of bromotriazoles was possible, affording access a repertoire of highly substituted involving electrophilic activation of the alkyne with the iridium catalyst, followed by complexation with the azide, leading to 296 (Scheme 38B).³⁹⁶ The stabilized iridium carbenoid complex (297b) further undergoes a Cope-like rearrangement providing intermediate 298, followed by reductive elimination, giving triazole 294 with the expected regiochemistry.³⁹⁶

The ability to include internal alkynes cycloaddition azide-alkyne (AAC) in chemistry will continue to remain a challenge. In this regard, the advances of Sun and coworkers are notable. These workers observed that the iridium-catalyzed AAC reaction between electron-rich thioalkynes and azides at room temperature and in air furnishes and substituted triazoles with fully good **40)**, 397 regiochemical control (Scheme Mechanistically, they propose coordination of the alkyne and the azide via its internal

nitrogen to the iridium catalyst, resulting in complex 301. Intermediate 302, arising from oxidative

cyclization, may be stabilized due to sulfur coordination to the iridium center. Presumed reductive

Scheme 41. Ir-Catalyzed Regioselective Azide-Alkyne Cycloaddition Reaction and Application in Biological Media

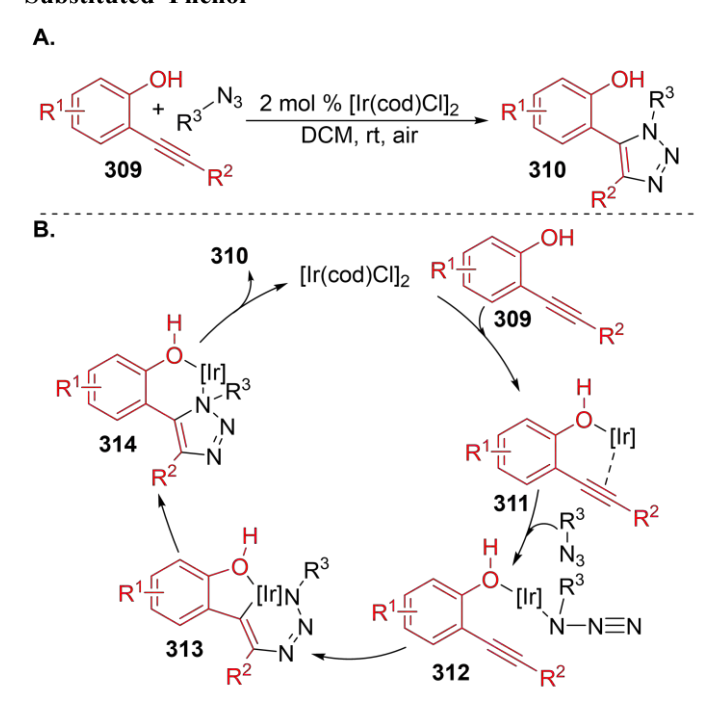


elimination from **302 then** provides triazole product **300** and regenerates the Ir(I) catalyst for another cycle. Various internal thioalkynes and azides successfully participate in this chemistry, leading to a diverse set of triazoles, albeit in modest yield.³⁹⁷

A similar observation was made by Song and coworkers in which an ynamide-alkyne cycloaddition mediated by

Ir proceeded regioselectively (**Scheme 41**) under conditions similar to those reported by Sun and coworkers (**Scheme 40**). Herein, the coordination of the ynamide carbonyl group with iridium

Scheme 42. Ir-Catalyzed Regioselective [3+2] Cycloaddition Reaction of Azide With Ortho-Alkynyl Substituted Phenol



may underlie the high regioselectivity for 5-amido-triazoles. The bioorthogonality of the cycloaddition reaction was tested under various biological conditions (Scheme 41A). 398 The reaction proved to be highly efficient in phosphate-buffer across a pH range of 5.7-8.0.³⁹⁸ The reaction also worked well in DMEM (Dulbeccos's modified eagle medium), as well as in cell lysates frequently used to simulate biological environments. Excellent yields and regioselectivity for the cycloaddition reaction were observed even in biological media including 50% normal mouse serum.³⁹⁸ The highly efficient cycloaddition was further applied to synthesize nonnatural carbohydrates using glycosyl azides and ynamides (Scheme 41B).³⁹⁸

Cui and coworkers also studied the Ir-catalyzed AAC to achieve regioselective access to diverse triazoles

using *o*-alkyne-substituted phenols (**Scheme 42A**).³⁹⁹ The hydroxyl group on such o-alkynyl phenols proved to be a crucial factor for regioselectivity, leading to the fully substituted 1,2,3-triazole products.³⁹⁹ These workers suggest initial coordination by the hydroxyl group to the Ir center, followed by coordination of the triple bond, leading to complex **311** (**Scheme 42B**).³⁹⁹ Subsequent intramolecular cyclization would give iridium complex **313**, followed by rapid

reductive elimination to triazole **310** with concomitant Ir(I) catalyst regeneration via **314** (Scheme **42 B**). The hydroxyl group also provides a handle for late-stage functionalization. The protocol was also tested in various biomimetic environments (phosphate-saline buffer, DMEM, and fetal bovine serum) and proved to be highly efficient suggesting a high level of biorthogonality for this chemistry. ³⁹⁹

3.1.2.2. Initial Screening Hit: Pyridine Ylide-Nitrile Cyclo-Condensation

The 1,3-dipolar cycloaddition between pyridinium salts and aromatic nitriles is one of the novel

Scheme 43. Rh-Catalyzed Pyridine Ylide-Nitrile Cyclo-Condensation

discovered hits high-throughput immunoassay screening (Scheme 34B).³⁸¹ Of the hits discovered during this screen, this cycloaddition displayed kinetics the fastest **5**).³⁸¹ (Table Mechanistic analysis on this novel 1,3-dipolar cycloaddition has not

yet been reported, but it is reasonable to hypothesize that the coordination between the Rh catalyst and triple bond of the aromatic nitrile leads to nitrile activation. This allows attack by the nucleophilic carbon, via a pyridinium ylide, upon the electrophilic nitrile carbon. Tautomerization followed by C-N bond formation/re-aromatization leads to fused azacyclic product. Although yields were moderate due to rapid degradation of the pyridinium substrates under the reaction conditions, four hits were reported (**Scheme 43**). There is a need for further mechanistic studies on this 1,3-dipolar cycloaddition between pyridinium salts and aromatic nitriles. Such

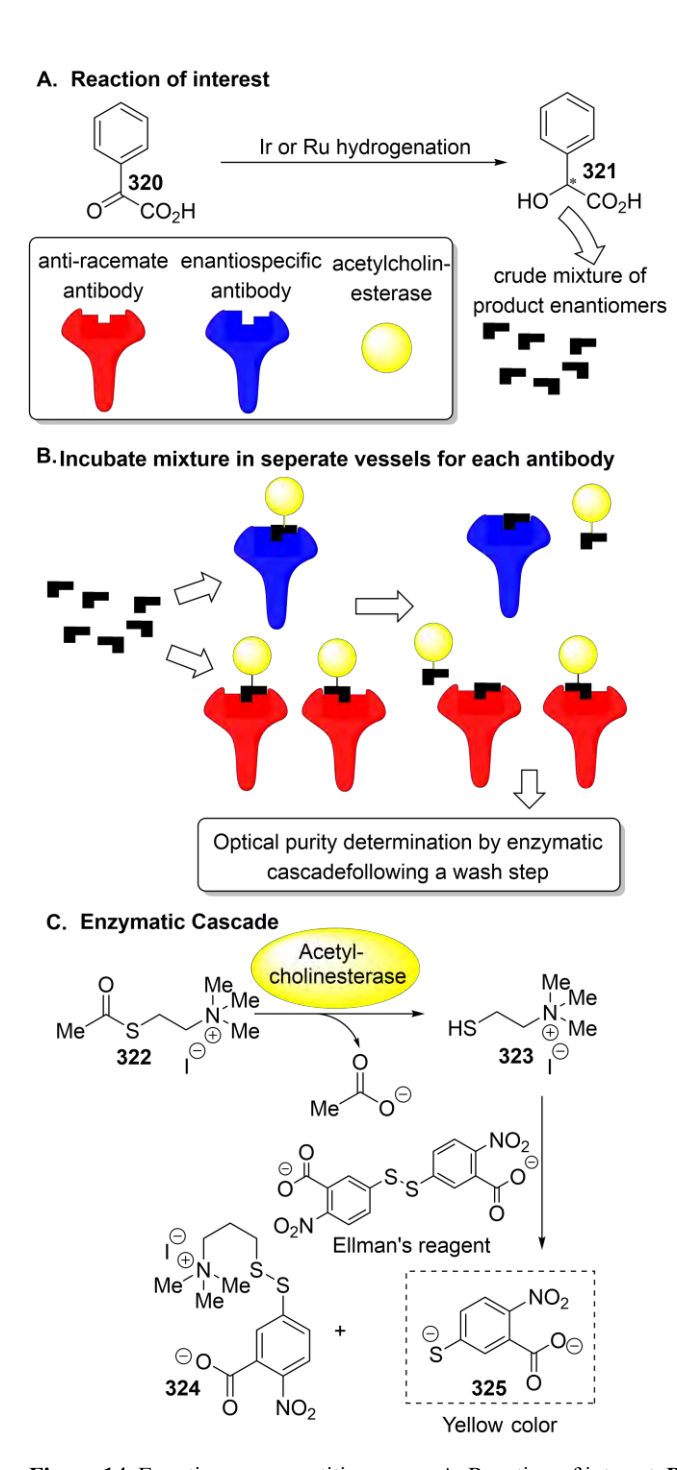


Figure 14. Enantiomer competition assay. **A.** Reaction of interest. **B.** Incubation mixture in separate vessels for each antibody. **C.** Enzymatic cascade for optical purity determination by assaying for acetylcholinesterase activity with an Ellman reagent derived colorimetric visualization screen by forming 5-thionitrobenzoic acid with absorbance maxima at 412 nm.

investigations, particularly those varying the metal have the potential to further optimize yields and substrate compatibility.

3.2. Immunoassay Screening for Enantioselective Catalysts

3.2.1. High-Throughput Screening of Enantioselective Catalyst by Immunoassay-Two Competitive Cat-ELISAs

Antibodies can also be employed in a competition-style assay to determine the conversion and enantioselectivity of a reaction. In pioneering work done by Mioskowski, Wagner and co-workers, a mAb-based assay was employed to study the transition metal-catalyzed hydrogenation of benzoylformate to mandelate. 400 This method availed itself of one monoclonal antibody that binds selectively to the the (S)-enantiomer of the product, but also another antibody that binds racemic product nonselectively. The screen begins with a pre-bound product-enzyme conjugate that is only displaced upon exposure to the desired product formed upon metalcatalyzed reduction. (Figure 14B). Reaction success can be monitored by placing the crude reaction product in the screening well alongside acetylcholinesterase (AChE) whereby enzyme-product conjugate displaced by the product (Figure 14B). Following a wash step, only the AChE enzyme present in the screen will be attached to the conjugate that has not been displaced from the antibodies (Figure 14B). Thus, lower amounts of AChE activity correspond to higher amounts of product formed in the reaction. This reporting enzyme catalyzes acetylthiocholine cleavage, producing a thiocholine anion that itself

reacts with Ellman's reagent to release 3-carboxy-4-nitrophenylthiolate anion. Upon formation of this anion, an increase in absorbance at 414 nm can be visualized (**Figure 14C**). 401

A calibration curve was established by measuring the absorbance readings for a series of known product concentrations. This curve was then used to estimate reaction product yield for a set of catalytic conditions. To estimate the corresponding *ee* values, the same procedure is was performed employing the antibody specific for the (*S*)-antipode of the product. By comparing data for the total product (rac-antibody screen) to that for (*S*)-product (anti-*S* antibody screen), the enantioselectivity could be conveniently estimated. For this assay, it was found mAb-15 binds both enantiomers with a relatively low affinity [apparent K_d values of 6.4 mM for the (*S*)-enantiomer and 7 mM for the (*R*)-enantiomer]. On the other hand, monoclonal antibody mAb-8 was found

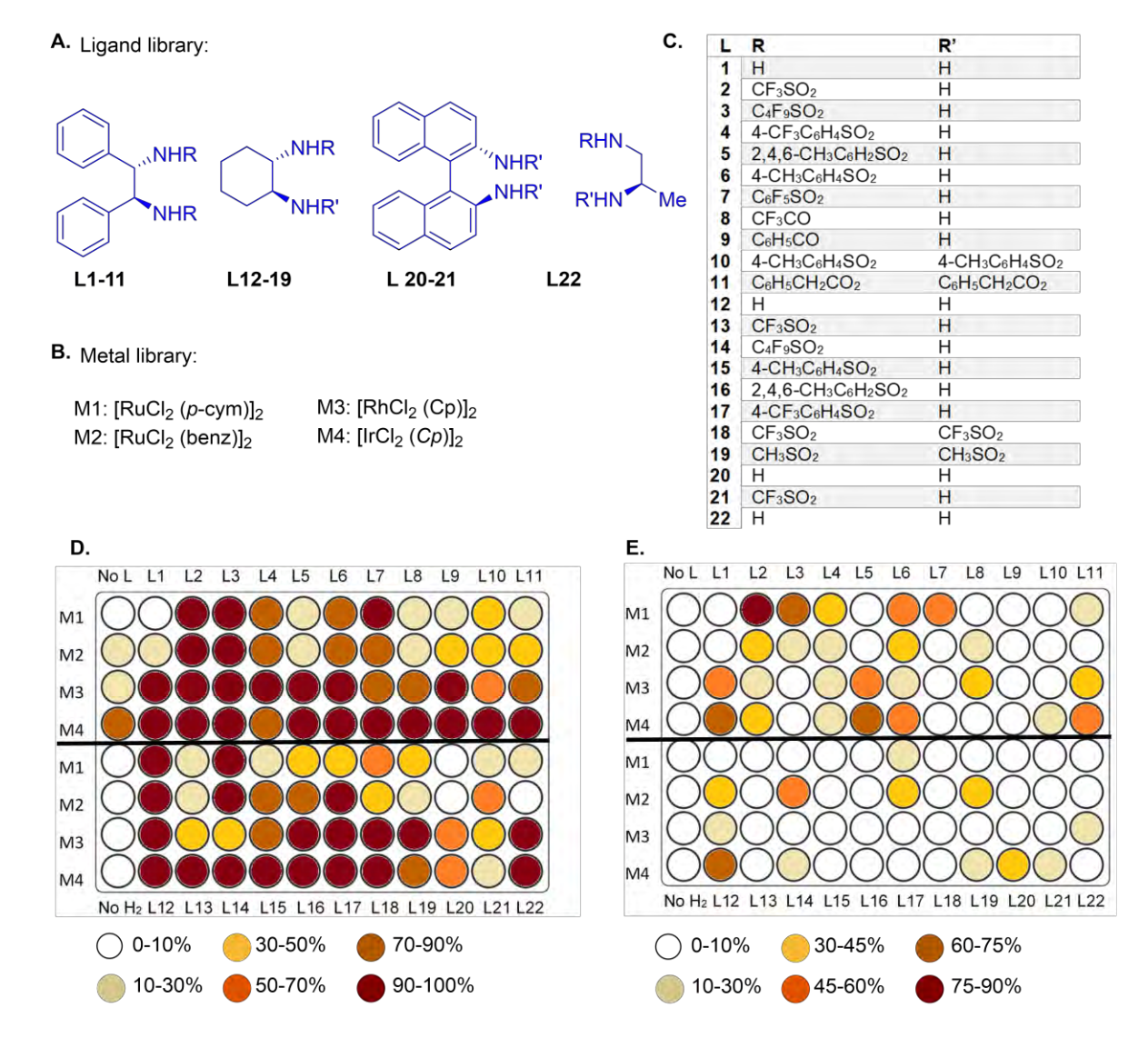


Figure 15. Immunoassay screening for enantioselective catalyst. **A.** General ligand scaffold library. **B.** Metal library. **C.** List of ligands with R and R' variations. **D.** Yield % of reactions for catalyst screening. **E.** % ee of reactions for catalyst screening.

to be selective for the (S)-enantiomer with a relatively high affinity (apparent $K_d = 55 \mu M$). ⁴⁰⁰

The screen, which studied various d⁸- and d⁹-metal catalyst candidates (**Figure 15B**) with different chiral diamines (**Figure 15A & C**),⁴⁰⁰ was conducted in a 96-well plate format, allowing a total of 192 reaction conditions to be screened. The reactions were performed using peroxide and

TEA as the hydrogen source and chiral catalyst (1.6 mol%) in DMF. The reaction is then diluted with assay buffer and transferred to the microtiter plate coated with mAB 203 and left to incubate for three hours, followed by an additional wash with buffer and then addition of a solution of the anti-tag 2 (mAb 46)-AChE conjugate. This protocal led to reproducibly good estimates of product ee as confirmed by chiral HPLC. The screen reported the best results for cases where peroxide and TEA were present and the best catalyst-ligand combination was found with M1 and L2, respectively (**Figure 15D & E**). 400

This is a powerful method, once established, as it provides stereochemical information rapidly in a highly parallel format. That said, the assay development stage is significant and requires some serendipity. Namely, two antibodies are required to get information on both yield and enantioselectivity. Interestingly, as alluded to above, for the study of the enantioselective reduction of α -keto acids by hydrogen transfer, the Wagner-Mioskowski group discovered one antibody that binds both enantiomers of the α -hydroxy acid product and another that selectively binds just one enantiomer of the product. Given the high levels of enantio-discrimination of antibodies, in general, it seems reasonable that one will be able to find monoclonal antibodies that bind each enantiomer of the product well, in most cases, particularly if one uses highly enantio-enriched haptens for selection, making it reasonable to expect that this technique can be expanded to a more diverse array of reactions in screening for both conversion and enantioselectivity.

4. SINGLE ANTIBODY-BASED SCREENING

4.1. A Remarkable Antibody-Based Optical Sensor: Stilbenoid Ligand-Antibody Co-Crystal Structure Provides Insight into Tryptophan Fluorescence Mechanism.

Janda and coworkers established the first example of which we are aware of a single antibody method for the screening of enantioselectivity for a catalytic asymmetric reaction of interest. A reaction is run and the chiral product incubated with the sensing antibody and the fluorescence is measured as a way of estimating ee. This method relies on the discovery of an antibody possessing two invaluable attributes

Figure 16. Structure of mAb 19G2-bound ligand

for this type of screening application; namely (i) the bound Ab-ligand complex exhibits fluorescence and (ii) the Ab shows significant enantioselectivity for ligand binding. Indeed, the system discovered by Janda and coworkers exploits the photophysics of the Ab-ligand complex resulting in a remarkable antibody-based optical sensor. This sensor is able to report directly on the dynamic interplay of specific ligands with protein residues within an antibody binding pocket. 402,403

This variant of biomacromolecular screens emanated from a fortuitous observation made by the Janda team of blue fluorescent behavior stemming from the interaction between a *trans*-stilbene hapten ligand and series of monoclonal antibodies. Specifically, the Janda group studied a library of monoclonal antibodies (mAb) raised against a *trans*-stilbene hapten 326.⁴⁰⁴ Subsequent crystallographic analysis established the chemical environment of the mAb 19G2 binding pocket with bound ligand 326 (Figure 16) at 2.4 Å resolution and 4 °C (277 K) (PDB 1FL3). One sees that the *trans*-stilbenoid ligand is likely π -stacked with tryptophan residue (Trp103) (Kabat numbering) (Figure 17A).⁴⁰⁴ The hydrophobic *trans*-stilbenoid-binding pocket is deep within the antibody, between the V_H and V_L domains (Figure 17B). The key residue, Trp103, typically participates in contacts between two domains that stabilize the antibody fold. For Trp103 to form

an exciplex with the *trans*-stilbenoid ligand, the interface between the two domains must rearrange. This interdomain distortion generates a surface depression that creates a portal to the deep binding pocket (**Figure 17A**).

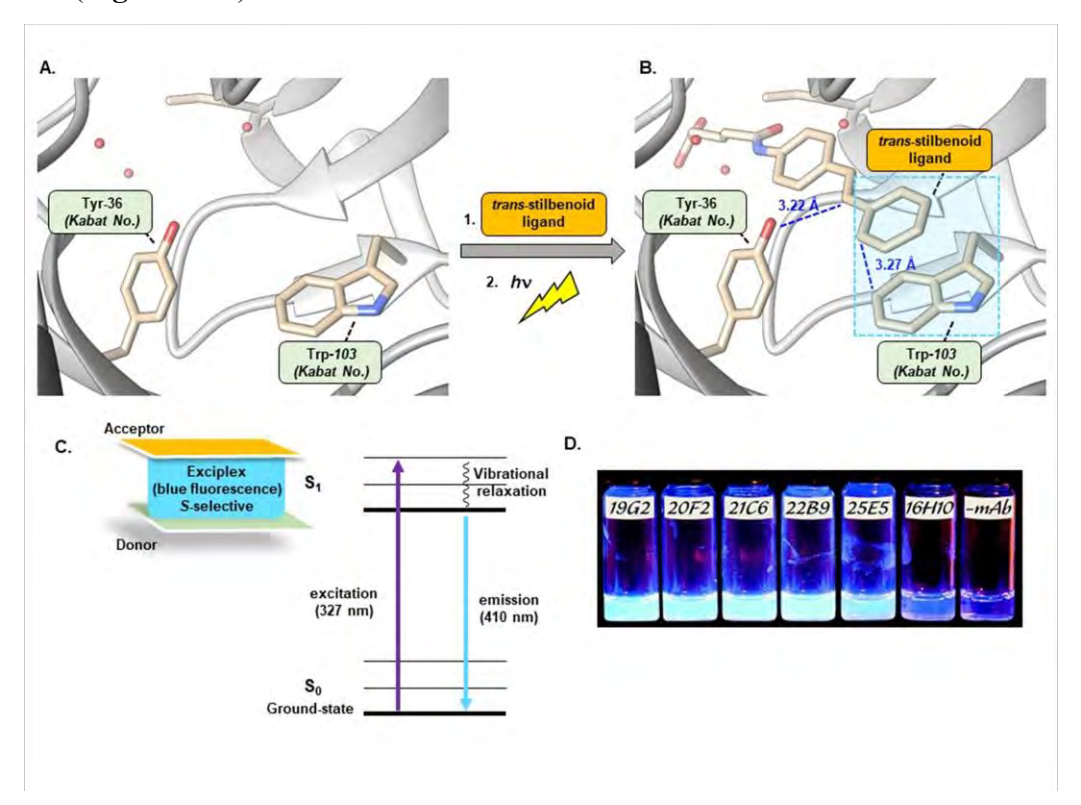


Figure 17. Blue fluorescence in mAb-ligand complexes. A. View of the unbound structure of mAb 19G2 (PDB 1FL3). B. View of *trans*-stilbenoid ligand 317 bound to mAb 19G2 showing apparent face-to-face π -stacking interaction, potentially leading to exciplex formation & blue fluorescence upon excitement (PDB 1FL3). C. Jablonski diagram illustration of electron transfer with excitation at 327 nm and emission at 410 nm upon the binding of the ligand. D. Members of the Janda mAb library bound to the *trans*-stilbenoid ligand showing the degree of blue fluorescence as a function of mAb. Panel D republished with permission from ref 404. Copyright © 2000 The American Association for the Advancement of Science.

Upon UV irradiation in solution, the mAb 19G2 complex displays blue fluorescence (**Figure 17A**). The origins of this blue fluorescence are thought to lie in the positioning of the distal phenyl ring of the stilbenoid ligand being involved in a face-to-face π-stacking interaction with the indole ring of the tryptophan-103 residue.⁴⁰⁴ The crystal structure of the mAb 19G2 complex at low temperature (100 K) was unchanged compared with the structure at 277 K, which indicates that main chain and side chain atoms of the antibody active site and the atomic coordinates of the bound stilbene are rather fixed.⁴⁰⁴ This structure establishes the key role played by Trp103 in the observed blue-fluorescence arising from presumed exciplex formation with the bound *trans*-stilbenoid ligand.⁴⁰⁴

4.2. Discovery of Antibody Showing Enantioselective Fluorescence with Stilbenoid Analytes

As mentioned, the Janda team developed a series of monoclonal antibodies (mAbs) prepared against the *trans*-stilbenoid hapten **326**; they then recognized that this might be the basis of a screen for enantioselective catalysis. ⁴⁰⁴ The authors discovered that upon binding such stilbenoid species, the antibody coded mAb 19G2 produced blue fluorescence in high quantum yield (excitation 327).

nm; emission 410 nm $\phi f = 0.78 \pm 10\%$). Follow-up work by Janda and co-workers in monoclonal antibody fluorescence led to the discovery that this same antibody could show significant

Figure 18. Blue-fluorescent mAb 19G2 ligands for asymmetric non-proteinogenic AA synthesis.

enantiodiscrimination. Thus, *trans-(S)-327* **(Figure 18)** upon binding to the mAb, afforded bright blue fluorescence whereas its enantiomer failed to give much discernable fluorescence.⁴⁰³

Later, Janda and co-workers explored the enantioselective fluorescent sensing technique to evaluate a pool of chiral transition metal-salen catalysts in the asymmetric epoxide opening reactions utilizing blue fluorescent antibody

sensor 19G2.⁴⁰² Enantiomerically pure (*R*)- and (*S*)-phenethylamine were coupled with different stilbene chains (**328-331**), and fluorescence properties were measured by utilizing the mAb 19G2

Figure 19. Structures of trans-stilbene tagged phenylethylamines.

fluorescence intensity of S-327 enantiomer is 1.2 times compared to its R-enantiomer yet the stereocenter is eight bonds apart from the stilbene moiety. Compounds bearing shorter spacers between the stilbene moiety and the stereocenter (328-331) showed less or very weak fluorescence. 402

The rationale put forward for the observed weak fluorescence was based on α -

Figure 20. Structures of trans-stilbene tagged chiral amines.

phenylethylamine moiety, which in the case of compound **328** is outside the binding pocket of 19G2 and may affect the conformation of stilbene moiety, leading to the diminished fluorescence intensity observed. This experiment led to a more detailed study of variety of chiral amines attached to *trans*-stilbenoid tags **332-337** (**Figure 20**). The (*S*)-enantiomer of **337** showed 3.1 times the fluorescence of its (*R*)-enantiomer counterpart, when complexed with 19G2.⁴⁰² The dissociation constant *K*_D for the (*S*)-enantiomer was 31 μM compared to 6.4 μM for the (*R*)-enantiomer. However,

the magnitude differential in these dissociation constants is not sufficient to explain the difference

in fluorescence emission, which is based on the experiment performed where an excess of **337** enantiomer is incubated with 19G2.⁴⁰²

4.3. Chiral Sensing with the Blue Fluorescent Antibody for Enantioselective Metal-Salen Catalyzed Epoxide Opening

The Janda group explored Jacobsen's catalyst in the asymmetric opening of epoxide (Scheme 44)

Scheme 44. Catalytic Asymmetric Opening of Epoxide Using Jacobsen Catalyst for the Synthesis of *Trans*-Stilbene Tagged Amino Alcohol

and performed a screening of the catalyst by using the blue-fluorescent antibody mAb 19G2. The racemic epoxide was treated with TMS-azide in the presence of metalsalen catalysts. This provided azido alcohol in four different enantiomeric purities and these products further converted to **341** by attaching trans-stilbene moiety. 402

To establish a calibration curve. standard chiral mixtures of defined enantiomeric purity, >99.99% ee, 50% ee, 0% ee each of (R)-337, and of (S)-337 were prepared as solutions in DMF. A standard was calibration curve established measuring fluorescence as a function of ee with 19G2. The results were cross-checked by comparing with chiral HPLC, showing good reliability of the fluorescence sensing method. Not surprisingly, the classical Jacobsen cobalt-salen catalyst 344 gave the best results with this test substrate, showing >99% ee with the new Ab-based readout, solidifying the technique. 402

4.4. Application of Blue-Fluorescent Antibody to Chiral PTC Library Screening for Asymmetric Unnatural Amino Acid Synthesis

Chiral phase-transfer catalysts (PTCs) based upon cinchona alkaloid-derived quaternary ammonium salts have been workhorses for methodology development in the areas of asymmetric C-C and C-heteroatom bond formation. 405,406 Optimization studies of such reactions involving

Scheme 45. Application of mAb 19G2 for Catalyst Screening: Using Cinchona Alkaloid-Based PTCs for Unnatural AA Synthesis

chiral phase transfer catalysts (PTCs) challenging are including multiple variables catalyst structure. solvent. temperature, and metalcounterion must be examined. Approaching a similar task in 1997. Reetz and co-workers developed one of the first high throughput screening (HTS) methods for the parallel determination of reaction ee values using UV/Vis spectroscopy. 407 Other such HTS methods include hose using IR-thermography, circular dichroism, capillary electrophoresis, fluorescence, mass spectrometry, chemo-sensing, competitive immunoassays, and enzymatic methods have also been utilized. 41,42,61,68,337 That said, most of these HTS methods have been used to screen the asymmetric reduction or hydrolysis reactions.

Against this backdrop, Janda and coworkers set out to be the first to demonstrate such a screen for a single monoclonal antibody platform, using their mAbs 19G2 for discriminating enantiomers. The study revealed that mAbs 19G2 shows high selectivity for chiral *trans*-stilbenoid-derived amino acid ester (*S*)-327 (Scheme 45). The (*R*)-antipode of 327 does bind to 19G2, but only the 19G2-(*S*)-327 complex exhibits blue-fluorescence. Therefore, 19G2 was further utilized for screening the library of derivatized PTC cinchona alkaloids for the asymmetric α -alkylation (Scheme 46) by using a fluorescence plate-reader format for the rapid estimation of alkylation product *ee* values.

A library containing 35 cinchona alkaloid ammonium salts was synthesized in high yield and with high purity by routine synthesis (**Scheme 46**). The derivatives of cinchona alkaloid ammonium salts were screened for the alkylation reaction of the N-(diphenylmethylene)glycine methyl ester **337** with 4-bromomethyl-*trans*-stilbene (**Scheme 45**). The benzophenone Schiff's base N-protecting group in **348** was then cleaved by mild acid hydrolysis, providing the mixture of enantiomers (*S*)-**327** and (*R*)-**327**. The *ee* values of the 35 product mixtures were determined using a calibration curve prepared by measuring the fluorescence of mixtures of (*S*)-**327** and (*R*)-**3277** of defined ee. The fluorescence values for each of the 35 product mixtures were obtained, and the corresponding *ee* values were calculated. The accuracy of HTS was cross-checked by randomly selecting 10 samples from HTS screening and analyzing further by chiral HPLC. The fluorescence sensor and HPLC measurements were quite comparable, showing agreement within 10%.

Scheme 46: Preparation of a Cinchona Alkaloid-Derived Catalyst Library

The blue fluorescent mAb sensor method helped to identify highly performing chiral catalysts competitive with the best previously reported chiral PTCs for such chemistry in the literature. This method has advantages of (i) sensitivity, allowing for fluorescence detection on a small amount of sample (10 nmol) and of (ii) throughput, allowing rapid ee screening in microtiter plate format and of (iii) high accuracy. It remains to be seen how many antibodies can be discovered or engineered to display this fascinating and useful property of ligand-induced fluorescence, presumably via exciplex formation, and to do so with a high level of enantiodiscrimination as well. This sort of sensing is likely to function best for reactions that involve products possessing aromatic rings, systems that might interact with tryptophan residues in the sensing Ab. The Janda work with blue-fluorescent mAb 19G2 certainly sets a valuable and informative precedent for future research in this direction.

5. Nucleic Acid-Based Screening Methods

5.1. DNA-Templated Methods

In the past decade, advancements in DNA-based technology have been pivotal for research in both the reaction discovery enterprise and in the chemical biology/medicinal chemistry space. For the former area, both DNA-templated reactions and DNA-encoded reaction technology have played a major role and both fall squarely under the purview of this review. For the latter area, DNA-encoded library (DEL) technology looms large and has had a profound effect on both academic and pharmaceutical industry research laboratories. The remarkable efforts in the DEL area are, in turn motivated by the success of chemical biology in teasing out new targets or uncovering new motifs for binding to established

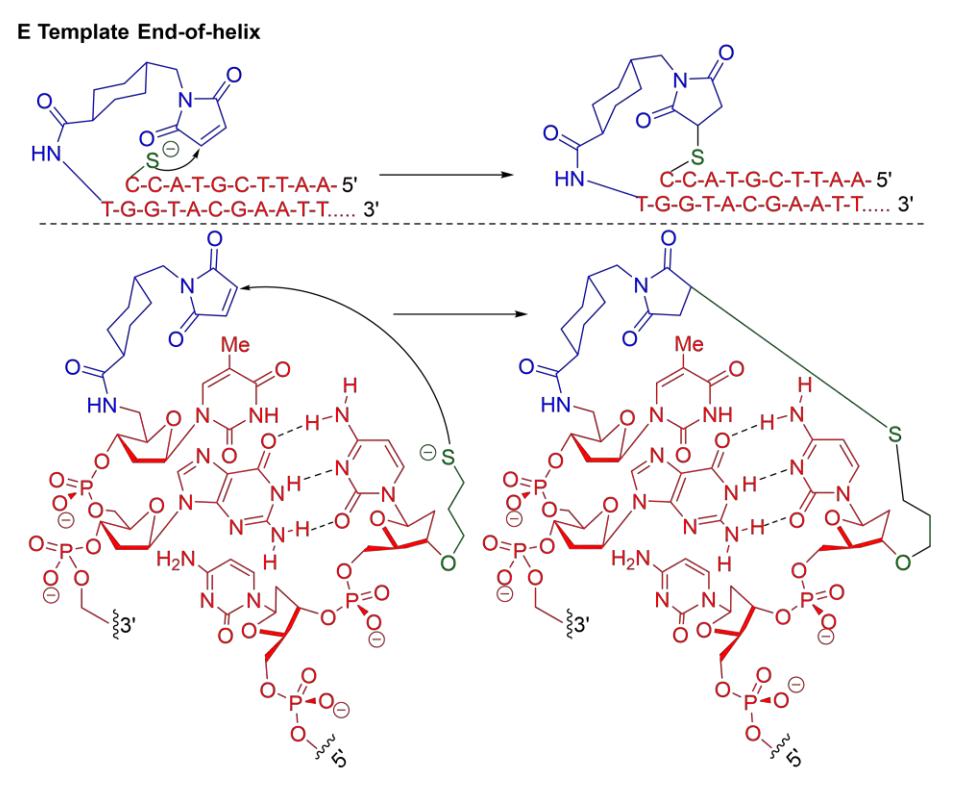


Figure 21. Synthesis directed by end-of-helix E template. Representation of hydrogen bonding interaction of base pairs.

targets. Indeed. the growth in DEL activity parallels the rise in the use of chemical biology probes to better understand disease progression and, identify potential leads in the development of new pharmaceutical candidates, many of which act on various biochemical pathways.408 Advantages using these DNA technologies, general, include the ability

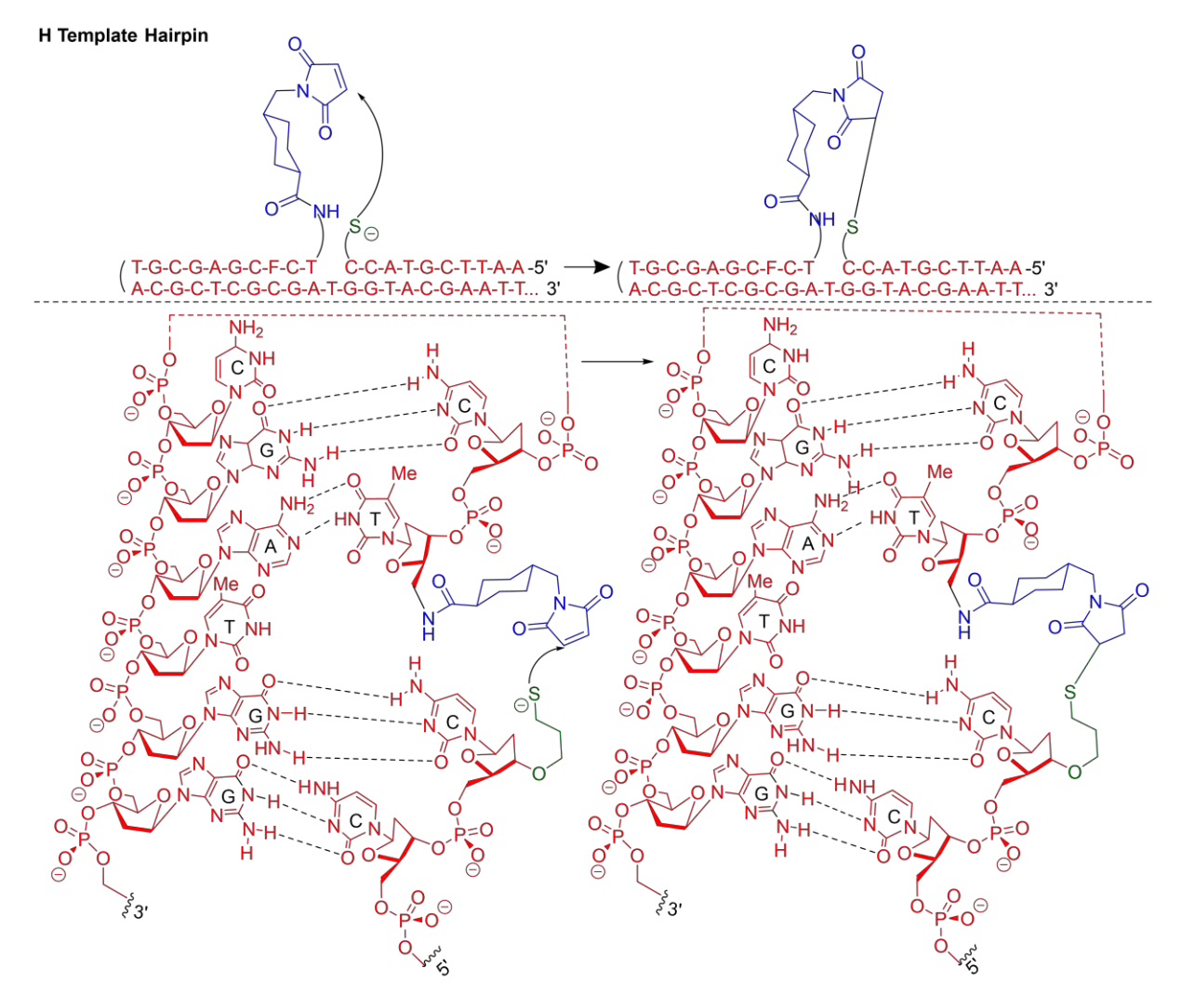


Figure 22. Synthesis directed by hairpin helix H template. Representation of hydrogen bonding interaction of base pairs.

sequence and amplify DNA at will. Also driving this field have been the notable advances in selection methods for small molecule discovery with an attached DNA sequence. 32,89,90,380,409-457

We begin this section on biomacromolecular technologies centered around DNA with a brief historical perspective. In 1992, Brenner and Lerner developed a solid-phase library, where selection occurred for an immobilized target. Unfortunately, this early example had the limitation of native conformational loss of immobilized targets. To improve upon this method, Liu and coworkers developed an Interaction-dependent PCR (IDPCR) selection method by utilizing DNA proximity to promote DNA hybridization of a self-priming hairpin. Moving on to a non-immobilized method, Li and coworkers developed a DNA-programmed affinity labeling (DPAL) selection. Here, a photocrosslinking moiety with the use of UV irradiation leads to a covalent attachment. A47,449,455 Other DNA selection methods that have been developed include encoded self-assembled chemical libraries (ESAC) by Neri and coworkers, Planton proximity ligation assays (PLA) by Landegren and coworkers and binder trap selection by the Vipergen biotechnology

company. 459,460 Extensive and informative reviews can be found in the literature on the development of amplified libraries of non-natural small molecules with the translation of DNA into synthetic structures. 89,90,461,462

5.1.1. Proof of Principle for Specific DNA-Encoded Reaction Pairs

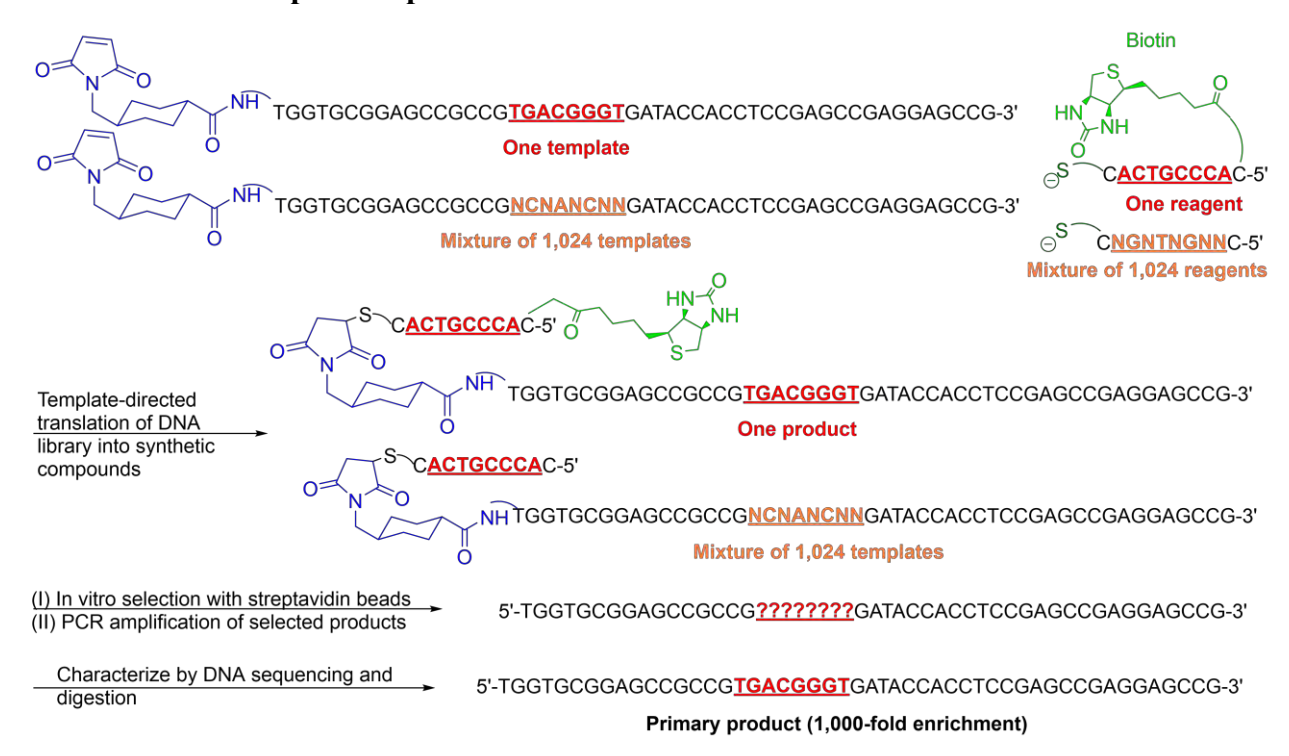


Figure 23. A model of translation, selection and amplification of synthetic molecules that bind streptavidin from DNA-encoded library. Synthesis directed by end-of-helix (E) DNA templates with 1,025 total starting materials and 1,025 total reagents.

Innovation of *in vitro* DNA-encoded libraries has been an enabling force for the reaction discovery process, increasing the probability of evaluating successful combinations of potential reactions among substrate library members. An early example from Liu and coworkers relied on DNA to direct chemical reactions by synthesizing reactants of interest bound to complementary DNA strands. This method was supported by solution-phase DNA-templated synthesis containing hairpin and end-of-helix templates. Both templates were covalently attached at the 5'-end to an electrophilic maleimide group and at the 3'-end to a nucleophilic thiolate group, thereby yielding thioether products (**Figures 21-22**). Set extensive work in this area, using end-of-helix templation, demonstrated the ability to orchestrate sequence-specific DNA-templated reactions with examples including S_N2 substitutions, additions to α,β -unsaturated carbonyl systems, and additions to vinyl sulfones with nucleophiles such as thiols and amines. Set $\frac{384,463,464}{4}$

Proof-of-principle DNAfor templated parallel synthesis was established whereby a library of 1,025 maleimide-linked E templates synthesized (Figure 23). Each contained an eight-base encoding region, and one of the sequences was chosen to code for a biotin attachment to the template.³⁸⁴ A library of thiolate-containing reagents linked to 1025 different oligonucleotides was also constructed. Bond formation leading to product was selected in vitro upon binding to immobilized streptavidin. This was followed by PCR-amplification and analyzed by restriction digestion, a process that cuts only the biotin-encoding These findings show the template. potential using DNA-templated synthesis study water-compatible organic reactions. 384,463,464

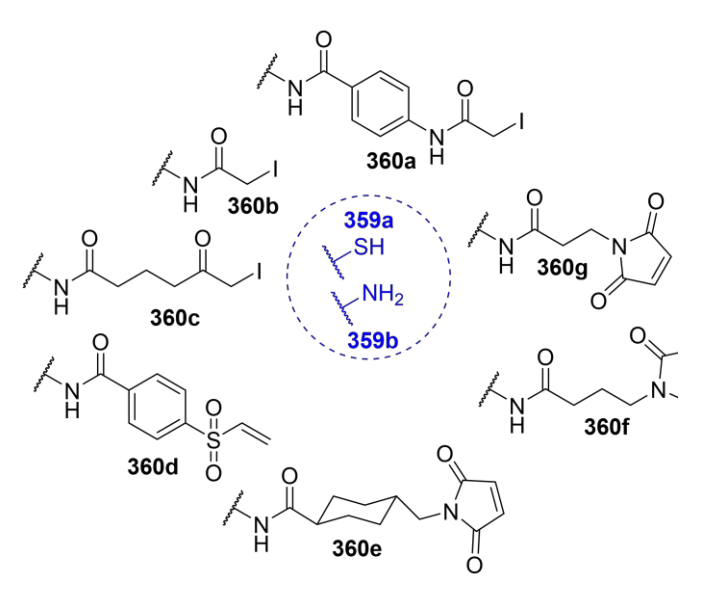


Figure 24. DNA-templated synthesis via nucleophilic and conjugate addition.

5.1.1.1 Reaction Scope with DNA-Templated Platform

Early on, Liu and co-workers explored a DNA-templated platform for reaction discovery, and chose to demonstrate this with conjugate addition and S_N2 reactions (**Figure 24**). This approach was piloted on DNA-templated electrophiles **360a-g** and DNA tagged thiolate reagent **359a** and proved to be successful.³⁸⁴ A DNA-templated amine **359b** was efficiently used as a nucleophile for conjugate addition on electrophiles **360d** and **360e** (**Figure 24**).-

Scheme 47. An Overview of DNA-Templated Bond Formation Across a Range of Chemistry

After establishing the viability of DNA templation to direct conjugate addition and S_N2 reactions, Liu and coworkers expanded the scope of DNA-templated synthesis to include a wide range of synthetic transformations. Thus, the Liu team explored DNA-templated reductive amination, peptide coupling, nitro-aldol, nitro-Michael, Wittig olefination, and 1,3 dipolar cycloadditions. The authors also reported on DNA-templated transition metal-catalyzed coupling reactions (e.g. Heck reaction) (Scheme 47). DNA templated synthesis was first utilized in a reductive amination reaction involving amine 361a and aldehyde 362a (Scheme 47) in the presence of NaBH₃CN (MES buffer, pH 6) and proved to be efficient.

A C-C bond forming nitro-aldol (Henry reaction) was explored in DNA-templated format, whereby nitro-alkane **361b** linked to a DNA template was reacted with template-linked aldehyde **362b**, giving expected product **363b** (**Scheme 47**) with high sequence specificity at pH 8.5 and 25 °C in [2-hydroxy-1,1-bis(hydroxymethyl)ethyl]amino-1-propanesulfonic acid (TAPS) buffer. Sequence-specific DNA-templated Wittig reactions were also examined. Here, coupling between phosphorus ylide **361c** and aldehyde **362c** (pH 6.0-8.0, TAPS buffer) afforded compound **363c** in excellent yield at 55 °C. The study also featured a 1,3-dipolar cycloaddition reaction between nitrone-linked reagent **361e** and vinyl sulfone **362f** as well as maleimide template **363e** at pH 7.5. The expected cyclic products **363e** and **363f**, respectively were each produced in moderate yield.

Liu and coworkers also applied a DNA-templated approach to a transition-metal-mediated Heck reaction in an aqueous medium at pH 5.0. Here, in the presence of Na₂PdCl₄, aryl iodide **361d** and olefin **362d** provided a moderate yield of **363d** (**Scheme 47**). Reaction scope was further expanded to different olefin-linked templates including maleimide, acrylamide, and vinyl sulfone functionalities. Reaction yields were improved by premixing two equivalents of P(*p*-SO₃C₆H₄)₃ per equivalent of Pd pre-catalyst. Control reactions containing mismatched sequences or lacking the Pd-pre-catalyst yielded no product.

DNA-templated peptide bond formation was successfully conducted by employing a water-stable activator, 4-(4,6-dimethoxy-1,3,5-triazin-2-yl)-4-methylmorpholinium chloride (DMT-MM) or 1-(3-dimethylaminopropyl)-3-ethylcarbodiimide (EDC), and *N*-hydroxysulfosuccinimide (sulfo-NHS) at pH 6.0 and 25 °C (**Scheme 48**). An optimized protocol

Scheme 48. DNA-Templated Amide Bond Formation

was established using chiral amines **364a-b** and chiral carboxylic acid **365c**. DNA-templated synthesis of diverse chiral amides is a striking feature of this novel DNA-templated approach.

5.1.2. Reaction Discovery Enabled By DNA-Templated Synthesis via Disulfide Cleavage Selection and DNA Microarray Readout

The first reaction discovery effort using DNA-templated chemical libraries was developed by Liu and coworkers (**Figure 25**). 409 The method relied on a selection-based approach via simultaneous

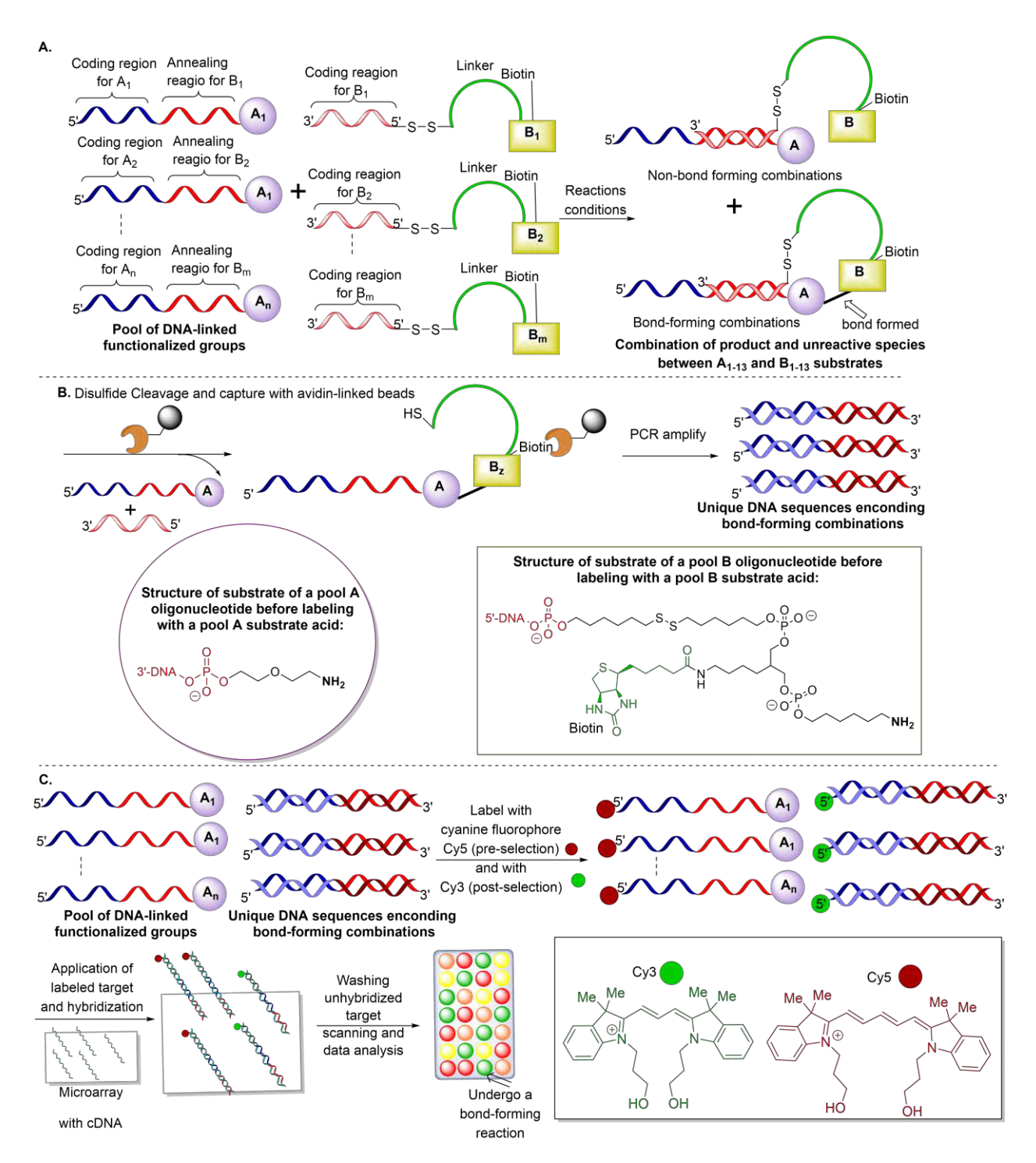


Figure 25. Reaction discovery enabled by DNA-templated synthesis and *in vitro* selection. A general one-pot selection method. A. Two pools of DNA-linked organic functional groups that associate each $A_n \times B_m$ substrate combinations with a unique DNA sequence, followed by bond formation and avidin pull-down of successful reaction. B. Structures pool A and B substrates before labeling with an acid functionalized substrate. C. Detection of bond-forming reaction by PCR amplification and DNA-microarray analysis. Spots that are significantly green suggest bond forming reaction, the yellow and orange represents the ratios of Cy3 to Cy5 fluorescence and red represent no reaction.

evaluation of a large population of molecules in a single aqueous solution to discover

all possible bond-forming reactions. This process, conducted at nanomolar concentrations, took place on a solid-phase platform where functional molecules can be easily separated from inactive variants. This discovery approach utilizes complementary DNA strands under templating conditions that lead to millimolar effective molarities, thereby enabling reactions at a significant rate. Reactions with non-complementary DNA strands do not benefit from such proximity effects and thus behave a true nanomolar concentration systems, leading to insignificant reaction rates. The screening process is designed by preparing two pools of DNA-linked substrates. Pool A contains n substrates covalently bound to the 5'-end of a set of DNA oligonucleotides that contain one coding region and a specific annealing region. Pool B contains n substrates covalently bound to the 3'-end of a set of DNA oligonucleotides that contain one coding region, a spacer with

Figure 26. Screen design and microarray analysis after avidin pull down selection. **A.** Coupling partners scaffolds. **B.** Screening result by DNA-microarray. The reactions were performed under five different conditions: EDC, sNHS at 25 °C for 1 h; Pd(II) at 37 °C for 1 h; Pd(II) at 25 °C for 20 min; Cu(I) at 25 °C for 10 min; and Reaction with no metal. Spots that are significantly green suggest bond forming reaction, the yellow and orange represents the ratios of bond/no bond formation and red represent no reaction. **Panel B republished with permission from ref 409.** Copyright © **2004 Springer Nature**

biotin, and a disulfide group (Figure 25). 409

Therefore, reactants are bound to complementary DNA strands and brought together via complementary base-pairing. In solution, various mixtures of these compounds are mixed while the annealing DNA code is used to bring the two reactants together in close proximity, mimicking an intramolecular transformation. If a bond is formed, the biotin becomes covalently linked to the

DNA strand encoding for the successful reactants. Thus, cleaving the disulfide uncouples biotin from unproductive reactions. Avidin pull-down is used to isolate successful reactions, followed by subsequent PCR amplification and DNA microarray analysis, highlighting the substrates that reacted by reading the code on the bound DNA (**Figure 25**). The microarray-based method provides a global profile for decoding complex populations of DNA sequences. The microarray contains all complementary DNA sequences (cDNA) possible for each pool member. 409

This approach simultaneously evaluates bond formation between any two substrates of a large collection of candidates under different possible reaction conditions (**Figure 26**). The screening method highlights the ability of reaction discovery directed by nucleic acids effective molarities and *in vitro* selection and amplification. The first screening was performed with a combination of substrates divided up into pool A and B, respectively. The substrates were outfitted with different reactive and non-reactive functional groups including ketones, carboxylic acids,

Scheme 49. Example of a Reaction Combination Performed by the First Generation of Reaction Discovery Enabled by DNA-Templated Synthesis and in Vitro Selection. The Structure of the Reaction Products was Analyzed by MALDI-TOF.

azide, cyano, epoxides, alkenes, alkynes, and cycles (Figure 26A). coupling partners subjected to various conditions, in a metal free, Pd(II) and with carboxyl-activating agent EDC, (Figure 26B). This work resulted in metal-catalyzed cross coupling reactions by employing pre-catalyst (Figure Na₂PdCl₄ **26B**). The discovery highlights a Pd(II)-mediated coupling reaction between alkynamides and alkenes trans-α,β-unsaturated ketones (Scheme 49).

This method allows for the possibility of evaluating thousands of combinations of substrates and reaction conditions in a two-day experiment. Requirements of this approach are based on: (i) the need for conditions and catalyst to be compatible with DNA, (ii) specialized techniques and PCR machinery, and (iii) **DNA** machinery.409 microarray Limitations include (i) the need for

DNA library design, (ii) the need for a water-soluble catalyst, and (iii) low-temperature conditions to facilitate DNA hybridization. Also, the microarray-based method is not suitable for analyzing DNA libraries with highly similar encoding sequences. Therefore, it is limited to the number of probes that can be arrayed on a chip. ⁹⁰

5.1.2.1 Initial Hit: Macrocyclization via Pd-Mediated, Oxidative Amido-Alkyne/Alkyne Coupling Reaction

Liu and coworkers discovered a novel reaction via DNA-templated synthesis involving highlighting an intramolecular Pd(II)-mediated carbon–carbon coupling between a simple terminal alkynamide

Scheme 50. Synthesis of Macrocycle via Pd (II) Catalyzed Alkyne-Alkene Coupling

(i) 1 equiv. Na_2PdCl_4 , 1 M NaCl in H_2O , 25 °C, 15 h, 86% (ii) 5 mol% Na_2PdCl_4 , 1 equiv. $CuCl_2$, 100 mM NaCl in H_2O , 25 °C, 2 h, 90% (iii) 5 mol% Na_2PdCl_4 , 1 equiv. $CuCl_2$, 9:1 THF: H_2O , 25 °C 4 h, 91% (iv) 15 mol% Na_2PdCl_4 , 1 atm O_2 , 9:1 THF: H_2O , 25 °C, 14 h, 73% (v) 1 equiv. $CuCl_2$, 100 mM NaCl in H_2O , 25 °C, 4 h, 0% (vi) 1 equiv. $CuCl_1$, 100 mM NaCl in H_2O , 25 °C, 4 h, 0%

also containing a terminal alkene **370** affording macrocyclic *trans*-enone product **371** (Scheme **50**). 409 Initial studies of this

novel process in the presence of 1 equivalent of Na₂PdCl₄ catalyst, 1M NaCl_(aq) resulted in the formation of a 20-membered macrocyclic trans-enone product **371** as a single olefin stereoisomer in 86% yield (15 h).

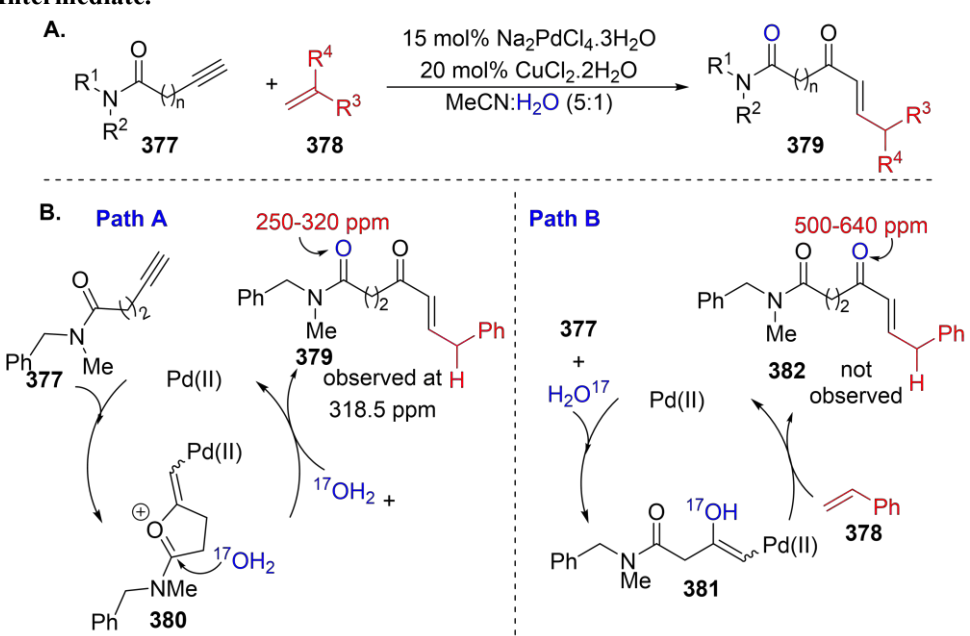
Scheme 51. Plausible Mechanism for Pd (II) Catalyzed Alkyne-Alkene

This synthetic transformation was conducted using a non-DNA-templated format, confirming the reaction is compatible to 109-fold scale compared to a DNA-templated form. This process, representing oxidative C-C coupling, attempted using was air CuCl₂ and for recycling catalytic Pd(0) Pd(II), whereby expected product was vielded (90%). The reaction was also compatible with mixed solvent systems like THF-H₂O. Further, exclusive use of O2 as an oxidant provided the expected product, albeit at a slower rate, whereas CuCl₂ and CuCl proved to be ineffective.

A plausible mechanism is depicted in **Scheme 51** and suggests activation of the alkynamide with Pd(II), providing cyclic oxypalladation intermediate **372** followed by hydration leading to acyclic intermediate **373**. Subsequently, an intramolecular Heck reaction on intermediate **373** provides Pd-alkene complex **374**. Next, β -hydride elimination generates a Pd-alkene complex **375**, and sequential internal hydrometaltion followed by β -hydride elimination results in migration of the olefin into conjugation with the carbonyl in **376**. Finally, the ligand exchange step releases the α , β -unsaturated ketone **371** and Pd(0), which is oxidized by air to regenerate Pd(II).

In follow-up work, the Liu group further investigated this novel Pd(II)-catalyzed oxidative coupling of alkenamide and alkenes to gain more mechanistic insight (**Scheme 52A**).⁴⁰⁹ The authors carried out an oxygen-labeling experiment which was performed between *N*-benzyl-*N*-

Scheme 52 A. Reaction scope of Pd(II)-Catalyzed Intermolecular Coupling of Alkynamides and Alkene and A Plausible Mechanisms for Cyclic Oxypalladation Intermediate.



methylpent-4vnamide 377 and styrene in MeCN- $H_2^{17}O$ (3:2).Analysis of the ¹⁷O NMR showed the presence of a peak at broad 318.5 ppm, characteristic of a $^{17}O = C$ labeled bond present in **379**. This observation strongly supports the mechanism proposed in path A (Scheme 52B), which proceeds cyclic via oxpalladation

intermediate **380**, followed by subsequent hydration by H₂¹⁷O to release product **379**. In contrast, path B represents a mechanism that would proceed via acyclic intermediate **381**, resulting from the direct hydration of a Pd(II)-alkyne complex which would have resulted in an expected enone ¹⁷O=C peak during the ¹⁷O NMR analysis for compound **382**, which was not observed in this experiment (**Scheme 52B**).

Notably, this process tolerated styrene, α -methylstyrenes, as well as unactivated long-chain olefins, affording a variety of terminal alkenes (99:1 E/Z) and good to excellent regioselectivity (>5:1 to >20:1) (long chain alkenes: styrenes). However, this protocol had one limitation in the case of the alkyneamide. It was observed that pentynamide or hexynamide proved to be successful compared to propyn-, butyn- and heptynamide. This could be rationalized by considering the cyclic oxypalladation mechanism proposed. Here, the cyclic oxypalladium intermediate **380** may not be forming due to increased strain in the case of propyn-, butyn- and heptynamide, in contrast to the pentynamide or hexynamide systems.

5.1.2.1.1. Hit Elaboration: Other Macrolide Formation

Related to the Liu-chemistry just described, Shridharan and coworkers established a Pd(II)-catalyzed nucleopalladation-initiated cascade approach to construct seven-membered benzo-fused nitrogen/oxygen heterocycles (**Scheme 53A**), which represent an important class of natural

Scheme 53 A. Intramolecular Syn-Oxypalladation-Olefin Insertion sp²-C-H Activation B. A Plausible Mechanism for the Syn Oxypalladation-Initiated Cascade

10 mol% PdCl₂ Α. CuCl₂.2H₂O (2.0 equiv.) H₂O (1.0 equiv) THF, 50 °C, 2-36 h R^1 (up to 88%) 384 X = NTs, NMs, O В. 384 Chlorination/ 383 Oxidation R^1 protodematallation 380 product 385 ÖMe [⊢]d^{||} 388 Intramolecular Syn-oxypalladation Rearrangement Pd^{II} (formation of π -benzyl Pd^{II} (\pm) 386 O olefin MeC insertion H_2O (±) 387 5-exo-trig β-H elimination not possible

products. This high atomand step-economical sequence cascade generated two heterocycle (seven and rings carbon fused) with three new bonds in a single synthetic operation.465 The process involves activating alkyne **383** via Pd(II) catalyst followed intramolecular synoxypalladation to generate σ-vinyl-palladium intermediate 386 species 385 (Scheme 53B). Subsequent olefin insertion comprising a 5-exo-trig cyclization generates intermediate 387 bearing the furanone ring system. The β-hydride elimination forbidden due geometrical constraints. Further, the o-chlorination process involving sp² C-H bond activation via σ - π - σ rearrangement of intermediate 387 to deliver species 388 via

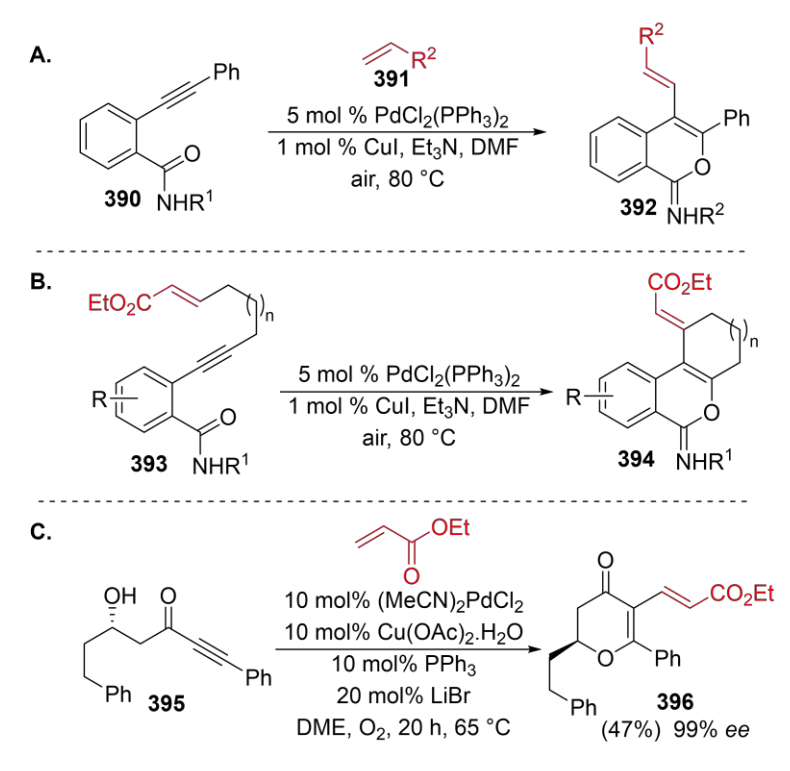
benzylpalladium(II) species involving the dearomatization reaction. Subsequently, rearomatization followed by the CuCl₂·2H₂O-mediated *ortho*-chlorination-oxidation sequence afforded the desired product **384** *via* intermediate **388**, and regenerating the Pd(II) species in the catalytic cycle.

5.1.2.1.2. Hit Elaboration: Six-Endo-Dig Cyclization Reactions

In 2012, Alvarej and coworkers reported the synthesis of various substituted isochromen-1-imine-based structures (**Schemes 54A & 54B**). He intermolecular and intramolecular nucleopalladation followed by Heck-type coupling on substrates **390** and **393** are reported, providing substituted isochromen-1-imine units **392** and **394**. Gouverneur and coworkers have established a novel palladium(II)-catalyzed Wacker-Heck process whereby two different electron-deficient species, hydroxy-ynones **395** and ethyl acrylate are coupled, providing highly functionalized dihydropyranones **396** in modest yield (**Scheme 54C**). He diene resulting from

this novel synthetic transformation is a key synthetic building block for the total synthesis of mycalamide A.

Scheme 54. Synthesis of Substituted Isochrome-1-Imines



A. Intermolecular coupling. **B.** Intramolecular coupling *via* nucleopalladation/oxidative Heck reaction. **C.** Pd(II)-catalyzed Wacker-Heck reaction for the synthesis of dihydrpyranone.

5.1.2.1.3. Hit Elaboration: Five-Endo and Exo-Dig Cyclization Reactions

The alkynamide scaffold, a generably valuable synthetic precursor, has been used in the synthesis of nitrogen-containing heterocycles via transition metalcatalyzed intramolecular aminometallation. In 2016, Jiang and co-workers described the Pdintramolecular cyclization of alkynamide enyne 397 to afford the heterocyclic compound 398 and 399 (Scheme 55 & B). 469 An amide-assisted Pd-catalyzed intramolecular Onucleopalladation followed by 6endo-trig cyclization Heck yielded compound 398 from enyne **397** (Scheme **55A**). 469 In contrast, switching from 6-endotrig Heck cyclization to 5-exocyclization via trig Heck judicious choice of oxidant from

O₂ to CuCl₂ gives **399**. This is an example of tuned reactivity from a Heck 6-endo-trig annulation to a 5-exo-trig cyclopropanation by varying oxidants yielded compound **399** in a moderate to good yield (**Scheme 55B**).

Scheme 55. Pd-Catalyzed Intramolecular Heck Reactions

A. 6-endo-trig Heck cyclization. B. 5-exo-trig Heck cyclization reaction.

5.1.2.1.4 Hit Elaboration: Intermolecular Amido-Alkyne/Alkene Coupling Reactions

Generally, previous reports have shown the trend in the intramolecular cyclization involving an alkyne was to activate the triple bond with a transition metal catalyst followed by nucleophilic attack and a subsequent Heck reaction. However, in 2013, the Zhu group reported the first effective cross-coupling reaction bearing two nucleophilic centers involving *o*-alkynyl

anilines and *o*-alkynyl benzamides (**Scheme 56**).⁴⁷⁰ Interestingly, the reaction proceeded *via* selective coordination of Pd-catalyst to the alkyne moiety of *o*-alkynylaniline followed by 5-*endo*-

Scheme 56. Cyclization via Cross-Coupling Between *o*-Alkynylanilines and *o*-Alkynylbenzamides and A Plausible Mechanism for the Reaction

5.1.3. Novel DNA Architectures for DNA-Templation

5.1.3.1. Use of a Double-Templated DNA Ternary Complex with Selection by Photocleavable Linker and PAGE Readout

Li and coworkers developed a system which does not require a pull-down mechanism to selectively choose the positive hit reactions. Their report shows a proof of principle utilizing photocleavable oligonucleotides, which can be synthesized by automated DNA synthesis with phosphoramidites. This method required the bond formation between substrate **A** and **B** (**Figure 27**), keeping the DNA strands in proximity to one another, due to the hydrogen-bonding interactions between the complementary base-pairs. Reaction bond formation followed by subsequent irradiation with light at 365 nm cleaves the photocleavable linker. The DNA strands with substrates **A** and **B** undergoing bond formation retain the ternary complex structure, and with the next step of religation by DNA ligase, a new template is formed. However, the DNA strands for substrates **A** and **B** that fail to undergo bond formation lose the hydrogen-bonding interaction between complementary base-pairs, and non-templated religation occurs. This process allows the selectivity of the hit reactions to be determined by comparing the quantity of religated

dig aminopalladation

403. The intermediate

templates for bond-forming vs. non-bond-forming reactions. Then, the qPCR threshold value (ΔC_T) is used to quantify the difference between the two cases.

Developing this screening method required an initial determination of how many bases between the reaction site and photocleavage site were needed to promote optimal selectivity, without hindering the ligase-mediated re-ligation process. Optimized results led to incorporating

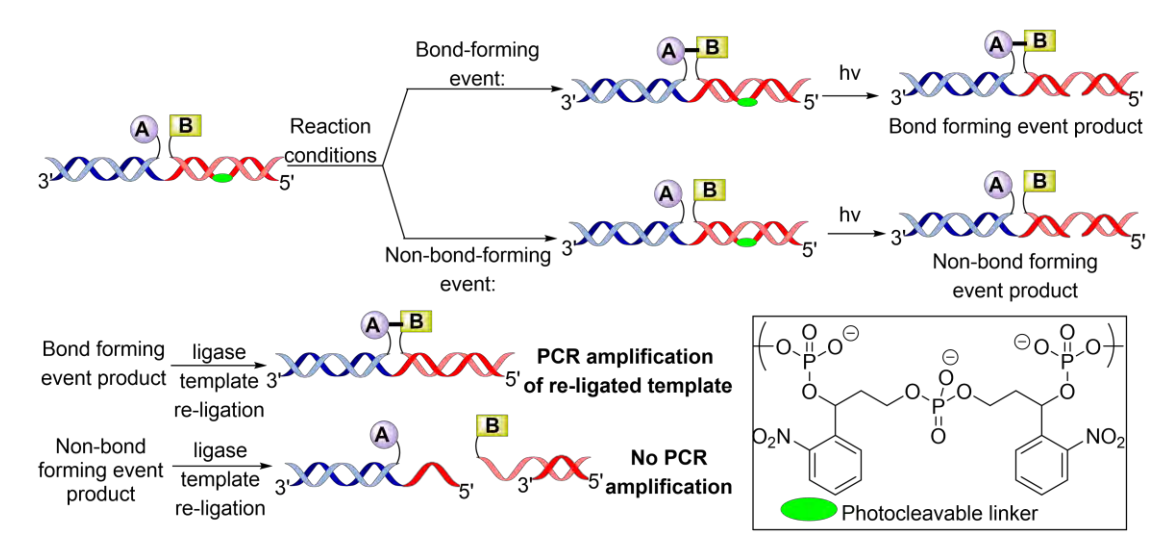


Figure 27. Approach to DNA-templated synthesis system for bond formation detection by using photocleavable linker. DNA-templated synthesis using where $\bf A$ and $\bf B$ are the different substrate. PNK/ E. coli ligase was used for the religation step and the PCR primer binding sites are located at the end of the template strand.

a PEG linker with 5 base-pairs, utilizing polynucleotide kinase (PNK) and *E. coli* DNA ligase. This DNA-templated system was applied in a proof-of-principle study with known reactions such as amidation, reductive amination, and azido-alkynyl click-reaction. The reaction progress was monitored by PAGE, and quantification was done via qPCR. Note that the selection capabilities of this system were proven by studying the bond-formation events versus a background of non-bond-forming DNA strands. By utilizing this selectivity method, a ratio of bond-forming to non-bond-forming events could be determined. Importantly, the process of photocleavage, ligase and qPCR afforded a high-enrichment fold for bond-forming results, proving to have a system with a capable detection limit comparable to other PCR amplification selection methods. 439

5.1.3.2. Exploration of Double-Helix-Templation with Intervening Elongator (E10) or Loop (Ω 5) Sequences with Selection by Sulfone Cleavage and MALDI-MS Product Identification

Advances in reaction discovery using DNA-templated synthesis promoted the urge to design a suitable system compatible with reagents and catalysts that are water sensible. Inspired by this, Liu and coworkers designed a DNA-templated synthesis method that is supported in organic solvents. ⁴⁷¹ This method enables further studies to be conducted with reaction manifolds that are not tolerated in aqueous environment. Demonstrating the stability of DNA double-strand hybridization interaction in organic solvent conditions is a highlight of this work. ⁴⁷¹ Guided by previous results, it has been demonstrated that in the presence of ammonium salts, DNA phosphate groups form ionic interactions, further enabling the complex to be soluble in organic solvents. ⁴⁷²⁻⁴⁷⁶

Liu and coworkers designed an approach supporting DNA-templated synthesis in organic solvents with different DNA-template architectures. This approach allows for pre-hybridization in aqueous solvent followed by transfer to an organic solvent and mixed with the relevant reaction conditions (**Figure 28**).⁴⁷¹ Specifically, the study involved (i) pre-hybridization in aqueous solvent of functionalized DNA strands, (ii) transfer of the complex to organic solvent under the pertinent

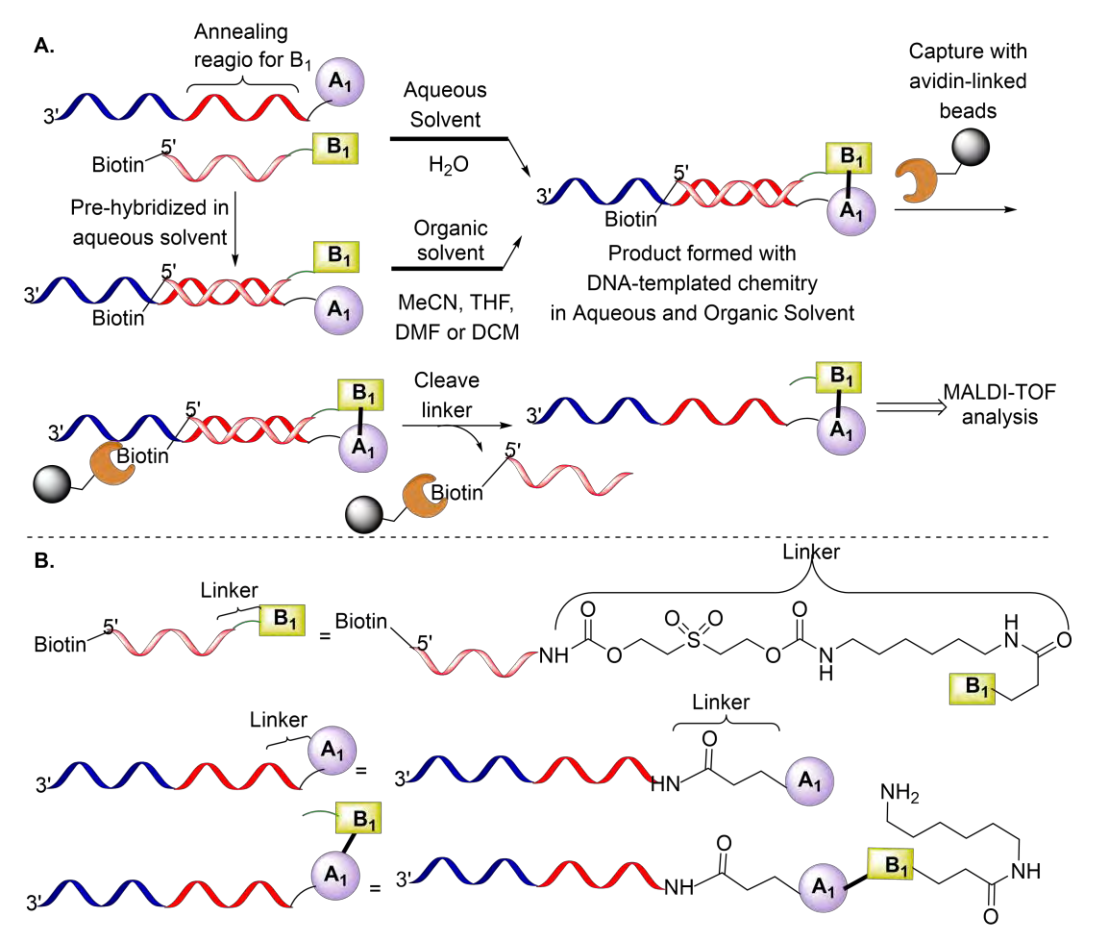


Figure 28. Approach to DNA-templated synthesis in organic solvent. **A.** Reaction studies with DNA pre-hybridization under aqueous conditions, followed by bond formation reaction under organic solvent conditions. Bond-formation product was selected by Avidin pull down and the analysis was performed by DNA PAGE gel and MALDI-TOF analysis. **B.** Representation of the structures attached to the DNA strands.

reaction conditions, (iii) analysis of the denaturing PAGE gel and Avidin pull-down followed by cleavage of the linker, and (iv) MALDI-TOF analysis (**Figure 28A**).⁴⁷¹ This method required for each DNA strand to be functionalized, the template is composed by a 5' linker attached to the substrate of interest A_x and the complementary strand is composed of a 5'-biotin and 3'-linker attached to the substrate of interest B_x (**Figure 28B**).⁴⁷¹

Screening was done with four different DNA template architectures: E1 an end-of-helix with juxtaposed reactants, E10 a long-distance end-ofhelix with ten intervening nucleotides between the hybridized reactants and $\Omega 5$ an "omega" shape with a five-base loop and a mismatched (noncomplementary oligonucleotide) linked to reagents (Figure 27).⁴⁷¹ A proof-of-principle study of this system was performed with known reactions including acylation of carboxylic acid primary amine, reductive amination of aldehyde, Wittig olefination between arvl aldehydes and phosphoranes, Pd(II)mediated alkene-alkyne coupling to generate an enone, pyrrolidine-catalyzed aldol reactions between an aldehyde and ketone, and Heck coupling between aryl iodine and alkene group.⁴⁷¹

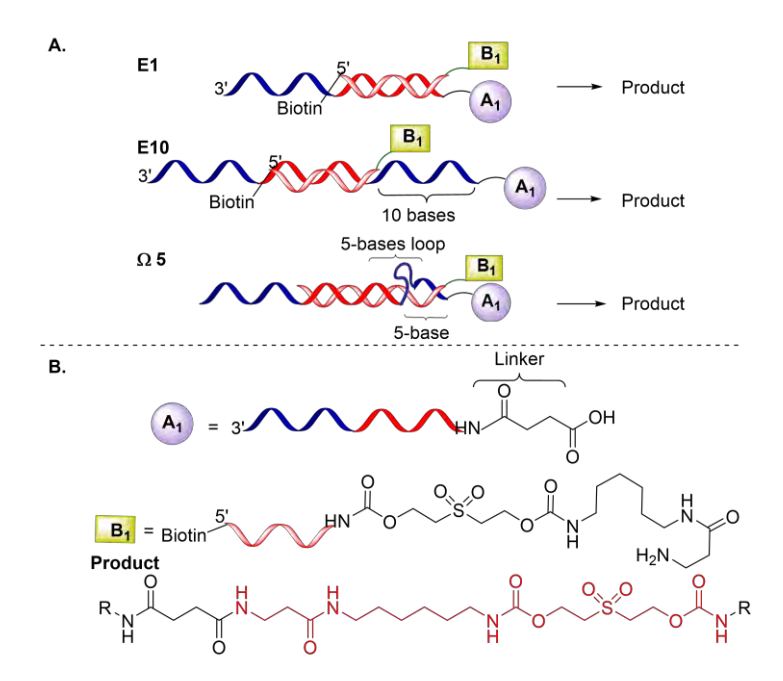


Figure 29. DNA template architectures. A. Reaction scheme: (E1) end-of-helix with juxtaposed reactants, (E10) long-distance end-of-helix with ten intervening nucleotides between the hybridized reactants, (Ω 5) a "omega" shape with a five-base loop. B. Representation of the structures of reaction performed by amine acylation in organic solvent.

5.1.3.3 Hairpin Formation via DNA-Templation with Selection via Disulfide Cleavage and Hairpin-Promoted PCR Readout

The DNA-templated system has been extensively studied to discover chemical reactivity. However, most of the methods need solution/solid-phase manipulations to indirectly select the library's bond forming product under study. To prevent the extra step for synthesizing the biotin-linked substrate, Liu and coworkers developed a new method which links bond formation products with amplification of desired sequences by DNA intermolecular stability. All Notably, it has been previously demonstrated that double-stranded oligonucleotides have different melting temperatures (Tm) for intramolecular and intermolecular hybridization. All The double-stranded oligonucleotides with intermolecular hybridization within the base pairs have higher Tm than intermolecular interaction. Therefore, the authors envisioned that selective PCR amplification could be used to differentiate DNA sequences presenting intramolecular from intermolecular interaction structure.

The method consists of a DNA-templated system undergoing bond formation between substrates of interests, leading to a self-priming DNA hairpin conformation (**Figure 30**). The non-bond formation will result in intermolecular duplex conformation, where PCR amplification will amplify only the sequences encoding DNA-hairpin formation (**Figure 30**). The reaction discovery method consists of a DNA strand with 5'end primer site, an encoding region for substrate of interest, and a complementary region covalently bound to substrate **A** (**Figure 30**). The DNA strand **B** contains a complementary region and a 3'end primer site with 8 nucleotide bases covalently bound to substrate **B** (**Figure 30**). The DNA-encoded library was synthetized by joining the DNA strands via a disulfide linker leading to a DNA hairpin structure (**Scheme 57**).

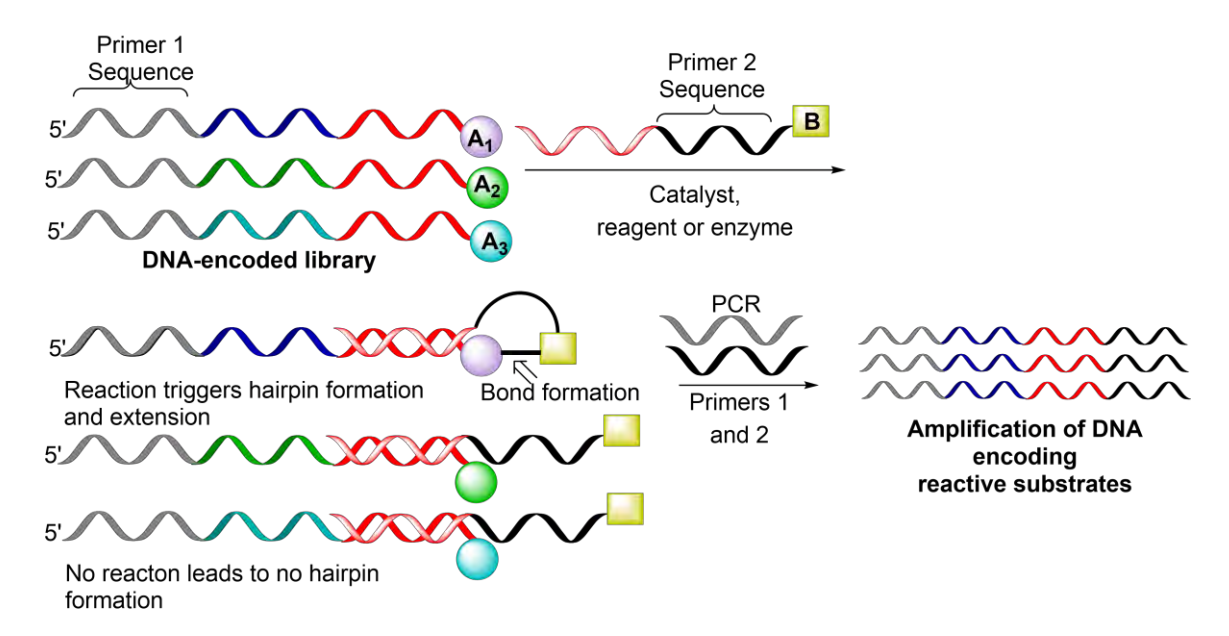


Figure 30. General approach for bond formation through DNA-templated hairpin formation.

Liu and coworkers presented proof-of-principle by studying known chemistry. The first reaction studied was an alkene and aryl iodine Pd-mediated Heck reaction in an aqueous buffer (**scheme 57**). The reaction study selection was based on the idea that after the bond formation occurs, the products will undergo disulfide cleavage, and only the bond-forming product will remain with a DNA hairpin structure (**Figure 31**). This hairpin structure will successfully go through PCR amplification (**Figure 31**). The ability of this approach was also studied with other known reactions such as Schmidt reaction in aqueous buffer and Cu(I)-catalyzed Huisgen cycloaddition reaction in 10% aqueous buffer. 420

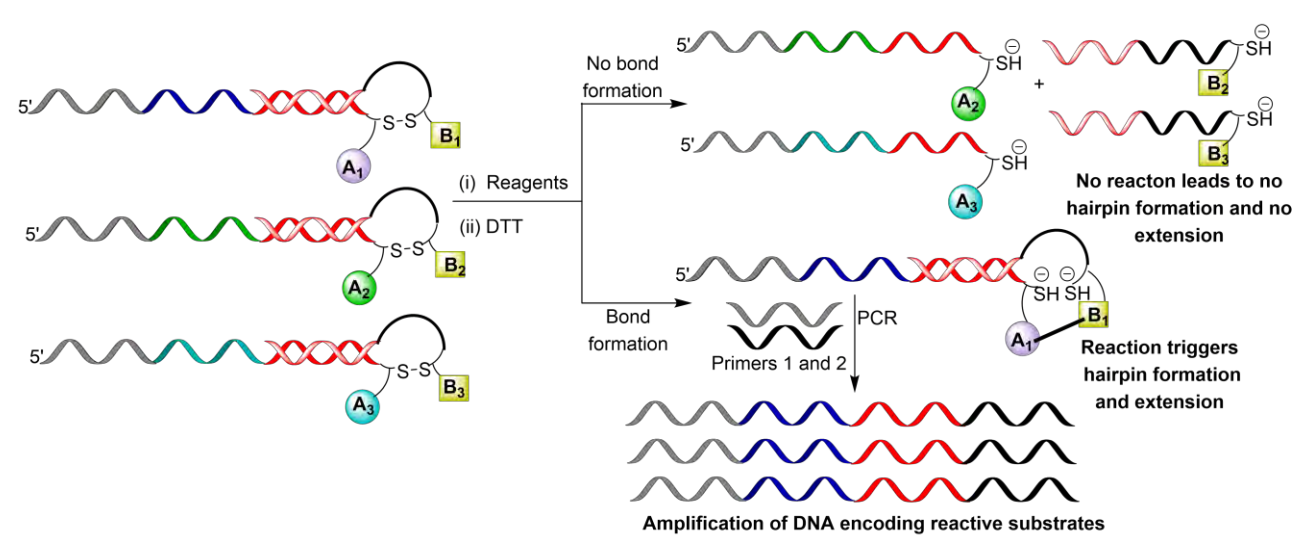


Figure 31 Reaction screening with hairpin DNA-templation and disulfide linkage via disulfide cleavage selection and hairpin promoted PCR read-out.

Scheme 57. DNA-Templated Synthesis of Hairpin Structure for Reaction Study of Alkene and Aryl Iodine Pd-Mediated Heck Reaction

A. Synthesis for B substrate. **B.** Synthesis for A substrate and cross coupling reaction.

Efficient PCR amplification of the bond-forming reaction product for this approach was detected by PAGE. This method provided an efficient way to study organic reactions without using solid-phase selection, which in theory allows for a more efficient screen involving DNA-templated synthesis. However, this combinatorial screening method still needs to be further optimized to expand substrate scope and reaction conditions to be able to be used in a high-throughput screen.

5.2. DNA-Ligation-Based Methods

5.2.1 Proof of Principle Platform for High-Throughput Screening of DNA-Encoded Catalyst Libraries in Organic Solvents via Biotin-Avidin Selection and DNA Sequencing Readout

Many exciting transition metal-mediated transformation that are compatible in organic conditions have been discovered. The use of bio-macromolecules in these discoveries provides the limitation of not being exclusively organic soluble. However, several groups have reported DNA molecules with surfactants and nanogels which improve DNA solubility in organic solvents. 480-488 For example, Hili and coworkers developed a method to study reaction transformation in organic solvent with modified DNA structures to increase its solubility. 489 The authors approach consisted of using a single-stranded DNA (ssDNA) conjugated to polyethylene glycol (PEG) to obtain an amphiphilic structure able to solubilize in organic solvents and aqueous media. 489 Their proof-of-principle to screen reaction transformation using ssDNA was designed with an optimal nucleotide length, an encoding region for the catalyst of interest, and two primer regions. The ssDNA contained a 3'end reactant A site, 3'-end catalyst site and a 5'-end PEG site (Figure 32). 489 The 3'-end contained an alkynyl group to functionalize further enroute to reactant A by coppercatalyzed click chemistry. 489 The 5'-end was functionalized with a thiol group, which coupled to the PEG maleimide (40,000 molecular mass). 489 The functionalization of the ssDNA was assisted by solid-phase DNA synthesis.

Figure 32. Single-stranded DNA-encoded architecture containing: 3' end primer site, 12 nucleotide encoding region and 5' end primer site. The ssDNA is functionalized at the 3' end with click site for reactant A attached to keto aldol reactant and with catalyst and catalyst attachment site. The 5' end is functionalized with thiol-maleimide and PEG moiety.

The proposed screening method consisted of modified ssDNA and a reactant (**B**) attached to a biotin tag. The reaction was performed in an organic solvent system and then the library was dissolved in aqueous buffer followed by a selection process via biotin-avidin affinity (**Figure 33**). The positive hits undergo PCR amplification and identification with DNA sequencing (**Figure 33**). To demonstrate the efficiency of the method, Hili and coworkers used a system to enrich the positive selection by adding an *Eco*RV restriction digest site with the encoding region, which allow it to be analyzed after restriction digestion, followed by PAGE analysis. As Negative control experiments were ran against this library containing only reactant A.

The system was further optimized by studying an amine-catalyzed aldol reaction (**Figure 33**). Various solvents were tested including 1,2-dichloroethane (DCE), acetonitrile (MeCN), heptane, 1,4-dioxane, and 1-octanol. ⁴⁸⁹ The findings of this study show that the highest yields were achieved when using DCE as the organic solvent. Hili and coworkers performed a high-throughput DNA sequencing of the aldol reaction with a library of 16.7 million different 12-nucleotide encoding regions to study its high-throughput screening potential. ⁴⁸⁹ It is important to note that for all of these library members, no aldol catalyst was attached, thus they were all negative control library members. For this study, an Illumina barcoded adapter did the screening readout instead of restriction digest. The authors analyzed the results by PCR amplification and Illumina Mi-seq paired-end sequencing, generating high-quality data. ⁴⁸⁹ This method demonstrated a proof of principle of a high-throughput screen with a specific amine-catalyzed aldol reaction. Furthermore, this method sets the stage for future studies looking at other transformations to be conducted.

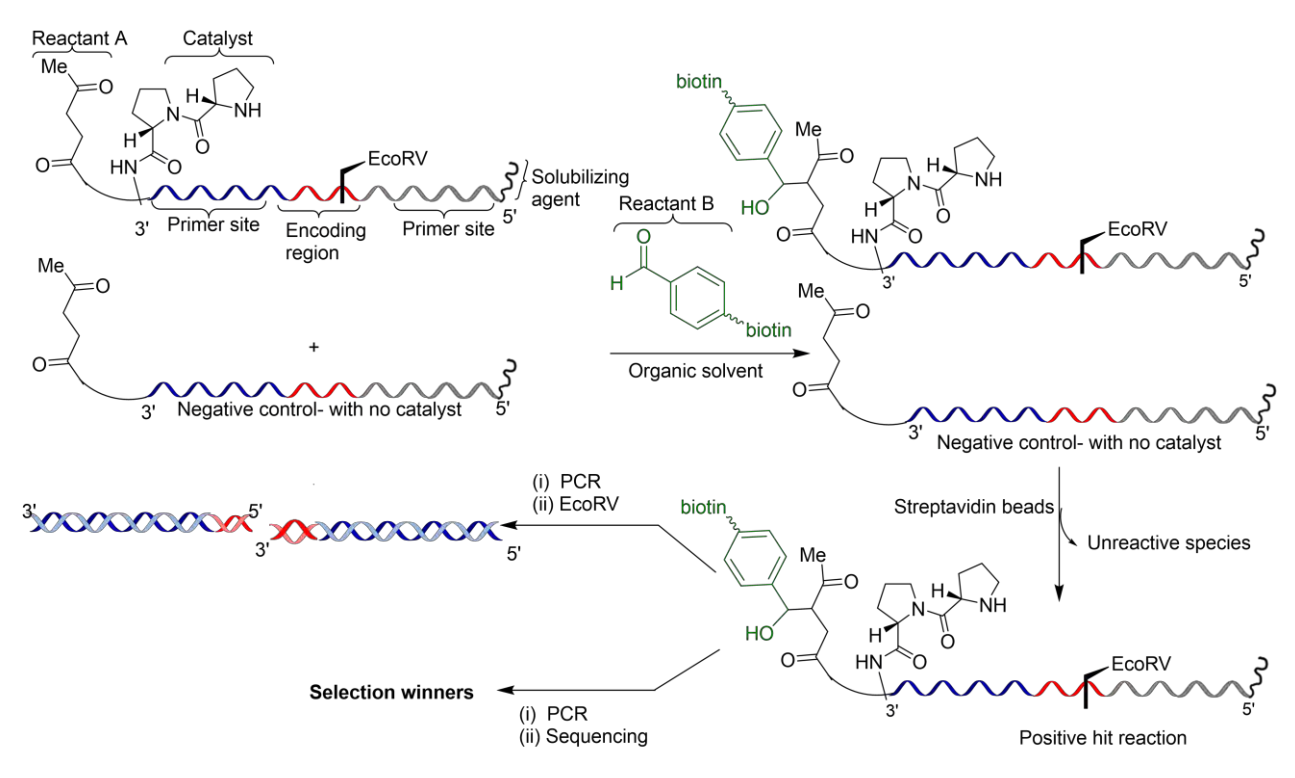


Figure 33. Proof of principle for reaction screening with ssDNA-encoded in organic solvent via biotin-avidin selection and DNA sequencing read-out. The system was used with an amine-catalyzed aldol reaction between reactant **A** ketone and reactant **B** aldehyde.

5.2.2. Reaction Discovery by Hybridization-Independent DNA-Encoded Reactions with Disulfide Cleavage Selection and DNA Microarray Readout

Liu and coworkers developed a second-generation method for the reaction discovery by DNA-encoded library. This approach was implemented using DNA-encoded systems without the need for reaction conditions that support DNA hybridization. Also, this system was well suited for the discovery in organic solvents conditions. However, similar to Liu's first-generation DNA-templated reaction discovery approach, the hybridization-independent reaction discovery

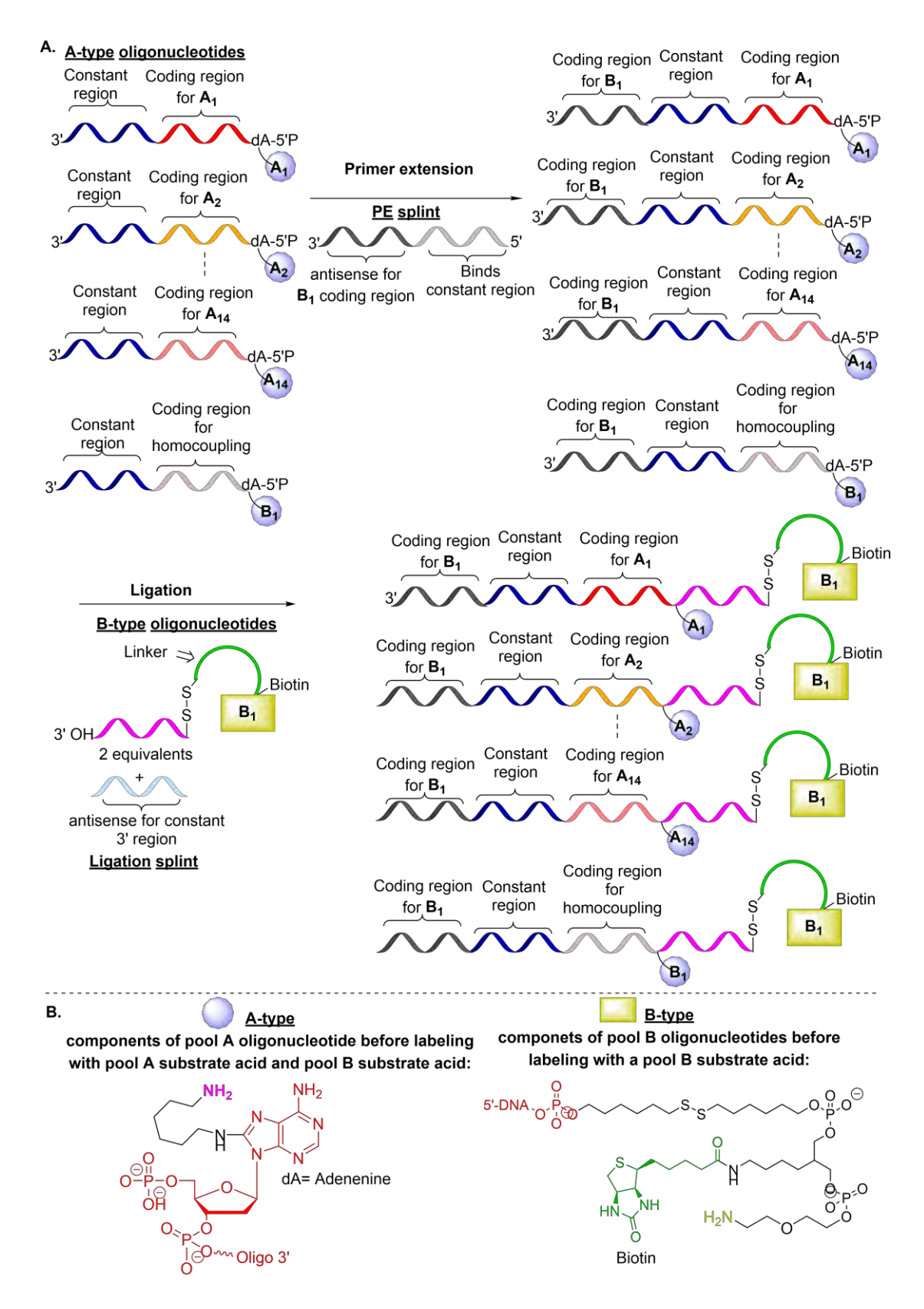


Figure 34 A. Modular assembly strategy for the hybridization-independent reaction discovery system. **B.** A-type and B-type oligonucleotides showing the reactive components structure.

requires (i) DNA encoding, (ii) DNA-programmed assembly of substrates pairs, (iii) *in vitro* selection, (iv) PCR amplification, and (v) DNA microarray analysis. 411,436

This hybridization-independent method requires a single strand of DNA outfitted with desired substrate attached to each strand (**Figure 34A**).⁴¹¹ The reaction discovery pool was synthesized using three types of oligonucleotides labeled as **A**-type, **B**-type, and a primer extension (PE). The **A**-type oligonucleotide is initially linked to **A** substrates, and the **B**-type oligonucleotide is initially linked to **B** substrates (**Figure 34B**). However, to study the homocoupling interactions, the authors prepared the **A**-type linked to **B** substrates and the **B**-type linked to **A** substrates.⁴¹¹

Scheme 58. T4 DNA Ligase Mechanism

Notably, the PE splint was used to extend the DNA strand for the **A**-type oligonucleotide (**Figure 34A**). The **A**-type is a 5' to 3' oligonucleotide comprised of 31-bases which include a unique 15-base coding region, an 8-base constant region, an amino deoxyadenosine (dA), a substrate

attachment site at carbon-6 (C6) of the linker (**Figure 34B**), and a 5'-phosphate group to undergo ligation with the 3'- hydroxyl group of the **B**-type strand during pool assembly. The **B**-type is a 5' to 3' oligonucleotide comprised of 5-bases a disulfide linker, a biotin group, and a 5' amidelinked substrate (**Figure 34B**). The PE is a 5' to 3' oligonucleotide comprised of 30-bases which include a 10-base antisense coding region to identify specific pool **B** substrates and an 8-base constant region complementary to the **A**-type which serves as a template for the enzyme-mediated

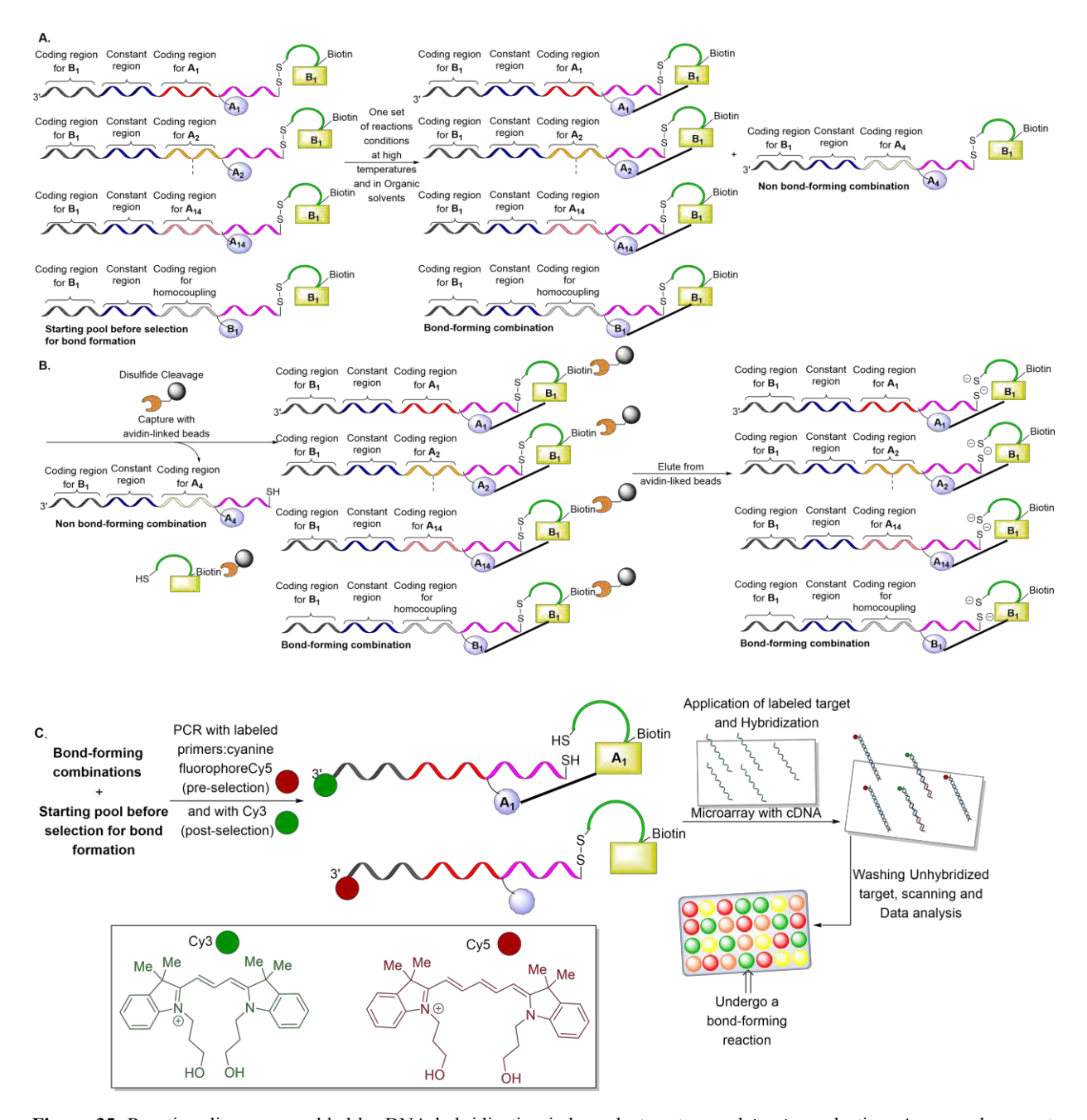
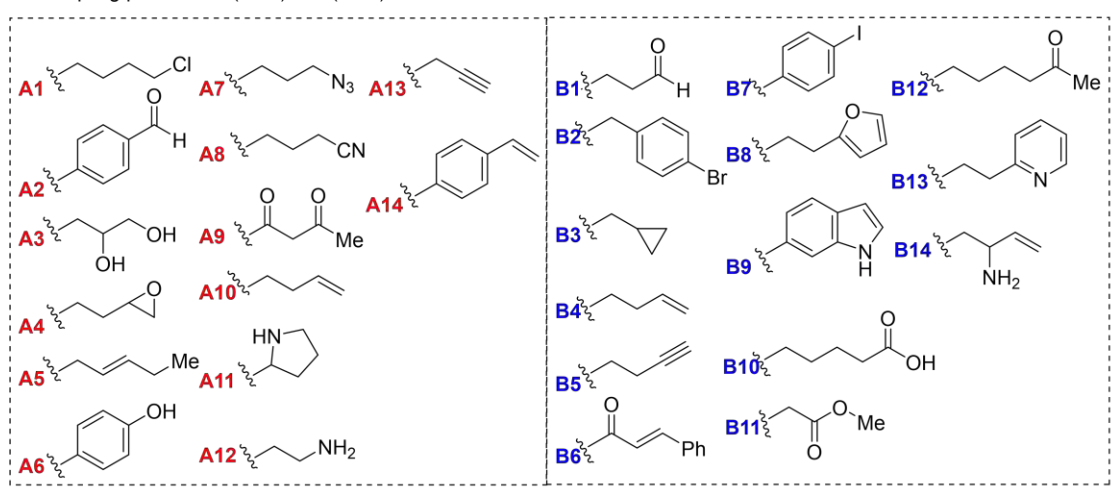


Figure 35. Reaction discovery enabled by DNA hybridization-independent system and *in vitro* selection. A. general one-pot selection method. B. Single strand DNA-linked organic functional groups that associate each $A_n \times B_m$ substrate combinations by bond formation and Avidin pull down of successful reaction. C. Detection of bond-forming reaction by PCR amplification and DNA-microarray analysis. Spots that are significantly green suggest bond forming reaction, the yellow and orange represents the ratios of Cy3 to Cy5 fluorescence and red represent no reaction.

primer extension reaction. As described above, single strand DNA of **A** and **B**-type contained each substrate pair and were assembled by PE followed by a ligation reaction which allows the identity of both substrates to be encoded (**Figure 34A**). 411,436

The catalyzed-phosphodiester bond formation for DNA extension was carried out using a T4 DNA-ligase in a three-step reaction mechanism (**Scheme 58**). First, ATP is used as a cofactor and converted to an activated enzyme bond phosphoramide intermediate upon nucleophilic attach by the essential lysine. Second, the phosphoramide intermediate is captured via nucleophilic addition of the 5'-phosphate, resulting in subsequent release of the lysine residue and formation of a phosphoranhydride. This is followed up by a nucleophilic attack from the 3' hydroxyl group of the other DNA strand, releasing AMP which results in the ligated phosphodiester bond (**Scheme 58**). How the strand is the second content of the strand is the second content of the s

A. Coupling partners: A (1-14) & B (1-14)



B. Screening result by DNA-microarray

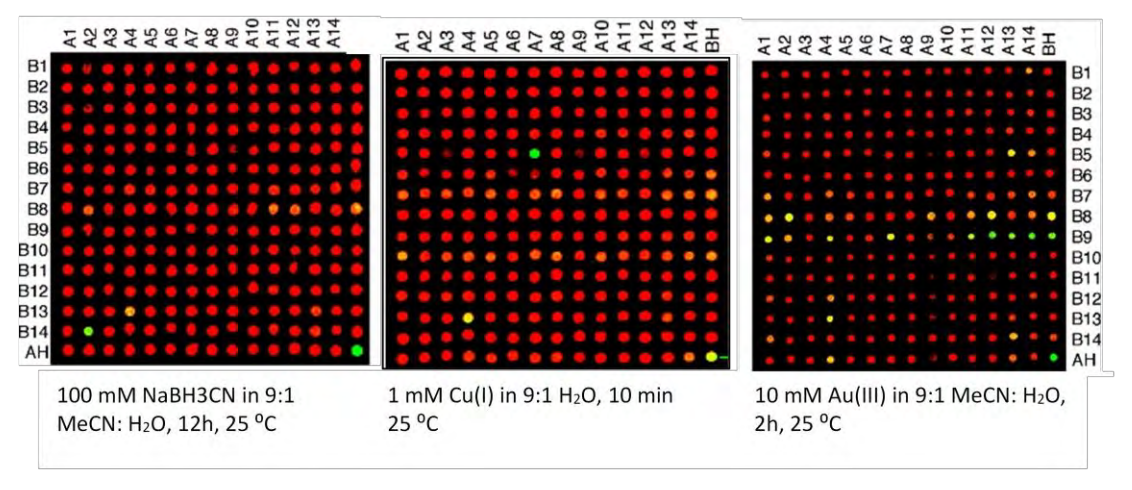


Figure 36. Screen design and microarray analysis after avidin pull down selection. **A.** Coupling partners scaffolds. **B.** Screening result by DNA-microarray. The reactions were performed under three different conditions: 1 mM Cu(l) in 9:1 dioxane:H₂O, at 25 °C for 10 min; 10 mM NaBH₃CN in 9:1 MeCN:H₂O at 25 °C for 12 h; and 10 mM Au(III) in 9:1 MeCN:H₂O at 25 °C for 2 h. Spots that are significantly green suggest bond forming reaction, the yellow and orange represents the ratios of bond/no bond formation and red represent no reaction. **Panel B republished with permission from ref 411.** Copyright © 2007 American Chemical Society.

Therefore, using this ligation method, the reaction discovery pool was done in a 15 x 15 substrate matrix with a single solution containing 1 picomol of the substrate pool. Then, after reaction completion, the disulfide cleavage uncouples biotin from unproductive reactions (**Figure 35**). An avidin pull-down follows this step to isolate the successful reactions. Then, PCR amplification and DNA microarray analysis highlight in a similar fashion as the first generation screening method (Section 5.1.2.) the substrates that reacted by looking at the coding region on the bound DNA (**Figure 35**).

Furthermore, this screening method has been used to study reactions in organic solvents such as acetonitrile, DMF, methanol, and dioxane with a 9:1 solvent ratio in H₂O.⁴¹¹ The substrates selected for the reaction discovery screen were chosen by their readily accessible functional groups, including primary halides, alkenes, alkynes, benzaldehydes, epoxides, nitriles, ketones, amines, aromatic halides, indoles, α.β-unsaturated systems, and carboxylic acids (**Figure 36A &**

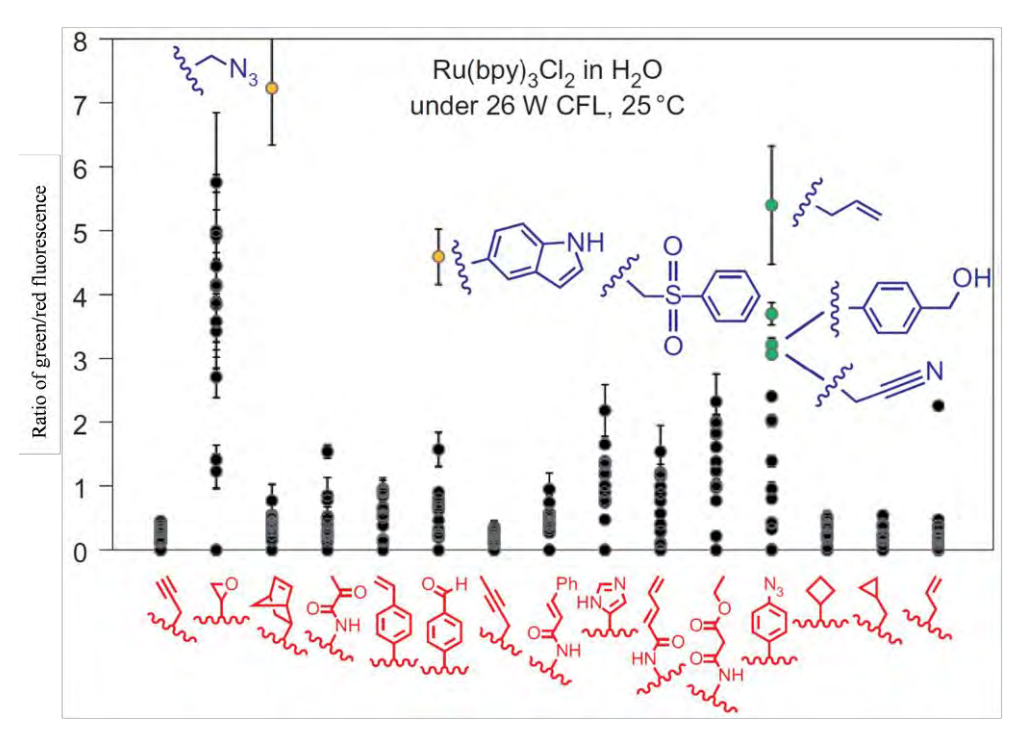


Figure 37. Screening result with 10 mM Ru(bpy) $_3C_{12}$ in 100 mM aqueous sodium carbonate, pH 9.5 , 25 °C , 1h under visible-light radiation (26 W CFL bulb). Spots that are significantly green suggest bond forming reaction, the yellow and orange represents the ratios of bond/no bond formation and red represent no reaction. Figure republished with permission from ref 436. Copyright © 2011 Springer Nature.

B).⁴¹¹ screening reported on a Cu(I) cycloaddition between alkyne and azide as positive hit (Figure 36A **& B**).⁴¹¹ The results were compared non-transition metals conditions such NaBH₃CN whereby a less efficient reaction was expected. In addition, new reactivity was explored with

Au(III), leading to the discovery of mild conditions for the selective Markovnikov-type hydroarylation of olefins with indoles (**Figure 36B**). Specifically, this Au-mediated coupling was achieved between indole and styrene scaffolds upon further Au-olefin activation of styrene, whereby the intramolecular hydroarylation between the styrene-indole system occurred. 411

This hybridization-independent DNA-encoded screening method was further explored to discover new reactions not easily predicted.⁴³⁶ The highlight of this screening was the use of tris(bipyridine)ruthenium (II) dichloride (Ru(bpy)₃Cl₂) in the presence of a visible-light source to undergo through photoredox reactions (**Figure 37**). The screening unveiled several positive hits from coupling between aryl azide and alkene, sulfone, phenol, and nitrile functionalities (**Figure**

37). 436 As shown, this azide-reduction reaction was compatible with several functional groups and efficient chemoselectivity was achieved, in contrast to known reactions. 436 These results presented the opportunity of developing an azide-reduction manifold in biological macromolecules. 436 In summary, Liu and coworkers designed two generations of screening systems, where DNAafforded high effective molarity, encoded reaction discovery around concentrations. 409,411,436 Furthermore, the conditions leverage the reactions to favor intermolecular bond formation, which would not normally be expected concentrations. 409,411,436 These methods also allow for a high-throughput screen of 105 to 106 products mixtures per day. 4,10,436

5.2.1.1 Application to Au(III)-Catalyzed Friedel-Crafts-Like Indole Alkylation

Liu and coworkers studied over 200 bond-forming combinations of substrates in a single step by

Scheme 59. Acid-Catalyzed Indole Hydroarylation Reaction

using the above technique, and it led the discovery of selective Markovnikov-type hydroarylation of olefins with indoles (Scheme **59**).⁴¹¹ The reactions characterized both in a DNA-linked format and also via conventional flask format. Further optimization of non-DNA-linked substrates carried out. The indole and styrene reaction compatibility were tested in the presence of different acids including AuCl₃, AgOTf, AgBF₄, Ag(O₂CCF₃), TfOH, and HCl while under various solvents conditions.

The combination of TfOH and DCM was found to be effective, providing the highest yield of indole-styrene coupling product in an open-air flask. The optimized protocol was tested on different substituted alkenes and showed excellent promise (**Scheme 59**). 411

5.2.2.2 Application to Visible-Light-Induced Azide Reduction

The second-generation DNA encoded reaction discovery by Liu and co-workers provides an innovative and bio-compatible screening method to report on the Ru(II)-catalyzed azide reduction which is promoted further by visible light. The different substrates linked with DNA were chosen under several reaction conditions for discovering novel hits.⁴³⁶ Here, an unprecedented bond-forming reaction between DNA-linked aryl azides **421** (**Scheme 59A**) and nitriles was observed in the presence of Ru(bpy)₃Cl₂ photoredox catalyst and visible-light.⁴³⁶

As these reactions were studied in a non-DNA-linked format, surprisingly the coupling product of the DNA-linked azide and nitrile did not lead to a significant coupling product, and an exclusively azide reduced product was observed (**Scheme 60B**). 436 After several combinations, the functional group compatibility of the azide reduction was tested under the optimized condition: 5 mol% Ru(bpy)₃Cl₂, 10 equiv. i-Pr₂NEt/HCOOH, 1.5 equiv. Hantzsch ester in DCM, hv, 25 °C. 436 The variety of substrates that contained protic functional groups, including free indoles, acids and alcohols, functional groups sensitive to hydrogenation, including alkenes, alkynes and aryl halides, functional groups sensitive to nucleophiles, including alkyl halides, alkyl mesylates and aldehydes,

(95%)

Scheme 60. Ru(bpy)₃Cl₂-Mediated, Induced by Visible Light Reduction

A. Aryl azide acetonitrile coupling reaction. B. Aryl azide reduction. C. Disulfide-linked DNA oligonucleotides aryl azide reduction. D. Naringin azide analogue in the presence of protein enzyme RNase A.

(>95%)

compatible were reaction with conditions

60B). (Scheme This remarkable azide reduction protocol was further tested in the presence biologically relevant molecules including nucleic acids, protein, and an oligosaccharide in aqueous solvent (Scheme 60C & **D**).436

The azide reduction on oligonucleotide **434** (Scheme 60C) provided cleanly expected the compound 435 in 95% yield without disulfide bond reduction. The authors also examined the compatibility of this novel methodology for azide-reduction in the presence of a

protein enzyme, RNase A, with standard aqueous reduction conditions (Scheme 60D). The reaction yielded the expected product 437 without forming any side product, and it did not alter the enzyme RNase A structure or activity. After completing the reduction reaction, an enzymatic assay of the isolated RNase A showed <10% loss of enzymatic activity. 436

5.3. DNA-Based Method for Enantioselectivity Readout

5.3.1. Enantioselectivity Readout Using Enantiomeric DNA Aptamers

A further example of a nucleic acid screen makes use of the availability of both D- and L-forms (spiegelomers) of DNA. ⁴⁹¹ The high-throughput screening of asymmetric reactions is known to be done with high-performance liquid chromatography (HPLC). However, this technique presents the limitation of analyzing up to approximately 800 samples per day and does not provide reaction yield information. ⁴⁹¹ Notably, Heemstra and coworkers have demonstrated the possibility of performing high-throughput chiral sensing of single small-molecule targets. ⁴⁹¹ It is possible to obtain information on both enantiomers of product with a sequence for a single-stranded DNA

Α. Mixture of enantiomers Ratio of dyes provides enantiomeric excess L-DNA В. tBu-FAM (fluorescein) **HEX** (hexachlorofluorescein) Excitation @ 495 nm Excitation @535 nm Emission @ 520 nm Emission @565 nm Color: Green/yellow Color: Pink ΝO2 O-CNEt Q Blackhole quencher 1 BHQ-1 Imax (nm)=534

Figure 38. Overview of single strand DNA aptamer employed to measure the optical purity of tyrosinamde mixtures. **A.** Chemical structures of native D-DNA and L-DNA (Spiegelomers). **B.** Enantiomeric structureswitching biosensors of DNA-aptamers with orthogonal fluorophores. **C.** Chemical structures of fluorophores and quencher.

aptamer selected to bind to a single enantiomer. 491

DNA aptamers are considered short-length oligonucleotides that bind with high affinity to specific targets. 492 Their binding affinity is comparable to that of monoclonal antibodies with a typical K_d (dissociation constant) range between 0.1 and 50 nM. 492 The method described by Heemstra and coworkers utilizes reciprocal chiral substrate selectivity with a structure-switching biosensor format to obtain a fluorescence readout. 491 The biosensor approach takes advantage of a hydrogenbonding interactions between the DNA aptamer labeled with a fluorophore and a complementary strand labeled with a fluorescence quencher (Figure 38). 491 The DNA aptamer will selectively bind to a small molecule of interest and displace the complementary strand. displacement with analyte, the aptamer is no longer proximal to this quenching agent. 491 Then, the fluorophores installed on the single-stranded aptamers are unquenched and can be monitored intensity relative concentration of the analyte in solution. The different dyes placed

on each aptamer can be compared, with the intensity ratio corresponding to the optical purity of the analyte. 491

Previous work from Peyrin and coworkers reported the design of DNA aptamers that selectively bind L-tyrosinamide and that can be assayed using a structure-switching aptamer with a fluorescence polarization readout. The assay is based on fluorescence anisotropy associated with the aptamer selectively binding to the molecule of interest. Further exploration by Heemstra and coworkers led them to develop an orthogonal fluorophore system to measure the enantiomeric excess of D-and L-tyrosinamide mixtures following their synthesis. The readout of this assay utilizes well-established fluorophores such as hexachlorofluorescein (HEX) and fluorescein (FAM), which have similar electronic properties (**Figure 38B**). The fluorophores HEX and FAM have excitation/emission wavelengths of 524/572 nm and 490/520 nm, respectively (**Figure 38B**). The fluorescent quencher, black hole quencher (BHQ1), is able to quench both fluorophores with a λ_{max} of 534 nm.

As shown in **Figure 38A**, the L- and D-DNA aptamer is complementary for opposite enantiomers displacing a weakly complementary DNA strand bound to the aptamer. The complementary strands contain a linked fluorescence quencher and can be employed in a screen for enantiomeric excess. ⁴⁹¹ This reported work demonstrates the ability of such an aptamer-based sensing method to provide for an accurate readout on analyte optical purity and to do so with rather high throughput. ⁴⁹¹ These early experiments have been conducted on samples that are relatively homogeneous and these examples suggest that such aptamer-based enantioselectivity readouts should be deployable to post-work-up product streams for reactions that follow largely a single reaction manifold, but differ in stereoselectivity as a function of the chiral catalyst. Going forward, it will be interesting to see for which reactions this method is best deployed and what sort of abbreviated work-up or product isolation procedure is most suitable. From this perspective, there may be reason to use robotics here to increase throughput eventually. Most importantly, there would appear to be a very wide window for exploration open to future investigators here as SELEX technology should permit for the selection of enantiomer-selective aptamers across a broad spectrum of product chemotypes.

6. CONCLUSIONS

As has been discussed in this overview, the same attributes that Nature selected for in the evolution biomacromolecules under Darwinian selection pressure also serve them well in the service of synthetic chemistry, particularly as tools to facilitate the search for new reactivity and for control of stereochemistry in developing synthetic methodology. The ability to recognize stereochemistry efficiently derives from the inherent chirality of DNA (RNA), antibodies and enzymes and their ability to form folded three-dimensional structures featuring chiral ligand binding pockets.

Through Darwinian evolution in biology, *nucleic acids* have been selected as the repository of 'bar-coded' genetic information, and for their ability to rapidly reproduce that information through templated processes. This makes nucleic acids an ideal platform for reaction templation, in general, and for the encoding of reactant information, as well. As has been discussed herein, DNA-templation has been used effectively for the HT-screening for novel chemical reactivity, particularly by the Liu group. 89,90,384,409,429,434,453,463,464,496 The approach is clearly biomimetic in that it exploits a common DNA-templation in an annealing region to bring together a set of reactant partner candidates, in pairwise fashion. Each partner carries an annealing sequence, that takes advantage of base-pairing to drive templation, and each partner also carries a separate coding

sequence, that may be regarded as the biomimetic bar code, essentially genetically encoding the reactant. Successful reaction effectively creates a new chemical ligation point, while cleavage of a built-in chemical switch--a disulfide, 409,436 a β -carbamoyloxy-sulfone linkage, 471 or a photocleavable o-nitrobenzyl phosphate ester (Li group) 439 essentially eliminates unreacted pairs from being amplified.

In terms of novel chemistry, Liu and co-workers were able to discover Pd(II)-mediated-oxypalladation Heck-like yne-ene coupling reaction that proceeds in both an intramolecular and an intermolecular sense and that proceeds in a six-endo-dig as well as in a five-endo-dig, and a five-exo-dig sense. Another interesting finding with this method was an Au(III)-catalyzed Friedel-Crafts-like indole alkylation reaction. Finally, the DNA-ligated and -encoded platform was shown to be biocompatible and suitable for the study of photoredox and visible-light chemistry, leading to the identification of Ru(II)-catalyzed azide reduction with visible light. Given advances in microfluidics technology by the DNA-encoding practitioners such as Harbury, 410,437 this approach can likely be multiplexed, and the throughput significantly increased going forward. Of course, it is important to note that parallel to the developments in DNA-templated and encoded-catalyst discovery, the field of DNA-encoded chemical libraries for drug discovery/chemical biology has burgeoned and shows great promise. 89,90,497-504

In terms of chiral sensing, the ceiling on the use of nucleic acids is high, with SELEX technology insuring that aptamers or spiegelomers with high levels of enantioselection can likely

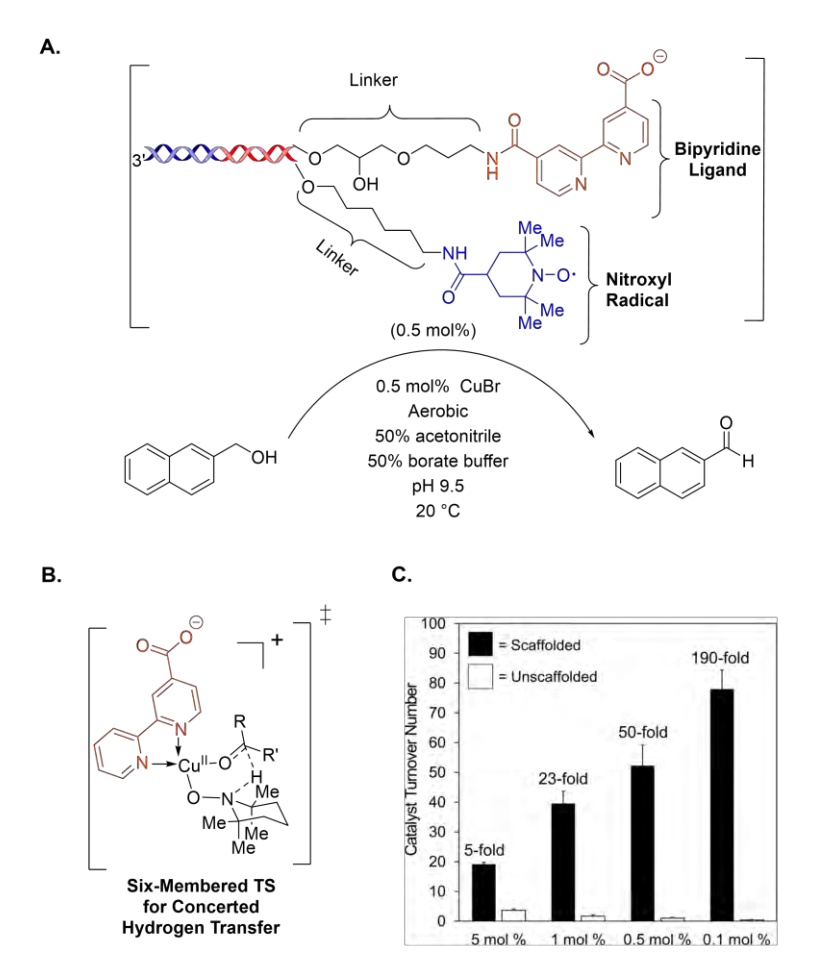


Figure 39. A. Martell group-utilization of DNA-scaffolded frameworks for exploring synergistic catalysis. B. Transition state for the Stahl oxidation involved highly cooperative catalysis between the copper-bipyridine and nitroxide components. C. The remarkable influence of effective molarity, as achieved by DNA-scaffolding on rate particularly as one dilutes the individual components particularly at low loading. Panel C republished with permission from ref 510. Copyright © 2021 American Chemical Society.

obtained chiral he for products/analytes of interest to the synthetic chemist, via repeated cycles of selection/amplification protocol originated by Ellington and Szostak.⁹⁴ With pioneering work on the use of aptamers for ee readout is by Peyrin^{91,505,506} and Heemstra, ^{491,507} and with the advent of aptamerswitching technology^{508,509} and the versatility of aptamer-recognition should motifs. there be heightened interest in the technology within the community.

Finally, the ability of nucleic acids to position candidate catalytic components at a potential reaction center has the possibility to really open up a much higher throughput exploration combinatorial catalysis space. The potential here is perhaps best illustrated by a recent disclosure from Pimentel and Martell⁵¹⁰ in which DNA scaffolding technology used demonstrate just how important effective molarity can be for the exploration of synergistic catalysis. As a platform reaction, the Wisconsin team utilized the Stahl oxidation^{511,512} of alcohols to aldehydes. As is illustrated in

Figure 39, this transformation requires the appropriate juxtaposition of both a Cu(II)-bipyridine center and the nitroxide catalytic component to permit for their synergistic oxidation of the coordinated alkoxide. As can be seen from the bar graphs, particularly at low catalyst loading, the profound acceleration of complementary component scaffolding is huge. The opportunity here for exploiting more complex DNA architectures and even exploring ternary catalytic combinations would appear to be very high indeed and this approach aligns well with the expanding field of DNA-conjugated small molecule catalysts or DCats. ⁵¹³⁻⁵¹⁶

As for *antibodies*, they have evolved a hypervariable region that is sometimes referred to as the 'complementarity determining region' (CDR) so that they might rapidly adopt a binding pocket of high affinity to an analyte of interest, often an offending xenobiotic in a biological

This highly selected for trait serves as an ideal property for reaction screening applications. The concept of utilizing antibodies for this purposes really harks back to the pioneering work of Tawfik⁵¹⁷ and the concept of catELISA⁵¹⁸ that he first put forward. Provided that the product for a reaction under study is known, it is then quite reasonable to expect that by utilizing hybridoma technology one can generate or purchase a set of monoclonal antibodies to that analyte. Moreover, with appropriate screening, as has been pointed out in this review, particularly from the examples reported by the groups of Wagner-Mioskowski, 400 and Janda-Lerner, 402,403 one can arrive at antibodies with complementary enantioselectivities, allowing one to probe both relative rate/conversion and enantioselectivity for a transformation of interest. This method has the advantage of high sensitivity, selectivity, and no requirement of an extra workup step, allowing the experimentalist to screen one thousand reaction combinations in a single day. And while the Taran laboratory, in particular, has really exploited enzyme-linked antibody readouts, much in the manner of the clinical ELISA approach, the potential for single, fluorescent antibody detection demonstrated by the Janda team is worth emphasizing. This group identified a set of blue-fluorescence antibodies that, at once, displayed high binding affinity, enantioselectivity and fluorescence upon analyte-binding, obviating the need for an enzyme conjugate. This type of single protein antibody sensing system is clearly under-developed at this stage and worthy of further exploration going forward.

In terms of the chemistry uncovered, such enzyme-conjugated antibody-based screening methods led to the discovery of efficient transition metal-mediated cycloaddition reactions of 1,3-dipolar systems of the sydnone variety alkyne dipolarophiles particularly from Taran and coworkers. And the follow-on discovery of a strain-promoted variant of this transformation opens up biorthogonal chemistry applications. Finally, in recent years this area has really expanded with the observation both of fluorescent probes based upon such sydnone cycloadditions in PET-imaging technology. S23

The final class of biomacromolecules to discuss is perhaps the most versatile class. Namely, *enzymes* have evolved roles that encompass both molecular recognition and catalysis. Moreover, at least for redox chemistry, a chromophore-change is often associated with that catalytic process. Thus, quite naturally from their roles in Nature and in metabolism, enzymes make ideal "sensors," providing advantages in terms of rapid analysis, specificity, and sensitivity. As has been discussed herein, parallel to the work by the groups of Seto³³⁵⁻³³⁷ and Moberg/Hult ^{338,360,524} on the EMDee (enzymatic method for determining ee), the Berkowitz group has developed the ISES (in situ enzymatic screening) method^{87,150,221-223} that provides a readout on catalyst performance in real-time without the need for quenching and/or work-up. This ISES technique runs under biphasic conditions to screen organometallic catalysts in an organic phase with the reporting enzymes providing a spectroscopic signal in real time in an adjacent buffered, aqueous phase. Efforts are underway to expand the sorts of chemistry explored by the ISES method by developing other sets of reporting enzymes, including thermostable enzymes.⁵²⁵ Looking ahead, advances in protein engineering and directed evolution 138,139,526,527 should allow for the generation 'reporting enzymes' for a much greater array of analytes and chemistries and should also permit the development of more organic solvent-tolerant enzymes as well. 528-532

In terms of the chemistry uncovered through the ISES method, the development of the first examples of asymmetric Ni(0)-mediated allylic amination chemistry is notable. This chemistry provides for an earth-abundant transition metal-mediated entry into the important PLP-enzyme inactivator, L- α -vinylglycine. Colorimetric ISES led to the discovery of a Rh(II)-

perfluorocarboxylate/LiBr-mediated bromorhodiation/carbocyclization transformation that was applied to the synthesis of the natural product cores corresponding to xanthanolide, zaluzanin A, linearifolin.²³⁰ Perhaps most significantly, fundamentally and the the thiocyanopalladation/carbocyclization transformation also arose out of the colorimetric-ISES screen (one well out of 1152 catalytic candidate combinations). 224 This new reaction allows for the construction of both C-SCN and C-C bonds with excellent stereocontrol, proceeding with high 1,2-anti- or 1,3-syn-selectivity, with allylic or propargylic substitution in the cyclization substrate. respectively.²²⁹ This chemistry shows great promise for diversity-oriented synthesis (DOS), as was demonstrated in constructing the oxabicyclo[3.2.1.]octyl core of the natural products annuionone A and massarilactone G and in decorating this core with a range of functionality through the rich tailoring chemistry open to the vinyl thiocyanate functionality.²²⁹

The double cuvette- 221 and cassette-ISES 222,223 methods provide for information on sense and magnitude of stereoinduction, as well as on relative rate, and these methods have been utilized to explore a broad range of chiral salen ligand space. Among the more promising new non- C_2 -symmetric salen ligand scaffolds discovered in this manner are those derived from the readily available terpenoid natural product, β -pinene, 223 and from D-fructopyranose and its carbocyclic analogue itself available from D-mannose. Finally, it must be said that for those practitioners who utilize enzymatic screening, there is both a challenge and a potential high end reward from the need to scope out appropriate enantioselective 'reporting enzymes' for such double cuvette-ISES techniques. Namely once such enantioselective enzymes have been identified that can not only be used to screen for a targeted enantioselective organometallic transformation say, but they can also be exploited in and of themselves for asymmetric biocatalysis. This approach has been taken to great avail for several ISES reporting enzymes in the Berkowitz group, including recombinant KRED enzymes from Codexis, 533,534 and the hyperthermophilic SSADH- 10525 from the archeon, *Sulfolobus solfataricus* and the remarkable *Clostridial* enzyme, CaADH that displays unusual substrate promiscuity, yet stereochemical fidelity.

AUTHOR INFORMATION

Corresponding Author

*E-mail: dberkowitz1@unl.edu

ORCID

David B. Berkowitz *0000-0001-7550-*0112

Notes

The authors declare no competing financial interests

Biographies

Stephany M. Ramos De Dios completed her B.S. degree in Chemistry at the University of Puerto Rico-Rio Piedras performing undergraduate research with Ingrid Montes. She is currently a Ph.D. candidate in the Berkowitz group at the University of Nebraska-(UNL). Her interests are squarely at the nexus of synthetic organic chemistry, mechanistic enzymology, and molecular biology. Her

thesis research is on the development of enzymatic screening methods for reaction discovery and catalyst optimization and on the development and deployment of a new, dual function assay for the important PLP-dependent enzyme, human serine racemase.

Virendra K. Tiwari completed his Ph.D. in 2016 at the Indian Institute of Science Education and Research (IISER) Bhopal India, under the supervision of Prof. Manmohan Kapur. Following an initial postdoctoral stint with Cheol-Min Park at the National Institute of Science and Technology, Ulsan, South Korea, he joined the Berkowitz group at UNL. His current research in the Berkowitz group is focused on the use of enzymes as analytical sensors for the catalyst screening and reaction discovery, including the development of the thiocyanopalladation/carbocyclization transformation uncovered by in situ enzymatic screening. Dr. Tiwari is also interested in the use of 'reporting enzymes' as chiral catalysts in asymmetric synthesis, highlighted by the recent disclosure of a new hybrid biocatalytic/sigmatropic rearrangement-based entry into the core of the important anti-influenza drug, oseltamivir (Tamiflu).

Christopher D. McCune pursued both his undergraduate and Ph.D. studies at UNL, both in the Berkowitz group, while also serving in the Nebraska Air National Guard. He has interests at the interface of synthetic bioorganic chemistry, mechanistic enzymology, and chemical biology. Dr. McCune developed new chemistry for the formal 'fluorovinylation' of amino acid enolate equivalents, leading to a new class of quaternary, α-(1'-fluoro)vinyl amino acids as mechanism-based inhibitors for PLP enzymes. He also helped develop and evaluate a class PLP-dependent cystathionine β-synthase (CBS) inhibitors that have demonstrated ability to attenuate cellular H₂S levels pursuant to stroke and reduce neuronal infarction in rat ischemic stroke models. He was recognized with a UNL graduate teaching award and has been actively engaged in undergraduate STEM education at UNL. He currently is working in STEM-related disciplines at the University of Nebraska-Omaha (UNO) and Doane University OLA, teaching and mentoring the next generation of scientists in the lecture hall, laboratory, and virtually.

Ranjeet A. Dhokale completed his Ph.D. studies at the CSIR-National Chemical Laboratory in Pune, India where he studied aryne-based methodologies and their application to natural product synthesis. He then joined the Berkowitz group where he has explored chemistry that has evolved out of In Situ Enzymatic Screening (ISES) with a particular focus on the bromorhodiation-carbocyclization transformation and its application to natural product core synthesis.

David B. Berkowitz is Willa Cather Professor of Chemistry at UNL and Director of the Chemistry Division at the National Science Foundation. He serves on the Chemical Sciences Roundtable at the National Academy of Sciences. He is a AAAS, JSPS and Sloan Fellow. He completed his undergraduate studies at the University of Chicago and his doctoral research at both Harvard University and the ETH-Zurich with Steven A. Benner, followed by postdoctoral studies with Samuel J. Danishefsky at Yale. Berkowitz has a longstanding interest in research at the chem-bio interface, with interests in stereocontrolled synthesis and reaction/catalyst development, on the interplay of biocatalytic and synthetic organic chemistry and on the study of enzyme mechanism and the development of mechanism-based enzyme inhibitors as tools for chemical biology.

ACKNOWLEDGMENTS

This work was supported by NSF grant CHE/CBET-2102705. These studies were facilitated by the IR/D program associated with DBB's appointment at the NSF. The authors thank the NIH (SIG-1-510-RR-06307) and the NSF (CHE-0091975 and MRI-0079750) for NMR instrumentation and the NIH (RR016544) for facilities.

REFERENCES

- (1) Collins, K. D.; Gensch, T.; Glorius, F. Contemporary Screening Approaches to Reaction Discovery and Development. *Nat Chem* **2014**, 6, 859-871.
- (2) Zhou, Q.-L. Transition-Metal Catalysis and Organocatalysis: Where Can Progress Be Expected? *Angew. Chem. Int. Ed.* **2016**, 55, 5352-5353.
- (3) Knowles, W. S. Asymmetric Hydrogenations (Nobel Lecture). *Angew. Chem. Int. Ed.* **2002**, 41, 1998-2007.
- (4) Sharpless, K. B. Searching for New Reactivity (Nobel Lecture). *Angew. Chem. Int. Ed.* **2002**, 41, 2024-2032.
- (5) Noyori, R. Asymmetric Catalysis: Science and Opportunities (Nobel Lecture). *Angew. Chem. Int. Ed.* **2002**, 41, 2008-2022.
- (6) Knowles, W. S. Asymmetric Hydrogenation. Acc. Chem. Res. 1983, 16, 106-112.
- (7) Vineyard, B. D.; Knowles, W. S.; Sabacky, M. J.; Bachman, G. L.; Weinkauff, D. J. Asymmetric Hydrogenation. Rhodium Chiral Bisphosphine Catalyst. *J. Am. Chem. Soc.* **1977**, 99, 5946-5952.
- (8) Hansen, K. B.; Hsiao, Y.; Xu, F.; Rivera, N.; Clausen, A.; Kubryk, M.; Krska, S.; Rosner, T.; Simmons, B.; Balsells, J.et al. Highly Efficient Asymmetric Synthesis of Sitagliptin. *J. Am. Chem. Soc.* **2009**, 131, 8798-8804.
- (9) Savile, C. K.; Janey, J. M.; Mundorff, E. C.; Moore, J. C.; Tam, S.; Jarvis, W. R.; Colbeck, J. C.; Krebber, A.; Fleitz, F. J.; Brands, J.et al. Biocatalytic Asymmetric Synthesis of Chiral Amines from Ketones Applied to Sitagliptin Manufacture. *Science* **2010**, 329, 305-309.
- (10) Huffman, M. A.; Fryszkowska, A.; Alvizo, O.; Borra-Garske, M.; Campos, K. R.; Canada, K. A.; Devine, P. N.; Duan, D.; Forstater, J. H.; Grosser, S. T.et al. Design of an in Vitro Biocatalytic Cascade for the Manufacture of Islatravir. *Science* **2019**, 366, 1255-1259.
- (11) Johnson, R. A.; Sharpless, K. B. Catalytic Asymmetric Epoxidation of Allylic Alcohols. *Catal. Asymmetric Synth.* **2000**, 231-280.
- (12) Sharpless, K. B.; Amberg, W.; Bennani, Y. L.; Crispino, G. A.; Hartung, J.; Jeong, K. S.; Kwong, H. L.; Morikawa, K.; Wang, Z. M. The Osmium-Catalyzed Asymmetric Dihydroxylation: A New Ligand Class and a Process Improvement. *J. Org. Chem.* **1992**, 57, 2768-2771.
- (13) Kolb, H. C.; Finn, M. G.; Sharpless, K. B. Click Chemistry: Diverse Chemical Function from a Few Good Reactions. *Angew. Chem. Int. Ed.* **2001**, 40, 2004-2021.
- (14) Wu, P.; Feldman, A. K.; Nugent, A. K.; Hawker, C. J.; Scheel, A.; Voit, B.; Pyun, J.; Fréchet, J. M. J.; Sharpless, K. B.; Fokin, V. V. Efficiency and Fidelity in a Click-Chemistry Route to Triazole Dendrimers by the Copper(I)-Catalyzed Ligation of Azides and Alkynes. *Angew. Chem. Int. Ed.* **2004**, 43, 3928-3932.
- (15) Oakdale, J. S.; Fokin, V. V. Preparation of 1,5-Disubstituted 1,2,3-Triazoles Via Ruthenium-Catalyzed Azide Alkyne Cycloaddition. *Org. Synth.* **2013**, 90, 96-104.

- (16) Boren, B. C.; Narayan, S.; Rasmussen, L. K.; Zhang, L.; Zhao, H.; Lin, Z.; Jia, G.; Fokin, V. V. Ruthenium-Catalyzed Azide-Alkyne Cycloaddition: Scope and Mechanism. *J. Am. Chem. Soc.* **2008**, 130, 8923-8930.
- (17) Shieh, P.; Siegrist, M. S.; Cullen, A. J.; Bertozzi, C. R. Imaging Bacterial Peptidoglycan with near-Infrared Fluorogenic Azide Probes. *Proc. Natl. Acad. Sci. U. S. A.* **2014**, 111, 5456-5461.
- (18) Yao, J. Z.; Uttamapinant, C.; Poloukhtine, A.; Baskin, J. M.; Codelli, J. A.; Sletten, E. M.; Bertozzi, C. R.; Popik, V. V.; Ting, A. Y. Fluorophore Targeting to Cellular Proteins Via Enzyme-Mediated Azide Ligation and Strain-Promoted Cycloaddition. J. Am. Chem. Soc. 2012, 134, 3720-3728.
- (19) Baskin, J. M.; Prescher, J. A.; Laughlin, S. T.; Agard, N. J.; Chang, P. V.; Miller, I. A.; Lo, A.; Codelli, J. A.; Bertozzi, C. R. Copper-Free Click Chemistry for Dynamic in Vivo Imaging. *Proc. Natl. Acad. Sci. U. S. A.* **2007**, 104, 16793-16797.
- (20) Agard, N. J.; Prescher, J. A.; Bertozzi, C. R. A Strain-Promoted [3+2] Azide-Alkyne Cycloaddition for Covalent Modification of Biomolecules in Living Systems. *J. Am. Chem. Soc.* **2004**, 126, 15046-15047.
- (21) Shoja, A.; Reid, J. P. Computational Insights into Privileged Stereocontrolling Interactions Involving Chiral Phosphates and Iminium Intermediates. *J. Am. Chem. Soc.* **2021**, 143, 7209-7215.
- (22) An, Q.; Shen, Y.; Fortunelli, A.; Goddard, W. A. Qm-Mechanism-Based Hierarchical High-Throughput in Silico Screening Catalyst Design for Ammonia Synthesis. *J. Am. Chem. Soc.* **2018**, 140, 17702-17710.
- (23) Gallarati, S.; Fabregat, R.; Laplaza, R.; Bhattacharjee, S.; Wodrich, M. d.; Corminboeuf, C. Reaction-Based Machine Learning Representations for Predicting the Enantioselectivity of Organocatalysts. *Chem. Sci.* **2021**, DOI:10.1039/d1sc00482d 10.1039/d1sc00482d, Ahead of Print.
- (24) See, X. Y.; Wen, X.; Wheeler, T. A.; Klein, C. K.; Goodpaster, J. D.; Reiner, B. R.; Tonks, I. A. Iterative Supervised Principal Component Analysis Driven Ligand Design for Regioselective Ti-Catalyzed Pyrrole Synthesis. *ACS Catal.* **2020**, 10, 13504-13517.
- (25) Nguyen, T. N.; Nakanowatari, S.; Nhat Tran, T. P.; Thakur, A.; Takahashi, L.; Takahashi, K.; Taniike, T. Learning Catalyst Design Based on Bias-Free Data Set for Oxidative Coupling of Methane. ACS Catal. 2021, 11, 1797-1809.
- (26) Xing, X.; Xu, C.; Chen, B.; Li, C.; Virgil, S. C.; Grubbs, R. H. Highly Active Platinum Catalysts for Nitrile and Cyanohydrin Hydration: Catalyst Design and Ligand Screening Via High-Throughput Techniques. *J. Am. Chem. Soc.* **2018**, 140, 17782-17789.
- (27) Fowler, B. S.; Laemmerhold, K. M.; Miller, S. J. Catalytic Site-Selective Thiocarbonylation and Deoxygenation of Vancomycin Reveal Hydroxyl-Dependent Conformational Effects. *J. Am. Chem. Soc.* **2012**, 134, 9755-9761.
- (28) Ding, K.; Du, H.; Yuan, Y.; Long, J. Combinatorial Chemistry Approach to Chiral Catalyst Engineering and Screening: Rational Design and Serendipity. *Chem. Eur. J.* **2004**, 10, 2872-2884.
- (29) Porte, A. M.; Reibenspies, J.; Burgess, K. Design and Optimization of New Phosphine Oxazoline Ligands Via High-Throughput Catalyst Screening. *J. Am. Chem. Soc.* **1998**, 120, 9180-9187.
- (30) Robbins, D. W.; Hartwig, J. F. A Simple, Multidimensional Approach to High-Throughput Discovery of Catalytic Reactions. *Science* **2011**, 333, 1423-1427.
- (31) Troshin, K.; Hartwig, J. F. Snap Deconvolution: An Informatics Approach to High-Throughput Discovery of Catalytic Reactions. *Science* **2017**, 357, 175-181.
- (32) McNally, A.; Prier, C. K.; MacMillan, D. W. C. Discovery of an Alpha-Amino C-H Arylation Reaction Using the Strategy of Accelerated Serendipity. *Science* **2011**, 334, 1114-1117.
- (33) Loskyll, J.; Stoewe, K.; Maier, W. F. Infrared Thermography as a High-Throughput Tool in Catalysis Research. *ACS Comb. Sci.* **2012**, 14, 295-303.

- (34) Reetz, M. T.; Becker, M. H.; Liebl, M.; Furstner, A. Ir-Thermographic Screening of Thermoneutral or Endothermic Transformations: The Ring-Closing Olefin Metathesis Reaction. *Angew. Chem., Int. Ed.* **2000**, 39, 1236-1239.
- (35) Taylor, S. J.; Morken, J. P. Thermographic Selection of Effective Catalysts from an Encoded Polymer-Bound Library. *Science (Washington, D. C.)* **1998**, 280, 267-270.
- (36) Reetz, M. T.; Becker, M. H.; Kuhling, K. M.; Holzwarth, A. Time-Resolved Ir-Thermographic Detection and Screening of Enantioselectivity in Catalytic Reactions. *Angew. Chem., Int. Ed.* **1998**, 37, 2647-2650.
- (37) Ebner, C.; Muller, C. A.; Markert, C.; Pfaltz, A. Determining the Enantioselectivity of Chiral Catalysts by Mass Spectrometric Screening of Their Racemic Forms. *J. Am. Chem. Soc.* **2011**, 133, 4710-4713.
- (38) Mueller, C. A.; Markert, C.; Teichert, A. M.; Pfaltz, A. Mass Spectrometric Screening of Chiral Catalysts and Catalyst Mixtures. *Chemical Communications (Cambridge, United Kingdom)* **2009**, DOI:10.1039/b822382c 10.1039/b822382c, 1607-1618.
- (39) Mueller, C. A.; Pfaltz, A. Mass Spectrometric Screening of Chiral Catalysts by Monitoring the Back Reaction of Quasienantiomeric Products: Palladium-Catalyzed Allylic Substitution. *Angew. Chem., Int. Ed.* **2008**, 47, 3363-3366.
- (40) Markert, C.; Pfaltz, A. Enantioselectivity Determination: Screening of Chiral Catalysts and Catalyst Mixtures by Mass Spectrometric Monitoring of Catalytic Intermediates. *Angew. Chem., Int. Ed.* **2004**, 43, 2498-2500.
- (41) Reetz, M. T.; Becker, M. H.; Klein, H.-W.; Stöckigt, D. A Method for High-Throughput Screening of Enantioselective Catalysts. *Angew. Chem. Int. Ed.* **1999**, 38, 1758-1761.
- (42) Guo, J.; Wu, J.; Siuzdak, G.; Finn, M. G. Measurement of Enantiomeric Excess by Kinetic Resolution and Mass Spectrometry. *Angew. Chem. Int. Ed.* **1999**, 38, 1755-1758.
- (43) Pluchinsky, A. J.; Wackelin, D. J.; Huang, X.; Arnold, F. H.; Mrksich, M. High Throughput Screening with Samdi Mass Spectrometry for Directed Evolution. *J. Am. Chem. Soc.* **2020**, 142, 19804-19808.
- (44) Bayly, A. A.; McDonald, B. R.; Mrksich, M.; Scheidt, K. A. High-Throughput Photocapture Approach for Reaction Discovery. *Proc. Natl. Acad. Sci.* **2020**, 117, 13261-13266.
- (45) O'Kane, P. T.; Dudley, Q. M.; McMillan, A. K.; Jewett, M. C.; Mrksich, M. High-Throughput Mapping of Coa Metabolites by Samdi-Ms to Optimize the Cell-Free Biosynthesis of Hmg-Coa. *Sci. Adv.* **2019**, 5, eaaw9180.
- (46) Szymczak, L. C.; Huang, C.-F.; Berns, E. J.; Mrksich, M. Combining Samdi Mass Spectrometry and Peptide Arrays to Profile Phosphatase Activities. *Methods Enzymol.* **2018**, 607, 389-403.
- (47) Cabrera-Pardo, J. R.; Chai, D. I.; Liu, S.; Mrksich, M.; Kozmin, S. A. Label-Assisted Mass Spectrometry for the Acceleration of Reaction Discovery and Optimization. *Nat. Chem.* **2013**, 5, 423-427.
- (48) Montavon, T. J.; Li, J.; Cabrera-Pardo, J. R.; Mrksich, M.; Kozmin, S. A. Three-Component Reaction Discovery Enabled by Mass Spectrometry of Self-Assembled Monolayers. *Nat. Chem.* **2012**, 4, 45-51.
- (49) Sun, J.; Jiang, Y.; Liu, H.; Huang, X.; Xiong, C.; Nie, Z. Ultrafast Photocatalytic Reaction Screening by Mass Spectrometry. *Anal. Chem.* **2020**, 92, 6564-6570.
- (50) Tielmann, P.; Boese, M.; Luft, M.; Reetz, M. T. A Practical High-Throughput Screening System for Enantioselectivity by Using Ftir Spectroscopy. *Chem. Eur. J.* **2003**, 9, 3882-3887.
- (51) Reetz, M. T.; Tielmann, P.; Eipper, A.; Ross, A.; Schlotterbeck, G. A High-Throughput Nmr-Based Ee-Assay Using Chemical Shift Imaging. *Chemical Communications (Cambridge, United Kingdom)* **2004**, 1366-1367.
- (52) Jung, E.; Kim, S.; Kim, Y.; Seo, S. H.; Lee, S. S.; Han, M. S.; Lee, S. A Colorimetric High-Throughput Screening Method for Palladium-Catalyzed Coupling Reactions of Aryl Iodides Using a Gold

- Nanoparticle-Based Iodide-Selective Probe. *Angew. Chem., Int. Ed.* **2011**, 50, 4386-4389, S4386/4381-S4386/4316.
- (53) Folmer-Andersen, J. F.; Lynch, V. M.; Anslyn, E. V. Colorimetric Enantiodiscrimination of Alpha-Amino Acids in Protic Media. *J. Am. Chem. Soc.* **2005**, 127, 7986-7987.
- (54) Loch, J. A.; Crabtree, R. H. Rapid Screening and Combinatorial Methods in Homogeneous Organometallic Catalysis. *Pure Appl. Chem.* **2001**, 73, 119-128.
- (55) Kawatsura, M.; Hartwig, J. F. Transition Metal-Catalyzed Addition of Amines to Acrylic Acid Derivatives. A High-Throughput Method for Evaluating Hydroamination of Primary and Secondary Alkylamines. *Organometallics* **2001**, 20, 1960-1964.
- (56) Lavastre, O.; Morken, J. P. Discovery of Novel Catalysts for Allylic Alkylation with a Visual Colorimetric Assay. *Angew. Chem., Int. Ed.* **1999**, 38, 3163-3165.
- (57) Wu, X.; Marks, J.; Wang, C.; Dickie, D.; Pu, L. Enantioselective Sensing in the Fluorous Phase for Catalyst Screening: Application of a Racemic Fluorescent Probe. *J. Org. Chem.* **2021**, 86, 4607-4615.
- (58) Belder, D.; Ludwig, M.; Wang, L.-W.; Reetz, M. T. Enantioselective Catalysis and Analysis on a Chip. *Angew. Chem., Int. Ed.* **2006**, 45, 2463-2466.
- (59) Moreira, R.; Havranek, M.; Sames, D. New Fluorogenic Probes for Oxygen and Carbene Transfer: A Sensitive Assay for Single Bead-Supported Catalysts. *J. Am. Chem. Soc.* **2001**, 123, 3927-3931.
- (60) Korbel, G. A.; Lalic, G.; Shair, M. D. Reaction Microarrays: A Method for Rapidly Determining the Enantiomeric Excess of Thousands of Samples. *J. Am. Chem. Soc.* **2001**, 123, 361-362.
- (61) Reetz, M. T.; Kühling, K. M.; Deege, A.; Hinrichs, H.; Belder, D. Super-High-Throughput Screening of Enantioselective Catalysts by Using Capillary Array Electrophoresis. *Angew. Chem. Int. Ed.* 2000, 39, 3891-3893.
- (62) Copeland, G. T.; Miller, S. J. A Chemosensor-Based Approach to Catalyst Discovery in Solution and on Solid Support. *J. Am. Chem. Soc.* **1999**, 121, 4306-4307.
- (63) Stauffer, S. R.; Hartwig, J. F. Fluorescence Resonance Energy Transfer (Fret) as a High-Throughput Assay for Coupling Reactions. Arylation of Amines as a Case Study. *J. Am. Chem. Soc.* **2003**, 125, 6977-6985.
- (64) Stambuli, J. P.; Stauffer, S. R.; Shaughnessy, K. H.; Hartwig, J. F. Screening of Homogeneous Catalysts by Fluorescence Resonance Energy Transfer. Identification of Catalysts for Room-Temperature Heck Reactions. *J. Am. Chem. Soc.* **2001**, 123, 2677-2678.
- (65) Pilicer, S. L.; Dragna, J. M.; Garland, A.; Welch, C. J.; Anslyn, E. V.; Wolf, C. High-Throughput Determination of Enantiopurity by Microplate Circular Dichroism. *J. Org. Chem.* **2020**, 85, 10858-10864.
- (66) Herrera, B. T.; Moor, S. R.; McVeigh, M.; Roesner, E. K.; Marini, F.; Anslyn, E. V. Rapid Optical Determination of Enantiomeric Excess, Diastereomeric Excess, and Total Concentration Using Dynamic-Covalent Assemblies: A Demonstration Using 2-Aminocyclohexanol and Chemometrics. *J. Am. Chem. Soc.* **2019**, 141, 11151-11160.
- (67) Giuliano, M. W.; Lin, C.-Y.; Romney, D. K.; Miller, S. J.; Anslyn, E. V. A Synergistic Combinatorial and Chiroptical Study of Peptide Catalysts for Asymmetric Baeyer-Villiger Oxidation. *Adv. Synth. Catal.* **2015**, 357, 2301-2309.
- (68) Ding, K.; Ishii, A.; Mikami, K. Super High Throughput Screening (Shts) of Chiral Ligands and Activators: Asymmetric Activation of Chiral Diol–Zinc Catalysts by Chiral Nitrogen Activators for the Enantioselective Addition of Diethylzinc to Aldehydes. *Angew. Chem. Int. Ed.* **1999**, 38, 497-501.
- (69) Shabbir, S. H.; Regan, C. J.; Anslyn, E. V. A General Protocol for Creating High-Throughput Screening Assays for Reaction Yield and Enantiomeric Excess Applied to Hydrobenzoin. *Proc. Natl. Acad. Sci. U. S. A.* **2009**, 106, 10487-10492, S10487/10481-S10487/10434.

- (70) Leung, D.; Folmer-Andersen, J. F.; Lynch, V. M.; Anslyn, E. V. Using Enantioselective Indicator Displacement Assays to Determine the Enantiomeric Excess of A-Amino Acids. *J. Am. Chem. Soc.* **2008**, 130, 12318-12327.
- (71) Zhu, L.; Zhong, Z.; Anslyn, E. V. Guidelines in Implementing Enantioselective Indicator-Displacement Assays for Alpha-Hydroxycarboxylates and Diols. J. Am. Chem. Soc. 2005, 127, 4260-4269.
- (72) Zhu, L.; Anslyn, E. V. Facile Quantification of Enantiomeric Excess and Concentration with Indicator-Displacement Assays: An Example in the Analyses of Alpha-Hydroxyacids. *J. Am. Chem. Soc.* **2004**, 126, 3676-3677.
- (73) Senkan, S.; Ozturk, S.; Krantz, K.; Onal, I. Photoionization Detection (Pid) as a High Throughput Screening Tool in Catalysis. *Appl. Catal., A* **2003**, 254, 97-106.
- (74) Senkan, S. M. High-Throughput Screening of Solid-State Catalyst Libraries. *Nature (London)* **1998**, 394, 350-353.
- (75) Hassan, D. S.; Kariapper, F. S.; Lynch, C. C.; Wolf, C. Accelerated Asymmetric Reaction Screening with Optical Assays. *Synthesis* **2022**, DOI:10.1055/a-1754-2271 10.1055/a-1754-2271, Ahead of Print.
- (76) Nelson, E.; Formen, J. S. S. K.; Wolf, C. Rapid Organocatalytic Chirality Analysis of Amines, Amino Acids, Alcohols, Amino Alcohols and Diols with Achiral Iso(Thio)Cyanate Probes. *Chem. Sci.* **2021**, 12, 8784-8790.
- (77) De los Santos, Z. A.; MacAvaney, S.; Russell, K.; Wolf, C. Tandem Use of Optical Sensing and Machine Learning for the Determination of Absolute Configuration, Enantiomeric and Diastereomeric Ratios, and Concentration of Chiral Samples. *Angew. Chem., Int. Ed.* **2020**, 59, 2440-2448.
- (78) Renom-Carrasco, M.; Lefort, L. Ligand Libraries for High Throughput Screening of Homogeneous Catalysts. *Chem. Soc. Rev.* **2018**, 47, 5038-5060.
- (79) Pfaltz, A. Design and Screening of Chiral Catalysts. *Chimia* **2010**, 64, 860-862.
- (80) Fonseca, M. H.; List, B. Combinatorial Chemistry and High-Throughput Screening for the Discovery of Organocatalysts. *Curr. Opin. Chem. Biol.* **2004**, 8, 319-326.
- (81) Stambuli, J. P.; Hartwig, J. F. Recent Advances in the Discovery of Organometallic Catalysts Using High-Throughput Screening Assays. *Curr. Opin. Chem. Biol.* **2003**, 7, 420-426.
- (82) Reetz, M. T. New Methods for the High-Throughput Screening of Enantioselective Catalysts and Biocatalysts. *Angew. Chem., Int. Ed.* **2002**, 41, 1335-1338.
- (83) Jo, H. H.; Lin, C.-Y.; Anslyn, E. V. Rapid Optical Methods for Enantiomeric Excess Analysis: From Enantioselective Indicator Displacement Assays to Exciton-Coupled Circular Dichroism. *Acc. Chem. Res.* **2014**, 47, 2212-2221.
- (84) Leung, D.; Kang, S. O.; Anslyn, E. V. Rapid Determination of Enantiomeric Excess: A Focus on Optical Approaches. *Chem. Soc. Rev.* **2012**, 41, 448-479.
- (85) Shevlin, M. Practical High-Throughput Experimentation for Chemists. *ACS Medicinal Chemistry Letters* **2017**, 8, 601-607.
- (86) Buitrago Santanilla, A.; Regalado, E. L.; Pereira, T.; Shevlin, M.; Bateman, K.; Campeau, L.-C.; Schneeweis, J.; Berritt, S.; Shi, Z.-C.; Nantermet, P.et al. Nanomole-Scale High-Throughput Chemistry for the Synthesis of Complex Molecules. *Science* **2015**, 347, 49.
- (87) Swyka, R. A.; Berkowitz, D. B. The in Situ Enzymatic Screening (Ises) Approach to Reaction Discovery and Catalyst Identification. *Curr. Protoc. Chem. Biol.* **2017**, 9, 285-305.
- (88) Créminon, C.; Taran, F. Enzyme Immunoassays as Screening Tools for Catalysts and Reaction Discovery. *Chem. Commun.* **2015**, 51, 7996-8009.
- (89) Chan, A. I.; McGregor, L. M.; Liu, D. R. Novel Selection Methods for DNA-Encoded Chemical Libraries. *Curr. Opin. Chem. Biol.* **2015**, 26, 55-61.

- (90) Kleiner, R. E.; Dumelin, C. E.; Liu, D. R. Small-Molecule Discovery from DNA-Encoded Chemical Libraries. *Chem. Soc. Rev.* **2011**, 40, 5707-5717.
- (91) Oukacine, F.; Ravelet, C.; Peyrin, E. Enantiomeric Sensing and Separation by Nucleic Acids. *TrAC, Trends Anal. Chem.* **2020**, 122, 115733.
- (92) Neveu, M.; Kim, H.-J.; Benner, S. A. The "Strong" Rna World Hypothesis: Fifty Years Old. *Astrobiology* **2013**, 13, 391-403.
- (93) Tuerk, C.; Gold, L. Systematic Evolution of Ligands by Exponential Enrichment: Rna Ligands to Bacteriophage T4 DNA Polymerase. *Science* **1990**, 249, 505-510.
- (94) Ellington, A. D.; Szostak, J. W. In Vitro Selection of Rna Molecules That Bind Specific Ligands. *Nature* **1990**, 346, 818-822.
- (95) Zhuo, Z.; Yu, Y.; Wang, M.; Li, J.; Zhang, Z.; Liu, J.; Wu, X.; Lu, A.; Zhang, G.; Zhang, B. Recent Advances in Selex Technology and Aptamer Applications in Biomedicine. *International journal of molecular sciences* **2017**, 18, 2142.
- (96) Fryszkowska, A.; Devine, P. N. Biocatalysis in Drug Discovery and Development. *Curr. Opin. Chem. Biol.* **2020**, 55, 151-160.
- (97) Woodley, J. M. Accelerating the Implementation of Biocatalysis in Industry. *Appl. Microbiol. Biotechnol.* **2019**, 103, 4733-4739.
- (98) Sheldon, R. A.; Woodley, J. M. Role of Biocatalysis in Sustainable Chemistry. *Chem. Rev.* **2018**, 118, 801-838.
- (99) Bommarius, A. S.; Blum, J. K.; Abrahamson, M. J. Status of Protein Engineering for Biocatalysts: How to Design an Industrially Useful Biocatalyst. *Curr. Opin. Chem. Biol.* **2011**, 15, 194-200.
- (100) Mattey Ashley, P.; Ford Grayson, J.; Citoler, J.; Baldwin, C.; Marshall James, R.; Palmer Ryan, B.; Turner Nicholas, J.; Cosgrove Sebastian, C.; Flitsch Sabine, L.; Thompson, M.et al. Development of Continuous Flow Systems to Access Secondary Amines through Previously Incompatible Biocatalytic Cascades*. *Angew Chem Int Ed Engl* **2021**.
- (101) Finnigan, W.; Hepworth, L. J.; Flitsch, S. L.; Turner, N. J. Retrobiocat as a Computer-Aided Synthesis Planning Tool for Biocatalytic Reactions and Cascades. *Nat. Catal.* **2021**, 4, 98-104.
- (102) Becker, A.; Boettcher, D.; Katzer, W.; Siems, K.; Mueller-Kuhrt, L.; Bornscheuer, U. T. An Adh Toolbox for Raspberry Ketone Production from Natural Resources Via a Biocatalytic Cascade. *Appl. Microbiol. Biotechnol.* **2021**, 105, 4189-4197.
- (103) Gandomkar, S.; Rocha, R.; Sorgenfrei, F. A.; Montero, L. M.; Fuchs, M.; Kroutil, W. Pqq-Dependent Dehydrogenase Enables One-Pot Bi-Enzymatic Enantio-Convergent Biocatalytic Amination of Racemic Sec-Allylic Alcohols. *ChemCatChem* **2021**, 13, 1290-1293.
- (104) Zhang, S.; Ruccolo, S.; Fryszkowska, A.; Klapars, A.; Marshall, N.; Strotman, N. A. Electrochemical Activation of Galactose Oxidase: Mechanistic Studies and Synthetic Applications. *ACS Catal.* **2021**, 11, 7270-7280.
- (105) Rother, D.; Malzacher, S. Computer-Aided Enzymatic Retrosynthesis. Nat. Catal. 2021, 4, 92-93.
- (106) Thorpe, T. W.; France, S. P.; Hussain, S.; Marshall, J. R.; Zawodny, W.; Mangas-Sanchez, J.; Montgomery, S. L.; Howard, R. M.; Daniels, D. S. B.; Kumar, R.et al. One-Pot Biocatalytic Cascade Reduction of Cyclic Enimines for the Preparation of Diastereomerically Enriched N-Heterocycles. *J. Am. Chem. Soc.* **2019**, 141, 19208-19213.
- (107) Ramsden, J. I.; Heath, R. S.; Derrington, S. R.; Montgomery, S. L.; Mangas-Sanchez, J.; Mulholland, K. R.; Turner, N. J. Biocatalytic N-Alkylation of Amines Using Either Primary Alcohols or Carboxylic Acids Via Reductive Aminase Cascades. *J. Am. Chem. Soc.* **2019**, 141, 1201-1206.
- (108) Rudroff, F. Whole-Cell Based Synthetic Enzyme Cascades-Light and Shadow of a Promising Technology. *Curr. Opin. Chem. Biol.* **2019**, 49, 84-90.

- (109) Schmermund, L.; Jurkas, V.; Oezgen, F. F.; Barone, G. D.; Buechsenschuetz, H. C.; Winkler, C. K.; Schmidt, S.; Kourist, R.; Kroutil, W. Photo-Biocatalysis: Biotransformations in the Presence of Light. *ACS Catal.* **2019**, 9, 4115-4144.
- (110) Erdmann, V.; Sehl, T.; Frindi-Wosch, I.; Simon, R. C.; Kroutil, W.; Rother, D. Methoxamine Synthesis in a Biocatalytic 1-Pot 2-Step Cascade Approach. *ACS Catal.* **2019**, *9*, 7380-7388.
- (111) Gandomkar, S.; Dennig, A.; Dordic, A.; Hammerer, L.; Pickl, M.; Haas, T.; Hall, M.; Faber, K. Biocatalytic Oxidative Cascade for the Conversion of Fatty Acids to A-Ketoacids Via Internal H2o2 Recycling. *Angew. Chem., Int. Ed.* **2018**, 57, 427-430.
- (112) Dennig, A.; Gandomkar, S.; Cigan, E.; Reiter, T. C.; Haas, T.; Hall, M.; Faber, K. Enantioselective Biocatalytic Formal A-Amination of Hexanoic Acid to L-Norleucine. *Org. Biomol. Chem.* **2018**, 16, 8030-8033.
- (113) Oeggl, R.; Massmann, T.; Jupke, A.; Rother, D. Four Atom Efficient Enzyme Cascades for All 4-Methoxyphenyl-1,2-Propanediol Isomers Including Product Crystallization Targeting High Product Concentrations and Excellent E-Factors. ACS Sustainable Chem. Eng. 2018, 6, 11819-11826.
- (114) France, S. P.; Hepworth, L. J.; Turner, N. J.; Flitsch, S. L. Constructing Biocatalytic Cascades: In Vitro and in Vivo Approaches to De Novo Multi-Enzyme Pathways. *ACS Catal.* **2017**, 7, 710-724.
- (115) Hernandez, K.; Bujons, J.; Joglar, J.; Charnock, S. J.; Dominguez de Maria, P.; Fessner, W. D.; Clapes, P. Combining Aldolases and Transaminases for the Synthesis of 2-Amino-4-Hydroxybutanoic Acid. *ACS Catal.* **2017**, 7, 1707-1711.
- (116) Faber, K.; Fessner, W.-D.; Turner, N. J. Engineering Biocatalysts for Synthesis Including Cascade Processes. *Adv. Synth. Catal.* **2015**, 357, 1565-1566.
- (117) Schmidt, S.; Scherkus, C.; Muschiol, J.; Menyes, U.; Winkler, T.; Hummel, W.; Groeger, H.; Liese, A.; Herz, H.-G.; Bornscheuer, U. T. An Enzyme Cascade Synthesis of E-Caprolactone and Its Oligomers. *Angew. Chem., Int. Ed.* **2015**, 54, 2784-2787.
- (118) Fessner, W.-D. Systems Biocatalysis: Development and Engineering of Cell-Free "Artificial Metabolisms" for Preparative Multi-Enzymatic Synthesis. *New Biotechnol.* **2015**, 32, 658-664.
- (119) Bayer, T.; Milker, S.; Wiesinger, T.; Rudroff, F.; Mihovilovic, M. D. Designer Microorganisms for Optimized Redox Cascade Reactions Challenges and Future Perspectives. *Adv. Synth. Catal.* **2015**, 357, 1587-1618.
- (120) Gall, M.; Thomsen, M.; Peters, C.; Pavlidis, I. V.; Jonczyk, P.; Gruenert, P. P.; Beutel, S.; Scheper, T.; Gross, E.; Backes, M.et al. Enzymatic Conversion of Flavonoids Using Bacterial Chalcone Isomerase and Enoate Reductase. *Angew. Chem., Int. Ed.* 2014, 53, 1439-1442.
- (121) Sehl, T.; Hailes, H. C.; Ward, J. M.; Wardenga, R.; von Lieres, E.; Offermann, H.; Westphal, R.; Pohl, M.; Rother, D. Two Steps in One Pot: Enzyme Cascade for the Synthesis of nor(Pseudo)Ephedrine from Inexpensive Starting Materials. *Angew. Chem., Int. Ed.* **2013**, 52, 6772-6775.
- (122) O'Reilly, E.; Ryan, J. Biocatalytic Cascades Go Viral. Science 2019, 366, 1199-1200.
- (123) Turner, N. J.; O'Reilly, E. Biocatalytic Retrosynthesis. Nat. Chem. Biol. 2013, 9, 285-288.
- (124) Moore, J. C.; Pollard, D. J.; Kosjek, B.; Devine, P. N. Advances in the Enzymatic Reduction of Ketones. *Acc. Chem. Res.* **2007**, 40, 1412-1419.
- (125) Schmidt, S.; Buechsenschuetz, H. C.; Scherkus, C.; Liese, A.; Groeger, H.; Bornscheuer, U. T. Biocatalytic Access to Chiral Polyesters by an Artificial Enzyme Cascade Synthesis. *ChemCatChem* **2015**, 7, 3951-3955.
- (126) Oberleitner, N.; Peters, C.; Muschiol, J.; Kadow, M.; Sass, S.; Bayer, T.; Schaaf, P.; Iqbal, N.; Rudroff, F.; Mihovilovic, M. D.et al. An Enzymatic Toolbox for Cascade Reactions: A Showcase for an in Vivo Redox Sequence in Asymmetric Synthesis. *ChemCatChem* **2013**, 5, 3524-3528.
- (127) Boettcher, D.; Schmidt, M.; Bornscheuer, U. T. Screens for Active and Stereoselective Hydrolytic Enzymes. *Methods Mol. Biol.* **2010**, 668, 169-176.

- (128) Bornscheuer, U. T.; Kazlauskas, R. J. Reaction Specificity of Enzymes: Catalytic Promiscuity in Biocatalysis: Using Old Enzymes to Form New Bonds and Follow New Pathways. *Angew. Chem., Int. Ed.* **2004**, 43, 6032-6040.
- (129) Schoenfeld, D. L.; Bornscheuer, U. T. Polarimetric Assay for the Medium-Throughput Determination of Alpha-Amino Acid Racemase Activity. *Anal. Chem.* **2004**, 76, 1184-1188.
- (130) Konarzycka-Bessler, M.; Bornscheuer, U. T. A High-Throughput-Screening Method for Determining the Synthetic Activity of Hydrolases. *Angew. Chem., Int. Ed.* **2003**, 42, 1418-1420.
- (131) Henke, E.; Bornscheuer Uwe, T. Fluorophoric Assay for the High-Throughput Determination of Amidase Activity. *Anal. Chem.* **2003**, 75, 255-260.
- (132) Baumann, M.; Sturmer, R.; Bornscheuer, U. T. A High-Throughput-Screening Method for the Identification of Active and Enantioselective Hydrolases. *Angew. Chem., Int. Ed.* **2001**, 40, 4201-4204.
- (133) Weissenborn, M. J.; Notonier, S.; Lang, S.-L.; Otte, K. B.; Herter, S.; Turner, N. J.; Flitsch, S. L.; Hauer, B. Whole-Cell Microtiter Plate Screening Assay for Terminal Hydroxylation of Fatty Acids by P450s. *Chemical Communications (Cambridge, United Kingdom)* **2016**, 52, 6158-6161.
- (134) Westley, C.; Xu, Y.; Carnell, A. J.; Turner, N. J.; Goodacre, R. Label-Free Surface Enhanced Raman Scattering Approach for High-Throughput Screening of Biocatalysts. *Anal. Chem.* **2016**, 88, 5898-5903.
- (135) Yan, C.; Schmidberger, J. W.; Parmeggiani, F.; Hussain, S. A.; Turner, N. J.; Flitsch, S. L.; Barran, P. Rapid and Sensitive Monitoring of Biocatalytic Reactions Using Ion Mobility Mass Spectrometry. *Analyst (Cambridge, United Kingdom)* **2016**, 141, 2351-2355.
- (136) Kohler, V.; Turner, N. J. Artificial Concurrent Catalytic Processes Involving Enzymes. *Chemical Communications (Cambridge, United Kingdom)* **2015**, 51, 450-464.
- (137) Turner, N. J.; Wells, A. The Enzyme Spring: Biocatalysis at Its Best. *ChemCatChem* **2014**, 6, 900-901.
- (138) Daugherty, A. B.; Horton, J. R.; Cheng, X.; Lutz, S. Structural and Functional Consequences of Circular Permutation on the Active Site of Old Yellow Enzyme. *ACS Catal.* **2015**, 5, 892-899.
- (139) Hollfelder, F.; Lutz, S. Just (Protein) Engineering? Curr. Opin. Struct. Biol. 2013, 23, 569-570.
- (140) Daugherty, A. B.; Govindarajan, S.; Lutz, S. Improved Biocatalysts from a Synthetic Circular Permutation Library of the Flavin-Dependent Oxidoreductase Old Yellow Enzyme. *J. Am. Chem. Soc.* **2013**, 135, 14425-14432.
- (141) Grognux, J.; Reymond, J.-L. A Red-Fluorescent Substrate Microarray for Lipase Fingerprinting. *Mol. BioSyst.* **2006**, 2, 492-498.
- (142) Yang, Y.; Babiak, P.; Reymond, J.-L. New Monofunctionalized Fluorescein Derivatives for the Efficient High-Throughput Screening of Lipases and Esterases in Aqueous Media. *Helv. Chim. Acta* **2006**, 89, 404-415.
- (143) Yang, Y.; Babiak, P.; Reymond, J.-L. Low Background Fret-Substrates for Lipases and Esterases Suitable for High-Throughput Screening under Basic (Ph 11) Conditions. *Org. Biomol. Chem.* **2006**, 4, 1746-1754.
- (144) Yang, Y.; Reymond, J.-L. Protease Profiling Using a Fluorescent Domino Peptide Cocktail. *Mol. BioSyst.* **2005**, 1, 57-63.
- (145) Sicard, R.; Chen, L. S.; Marsaioli, A. J.; Reymond, J.-L. A Fluorescence-Based Assay for Baeyer-Villiger Monooxygenases, Hydroxylases and Lactonases. *Adv. Synth. Catal.* **2005**, 347, 1041-1050.
- (146) Reetz, M. T.; Kahakeaw, D.; Sanchis, J. Shedding Light on the Efficacy of Laboratory Evolution Based on Iterative Saturation Mutagenesis. *Mol. BioSyst.* **2009**, 5, 115-122.
- (147) Reetz, M. T. Directed Evolution of Enzymes for Asymmetric Syntheses. *Asymmetric Synthesis* **2007**, 207-211.

- (148) Reetz, M. T.; Bocola, M.; Carballeira, J. D.; Zha, D.; Vogel, A. Expanding the Range of Substrate Acceptance of Enzymes: Combinatorial Active-Site Saturation Test. *Angew. Chem., Int. Ed.* **2005**, 44, 4192-4196.
- (149) Reetz, M. T.; Kuhling, K. M.; Wilensek, S.; Husmann, H.; Hausig, U. W.; Hermes, M. A Gc-Based Method for High-Throughput Screening of Enantioselective Catalysts. *Catal. Today* **2001**, 67, 389-396.
- (150) Berkowitz, D. B.; Bose, M.; Choi, S. In Situ Enzymatic Screening (Ises): A Tool for Catalyst Discovery and Reaction Development. *Angew. Chem., Int. Ed.* **2002**, 41, 1603-1607.
- (151) Alberty, R. A. Thermodynamics of Reactions of Nicotinamide Adenine Dinucleotide and Nicotinamide Adenine Dinucleotide Phosphate. *Arch. Biochem. Biophys.* **1993**, 307, 8-14.
- (152) McCune, C. D.; Beio, M. L.; Sturdivant, J. M.; de la Salud-Bea, R.; Darnell, B. M.; Berkowitz, D. B. Synthesis and Deployment of an Elusive Fluorovinyl Cation Equivalent: Access to Quaternary A-(1'-Fluoro)Vinyl Amino Acids as Potential Plp Enzyme Inactivators. *J. Am. Chem. Soc.* **2017**, 139, *ASAP*.
- (153) Berkowitz, D. B.; Chisowa, E.; McFadden, J. M. Stereocontrolled Synthesis of Quaternary Beta, Gamma-Unsaturated Amino Acids: Chain Extension of D- and L-Alpha-(2-Tributylstannyl) Vinyl Amino Acids. *Tetrahedron* **2001**, 57, 6329-6343.
- (154) Berkowitz, D. B.; McFadden, J. M.; Sloss, M. K. Engineering Acyclic Stereocontrol in the Alkylation of Vinylglycine-Derived Dianions: Asymmetric Synthesis of Higher Alpha-Vinyl Amino Acids. *J. Org. Chem.* **2000**, 65, 2907-2918.
- (155) Berkowitz, D. B.; McFadden, J. M.; Chisowa, E.; Semerad, C. L. Organoselenium-Based Entry into Versatile, Alpha-(2-Tributylstannyl)Vinyl Amino Acids in Scalemic Form: A New Route to Vinyl Stannanes. *J. Am. Chem. Soc.* **2000**, 122, 11031-11032.
- (156) Berkowitz, D. B.; Pedersen, M. L.; Jahng, W.-J. Synthesis of Higher Alpha-Chlorovinyl and Alpha-Bromovinyl Amino Acids: The Amino Protecting Group Determines the Reaction Course. *Tetrahedron Lett.* **1996**, 37, 4309-4312.
- (157) Berkowitz, D. B.; Jahng, W.-J.; Pedersen, M. L. Alpha-Vinyllysine and Alpha-Vinylarginine Are Time-Dependent Inhibitors of Their Cognate Decarboxylases. *Bioorg. Med. Chem. Lett.* **1996**, 6, 2151-2156.
- (158) Berkowitz, D. B.; Pedersen, M. L. Free Alpha-Oxiranyl Amino Acids. *J. Org. Chem.* **1995**, 60, 5368-5369
- (159) Berkowitz, D. B.; Pumphrey, J. A.; Shen, Q. Enantiomerically Enriched Alpha-Vinyl Amino Acids Via Lipase-Mediated Reverse Transesterification. *Tetrahedron Lett.* **1994**, 35, 8743-8746.
- (160) Pedersen, M. L.; Berkowitz, D. B. Formal Alpha-Vinylation of Amino Acids. Use of a New Benzeneselenolate Equivalent. *J. Org. Chem.* **1993**, 58, 6966-6975.
- (161) Berkowitz, D. B.; Smith, M. K. Enantiomerically Enriched .Alpha.-Methyl Amino Acids. Use of an Acyclic, Chiral Alanine-Derived Dianion with a High Diastereofacial Bias. *Journal of Organic Chemistry* **1995**, 60, 1233-1238.
- (162) Berkowitz, D. B.; Charette, B. D.; Karukurichi, K. R.; McFadden, J. M. A-Vinylic Amino Acids: Occurrence, Asymmetric Synthesis and Biochemical Mechanisms. *Tetrahedron, asymmetry* **2006**, 17, 869-882.
- (163) Berkowitz, D. B.; Wu, B.; Li, H. A Formal [3,3]-Sigmatropic Rearrangement Route to Quaternary A-Vinyl Amino Acids: Use of Allylic N-Pmp Trifluoroacetimidates. *Org. Lett.* **2006**, 8, 971-974.
- (164) Berkowitz, D. B.; Karukurichi, K. R.; de la Salud-Bea, R.; Maiti, G.; McFadden, J. M.; Morris, M. L. In *Asymmetric Synthesis and Application of A-Amino Acids*; American Chemical Society, 2009; Vol. 1009.
- (165) Berkowitz, D. B.; de la Salud-Bea, R.; Jahng, W.-J. Synthesis of Quaternary Amino Acids Bearing a (2'Z)-Fluorovinyl Alpha-Branch: Potential Plp Enzyme Inactivators. *Org. Lett.* **2004**, 6, 1821-1824.

- (166) Karukurichi, K. R.; de la Salud-Bea, R.; Jahng, W. J.; Berkowitz, D. B. Examination of the New R-(2'Z-Fluoro)Vinyl Trigger with Lysine Decarboxylase: The Absolute Stereochemistry Dictates the Reaction Course. *J. Am. Chem. Soc* **2007**, 129, 258-259.
- (167) Capitani, G.; Tschopp, M.; Eliot, A. C.; Kirsch, J. F.; Grütter, M. G. Structure of Acc Synthase Inactivated by the Mechanism-Based Inhibitor L-Vinylglycine. *FEBS Lett.* **2005**, 579, 2458-2462.
- (168) Berkowitz, D. B.; Smith, M. K. A Convenient Synthesis of L-A-Vinylglycine from L-Homoserine Lactone. *Synthesis* **1996**, 1996, 39-41.
- (169) Trost, B. M.; Machacek, M. R.; Aponick, A. Predicting the Stereochemistry of Diphenylphosphino Benzoic Acid (Dppba)-Based Palladium-Catalyzed Asymmetric Allylic Alkylation Reactions: A Working Model. *Acc. Chem. Res.* **2006**, 39, 747-760.
- (170) Trost, B. M. Asymmetric Allylic Alkylation, an Enabling Methodology. *The Journal of Organic Chemistry* **2004**, 69, 5813-5837.
- (171) Trost, B. M.; Bunt, R. C.; Lemoine, R. C.; Calkins, T. L. Dynamic Kinetic Asymmetric Transformation of Diene Monoepoxides: A Practical Asymmetric Synthesis of Vinylglycinol, Vigabatrin, and Ethambutol. *J. Am. Chem. Soc.* **2000**, 122, 5968-5976.
- (172) Berkowitz, D. B.; Maiti, G. Following an Ises Lead: The First Examples of Asymmetric Ni(0)-Mediated Allylic Amination. *Org. Lett.* **2004**, *6*, 2661-2664.
- (173) Berkowitz, D. B.; Shen, W.; Maiti, G. In Situ Enzymatic Screening (Ises) of P,N-Ligands for Ni(0)-Mediated Asymmetric Intramolecular Allylic Amination. *Tetrahedron: Asymmetry* **2004**, 15, 2845-2851.
- (174) Trost, B. M.; Fullerton, T. J. New Synthetic Reactions. Allylic Alkylation. *J. Am. Chem. Soc.* **1973**, 95, 292-294.
- (175) Li, G.; Huo, X.; Jiang, X.; Zhang, W. Asymmetric Synthesis of Allylic Compounds Via Hydrofunctionalisation and Difunctionalisation of Dienes, Allenes, and Alkynes. *Chem. Soc. Rev.* **2020**, 49, 2060-2118.
- (176) Huang, H. M.; Bellotti, P.; Glorius, F. Transition Metal-Catalysed Allylic Functionalization Reactions Involving Radicals. *Chem. Soc. Rev.* **2020**, 49, 6186-6197.
- (177) Butt, N. A.; Zhang, W. Transition Metal-Catalyzed Allylic Substitution Reactions with Unactivated Allylic Substrates. *Chem. Soc. Rev.* **2015**, 44, 7929-7967.
- (178) Sundararaju, B.; Achard, M.; Bruneau, C. Transition Metal Catalyzed Nucleophilic Allylic Substitution: Activation of Allylic Alcohols Via Pi-Allylic Species. *Chem. Soc. Rev.* **2012**, 41, 4467-4483.
- (179) Trost, B. M.; Crawley, M. L. Asymmetric Transition-Metal-Catalyzed Allylic Alkylations: Applications in Total Synthesis. *Chem. Rev.* **2003**, 103, 2921-2944.
- (180) Trost, B. M.; Van Vranken, D. L. Asymmetric Transition Metal-Catalyzed Allylic Alkylations. *Chem. Rev.* **1996**, 96, 395-422.
- (181) Lu, Z.; Ma, S. Metal-Catalyzed Enantioselective Allylation in Asymmetric Synthesis. *Angew. Chem. Int. Ed.* **2008**, 47, 258-297.
- (182) Cheng, Q.; Tu, H.-F.; Zheng, C.; Qu, J.-P.; Helmchen, G.; You, S.-L. Iridium-Catalyzed Asymmetric Allylic Substitution Reactions. *Chem. Rev.* **2019**, 119, 1855-1969.
- (183) Qu, J.; Helmchen, G. Applications of Iridium-Catalyzed Asymmetric Allylic Substitution Reactions in Target-Oriented Synthesis. *Acc. Chem. Res.* **2017**, 50, 2539-2555.
- (184) Spielmann, K.; Niel, G.; de Figueiredo, R. M.; Campagne, J. M. Catalytic Nucleophilic 'Umpoled' Pi-Allyl Reagents. *Chem. Soc. Rev.* **2018**, 47, 1159-1173.
- (185) Wright, T. B.; Turnbull, B. W. H.; Evans, P. A. Enantioselective Rhodium-Catalyzed Allylic Alkylation of Beta, Gamma-Unsaturated Alpha-Amino Nitriles: Synthetic Homoenolate Equivalents. *Angew. Chem. Int. Ed.* **2019**, 58, 9886-9890.

- (186) Turnbull, B. W. H.; Evans, P. A. Asymmetric Rhodium-Catalyzed Allylic Substitution Reactions: Discovery, Development and Applications to Target-Directed Synthesis. *J. Org. Chem.* **2018**, 83, 11463-11479.
- (187) Evans, P. A.; Leahy, D. K. Regio- and Enantiospecific Rhodium-Catalyzed Allylic Etherification Reactions Using Copper(I) Alkoxides: Influence of the Copper Halide Salt on Selectivity. *J. Am. Chem. Soc.* **2002**, 124, 7882-7883.
- (188) Kanbayashi, N.; Hosoda, K.; Okamura, T.-a.; Aoshima, S.; Onitsuka, K. Enantio- and Diastereoselective Polymerization: Asymmetric Allylic Alkylation Catalyzed by a Planar-Chiral Cp'Ru Complex. *Polymer Chemistry* **2016**, 7, 3691-3699.
- (189) Kanbayashi, N.; Hosoda, K.; Kato, M.; Takii, K.; Okamura, T. A.; Onitsuka, K. Enantio- and Diastereoselective Asymmetric Allylic Alkylation Catalyzed by a Planar-Chiral Cyclopentadienyl Ruthenium Complex. *Chemical Communications (Cambridge, United Kingdom)* **2015**, 51, 10895-10898.
- (190) Bayer, A.; Kazmaier, U. Ruthenium-Catalyzed Allylic Alkylations of Chelated Enolates Using Vinyl Dioxolanon-2-Ones. *J. Org. Chem.* **2014**, 79, 8498-8504.
- (191) Trost, B. M.; Rao, M.; Dieskau, A. P. A Chiral Sulfoxide-Ligated Ruthenium Complex for Asymmetric Catalysis: Enantio- and Regioselective Allylic Substitution. *J. Am. Chem. Soc.* **2013**, 135, 18697-18704.
- (192) Farthing, C. N.; Kočovský, P. The Stereochemical Dichotomy in Palladium(0)- and Nickel(0)-Catalyzed Allylic Substitution. *J. Am. Chem. Soc.* **1998**, 120, 6661-6672.
- (193) Tolman, C. A. Chemistry of Tetrakis(Triethyl Phosphite) Nickel Hydride, Hni[P(Oet)3]4+. Iii. Proton Nuclear Magnetic Resonance Study of Reactions with Dienes. *J. Am. Chem. Soc.* **1970**, 92, 6785-6790.
- (194) Yamamoto, T.; Ishizu, J.; Yamamoto, A. Interaction of Nickel(0) Complexes with Allyl Carboxylates, Allyl Ethers, Allylic Alcohols, and Vinyl Acetate. .Pi.-Complex Formation and Oxidative Addition to Nickel Involving Cleavage of the Alkenyl-Oxygen Bond. J. Am. Chem. Soc. 1981, 103, 6863-6869.
- (195) Yamamoto, T.; Ishizu, J.; Kohara, T.; Komiya, S.; Yamamoto, A. Oxidative Addition of Aryl Carboxylates to Nickel(0) Complexes Involving Cleavage of the Acyl-Oxygen Bond. *J. Am. Chem. Soc.* **1980**, 102, 3758-3764.
- (196) Hiyama, T.; Wakasa, N. Asymmetric Coupling of Arylmagnesium Bromides with Allylic Esters. *Tetrahedron Lett.* **1985**, 26, 3259-3262.
- (197) Consiglio, G.; Piccolo, O.; Roncetti, L.; Morandini, F. Asymmetric Nickel-Catalyzed Cross-Coupling Reaction of Allylic Substrates with Grignard Reagents. *Tetrahedron* **1986**, 42, 2043-2053.
- (198) Consiglio, G.; Morandini, F.; Piccolo, O. Stereochemical Aspects of the Nickel-Catalyzed Alkylation of Allylic Alcohols. *J. Am. Chem. Soc.* **1981**, 103, 1846-1847.
- (199) Nomura, N.; RajanBabu, T. V. Nickel-Catalyzed Asymmetric Allylation of Alkyl Grignard Reagents. Effect of Ligands, Leaving Groups and a Kinetic Resolution with a Hard Nucleophile. *Tetrahedron Lett.* **1997**, 38, 1713-1716.
- (200) Didiuk, M. T.; Morken, J. P.; Hoveyda, A. H. Phosphine-Directed Stereo- & Regioselective Ni-Catalyzed Reactions of Grignard Reagents with Allylic Ethers. *Tetrahedron* **1998**, 54, 1117-1130.
- (201) Didiuk, M. T.; Morken, J. P.; Hoveyda, A. H. Directed Regio- and Stereoselective Nickel-Catalyzed Addition of Alkyl Grignard Reagents to Allylic Ethers. *J. Am. Chem. Soc.* **1995**, 117, 7273-7274.
- (202) Moberg, C. Stereochemistry of Nucleophilic Attack by Amine on a Cationic Π-Allylnickel Complex. *Tetrahedron Lett.* **1980**, 21, 4539-4542.
- (203) Bricout, H.; Carpentier, J.-F.; Mortreux, A. Nickel-Catalyzed Substitution Reactions of Allylic Compounds with Soft Nucleophiles: An Efficient Alternative to Palladium Catalysis. *J. Chem. Soc., Chem. Commun.* **1995**, DOI:10.1039/c39950001863 10.1039/c39950001863, 1863-1864.

- (204) Evans, P.; Grange, R.; Clizbe, E. Recent Developments in Asymmetric Allylic Amination Reactions. *Synthesis* **2016**, 48, 2911-2968.
- (205) Kita, Y.; Sakaguchi, H.; Hoshimoto, Y.; Nakauchi, D.; Nakahara, Y.; Carpentier, J. F.; Ogoshi, S.; Mashima, K. Pentacoordinated Carboxylate Pi-Allyl Nickel Complexes as Key Intermediates for the Ni-Catalyzed Direct Amination of Allylic Alcohols. *Chemistry* **2015**, 21, 14571-14578.
- (206) Sweeney, J. B.; Ball, A. K.; Lawrence, P. A.; Sinclair, M. C.; Smith, L. J. A Simple, Broad-Scope Nickel(0) Precatalyst System for the Direct Amination of Allyl Alcohols. *Angew. Chem. Int. Ed.* **2018**, 57, 10202-10206.
- (207) Blieck, R.; Azizi, M. S.; Mifleur, A.; Roger, M.; Persyn, C.; Sauthier, M.; Bonin, H. Nickel-Catalysed Bis-Allylation of Activated Nucleophiles with Allyl -Alcohol. *Eur. J. Org. Chem.* **2016**, 2016, 1194-1198.
- (208) Sweeney, J. B.; Ball, A. K.; Smith, L. J. Catalytic C-C Bond Formation Using a Simple Nickel Precatalyst System: Base- and Activator-Free Direct C-Allylation by Alcohols and Amines. *Chemistry* **2018**, 24, 7354-7357.
- (209) Sha, S.-C.; Jiang, H.; Mao, J.; Bellomo, A.; Jeong, S. A.; Walsh, P. J. Nickel-Catalyzed Allylic Alkylation with Diarylmethane Pronucleophiles: Reaction Development and Mechanistic Insights. *Angew. Chem. Int. Ed.* **2016**, 55, 1070-1074.
- (210) Kita, Y.; Kavthe, R. D.; Oda, H.; Mashima, K. Asymmetric Allylic Alkylation of Beta-Ketoesters with Allylic Alcohols by a Nickel/Diphosphine Catalyst. *Angew. Chem. Int. Ed.* **2016**, 55, 1098-1101.
- (211) Nagae, H.; Xia, J.; Kirillov, E.; Higashida, K.; Shoji, K.; Boiteau, V.; Zhang, W.; Carpentier, J.-F.; Mashima, K. Asymmetric Allylic Alkylation of B-Ketoesters Via C–N Bond Cleavage of N-Allyl-N-Methylaniline Derivatives Catalyzed by a Nickel–Diphosphine System. *ACS Catalysis* **2020**, 10, 5828-5839.
- (212) Ngamnithiporn, A.; Jette, C. I.; Bachman, S.; Virgil, S. C.; Stoltz, B. M. Nickel-Catalyzed Enantioselective Allylic Alkylation of Lactones and Lactams with Unactivated Allylic Alcohols. *Chem Sci* **2018**, 9, 2547-2551.
- (213) Long, J.; Yu, R.; Gao, J.; Fang, X. Access to 1,3-Dinitriles by Enantioselective Auto-Tandem Catalysis: Merging Allylic Cyanation with Asymmetric Hydrocyanation. *Angew. Chem. Int. Ed.* **2020**, 59, 6785-6789.
- (214) Trost, B. M.; Spagnol, M. D. Nickel Catalyzed Coupling of Allylamines and Boronic Acids. *J. Chem. Soc., Perkin Trans.* 1 **1995**, 2083-2096.
- (215) Kobayashi, Y.; Tokoro, Y.; Watatani, K. Preparation of Functionalized Zinc Borates and Their Coupling Reaction with Allylic Acetates. *Tetrahedron Lett.* **1998**, 39, 7537-7540.
- (216) Kobayashi, Y.; Takahisa, E.; Usmani, S. B. Realization of High Regioselectivity in the Coupling Reaction of a Cyclopentadiene Monoepoxide Equivalent and Aryl Nucleophiles. *Tetrahedron Lett.* **1998**, 39, 597-600.
- (217) Kobayashi, Y.; Watatani, K.; Kikori, Y.; Mizojiri, R. A New Approach to (+)-Brefeldin a Via a Nickel-Catalyzed Coupling Reaction of Cyclopentenyl Acetate and Lithium 2-Furylborate. *Tetrahedron Lett.* **1996**, 37, 6125-6128.
- (218) Kobayashi, Y.; Mizojiri, R.; Ikeda, E. Nickel-Catalyzed Coupling Reaction of 1,3-Disubstituted Secondary Allylic Carbonates and Lithium Aryl- and Alkenylborates. *The Journal of Organic Chemistry* **1996**, 61, 5391-5399.
- (219) Kobayashi, Y.; Tokoro, Y.; Watatani, K. Zinc Borates: Functionalized Hard Nucleophiles for Coupling Reactions with Secondary Allylic Acetates. *Eur. J. Org. Chem.* **2000**, 2000, 3825-3834.
- (220) Chung, K.-G.; Miyake, Y.; Uemura, S. Nickel(0)-Catalyzed Asymmetric Cross-Coupling Reactions of Allylic Compounds with Arylboronic Acids. *Perkin 1* **2000**, 15-18.

- (221) Dey, S.; Karukurichi, K. R.; Shen, W.; Berkowitz, D. B. Double-Cuvette Ises: In Situ Estimation of Enantioselectivity and Relative Rate for Catalyst Screening. *J. Am. Chem. Soc.* **2005**, 127, 8610-8611.
- (222) Karukurichi, K. R.; Fei, X.; Swyka, R. A.; Broussy, S.; Shen, W.; Dey, S.; Roy, S. K.; Berkowitz, D. B. Mini-Ises Identifies Promising Carbafructopyranose-Based Salens for Asymmetric Catalysis: Tuning Ligand Shape Via the Anomeric Effect. *Sci Adv* **2015**, 1.
- (223) Dey, S.; Powell, D. R.; Hu, C.; Berkowitz, D. B. Cassette in Situ Enzymatic Screening Identifies Complementary Chiral Scaffolds for Hydrolytic Kinetic Resolution across a Range of Epoxides. *Angew. Chem., Int. Ed.* **2007**, 46, 7010-7014.
- (224) Friest, J. A.; Broussy, S.; Chung, W. J.; Berkowitz, D. B. Combinatorial Catalysis Employing a Visible Enzymatic Beacon in Real Time: Synthetically Versatile (Pseudo)Halometalation/Carbocyclizations. *Angew. Chem. Int. Ed.* **2011**, 50, 8895-8899.
- (225) Zhou, F.; Han, X.; Lu, X. Palladium(Ii)-Catalyzed Synthesis of Functionalized Indenes from O-Alkynylbenzylidene Ketones. *J. Org. Chem.* **2011**, 76, 1491-1494.
- (226) Ji, J.; Zhang, C.; Lu, X. Palladium-Templated Regio- and Stereoselective Cyclization of 2'-Alkenyl 2-Alkynoates and Its Synthetic Applications. *J. Org. Chem.* **1995**, 60, 1160-1169.
- (227) Ma, S.; Lu, X. Divalent Palladium Catalyzed Stereoselective Synthesis of A-(Z)-(Halomethylene)-Γ-Butyrolactone Derivatives and Its Mechanism. *J. Org. Chem.* **1991**, 56, 5120-5125.
- (228) Ma, S.; Lu, X. Palladium Dihalide Catalyzed Stereoselective Synthesis of A-(Z)-Halomethylene-Γ-Butyrolactone Derivatives. *J. Chem. Soc., Chem. Commun.* **1990**, DOI:10.1039/C39900000733 10.1039/C39900000733, 733-734.
- (229) Malik, G.; Swyka, R. A.; Tiwari, V. K.; Fei, X.; Applegate, G. A.; Berkowitz, D. B. A Thiocyanopalladation/Carbocyclization Transformation Identified through Enzymatic Screening: Stereocontrolled Tandem C-Scn and C-C Bond Formation. *Chem. Sci.* **2017**, 8, 8050-8060.
- (230) Ginotra, S. K.; Friest, J. A.; Berkowitz, D. B. Halocarbocyclization Entry into the Oxabicyclo[4.3.1]Decyl Exomethylene-Δ-Lactone Cores of Linearifolin and Zaluzanin A: Exploiting Combinatorial Catalysis. *Org. Lett.* **2012**, 14, 968-971.
- (231) Lu, X. Y.; Zhu, G. X.; Wang, Z. Enyne Coupling as the Potent Methodology for the Synthesis of Bioactive Molecules. *Synlett* **1998**, DOI:10.1055/s-1998-1585 10.1055/s-1998-1585, 115-121.
- (232) Tong, X.; Zhang, Z.; Zhang, X. Novel Rhodium-Catalyzed Cycloisomerization of 1,6-Enynes with an Intramolecular Halogen Shift. *J. Am. Chem. Soc.* **2003**, 125, 6370-6371.
- (233) Lu, X.; Zhu, G.; Wang, Z.; Ma, S.; Ji, J.; Zhang, Z. Enyne Cyclization Methodology for the Synthesis of Bioactive Lactones. *Pure Appl. Chem.* **1997**, 69, 553-558.
- Zhang, Q.; Lu, X. Highly Enantioselective Palladium(Ii)-Catalyzed Cyclization of (Z)-4'-Acetoxy-2'-Butenyl 2-Alkynoates: An Efficient Synthesis of Optically Active Γ-Butyrolactones. *J. Am. Chem. Soc.* **2000**, 122, 7604-7605.
- (235) Welbes, L. L.; Lyons, T. W.; Cychosz, K. A.; Sanford, M. S. Synthesis of Cyclopropanes Via Pd(Ii/Iv)-Catalyzed Reactions of Enynes. *J. Am. Chem. Soc.* **2007**, 129, 5836-5837.
- (236) Jackowski, O.; Wang, J.; Xie, X.; Ayad, T.; Zhang, Z.; Ratovelomanana-Vidal, V. Enantioselective Rhodium-Catalyzed Synthesis of A-Chloromethylene-Γ-Butyrolactams from N-Allylic Alkynamides. *Org. Lett.* **2012**, 14, 4006-4009.
- (237) Wang, J.; Tong, X.; Xie, X.; Zhang, Z. Rhodium-Catalyzed Activation of C(Sp3)–X (X = Cl, Br) Bond: An Intermolecular Halogen Exchange Case. *Org. Lett.* **2010**, 12, 5370-5373.
- (238) Tong, X.; Li, D.; Zhang, Z.; Zhang, X. Rhodium-Catalyzed Cycloisomerization of 1,6-Enynes with an Intramolecular Halogen Shift: Reaction Scope and Mechanism. *J. Am. Chem. Soc.* **2004**, 126, 7601-7607.
- (239) Shen, K.; Han, X.; Lu, X. Cationic Pd(Ii)-Catalyzed Reductive Cyclization of Alkyne-Tethered Ketones or Aldehydes Using Ethanol as Hydrogen Source. *Org. Lett.* **2013**, 15, 1732-1735.

- (240) Yin, G.; Liu, G. Palladium-Catalyzed Oxidative Cyclization of Enynes with Hydrogen Peroxide as the Oxidant. *Angew. Chem. Int. Ed. Engl.* **2008**, 47, 5442-5445.
- (241) Zhang, Z.; Lu, X.; Xu, Z.; Zhang, Q.; Han, X. Role of Halide Ions in Divalent Palladium-Mediated Reactions: Competition between B-Heteroatom Elimination and B-Hydride Elimination of a Carbon-Palladium Bond. *Organometallics* **2001**, 20, 3724-3728.
- (242) Wang, Z.; Lu, X. Palladium-Catalyzed Nucleophile-Alkyne-A,B-Unsaturated Carbonyl Coupling through Tandem Nucleopalladation and Conjugate Addition. *J. Org. Chem.* **1996**, 61, 2254-2255.
- (243) Ji, J.; Wang, Z.; Lu, X. Studies on [Pdh]- and [Pdcl] Catalyzed Intramolecular Cyclization: The Search for a Better Solution to Selective Enyne Coupling. *Organometallics* **1996**, 15, 2821-2828.
- Lu, X.; Ma, S.; Ji, J.; Zhu, G.; Jiang, H. Construction of A-Alkylidene-Γ-Butyrolactones from Acyclic Ester Precursors. *Pure Appl. Chem.* **1994**, 66, 1501-1508.
- (245) Ma, S.; Lu, X. Stereoselective Synthesis Of .Alpha.-Chloromethylene-.Gamma.-Butyrolactone Derivatives from Acyclic Allylic 2-Alkynoates. *Journal of Organic Chemistry* **1993**, 58, 1245-1250.
- (246) Ma, S.; Lu, X. A Novel Stereospecific Hydrohalogenation Reaction of Propiolates and Propiolic Acid. *J. Chem. Soc., Chem. Commun.* **1990**, DOI:10.1039/c39900001643 10.1039/c39900001643, 1643-1644.
- (247) Shen, C.; Zhang, P.; Sun, Q.; Bai, S.; Hor, T. S.; Liu, X. Recent Advances in C-S Bond Formation Via C-H Bond Functionalization and Decarboxylation. *Chem. Soc. Rev.* **2015**, 44, 291-314.
- (248) Slocum, J. D.; Webb, L. J. Nitrile Probes of Electric Field Agree with Independently Measured Fields in Green Fluorescent Protein Even in the Presence of Hydrogen Bonding. *J. Am. Chem. Soc.* **2016**, 138, 6561-6570.
- (249) Layfield, J. P.; Hammes-Schiffer, S. Calculation of Vibrational Shifts of Nitrile Probes in the Active Site of Ketosteroid Isomerase Upon Ligand Binding. *J. Am. Chem. Soc.* **2013**, 135, 717-725.
- (250) Kim, H.; Cho, M. Infrared Probes for Studying the Structure and Dynamics of Biomolecules. *Chem Rev* **2013**, 113, 5817-5847.
- (251) Xu, L.; Cohen, A. E.; Boxer, S. G. Electrostatic Fields near the Active Site of Human Aldose Reductase: 2. New Inhibitors and Complications Caused by Hydrogen Bonds. *Biochemistry* **2011**, 50, 8311-8322.
- (252) McMahon, H. A.; Alfieri, K. N.; Clark, K. A. A.; Londergan, C. H. Cyanylated Cysteine: A Covalently Attached Vibrational Probe of Protein–Lipid Contacts. *The Journal of Physical Chemistry Letters* **2010**, 1, 850-855.
- (253) Edelstein, L.; Stetz, M. A.; McMahon, H. A.; Londergan, C. H. The Effects of A-Helical Structure and Cyanylated Cysteine on Each Other. *The Journal of Physical Chemistry B* **2010**, 114, 4931-4936.
- (254) Sigala, P. A.; Fafarman, A. T.; Bogard, P. E.; Boxer, S. G.; Herschlag, D. Do Ligand Binding and Solvent Exclusion Alter the Electrostatic Character within the Oxyanion Hole of an Enzymatic Active Site? *J. Am. Chem. Soc.* **2007**, 129, 12104-12105.
- (255) Fafarman, A. T.; Webb, L. J.; Chuang, J. I.; Boxer, S. G. Site-Specific Conversion of Cysteine Thiols into Thiocyanate Creates an Ir Probe for Electric Fields in Proteins. *J. Am. Chem. Soc.* **2006**, 128, 13356-13357.
- (256) Charette, B. D.; MacDonald, R. G.; Wetzel, S.; Berkowitz, D. B.; Waldmann, H. Protein Structure Similarity Clustering: Dynamic Treatment of Pdb Structures Facilitates Clustering. *Angew. Chem. Int. Ed.* **2006**, 45, 7766-7770.
- (257) Tan, D. S. Diversity-Oriented Synthesis: Exploring the Intersections between Chemistry and Biology. *Nature Chemical Biology* **2005**, 1, 74-84.
- (258) Burke, M. D.; Schreiber, S. L. A Planning Strategy for Diversity-Oriented Synthesis. *Angew. Chem. Int. Ed.* **2004**, 43, 46-58.
- (259) Schreiber, S. L. Target-Oriented and Diversity-Oriented Organic Synthesis in Drug Discovery. *Science* **2000**, 287, 1964.

- (260) Yi, S.; Varun, B. V.; Choi, Y.; Park, S. B. A Brief Overview of Two Major Strategies in Diversity-Oriented Synthesis: Build/Couple/Pair and Ring-Distortion. *Front Chem* **2018**, 6, 507.
- (261) Lenci, E.; Innocenti, R.; Menchi, G.; Trabocchi, A. Diversity-Oriented Synthesis and Chemoinformatic Analysis of the Molecular Diversity of Sp(3)-Rich Morpholine Peptidomimetics. *Front Chem* **2018**, 6, 522.
- (262) Galloway, W. R. J. D.; Isidro-Llobet, A.; Spring, D. R. Diversity-Oriented Synthesis as a Tool for the Discovery of Novel Biologically Active Small Molecules. *Nature Communications* **2010**, 1, 80.
- (263) Wu, H.-Q.; Yang, K.; Luo, S.-H.; Wu, X.-Y.; Wang, N.; Chen, S.-H.; Wang, Z.-Y. C4-Selective Synthesis of Vinyl Thiocyanates and Selenocyanates through 3,4-Dihalo-2(5h
-)-Furanones. Eur. J. Org. Chem. 2019, 2019, 4572-4580.
- (264) Song, X.-F.; Ye, A.-H.; Xie, Y.-Y.; Dong, J.-W.; Chen, C.; Zhang, Y.; Chen, Z.-M. Lewis-Acid-Mediated Thiocyano Semipinacol Rearrangement of Allylic Alcohols for Construction of A-Quaternary Center B-Thiocyano Carbonyls. *Org. Lett.* **2019**, 21, 9550-9554.
- (265) Dwivedi, V.; Rajesh, M.; Kumar, R.; Kant, R.; Sridhar Reddy, M. A Stereoselective Thiocyanate Conjugate Addition to Electron Deficient Alkynes and Concomitant Cyclization to N,S-Heterocycles. *Chemical Communications (Cambridge, United Kingdom)* **2017**, 53, 11060-11063.
- (266) Chen, Q.; Lei, Y.; Wang, Y.; Wang, C.; Wang, Y.; Xu, Z.; Wang, H.; Wang, R. Direct Thiocyanation of Ketene Dithioacetals under Transition-Metal-Free Conditions. *Organic Chemistry Frontiers* **2017**, 4, 369-372.
- (267) Chen, J.; Yang, H.; Zhang, M.; Chen, H.; Liu, J.; Yin, K.; Chen, S.; Shao, A. Electrochemical-Induced Regioselective C-3 Thiocyanation of Imidazoheterocycles with Hydrogen Evolution. *Tetrahedron Lett.*2021, DOI:https://doi.org/10.1016/j.tetlet.2020.152755, 152755.
- (268) Zhang, Y.-A.; Ding, Z.; Liu, P.; Guo, W.-S.; Wen, L.-R.; Li, M. Access to Scn-Containing Thiazolines Via Electrochemical Regioselective Thiocyanothiocyclization of N-Allylthioamides. *Organic Chemistry Frontiers* **2020**, 7, 1321-1326.
- (269) Liang, Z.; Wang, F.; Chen, P.; Liu, G. Copper-Catalyzed Intermolecular Trifluoromethylthiocyanation of Alkenes: Convenient Access to Cf3-Containing Alkyl Thiocyanates. *Org. Lett.* **2015**, 17, 2438-2441.
- (270) Wang, L.-J.; Ren, P.-X.; Qi, L.; Chen, M.; Lu, Y.-L.; Zhao, J.-Y.; Liu, R.; Chen, J.-M.; Li, W. Copper-Mediated Aminoazidation, Aminohalogenation, and Aminothiocyanation of Β,Γ-Unsaturated Hydrazones: Synthesis of Versatile Functionalized Pyrazolines. *Org. Lett.* **2018**, 20, 4411-4415.
- (271) Meng, F.; Zhang, H.; He, H.; Xu, N.; Fang, Q.; Guo, K.; Cao, S.; Shi, Y.; Zhu, Y. Copper-Catalyzed Domino Cyclization/Thiocyanation of Unactivated Olefins: Access to Scn-Containing Pyrazolines. *Adv. Synth. Catal.* **2020**, 362, 248-254.
- (272) Schaus, S. E.; Brandes, B. D.; Larrow, J. F.; Tokunaga, M.; Hansen, K. B.; Gould, A. E.; Furrow, M. E.; Jacobsen, E. N. Highly Selective Hydrolytic Kinetic Resolution of Terminal Epoxides Catalyzed by Chiral (Salen)Coiii Complexes. Practical Synthesis of Enantioenriched Terminal Epoxides and 1,2-Diols. J. Am. Chem. Soc. 2002, 124, 1307-1315.
- (273) Nielsen, L. P. C.; Stevenson, C. P.; Blackmond, D. G.; Jacobsen, E. N. Mechanistic Investigation Leads to a Synthetic Improvement in the Hydrolytic Kinetic Resolution of Terminal Epoxides. *J. Am. Chem. Soc.* **2004**, 126, 1360-1362.
- (274) Snider, B. B.; Lin, H. An Improved Procedure for the Conversion of Alkenes and Glycals to 1,2-Diazides Using Mn(Oac)3·2h2o in Acetonitrile Containing Trifluoroacetic Acid. *Synth. Commun.* 1998, 28, 1913-1922.
- (275) Yoon, T. P.; Jacobsen, E. N. Privileged Chiral Catalysts. Science 2003, 299, 1691.

- (276) Wassenaar, J.; Reek, J. N. H. Hybrid Bidentate Phosphorus Ligands in Asymmetric Catalysis: Privileged Ligand Approach Vs. Combinatorial Strategies. *Organic & Biomolecular Chemistry* **2011**, 9. 1704-1713.
- (277) Fu, G. C. Applications of Planar-Chiral Heterocycles as Ligands in Asymmetric Catalysis. *Acc. Chem. Res.* **2006**, 39, 853-860.
- (278) Guthrie, D. B.; Curran, D. P. Asymmetric Radical and Anionic Cyclizations of Axially Chiral Carbamates[†]. *Org. Lett.* **2008**, 11, 249-251.
- (279) Pye, P. J.; Rossen, K.; Reamer, R. A.; Tsou, N. N.; Volante, R. P.; Reider, P. J. A New Planar Chiral Bisphosphine Ligand for Asymmetric Catalysis: Highly Enantioselective Hydrogenations under Mild Conditions. *J. Am. Chem. Soc.* **1997**, 119, 6207-6208.
- (280) Togni, A.; Breutel, C.; Schnyder, A.; Spindler, F.; Landert, H.; Tijani, A. A Novel Easily Accessible Chiral Ferrocenyldiphosphine for Highly Enantioselective Hydrogenation, Allylic Alkylation, and Hydroboration Reactions. *J. Am. Chem. Soc.* **1994**, 116, 4062-4066.
- (281) Fu, G. C. Enantioselective Nucleophilic Catalysis with "Planar-Chiral" Heterocycles. *Acc. Chem. Res.* **2000**, 33, 412-420.
- (282) Martinez, A.; van Gemmeren, M.; List, B. Unexpected Beneficial Effect of Ortho-Substituents on the (S)-Proline-Catalyzed Asymmetric Aldol Reaction of Acetone with Aromatic Aldehydes. *Synlett* **2014**, 25, 961-964.
- (283) Narcis, M. J.; Takenaka, N. Helical-Chiral Small Molecules in Asymmetric Catalysis. *Eur. J. Org. Chem.* **2014**, 2014, 21-34.
- (284) Takenaka, N.; Chen, J.; Captain, B.; Sarangthem, R. S.; Chandrakumar, A. Helical Chiral 2-Aminopyridinium Ions: A New Class of Hydrogen Bond Donor Catalysts. *J. Am. Chem. Soc.* **2010**, 132, 4536-4537.
- (285) Bisai, V.; Bisai, A.; Singh, V. K. Enantioselective Organocatalytic Aldol Reaction Using Small Organic Molecules. *Tetrahedron* **2012**, 68, 4541-4580.
- (286) Knudsen, K. R.; Mitchell, C. E. T.; Ley, S. V. Asymmetric Organocatalytic Conjugate Addition of Malonates to Enones Using a Proline Tetrazole Catalyst. *Chem. Commun. (Cambridge, U. K.)* **2006**, DOI:10.1039/b514636d 10.1039/b514636d, 66-68.
- (287) Xie, H.; Zu, L.; Li, H.; Wang, J.; Wang, W. Organocatalytic Enantioselective Cascade Michael-Alkylation Reactions: Synthesis of Chiral Cyclopropanes and Investigation of Unexpected Organocatalyzed Stereoselective Ring Opening of Cyclopropanes. *J. Am. Chem. Soc.* **2007**, 129, 10886-10894.
- (288) Yang, H.; Carter, R. G. Synthesis of All-Carbon, Quaternary Center-Containing Cyclohexenones through an Organocatalyzed, Multicomponent Coupling. *Org. Lett.* **2010**, 12, 3108-3111.
- (289) Brown, S. P.; Brochu, M. P.; Sinz, C. J.; MacMillan, D. W. C. The Direct and Enantioselective Organocatalytic Alpha-Oxidation of Aldehydes. *J. Am. Chem. Soc.* **2003**, 125, 10808-10809.
- (290) Enders, D.; Grondal, C.; Vrettou, M.; Raabe, G. Asymmetric Synthesis of Selectively Protected Amino Sugars and Derivatives by a Direct Organo-Catalytic Mannich Reaction. *Angew. Chem., Int. Ed.* **2005**, 44, 4079-4083.
- (291) Steiner, D. D.; Mase, N.; Barbas, C. F., III. Direct Asymmetric Alpha-Fluorination of Aldehydes. *Angew. Chem., Int. Ed.* **2005**, 44, 3706-3710.
- (292) Corey, E. J.; Helal, C. J. Reduction of Carbonyl Compounds with Chiral Oxazaborolidine Catalysts: A New Paradigm for Enantioselective Catalysis and a Powerful New Synthetic Method. *Angew. Chem., Int. Ed.* **1998**, 37, 1986-2012.
- (293) Fiori, K. W.; Puchlopek, A. L. A.; Miller, S. J. Enantioselective Sulfonylation Reactions Mediated by a Tetrapeptide Catalyst. *Nat. Chem.* **2009**, 1, 630-634.
- (294) Gustafson, J. L.; Lim, D.; Miller, S. J. Dynamic Kinetic Resolution of Biaryl Atropisomers Via Peptide-Catalyzed Asymmetric Bromination. *Science* **2010**, 328, 1251-1255.

- (295) Han, S.; Miller, S. J. Asymmetric Catalysis at a Distance: Catalytic, Site-Selective Phosphorylation of Teicoplanin. *J. Am. Chem. Soc.* **2013**, 135, 12414-12421.
- (296) Inoue, T.; Sato, D.; Komura, K.; Itsuno, S. Enantiometrically Pure 2-Piperazinemethanols as Novel Chiral Ligands of Oxazaborolidine Catalysts in Enantioselective Borane Reductions. *Tetrahedron Lett.* **1999**, 40, 5379-5382.
- (297) Pathak, T. P.; Miller, S. J. Chemical Tailoring of Teicoplanin with Site-Selective Reactions. *J. Am. Chem. Soc.* **2013**, 135, 8415-8422.
- (298) Lewis, C. A.; Miller, S. J. Site-Selective Derivatization and Remodeling of Erythromycin a by Using Simple Peptide-Based Chiral Catalysts. *Angew. Chem., Int. Ed.* **2006**, 45, 5616-5619.
- (299) Lygo, B.; Andrews, B. I. Asymmetric Phase-Transfer Catalysis Utilizing Chiral Quaternary Ammonium Salts: Asymmetric Alkylation of Glycine Imines. *Acc. Chem. Res.* **2004**, 37, 518-525.
- (300) O'Donnell, M. J. The Enantioselective Synthesis of A-Amino Acids by Phase-Transfer Catalysis with Achiral Schiff Base Esters. *Acc. Chem. Res.* **2004**, 37, 506-517.
- (301) Carlier, P. R.; Mungall, W. S.; Schroder, G.; Sharpless, K. B. Enhanced Kinetic Resolution and Enzyme-Like Shape Selectivity. *J. Am. Chem. Soc.* **1988**, 110, 2978-2979.
- (302) Corey, E. J.; Xu, F.; Noe, M. C. A Rational Approach to Catalytic Enantioselective Enolate Alkylation Using a Structurally Rigidified and Defined Chiral Quaternary Ammonium Salt under Phase Transfer Conditions. *J. Am. Chem. Soc.* **1997**, 119, 12414-12415.
- (303) Lam, Y.-h.; Houk, K. N. How Cinchona Alkaloid-Derived Primary Amines Control Asymmetric Electrophilic Fluorination of Cyclic Ketones. *J. Am. Chem. Soc.* **2014**, 136, 9556-9559.
- (304) Mohar, B.; Baudoux, J.; Plaquevent, J.-C.; Cahard, D. Electrophilic Fluorination Mediated by Cinchona Alkaloids: Highly Enantioselective Synthesis of Alpha-Fluoro-Alpha-Phenylglycine Derivatives. *Angew. Chem., Int. Ed.* **2001**, 40, 4214-4216.
- (305) Fananas-Mastral, M.; Perez, M.; Bos, P. H.; Rudolph, A.; Harutyunyan, S. R.; Feringa, B. L. Enantioselective Synthesis of Tertiary and Quaternary Stereogenic Centers: Copper/Phosphoramidite-Catalyzed Allylic Alkylation with Organolithium Reagents. Angew. Chem., Int. Ed. 2012, 51, 1922-1925, S1922/1921-S1922/1942.
- (306) Giannerini, M.; Fananas-Mastral, M.; Feringa, B. L. Z-Selective Copper-Catalyzed Asymmetric Allylic Alkylation with Grignard Reagents. *J. Am. Chem. Soc.* **2012**, 134, 4108-4111.
- (307) Madrahimov, S. T.; Hartwig, J. F. Origins of Enantioselectivity During Allylic Substitution Reactions Catalyzed by Metallacyclic Iridium Complexes. *J. Am. Chem. Soc.* **2012**, 134, 8136-8147.
- (308) Seebach, D.; Beck, A. K.; Heckel, A. Taddols, Their Derivatives, and Taddol Analogs: Versatile Chiral Auxiliaries. *Angew. Chem., Int. Ed.* **2001**, 40, 92-138.
- (309) Teichert, J. F.; Feringa, B. L. Phosphoramidites: Privileged Ligands in Asymmetric Catalysis. *Angew. Chem., Int. Ed.* **2010**, 49, 2486-2528.
- (310) Kiener, C. A.; Shu, C.; Incarvito, C.; Hartwig, J. F. Identification of an Activated Catalyst in the Iridium-Catalyzed Allylic Amination and Etherification. Increased Rates, Scope, and Selectivity. *J. Am. Chem. Soc.* **2003**, 125, 14272-14273.
- (311) Markovic, D.; Hartwig, J. F. Resting State and Kinetic Studies on the Asymmetric Allylic Substitutions Catalyzed by Iridium-Phosphoramidite Complexes. *J. Am. Chem. Soc.* **2007**, 129, 11680-11681.
- (312) Sigman, M. S.; Jacobsen, E. N. Schiff Base Catalysts for the Asymmetric Strecker Reaction Identified and Optimized from Parallel Synthetic Libraries. *J. Am. Chem. Soc.* **1998**, 120, 4901-4902.
- (313) Joshi, H.; Singh, V. K. Cinchona Derivatives as Bifunctional H-Bonding Organocatalysts in Asymmetric Vinylogous Conjugate Addition Reactions. *Asian J. Org. Chem.* **2022**, DOI:10.1002/ajoc.202100053 10.1002/ajoc.202100053, Ahead of Print.

- (314) Yousefi, R.; Sarkar, A.; Ashtekar, K. D.; Whitehead, D. C.; Kakeshpour, T.; Holmes, D.; Reed, P.; Jackson, J. E.; Borhan, B. Mechanistic Insights into the Origin of Stereoselectivity in an Asymmetric Chlorolactonization Catalyzed by (Dhqd)2phal. *J. Am. Chem. Soc.* **2020**, 142, 7179-7189.
- (315) Hu, B.; Bezpalko, M. W.; Fei, C.; Dickie, D. A.; Foxman, B. M.; Deng, L. Origin of and a Solution for Uneven Efficiency by Cinchona Alkaloid-Derived, Pseudoenantiomeric Catalysts for Asymmetric Reactions. *J. Am. Chem. Soc.* **2018**, 140, 13913-13920.
- (316) Grayson, M. N.; Houk, K. N. Cinchona Alkaloid-Catalyzed Asymmetric Conjugate Additions: The Bifunctional Bronsted Acid-Hydrogen Bonding Model. *J. Am. Chem. Soc.* **2016**, 138, 1170-1173.
- (317) Wolstenhulme, J. R.; Gouverneur, V. Asymmetric Fluorocyclizations of Alkenes. *Acc. Chem. Res.* **2014**, 47, 3560-3570.
- (318) Ramachandran, P. V.; Madhi, S.; Bland-Berry, L.; Reddy, M. V. R.; O'Donnell, M. J. Catalytic Enantioselective Synthesis of Glutamic Acid Derivatives Via Tandem Conjugate Addition-Elimination of Activated Allylic Acetates under Chiral Ptc Conditions. *J. Am. Chem. Soc.* **2005**, 127, 13450-13451.
- (319) Lou, S.; Taoka, B. M.; Ting, A.; Schaus, S. E. Asymmetric Mannich Reactions of B-Keto Esters with Acyl Imines Catalyzed by Cinchona Alkaloids. *J. Am. Chem. Soc.* **2005**, 127, 11256-11257.
- (320) Zhu, C.; Shen, X.; Nelson, S. G. Cinchona Alkaloid-Lewis Acid Catalyst Systems for Enantioselective Ketene-Aldehyde Cycloadditions. *J. Am. Chem. Soc.* **2004**, 126, 5352-5353.
- (321) Fokin, V. V.; Sharpless, K. B. A Practical and Highly Efficient Aminohydroxylation of Unsaturated Carboxylic Acids. *Angew. Chem., Int. Ed.* **2001**, 40, 3455-3457.
- (322) Crispino, G. A.; Ho, P. T.; Sharpless, K. B. Selective Perhydroxylation of Squalene: Taming the Arithmetic Demon. *Science (Washington, D. C., 1883-)* **1993**, 259, 64-66.
- (323) Jacobsen, E. N.; Marko, I.; Mungall, W. S.; Schroeder, G.; Sharpless, K. B. Asymmetric Dihydroxylation Via Ligand-Accelerated Catalysis. *J. Am. Chem. Soc.* **1988**, 110, 1968-1970.
- (324) Edwards, M. G.; Kenworthy, M. N.; Kitson, R. R. A.; Scott, M. S.; Taylor, R. J. K. The Telescoped Intramolecular Michael/Olefination (Timo) Approach to A-Alkylidene-Γ-Butyrolactones: Synthesis of (+)-Paeonilactone B. *Angew. Chem., Int. Ed.* **2008**, 47, 1935-1937.
- (325) Kalidindi, S.; Jeong, W. B.; Schall, A.; Bandichhor, R.; Nosse, B.; Reiser, O. Enantioselective Synthesis of Arglabin. *Angew. Chem., Int. Ed.* **2007**, 46, 6361-6363.
- (326) Nosse, B.; Chhor, R. B.; Jeong, W. B.; Boehm, C.; Reiser, O. Facile Asymmetric Synthesis of the Core Nuclei of Xanthanolides, Guaianolides, and Eudesmanolides. *Org. Lett.* **2003**, 5, 941-944.
- (327) Han, C.; Barrios, F. J.; Riofski, M. V.; Colby, D. A. Semisynthetic Derivatives of Sesquiterpene Lactones by Palladium-Catalyzed Arylation of the A-Methylene-Γ-Lactone Substructure. *J. Org. Chem.* **2009**, 74, 7176-7179.
- (328) Riofski, M. V.; John, J. P.; Zheng, M. M.; Kirshner, J.; Colby, D. A. Exploiting the Facile Release of Trifluoroacetate for the A-Methylenation of the Sterically Hindered Carbonyl Groups on (+)-Sclareolide and (-)-Eburnamonine. *J. Org. Chem.* **2011**, 76, 3676-3683.
- (329) Merfort, I. Perspectives on Sesquiterpene Lactones in Inflammation and Cancer. *Curr. Drug Targets* **2011**, 12, 1560-1573.
- (330) Wagner, S.; Hofmann, A.; Siedle, B.; Terfloth, L.; Merfort, I.; Gasteiger, J. Development of a Structural Model for Nf-Kb Inhibition of Sesquiterpene Lactones Using Self-Organizing Neural Networks. *J. Med. Chem.* **2006**, 49, 2241-2252.
- (331) Peng, X.; Li, P.; Shi, Y. Synthesis of (+)-Ambrisentan Via Chiral Ketone-Catalyzed Asymmetric Epoxidation. *J. Org. Chem.* **2012**, 77, 701-703.
- (332) Wong, O. A.; Shi, Y. Asymmetric Epoxidation of Fluoroolefins by Chiral Dioxirane. Fluorine Effect on Enantioselectivity. *J. Org. Chem.* **2009**, 74, 8377-8380.
- (333) Burke, C. P.; Shi, Y. Regio- and Enantioselective Epoxidation of Dienes by a Chiral Dioxirane: Synthesis of Optically Active Vinyl Cis-Epoxides. *Angew. Chem., Int. Ed.* **2006**, 45, 4475-4478.

- (334) Shing, T. K. M.; Tang, Y. A New Approach to Pseudo-Sugars from (-)-Quinic Acid: Facile Syntheses of Pseudo-Beta-D-Mannopyranose and Pseudo-Beta-D-Fructopyranose. *J. C. S. Chem. Comm.* **1990**, 748-749.
- (335) Sprout, C. M.; Seto, C. T. Using Enzyme Inhibition as a High Throughput Method to Measure the Enantiomeric Excess of a Chiral Sulfoxide. *Org. Lett.* **2005**, 7, 5099-5102.
- (336) Onaran, M. B.; Seto, C. T. Using a Lipase as a High-Throughput Screening Method for Measuring the Enantiomeric Excess of Allylic Acetates. *J. Org. Chem.* **2003**, 68, 8136-8141.
- (337) Abato, P.; Seto, C. T. Emdee: An Enzymatic Method for Determining Enantiomeric Excess. *J. Am. Chem. Soc.* **2001**, 123, 9206-9207.
- (338) Hamberg, A.; Lundgren, S.; Penhoat, M.; Moberg, C.; Hult, K. High-Throughput Enzymatic Method for Enantiomeric Excess Determination of O-Acetylated Cyanohydrins. *J. Am. Chem. Soc.* **2006**, 128, 2234-2235.
- (339) Lundgren, S.; Wingstrand, E.; Penhoat, M.; Moberg, C. Dual Lewis Acid–Lewis Base Activation in Enantioselective Cyanation of Aldehydes Using Acetyl Cyanide and Cyanoformate as Cyanide Sources. J. Am. Chem. Soc. 2005, 127, 11592-11593.
- (340) Moberg, C. Recycling in Asymmetric Catalysis. Acc. Chem. Res. 2016, 49, 2736-2745.
- (341) Bracco, P.; Busch, H.; von Langermann, J.; Hanefeld, U. Enantioselective Synthesis of Cyanohydrins Catalysed by Hydroxynitrile Lyases a Review. *Org Biomol Chem* **2016**, 14, 6375-6389.
- (342) Effenberger, F. Synthesis and Reactions of Optically Active Cyanohydrins. *Angewandte Chemie International Edition in English* **1994**, 33, 1555-1564.
- (343) Marvel, C. S.; Brace, N. O.; Miller, F. A.; Johnson, A. R. Benzoyl Cyanide Dimer and the Addition of Benzoyl Cyanide to Aromatic Aldehydes. *J. Am. Chem. Soc.* **1949**, 71, 34-36.
- (344) Oaksmith, J. M.; Peters, U.; Ganem, B. Three-Component Condensation Leading to B-Amino Acid Diamides: Convergent Assembly of B-Peptide Analogues. *J. Am. Chem. Soc.* **2004**, 126, 13606-13607.
- (345) Watahiki, T.; Ohba, S.; Oriyama, T. Cyanobenzoylation and Hydrocyanation of Aldehydes with Benzoyl Cyanide Using No Catalyst. *Org. Lett.* **2003**, 5, 2679-2681.
- (346) Okimoto, M.; Chiba, T. A Convenient and Improved Method for the Preparation of Cyanohydrin Esters from Acyl Cyanides and Aldehydes. *Synthesis* **1996**, DOI:10.1055/s-1996-4361 10.1055/s-1996-4361, 1188-1190.
- (347) Baeza, A.; Najera, C.; de Gracia Retamosa, M.; Sansano, J. M. Solvent-Free Synthesis of Cyanohydrin Derivatives Catalysed by Triethylamine. *Synthesis* **2005**, DOI:10.1055/s-2005-872096 10.1055/s-2005-872096, 2787-2797.
- (348) Zhang, W.; Shi, M. Dbu Catalyzed Cyanoacylation of Ketones with Acyl Cyanides. *Org. Biomol. Chem.* **2006**, 4, 1671-1674.
- (349) Li, F.; Widyan, K.; Wingstrand, E.; Moberg, C. Chiral Lewis Base Catalyzed Enantioselective Acetylcyanation of A-Oxo Esters. *Eur. J. Org. Chem.* **2009**, DOI:10.1002/ejoc.200900055 10.1002/ejoc.200900055, 3917-3922, S3917/3911-S3917/3910.
- (350) Wingstrand, E.; Laurell, A.; Fransson, L.; Hult, K.; Moberg, C. Minor Enantiomer Recycling: Metal Catalyst, Organocatalyst and Biocatalyst Working in Concert. *Chem. Eur. J.* **2009**, 15, 12107-12113, S12107/12101-S12107/12127.
- (351) Scholl, M.; Lim, C.-K.; Fu, G. C. Convenient and Efficient Conversion of Aldehydes to Acylated Cyanohydrins Using Tributyltin Cyanide as Catalyst. *J. Org. Chem.* **1995**, 60, 6229-6231.
- (352) Zhang, H.; Liu, R.; Liu, J.; Fan, B.; Li, R.; Qiao, Y.; Zhou, R. Chemoselective Phosphine-Catalyzed Cyanoacylation of A-Dicarbonyl Compounds: A General Method for the Synthesis of Cyanohydrin Esters with One Quaternary Stereocenter. *New J. Chem.* **2018**, 42, 19720-19728.

- (353) Ishino, Y.; Mihara, M.; Takeuchi, T.; Takemoto, M. Zinc-Metal Promoted Selective A-Haloacylation and Gem-Bisacylation of Alkylaldehydes in the Presence of Chlorotrimethylsilane. *Tetrahedron Lett.* **2004**, 45, 3503-3506.
- (354) Baeza, A.; Najera, C.; Sansano, J. M.; Saa, J. M. Asymmetric Synthesis of O-Benzoyl Cyanohydrins by Reaction of Aldehydes with Benzoyl Cyanide Catalyzed by Binolam-Ti(Iv) Complexes. *Tetrahedron: Asymmetry* **2005**, 16, 2385-2389.
- (355) Lundgren, S.; Wingstrand, E.; Moberg, C. Lewis Acid-Lewis Base-Catalysed Enantioselective Addition of A-Ketonitriles to Aldehydes. *Adv. Synth. Catal.* **2007**, 349, 364-372.
- (356) Lundgren, S.; Ihre, H.; Moberg, C. Enantioselective Cyanation of Benzaldehyde: An Asymmetric Polymeric Catalyst in a Microreactor. *ARKIVOC (Gainesville, FL, U. S.)* **2008**, DOI:10.3998/ark.5550190.0009.607 10.3998/ark.5550190.0009.607, 73-80.
- (357) North, M.; Usanov, D. L.; Young, C. Lewis Acid Catalyzed Asymmetric Cyanohydrin Synthesis. *Chem. Rev.* **2008**, 108, 5146-5226.
- (358) Baeza, A.; Najera, C.; Sansano, J. M.; Saa, J. M. Mechanistic Studies on the Enantioselective Binolam/Titanium(Iv)-Catalyzed Cyanobenzoylation of Aldehydes: Part 1. *Tetrahedron: Asymmetry* **2011**, 22, 1282-1291.
- (359) Laurell, A.; Moberg, C. Opposite Enantiomers from Minor Enantiomer Recycling and Dynamic Kinetic Resolution Using a Single Biocatalyst. *Eur. J. Org. Chem.* **2011**, 2011, 3980-3984, S3980/3981-S3980/3987.
- (360) Hertzberg, R.; Widyan, K.; Heid, B.; Moberg, C. Enantioenriched Ω-Bromocyanohydrin Derivatives. Improved Selectivity by Combination of Two Chiral Catalysts. *Tetrahedron* **2012**, 68, 7680-7684.
- (361) Hertzberg, R.; Moberg, C. One-Step Preparation of O-(A-Bromoacyl) Cyanohydrins by Minor Enantiomer Recycling: Synthesis of 4-Amino-2(5h)-Furanones. *J. Org. Chem.* **2013**, 78, 9174-9180.
- (362) Wen, Y.-Q.; Hertzberg, R.; Gonzalez, I.; Moberg, C. Minor Enantiomer Recycling: Application to Enantioselective Syntheses of Beta Blockers. *Chemistry A European Journal* **2014**, 20, 3806-3812.
- (363) Hertzberg, R.; Monreal Santiago, G.; Moberg, C. Synthesis of the B3-Adrenergic Receptor Agonist Solabegron and Analogous N-(2-Ethylamino)-B-Amino Alcohols from O-Acylated Cyanohydrins Expanding the Scope of Minor Enantiomer Recycling. *J. Org. Chem.* **2015**, 80, 2937-2941.
- (364) Yoshioka, M.; Kawakita, T.; Ohno, M. Asymmetric Induction Catalyzed by Conjugate Bases of Chiral Proton Acids as Ligands: Enantioselective Addition of Dialkylzinc-Orthotitanate Complex to Benzaldehyde with Catalytic Ability of a Remarkable High Order. *Tetrahedron Lett.* **1989**, 30, 1657-1660.
- (365) Schmidt, B.; Seebach, D. Catalytic and Stoichiometric Enantioselective Addition of Diethylzinc to Aldehydes Using a Novel Chiral Spirotitanate. *Angewandte Chemie International Edition in English* **1991**, 30, 99-101.
- (366) Soai, K.; Yokoyama, S.; Hayasaka, T. Chiral N,N-Dialkylnorephedrines as Catalysts of the Highly Enantioselective Addition of Dialkylzincs to Aliphatic and Aromatic Aldehydes. The Asymmetric Synthesis of Secondary Aliphatic and Aromatic Alcohols of High Optical Purity. *Journal of Organic Chemistry* **1991**, 56, 4264-4268.
- (367) Kitamura, M.; Suga, S.; Kawai, K.; Noyori, R. Catalytic Asymmetric Induction. Highly Enantioselective Addition of Dialkylzincs to Aldehydes. *J. Am. Chem. Soc.* **1986**, 108, 6071-6072.
- (368) Prasad, K. R. K.; Joshi, N. N. Chiral Zinc Amides as the Catalysts for the Enantioselective Addition of Diethylzinc to Aldehydes. *Journal of Organic Chemistry* **1997**, 62, 3770-3771.
- (369) Li, Z.; Buetikofer, L.; Witholt, B. High-Throughput Measurement of the Enantiomeric Excess of Chiral Alcohols by Using Two Enzymes. *Angew. Chem., Int. Ed.* **2004**, 43, 1698-1702.
- (370) Zhao, S. H.; Samuel, O.; Kagan, H. B. Asymmetric Oxidation of Sulfides Mediated by Chiral Titanium Complexes: Mechanistic and Synthetic Aspects. *Tetrahedron* **1987**, 43, 5135-5144.

- (371) Yan, L.; Nan, X.; Zhang, C.; Wang, H.; Huang, X.; Hu, J.; Liu, Y. Development of an Enzyme-Linked Immunosorbent Assay for Camptothecin. *Mol Med Rep* **2019**, 20, 959-966.
- (372) Darwish, I. A. Immunoassay Methods and Their Applications in Pharmaceutical Analysis: Basic Methodology and Recent Advances. *International journal of biomedical science : IJBS* **2006**, 2, 217-235.
- (373) MacBeath, G.; Hilvert, D. Monitoring Catalytic Activity by Immunoassay: Implications for Screening. *J. Am. Chem. Soc.* **1994**, 116, 6101-6106.
- (374) KÖHler, G.; Milstein, C. Continuous Cultures of Fused Cells Secreting Antibody of Predefined Specificity. *Nature* **1975**, 256, 495-497.
- (375) Li, F.; Vijayasankaran, N.; Shen, A.; Kiss, R.; Amanullah, A. Cell Culture Processes for Monoclonal Antibody Production. *mAbs* **2010**, 2, 466-479.
- (376) Taran, F.; Renard, P. Y.; Bernard, H.; Mioskowski, C.; Frobert, Y.; Pradelles, P.; Grassi, J. Antibody-Catalyzed Decarboxylative Oxidation of Vanillylmandelic Acid. *J. Am. Chem. Soc.* **1998**, 120, 3332-3339.
- (377) Tawfik, D. S.; Green, B. S.; Chap, R.; Sela, M.; Eshhar, Z. Catelisa: A Facile General Route to Catalytic Antibodies. *Proc. Natl. Acad. Sci. U. S. A.* **1993**, 90, 373-377.
- (378) Tawfik, D. S.; Green, B. S.; Eshhar, Z. Detection of Catalytic Monoclonal Antibodies. *Anal. Biochem.* **1992**, 202, 35-39.
- (379) Vicennati, P.; Bensel, N.; Wagner, A.; Creminon, C.; Taran, F. Sandwich Immunoassay as a High-Throughput Screening Method for Cross-Coupling Reactions. *Angewandte Chemie-International Edition* **2005**, 44, 6863-6866.
- (380) Quinton, J.; Kolodych, S.; Chaumonet, M.; Bevilacqua, V.; Nevers, M.-C.; Volland, H.; Gabillet, S.; Thuery, P.; Creminon, C.; Taran, F. Reaction Discovery by Using a Sandwich Immunoassay. *Angew. Chem., Int. Ed.* **2012**, 51, 6144-6148, S6144/6141-S6144/6153.
- (381) Kolodych, S.; Rasolofonjatovo, E.; Chaumontet, M.; Nevers, M.-C.; Creminon, C.; Taran, F. Discovery of Chemoselective and Biocompatible Reactions Using a High-Throughput Immunoassay Screening. *Angew. Chem., Int. Ed.* **2013**, 52, 12056-12060.
- (382) Sletten, E. M.; Bertozzi, C. R. Bioorthogonal Chemistry: Fishing for Selectivity in a Sea of Functionality. *Angew. Chem. Int. Ed.* **2009**, 48, 6974-6998.
- (383) Agard, N. J.; Prescher, J. A.; Bertozzi, C. R. A Strain-Promoted [3 + 2] Azide–Alkyne Cycloaddition for Covalent Modification of Biomolecules in Living Systems [J. Am. Chem. Soc. 2004, 126, 15046–15047]. J. Am. Chem. Soc. 2005, 127, 11196-11196.
- (384) Gartner, Z. J.; Liu, D. R. The Generality of DNA-Templated Synthesis as a Basis for Evolving Non-Natural Small Molecules. *J. Am. Chem. Soc.* **2001**, 123, 6961-6963.
- (385) Thirumurugan, P.; Matosiuk, D.; Jozwiak, K. Click Chemistry for Drug Development and Diverse Chemical–Biology Applications. *Chem. Rev.* **2013**, 113, 4905-4979.
- (386) Decuypere, E.; Bernard, S.; Feng, M.; Porte, K.; Riomet, M.; Thuéry, P.; Audisio, D.; Taran, F. Copper-Catalyzed Aza-Iminosydnone-Alkyne Cycloaddition Reaction Discovered by Screening. *ACS Catalysis* **2018**, 8, 11882-11888.
- (387) Specklin, S.; Decuypere, E.; Plougastel, L.; Aliani, S.; Taran, F. One-Pot Synthesis of 1,4-Disubstituted Pyrazoles from Arylglycines Via Copper-Catalyzed Sydnone-Alkyne Cycloaddition Reaction. *J. Org. Chem.* **2014**, 79, 7772-7777.
- (388) Decuypere, E.; Specklin, S.; Gabillet, S.; Audisio, D.; Liu, H.; Plougastel, L.; Kolodych, S.; Taran, F. Copper(I)-Catalyzed Cycloaddition of 4-Bromosydnones and Alkynes for the Regioselective Synthesis of 1,4,5-Trisubstituted Pyrazoles. *Org. Lett.* **2015**, 17, 362-365.
- (389) Comas-Barcelo, J.; Foster, R. S.; Fiser, B.; Gomez-Bengoa, E.; Harrity, J. P. Cu-Promoted Sydnone Cycloadditions of Alkynes: Scope and Mechanism Studies. *Chemistry* **2015**, 21, 3257-3263.

- (390) Wezeman, T.; Comas-Barcelo, J.; Nieger, M.; Harrity, J. P.; Brase, S. Synthesis of Aminopyrazoles from Sydnones and Ynamides. *Org Biomol Chem* **2017**, 15, 1575-1579.
- (391) Lu, J.; Man, Y.; Zhang, Y.; Lin, B.; Lin, Q.; Weng, Z. Copper-Catalyzed Chemoselective Synthesis of 4-Trifluoromethyl Pyrazoles. *RSC Advances* **2019**, 9, 30952-30956.
- (392) McCormack, P. L. Celecoxib: A Review of Its Use for Symptomatic Relief in the Treatment of Osteoarthritis, Rheumatoid Arthritis and Ankylosing Spondylitis. *Drugs* **2011**, 71, 2457-2489.
- (393) Culbreath, A. K.; Brenneman, T. B.; Kemerait Jr, R. C.; Hammes, G. G. Effect of the New Pyrazole Carboxamide Fungicide Penthiopyrad on Late Leaf Spot and Stem Rot of Peanut. *Pest Management Science* **2009**, 65, 66-73.
- (394) Zhang, D.; Raghavan, N.; Chen, S.-Y.; Zhang, H.; Quan, M.; Lecureux, L.; Patrone, L. M.; Lam, P. Y. S.; Bonacorsi, S. J.; Knabb, R. M.et al. Reductive Isoxazole Ring Opening of the Anticoagulant Razaxaban Is the Major Metabolic Clearance Pathway in Rats and Dogs. *Drug Metabolism and Disposition* **2008**, 36, 303.
- (395) Bernard, S.; Audisio, D.; Riomet, M.; Bregant, S.; Sallustrau, A.; Plougastel, L.; Decuypere, E.; Gabillet, S.; Kumar, R. A.; Elyian, J.et al. Bioorthogonal Click and Release Reaction of Iminosydnones with Cycloalkynes. *Angew. Chem. Int. Ed.* **2017**, 56, 15612-15616.
- (396) Rasolofonjatovo, E.; Theeramunkong, S.; Bouriaud, A.; Kolodych, S.; Chaumontet, M.; Taran, F. Iridium-Catalyzed Cycloaddition of Azides and 1-Bromoalkynes at Room Temperature. *Org. Lett.* **2013**, 15, 4698-4701.
- (397) Ding, S.; Jia, G.; Sun, J. Iridium-Catalyzed Intermolecular Azide-Alkyne Cycloaddition of Internal Thioalkynes under Mild Conditions. *Angew. Chem. Int. Ed. Engl.* **2014**, 53, 1877-1880.
- (398) Song, W.; Zheng, N. Iridium-Catalyzed Highly Regioselective Azide-Ynamide Cycloaddition to Access 5-Amido Fully Substituted 1,2,3-Triazoles under Mild, Air, Aqueous, and Bioorthogonal Conditions. *Org. Lett.* **2017**, 19, 6200-6203.
- (399) Chen, R.; Zeng, L.; Lai, Z.; Cui, S. Iridium-Catalyzed Hydroxyl-Enabled Cycloaddition of Azides and Alkynes. *Adv. Synth. Catal.* **2019**, 361, 989-994.
- (400) Taran, F.; Gauchet, C.; Mohar, B.; Meunier, S.; Valleix, A.; Renard, P. Y.; Créminon, C.; Grassi, J.; Wagner, A.; Mioskowski, C. High-Throughput Screening of Enantioselective Catalysts by Immunoassay. *Angew. Chem. Int. Ed.* **2002**, 41, 124-127.
- (401) Worek, F.; Eyer, P.; Thiermann, H. Determination of Acetylcholinesterase Activity by the Ellman Assay: A Versatile Tool for in Vitro Research on Medical Countermeasures against Organophosphate Poisoning. *Drug Testing and Analysis* **2012**, *4*, 282-291.
- (402) Matsushita, H.; Yamamoto, N.; Meijler, M. M.; Wirsching, P.; Lerner, R. A.; Matsushita, M.; Janda, K. D. Chiral Sensing Using a Blue Fluorescent Antibody. *Molecular BioSystems* **2005**, 1, 303-306.
- (403) Matsushita, M.; Yoshida, K.; Yamamoto, N.; Wirsching, P.; Lerner, R. A.; Janda, K. D. High-Throughput Screening by Using a Blue-Fluorescent Antibody Sensor. *Angew. Chem. Int. Ed.* **2003**, 42, 5984-5987.
- (404) Simeonov, A.; Matsushita, M.; Juban, E. A.; Thompson, E. H. Z.; Hoffman, T. Z.; Beuscher Iv, A. E.; Taylor, M. J.; Wirsching, P.; Rettig, W.; McCusker, J. K.et al. Blue-Fluorescent Antibodies. *Science* **2000**, 290, 307.
- (405) Kaufman, T. S.; Rúveda, E. A. The Quest for Quinine: Those Who Won the Battles and Those Who Won the War. *Angew. Chem. Int. Ed.* **2005**, 44, 854-885.
- (406) Ha, M. W.; Park, H.-g. In Sustainable Catalysis: Without Metals or Other Endangered Elements, Part 2; The Royal Society of Chemistry, 2016, DOI:10.1039/9781782626435-00082 10.1039/9781782626435-00082.
- (407) Reetz, M. T.; Zonta, A.; Schimossek, K.; Jaeger, K.-E.; Liebeton, K. Creation of Enantioselective Biocatalysts for Organic Chemistry by in Vitro Evolution. *Angewandte Chemie International Edition in English* **1997**, 36, 2830-2832.

- (408) Brenner, S.; Lerner, R. A. Encoded Combinatorial Chemistry. *Proceedings of the National Academy of Sciences* **1992**, 89, 5381.
- (409) Kanan, M. W.; Rozenman, M. M.; Sakurai, K.; Snyder, T. M.; Liu, D. R. Reaction Discovery Enabled by DNA-Templated Synthesis and in Vitro Selection. *Nature* **2004**, 431, 545-549.
- (410) Wrenn, S. J.; Weisinger, R. M.; Halpin, D. R.; Harbury, P. B. Synthetic Ligands Discovered by in Vitro Selection. *J. Am. Chem. Soc.* **2007**, 129, 13137-13143.
- (411) Rozenman, M. M.; Kanan, M. W.; Liu, D. R. Development and Initial Application of a Hybridization-Independent, DNA-Encoded Reaction Discovery System Compatible with Organic Solvents. *J. Am. Chem. Soc.* **2007**, 129, 14933-14938.
- (412) Melkko, S.; Zhang, Y.; Dumelin, C. E.; Scheuermann, J.; Neri, D. Isolation of High-Affinity Trypsin Inhibitors from a DNA-Encoded Chemical Library. *Angew. Chem. Int. Ed.* **2007**, 46, 4671-4674.
- (413) Fredriksson, S.; Dixon, W.; Ji, H.; Koong, A. C.; Mindrinos, M.; Davis, R. W. Multiplexed Protein Detection by Proximity Ligation for Cancer Biomarker Validation. *Nat. Methods* **2007**, 4, 327-329.
- (414) Beeler, A. B.; Su, S.; Singleton, C. A.; Porco, J. A., Jr. Discovery of Chemical Reactions through Multidimensional Screening. *J. Am. Chem. Soc.* **2007**, 129, 1413-1419.
- (415) Shendure, J.; Porreca, G. J.; Reppas, N. B.; Lin, X.; McCutcheon, J. P.; Rosenbaum, A. M.; Wang, M. D.; Zhang, K.; Mitra, R. D.; Church, G. M. Accurate Multiplex Polony Sequencing of an Evolved Bacterial Genome. *Science* **2005**, 309, 1728-1732.
- (416) Melkko, S.; Scheuermann, J.; Dumelin, C. E.; Neri, D. Encoded Self-Assembling Chemical Libraries. *Nat. Biotechnol.* **2004**, 22, 568-574.
- (417) Zhu, Z.; Cuozzo, J. High-Throughput Affinity-Based Technologies for Small-Molecule Drug Discovery. *J. Biomol. Screening* **2009**, 14, 1157-1164.
- (418) Wu, Z.; Zhen, Z.; Jiang, J.-H.; Shen, G.-L.; Yu, R.-Q. Terminal Protection of Small-Molecule-Linked DNA for Sensitive Electrochemical Detection of Protein Binding Via Selective Carbon Nanotube Assembly. *J. Am. Chem. Soc.* **2009**, 131, 12325-12332.
- (419) Hansen, M. H.; Blakskjaer, P.; Petersen, L. K.; Hansen, T. H.; Hoejfeldt, J. W.; Gothelf, K. V.; Hansen, N. J. V. A Yoctoliter-Scale DNA Reactor for Small-Molecule Evolution. J. Am. Chem. Soc. 2009, 131, 1322-1327.
- (420) Gorin, D. J.; Kamlet, A. S.; Liu, D. R. Reactivity-Dependent Pcr: Direct, Solution-Phase in Vitro Selection for Bond Formation. *J. Am. Chem. Soc.* **2009**, 131, 9189-9191.
- (421) Clarke, J.; Wu, H.-C.; Jayasinghe, L.; Patel, A.; Reid, S.; Bayley, H. Continuous Base Identification for Single-Molecule Nanopore DNA Sequencing. *Nat. Nanotechnol.* **2009**, 4, 265-270.
- (422) Clark, M. A.; Acharya, R. A.; Arico-Muendel, C. C.; Belyanskaya, S. L.; Benjamin, D. R.; Carlson, N. R.; Centrella, P. A.; Chiu, C. H.; Creaser, S. P.; Cuozzo, J. W.et al. Design, Synthesis and Selection of DNA-Encoded Small-Molecule Libraries. *Nat. Chem. Biol.* 2009, 5, 647-654.
- (423) Buller, F.; Zhang, Y.; Scheuermann, J.; Schafer, J.; Buhlmann, P.; Neri, D. Discovery of Tnf Inhibitors from a DNA-Encoded Chemical Library Based on Diels-Alder Cycloaddition. *Chem. Biol.* (*Cambridge, MA, U. S.*) **2009**, 16, 1075-1086.
- (424) Tse, B. N.; Snyder, T. M.; Shen, Y.; Liu, D. R. Translation of DNA into a Library of 13 000 Synthetic Small-Molecule Macrocycles Suitable for in Vitro Selection. *J. Am. Chem. Soc.* **2008**, 130, 15611-15626.
- (425) Scheuermann, J.; Dumelin, C. E.; Melkko, S.; Zhang, Y.; Mannocci, L.; Jaggi, M.; Sobek, J.; Neri, D. DNA-Encoded Chemical Libraries for the Discovery of Mmp-3 Inhibitors. *Bioconjugate Chem.* **2008**, 19, 778-785.
- (426) Gustafsdottir, S. M.; Wennstroem, S.; Fredriksson, S.; Schallmeiner, E.; Hamilton, A. D.; Sebti, S. M.; Landegren, U. Use of Proximity Ligation to Screen for Inhibitors of Interactions between Vascular Endothelial Growth Factor a and Its Receptors. Clin. Chem. 2008, 54, 1218-1225.

- (427) Mie, M.; Sugita, R.; Endoh, T.; Kobatake, E. Evaluation of Small Ligand-Protein Interactions by Using T7 Rna Polymerase with DNA-Modified Ligand. *Anal. Biochem.* **2010**, 405, 109-113.
- (428) McGregor, L. M.; Gorin, D. J.; Dumelin, C. E.; Liu, D. R. Interaction-Dependent Pcr: Identification of Ligand–Target Pairs from Libraries of Ligands and Libraries of Targets in a Single Solution-Phase Experiment. *J. Am. Chem. Soc.* **2010**, 132, 15522-15524.
- (429) He, Y.; Liu, D. R. Autonomous Multistep Organic Synthesis in a Single Isothermal Solution Mediated by a DNA Walker. *Nat. Nanotechnol.* **2010**, 5, 778-782.
- (430) Buller, F.; Steiner, M.; Scheuermann, J.; Mannocci, L.; Nissen, I.; Kohler, M.; Beisel, C.; Neri, D. High-Throughput Sequencing for the Identification of Binding Molecules from DNA-Encoded Chemical Libraries. *Bioorg. Med. Chem. Lett.* **2010**, 20, 4188-4192.
- (431) Blokzijl, A.; Friedman, M.; Ponten, F.; Landegren, U. Profiling Protein Expression and Interactions: Proximity Ligation as a Tool for Personalized Medicine. *J. Intern. Med.* **2010**, 268, 232-245.
- (432) Wu, Z.; Wang, H.; Guo, M.; Tang, L.-J.; Yu, R.-Q.; Jiang, J.-H. Terminal Protection of Small Molecule-Linked DNA: A Versatile Biosensor Platform for Protein Binding and Gene Typing Assay. *Anal. Chem.* **2011**, 83, 3104-3111.
- (433) Lundberg, M.; Eriksson, A.; Tran, B.; Assarsson, E.; Fredriksson, S. Homogeneous Antibody-Based Proximity Extension Assays Provide Sensitive and Specific Detection of Low-Abundant Proteins in Human Blood. *Nucleic Acids Res.* **2011**, 39, e102.
- (434) He, Y.; Liu, D. R. A Sequential Strand-Displacement Strategy Enables Efficient Six-Step DNA-Templated Synthesis. *J. Am. Chem. Soc.* **2011**, 133, 9972-9975.
- (435) Darmanis, S.; Nong, R. Y.; Vaenelid, J.; Siegbahn, A.; Ericsson, O.; Fredriksson, S.; Baecklin, C.; Gut, M.; Heath, S.; Gut, I. G.et al. Proteinseq: High-Performance Proteomic Analyses by Proximity Ligation and Next Generation Sequencing. *PLoS One* **2011**, 6, e25583.
- (436) Chen, Y.; Kamlet, A. S.; Steinman, J. B.; Liu, D. R. A Biomolecule-Compatible Visible-Light-Induced Azide Reduction from a DNA-Encoded Reaction-Discovery System. *Nat. Chem.* **2011**, 3, 146-153.
- (437) Weisinger, R. M.; Jarrett Wrenn, S.; Harbury, P. B. Highly Parallel Translation of DNA Sequences into Small Molecules. *PLoS One* **2012**, *7*, e28056.
- (438) Scott, D. E.; Coyne, A. G.; Hudson, S. A.; Abell, C. Fragment-Based Approaches in Drug Discovery and Chemical Biology. *Biochemistry* **2012**, 51, 4990-5003.
- (439) Li, Y.; Zhang, M.; Zhang, C.; Li, X. Detection of Bond Formations by DNA-Programmed Chemical Reactions and Pcr Amplification. *Chem. Commun.* **2012**, 48, 9513-9515.
- (440) Leimbacher, M.; Zhang, Y.; Mannocci, L.; Stravs, M.; Geppert, T.; Scheuermann, J.; Schneider, G.; Neri, D. Discovery of Small-Molecule Interleukin-2 Inhibitors from a DNA-Encoded Chemical Library. *Chem. Eur. J.* **2012**, 18, 7729-7737, S7729/7721-S7729/7120.
- (441) Hammond, M.; Nong, R. Y.; Ericsson, O.; Pardali, K.; Landegren, U. Profiling Cellular Protein Complexes by Proximity Ligation with Dual Tag Microarray Readout. *PLoS One* **2012**, 7, e40405.
- (442) Deng, H.; O'Keefe, H.; Davie, C. P.; Lind, K. E.; Acharya, R. A.; Franklin, G. J.; Larkin, J.; Matico, R.; Neeb, M.; Thompson, M. M.et al. Discovery of Highly Potent and Selective Small Molecule Adamts-5 Inhibitors That Inhibit Human Cartilage Degradation Via Encoded Library Technology (Elt). *J. Med. Chem.* **2012**, 55, 7061-7079.
- (443) Cao, Y.; Zhu, S.; Yu, J.; Zhu, X.; Yin, Y.; Li, G. Protein Detection Based on Small Molecule-Linked DNA. *Anal. Chem.* **2012**, 84, 4314-4320.
- (444) Zhu, J.; Larman, H. B.; Gao, G.; Somwar, R.; Zhang, Z.; Laserson, U.; Ciccia, A.; Pavlova, N.; Church, G.; Zhang, W.et al. Protein Interaction Discovery Using Parallel Analysis of Translated Orfs (Plato). *Nat. Biotechnol.* **2013**, 31, 331-334.
- (445) Podolin, P. L.; Bolognese, B. J.; Foley, J. F.; Long, E.; Peck, B.; Umbrecht, S.; Zhang, X.; Zhu, P.; Schwartz, B.; Xie, W.et al. In Vitro and in Vivo Characterization of a Novel Soluble Epoxide Hydrolase Inhibitor. *Prostaglandins Other Lipid Mediators* **2013**, 104-105, 25-31.

- (446) Li, Y.; Zhao, P.; Zhang, M.; Zhao, X.; Li, X. Multistep DNA-Templated Synthesis Using a Universal Template. *J. Am. Chem. Soc.* **2013**, 135, 17727-17730.
- (447) Li, G.; Liu, Y.; Liu, Y.; Chen, L.; Wu, S.; Liu, Y.; Li, X. Photoaffinity Labeling of Small-Molecule-Binding Proteins by DNA-Templated Chemistry. *Angew. Chem. Int. Ed.* **2013**, 52, 9544-9549.
- (448) Kawakami, T.; Ishizawa, T.; Fujino, T.; Reid, P. C.; Suga, H.; Murakami, H. In Vitro Selection of Multiple Libraries Created by Genetic Code Reprogramming to Discover Macrocyclic Peptides That Antagonize Vegfr2 Activity in Living Cells. *ACS Chem. Biol.* **2013**, *8*, 1205-1214.
- (449) Zhao, P.; Chen, Z.; Li, Y.; Sun, D.; Gao, Y.; Huang, Y.; Li, X. Selection of DNA-Encoded Small Molecule Libraries against Unmodified and Non-Immobilized Protein Targets. *Angew. Chem. Int. Ed.* **2014**, 53, 10056-10059.
- (450) Zhang, Z.; Hejesen, C.; Kjelstrup, M. B.; Birkedal, V.; Gothelf, K. V. A DNA-Mediated Homogeneous Binding Assay for Proteins and Small Molecules. *J. Am. Chem. Soc.* **2014**, 136, 11115-11120.
- (451) Xu, Y.; Jiang, B.; Xie, J.; Xiang, Y.; Yuan, R.; Chai, Y. Terminal Protection of Small Molecule-Linked Ssdna for Label-Free and Sensitive Fluorescent Detection of Folate Receptor. *Talanta* **2014**, 128, 237-241.
- (452) Novoa, A.; Machida, T.; Barluenga, S.; Imberty, A.; Winssinger, N. Pna-Encoded Synthesis (Pes) of a 10 000-Member Hetero-Glycoconjugate Library and Microarray Analysis of Diverse Lectins. *ChemBioChem* **2014**, 15, 2058-2065.
- (453) McGregor, L. M.; Jain, T.; Liu, D. R. Identification of Ligand–Target Pairs from Combined Libraries of Small Molecules and Unpurified Protein Targets in Cell Lysates. *J. Am. Chem. Soc.* **2014**, 136, 3264-3270.
- (454) Maianti, J. P.; McFedries, A.; Foda, Z. H.; Kleiner, R. E.; Du, X. Q.; Leissring, M. A.; Tang, W.-J.; Charron, M. J.; Seeliger, M. A.; Saghatelian, A.et al. Anti-Diabetic Activity of Insulin-Degrading Enzyme Inhibitors Mediated by Multiple Hormones. *Nature* **2014**, 511, 94-98.
- (455) Li, G.; Liu, Y.; Yu, X.; Li, X. Multivalent Photoaffinity Probe for Labeling Small Molecule Binding Proteins. *Bioconjugate Chem.* **2014**, 25, 1172-1180.
- (456) Gu, L.; Li, C.; Aach, J.; Hill, D. E.; Vidal, M.; Church, G. M. Multiplex Single-Molecule Interaction Profiling of DNA-Barcoded Proteins. *Nature* **2014**, 515, 554-557.
- (457) Chen, T.-C.; Lin, K.-T.; Chen, C.-H.; Lee, S.-A.; Lee, P.-Y.; Liu, Y.-W.; Kuo, Y.-L.; Wang, F.-S.; Lai, J.-M.; Huang, C.-Y. F. Using an in Situ Proximity Ligation Assay to Systematically Profile Endogenous Protein-Protein Interactions in a Pathway Network. *J. Proteome Res.* **2014**, 13, 5339-5346.
- (458) Fredriksson, S.; Gullberg, M.; Jarvius, J.; Olsson, C.; Pietras, K.; Gústafsdóttir, S. M.; Östman, A.; Landegren, U. Protein Detection Using Proximity-Dependent DNA Ligation Assays. *Nat. Biotechnol.* **2002**, 20, 473-477.
- (459) Blakskjaer, P.; Heitner, T.; Hansen, N. J. V. Fidelity by Design: Yoctoreactor and Binder Trap Enrichment for Small-Molecule DNA-Encoded Libraries and Drug Discovery. *Curr. Opin. Chem. Biol.* **2015**, 26, 62-71.
- (460) Petersen, L. K.; Christensen, A. B.; Andersen, J.; Folkesson, C. G.; Kristensen, O.; Andersen, C.; Alzu, A.; Sløk, F. A.; Blakskjær, P.; Madsen, D.et al. Screening of DNA-Encoded Small Molecule Libraries inside a Living Cell. *Journal of American Chemical Society* **2021**, 143, 2751-2756.
- (461) O'Reilly, R. K.; Turberfield, A. J.; Wilks, T. R. The Evolution of DNA-Templated Synthesis as a Tool for Materials Discovery. *Acc. Chem. Res.* **2017**, 50, 2496-2509.
- (462) Oukacine, F.; Ravelet, C.; Peyrin, E. Enantiomeric Sensing and Separation by Nucleic Acids. *TrAC, Trends Anal. Chem.* **2019**, DOI:10.1016/j.trac.2019.115733 10.1016/j.trac.2019.115733, Ahead of Print.
- (463) Gartner, Z. J.; Kanan, M. W.; Liu, D. R. Expanding the Reaction Scope of DNA-Templated Synthesis. *Angew. Chem., Int. Ed.* **2002**, 41, 1796-1800.

- (464) Calderone, C. T.; Puckett, J. W.; Gartner, Z. J.; Liu, D. R. Directing Otherwise Incompatible Reactions in a Single Solution by Using DNA-Templated Organic Synthesis. *Angew. Chem. Int. Ed.* **2002**, 41, 4104-4108.
- (465) Karuppasamy, M.; Vachan, B. S.; Vinoth, P.; Muthukrishnan, I.; Nagarajan, S.; Ielo, L.; Pace, V.; Banik, S.; Maheswari, C. U.; Sridharan, V. Direct Access to 9-Chloro-1h-Benzo[B]Furo[3,4-E]Azepin-1-Ones Via Palladium(Ii)-Catalyzed Intramolecular Syn-Oxypalladation/Olefin Insertion/Sp2-C–H Bond Activation Cascade. *Org. Lett.* **2019**, 21, 5784-5788.
- (466) Martínez, C.; Aurrecoechea, J. M.; Madich, Y.; Denis, J. G.; de Lera, A. R.; Álvarez, R. Synthesis of Tetrahydrodibenzofuran and Tetrahydrophenanthridinone Skeletons by Intramolecular Nucleopalladation/Oxidative Heck Cascades. *Eur. J. Org. Chem.* **2012**, 2012, 99-106.
- (467) Álvarez, R.; Martínez, C.; Madich, Y.; Denis, J. G.; Aurrecoechea, J. M.; de Lera, Á. R. Corrigendum: A General Synthesis of Alkenyl-Substituted Benzofurans, Indoles, and Isoquinolones by Cascade Palladium-Catalyzed Heterocyclization/Oxidative Heck Coupling. *Chemistry A European Journal* **2012**, 18, 13894-13896.
- (468) Silva, F.; Reiter, M.; Mills-Webb, R.; Sawicki, M.; Klär, D.; Bensel, N.; Wagner, A.; Gouverneur, V. Pd(Ii)-Catalyzed Cascade Wacker–Heck Reaction: Chemoselective Coupling of Two Electron-Deficient Reactants. *The Journal of Organic Chemistry* **2006**, 71, 8390-8394.
- (469) Zheng, J.; Li, Z.; Wu, W.; Jiang, H. Controllable O-Nucleometalation Cyclization Strategy: Access to Divergent Ring-Functionalized Molecules. *Org. Lett.* **2016**, 18, 6232-6235.
- (470) Yao, B.; Wang, Q.; Zhu, J. Palladium(Ii)-Catalyzed Cyclizative Cross-Coupling of Ortho-Alkynylanilines with Ortho-Alkynylbenzamides under Aerobic Conditions. *Angew. Chem. Int. Ed.* **2013**, 52, 12992-12996.
- (471) Rozenman, M. M.; Liu, D. R. DNA-Templated Synthesis in Organic Solvents. *ChemBioChem* **2006**, 7, 253-256.
- (472) Sergeyev, V. G.; Pyshkina, O. A.; Lezov, A. V.; Mel'nikov, A. B.; Ryumtsev, E. I.; Zezin, A. B.; Kabanov, V. A. DNA Complexed with Oppositely Charged Amphiphile in Low-Polar Organic Solvents. *Langmuir* **1999**, 15, 4434-4440.
- (473) Sergeyev, V. G.; Mikhailenko, S. V.; Pyshkina, O. A.; Yaminsky, I. V.; Yoshikawa, K. How Does Alcohol Dissolve the Complex of DNA with a Cationic Surfactant? *J. Am. Chem. Soc.* **1999**, 121, 1780-1785.
- (474) Mel'nikov, S. M.; Sergeyev, V. G.; Yoshikawa, K. Discrete Coil-Globule Transition of Large DNA Induced by Cationic Surfactant. *J. Am. Chem. Soc.* **1995**, 117, 2401-2408.
- (475) Mel'nikov, S. M.; Sergeyev, V. G.; Yoshikawa, K. Transition of Double-Stranded DNA Chains between Random Coil and Compact Globule States Induced by Cooperative Binding of Cationic Surfactant. *J. Am. Chem. Soc.* **1995**, 117, 9951-9956.
- (476) Bromberg, L. E.; Klibanov, A. M. Detergent-Enabled Transport of Proteins and Nucleic Acids through Hydrophobic Solvents. *Proceedings of the National Academy of Sciences of the United States of America* **1994**, 91, 143-147.
- (477) Ogawa, A.; Maeda, M. Aptazyme-Based Riboswitches as Label-Free and Detector-Free Sensors for Cofactors. *Bioorganic & Medicinal Chemistry Letters* **2007**, 17, 3156-3160.
- (478) Lee, G. U.; Chrisey, L. A.; Colton, R. J. Direct Measurement of the Forces between Complementary Strands of DNA. *Science* **1994**, 266, 771-773.
- (479) Privalov, P. L.; Crane-Robinson, C. Forces Maintaining the DNA Double Helix and Its Complexes with Transcription Factors. *Prog. Biophys. Mol. Biol.* **2018**, 135, 30-48.
- (480) Ijiro, K.; Okahata, Y. A DNA–Lipid Complex Soluble in Organic Solvents. *J. Chem. Soc., Chem. Commun.* **1992**, DOI:10.1039/C39920001339 10.1039/C39920001339, 1339-1341.
- (481) Tanaka, K.; Okahata, Y. A DNA–Lipid Complex in Organic Media and Formation of an Aligned Cast Film1. *J. Am. Chem. Soc.* **1996**, 118, 10679-10683.

- (482) Mel'nikov, S. M.; Lindman, B. Solubilization of DNA–Cationic Lipid Complexes in Hydrophobic Solvents. A Single-Molecule Visualization by Fluorescence Microscopy. *Langmuir* **1999**, 15, 1923-1928
- (483) Bonner, G.; Klibanov, A. M. Structural Stability of DNA in Nonaqueous Solvents. *Biotechnol. Bioeng.* **2000**, 68, 339-344.
- (484) Ganguli, M.; Jayachandran, K. N.; Maiti, S. Nanoparticles from Cationic Copolymer and DNA That Are Soluble and Stable in Common Organic Solvents. *J. Am. Chem. Soc.* **2004**, 126, 26-27.
- (485) Mok, H.; Kim, H. J.; Park, T. G. Dissolution of Biomacromolecules in Organic Solvents by Nano-Complexing with Poly(Ethylene Glycol). *Int. J. Pharm.* **2008**, 356, 306-313.
- (486) Abe, H.; Abe, N.; Shibata, A.; Ito, K.; Tanaka, Y.; Ito, M.; Saneyoshi, H.; Shuto, S.; Ito, Y. Structure Formation and Catalytic Activity of DNA Dissolved in Organic Solvents. *Angew. Chem. Int. Ed.* **2012**, 51, 6475-6479.
- (487) Shibata, T.; Dohno, C.; Nakatani, K. G-Quadruplex Formation of Entirely Hydrophobic DNA in Organic Solvents. *Chem. Commun.* **2013**, 49, 5501-5503.
- (488) Liu, K.; Zheng, L.; Liu, Q.; de Vries, J. W.; Gerasimov, J. Y.; Herrmann, A. Nucleic Acid Chemistry in the Organic Phase: From Functionalized Oligonucleotides to DNA Side Chain Polymers. *J. Am. Chem. Soc.* **2014**, 136, 14255-14262.
- (489) Hook, K. D.; Chambers, J. T.; Hili, R. A Platform for High-Throughput Screening of DNA-Encoded Catalyst Libraries in Organic Solvents. *Chemical Science* **2017**, 8, 7072-7076.
- (490) Rossi, R.; Montecucco, A.; Ciarrocchi, G.; Biamonti, G. Functional Characterization of the T4 DNA Ligase: A New Insight into the Mechanism of Action. *Nucleic Acids Res.* **1997**, 25, 2106-2113.
- (491) Feagin, T. A.; Olsen, D. P. V.; Headman, Z. C.; Heemstra, J. M. High-Throughput Enantiopurity Analysis Using Enantiomeric DNA-Based Sensors. *J. Am. Chem. Soc.* **2015**, 137, 4198-4206.
- (492) Zhu, Q.; Liu, G.; Kai, M. DNA Aptamers in the Diagnosis and Treatment of Human Diseases. *Molecules* **2015**, 20, 20979-20997.
- (493) Zhu, Z.; Schmidt, T.; Mahrous, M.; Guieu, V.; Perrier, S.; Ravelet, C.; Peyrin, E. Optimization of the Structure-Switching Aptamer-Based Fluorescence Polarization Assay for the Sensitive Tyrosinamide Sensing. *Anal. Chim. Acta* **2011**, 707, 191-196.
- (494) Kidd, A.; Guieu, V.; Perrier, S.; Ravelet, C.; Peyrin, E. Fluorescence Polarization Biosensor Based on an Aptamer Enzymatic Cleavage Protection Strategy. *Analytical and Bioanalytical Chemistry* **2011**, 401, 3229-3234.
- (495) Vianini, E.; Palumbo, M.; Gatto, B. In Vitro Selection of DNA Aptamers That Bind L-Tyrosinamide. *Biorg. Med. Chem.* **2001**, 9, 2543-2548.
- (496) Sakurai, K.; Snyder, T. M.; Liu, D. R. DNA-Templated Functional Group Transformations Enable Sequence-Programmed Synthesis Using Small-Molecule Reagents. *J. Am. Chem. Soc.* **2005**, 127, 1660-1661.
- (497) Krumb, M.; Kammer, L. M.; Badir, S. O.; Cabrera-Afonso, M. J.; Wu, V. E.; Huang, M.; Csakai, A.; Marcaurelle, L. A.; Molander, G. A. Photochemical C-H Arylation of Heteroarenes for DNA-Encoded Library Synthesis. *Chem. Sci.* 2022, 13, 1023-1029.
- (498) Xia, B.; Franklin, G. J.; Lu, X.; Bedard, K. L.; Grady, L. C.; Summerfield, J. D.; Shi, E. X.; King, B. W.; Lind, K. E.; Chiu, C.et al. DNA-Encoded Library Hit Confirmation: Bridging the Gap between on-DNA and Off-DNA Chemistry. ACS Med. Chem. Lett. 2021, 12, 1166-1172.
- (499) Ede, S.; Schenk, M.; Bierer, D.; Weinmann, H.; Graham, K. Improved Diazo-Transfer Reaction for DNA-Encoded Chemistry and Its Potential Application for Macrocyclic Del-Libraries. *Molecules* **2021**, 26, 1790.
- (500) Badir, S. O.; Lipp, A.; Krumb, M.; Cabrera-Afonso, M. J.; Kammer, L. M.; Wu, V. E.; Huang, M.; Csakai, A.; Marcaurelle, L. A.; Molander, G. A. Photoredox-Mediated Hydroalkylation and

- Hydroarylation of Functionalized Olefins for DNA-Encoded Library Synthesis. *Chem. Sci.* **2021**, 12, 12036-12045.
- (501) Song, M.; Hwang, G. T. DNA-Encoded Library Screening as Core Platform Technology in Drug Discovery: Its Synthetic Method Development and Applications in Del Synthesis. *J. Med. Chem.* **2020**, 63, 6578-6599.
- (502) Zimmermann, G.; Neri, D. DNA-Encoded Chemical Libraries: Foundations and Applications in Lead Discovery. *Drug Discovery Today* **2016**, 21, 1828-1834.
- (503) Li, Y.; Gabriele, E.; Samain, F.; Favalli, N.; Sladojevich, F.; Scheuermann, J.; Neri, D. Optimized Reaction Conditions for Amide Bond Formation in DNA-Encoded Combinatorial Libraries. *ACS Comb. Sci.* **2016**, 18, 438-443.
- (504) Franzini, R. M.; Neri, D.; Scheuermann, J. DNA-Encoded Chemical Libraries: Advancing Beyond Conventional Small-Molecule Libraries. *Acc. Chem. Res.* **2014**, 47, 1247-1255.
- (505) Chovelon, B.; Fiore, E.; Faure, P.; Peyrin, E.; Ravelet, C. Kissing Interactions for the Design of a Multicolor Fluorescence Anisotropy Chiral Aptasensor. *Talanta* **2019**, 205, 120098.
- (506) Challier, L.; Mavre, F.; Moreau, J.; Fave, C.; Schollhorn, B.; Marchal, D.; Peyrin, E.; Noel, V.; Limoges, B. Simple and Highly Enantioselective Electrochemical Aptamer-Based Binding Assay for Trace Detection of Chiral Compounds. *Anal. Chem.* 2012, 84, 5415-5420.
- (507) Tan, Z.; Heemstra, J. M. High-Throughput Measurement of Small-Molecule Enantiopurity by Using Flow Cytometry. *ChemBioChem* **2018**, 19, 1853-1857.
- (508) Sanford, A. A.; Rangel, A. E.; Feagin, T. A.; Lowery, R. G.; Argueta-Gonzalez, H. S.; Heemstra, J. M. Re-Selex: Restriction Enzyme-Based Evolution of Structure-Switching Aptamer Biosensors. *ChemRxiv* **2021**, 1-12.
- (509) Lackey, H. H.; Peterson, E. M.; Harris, J. M.; Heemstra, J. M. Probing the Mechanism of Structure-Switching Aptamer Assembly by Super-Resolution Localization of Individual DNA Molecules. *Anal. Chem.* **2020**, 92, 6909-6917.
- (510) Pimentel, E. B.; Peters-Clarke, T. M.; Coon, J. J.; Martell, J. D. DNA-Scaffolded Synergistic Catalysis. *J. Am. Chem. Soc.* **2021**, 143, 21402-21409.
- (511) Nutting, J. E.; Rafiee, M.; Stahl, S. S. Tetramethylpiperidine N-Oxyl (Tempo), Phthalimide N-Oxyl (Pino), and Related N-Oxyl Species: Electrochemical Properties and Their Use in Electrocatalytic Reactions. *Chem. Rev.* **2018**, 118, 4834-4885.
- (512) Ryland, B. L.; McCann, S. D.; Brunold, T. C.; Stahl, S. S. Mechanism of Alcohol Oxidation Mediated by Copper(Ii) and Nitroxyl Radicals. *J. Am. Chem. Soc.* **2014**, 136, 12166-12173.
- (513) Punt, P. M.; Langenberg, M. D.; Altan, O.; Clever, G. H. Modular Design of G-Quadruplex Metallodnazymes for Catalytic C-C Bond Formations with Switchable Enantioselectivity. *J. Am. Chem. Soc.* **2021**, 143, 3555-3561.
- (514) Anzola, M.; Winssinger, N. Turn on of a Ruthenium(Ii) Photocatalyst by DNA-Templated Ligation. *Chem. Eur. J.* **2019**, 25, 334-342.
- (515) Flanagan, M. L.; Arguello, A. E.; Colman, D. E.; Kim, J.; Krejci, J. N.; Liu, S.; Yao, Y.; Zhang, Y.; Gorin, D. J. A DNA-Conjugated Small Molecule Catalyst Enzyme Mimic for Site-Selective Ester Hydrolysis. Chem. Sci. 2018, 9, 2105-2112.
- (516) Chang, D.; Lindberg, E.; Winssinger, N. Critical Analysis of Rate Constants and Turnover Frequency in Nucleic Acid-Templated Reactions: Reaching Terminal Velocity. *J. Am. Chem. Soc.* **2017**, 139, 1444-1447.
- (517) Jackson, C.; Toth-Petroczy, A.; Kolodny, R.; Hollfelder, F.; Fuxreiter, M.; Kamerlin, S. C. L.; Tokuriki, N. Adventures on the Routes of Protein Evolution-in Memoriam Dan Salah Tawfik (1955-2021). *J. Mol. Biol.* **2022**, 434, 167462.
- (518) Tawfik, D. S.; Green, B. S.; Chap, R.; Sela, M.; Eshhar, Z. Catelisa: A Facile General Route to Catalytic Antibodies. *Proc Natl Acad Sci U S A* **1993**, 90, 373-377.

- (519) Plougastel, L.; Lamaa, D.; Yen-Pon, E.; Audisio, D.; Taran, F. Fluorogenic Probes Based on Polycyclic Sydnone Scaffolds. *Tetrahedron* **2020**, 76, 131250.
- (520) Plougastel, L.; Pattanayak, M. R.; Riomet, M.; Bregant, S.; Sallustrau, A.; Nothisen, M.; Wagner, A.; Audisio, D.; Taran, F. Sydnone-Based Turn-on Fluorogenic Probes for No-Wash Protein Labeling and in-Cell Imaging. *Chem. Commun.* **2019**, 55, 4582-4585.
- (521) Decuypere, E.; Riomet, M.; Sallustrau, A.; Bregant, S.; Thai, R.; Pieters, G.; Clavier, G.; Audisio, D.; Taran, F. Sydnone-Coumarins as Clickable Turn-on Fluorescent Sensors for Molecular Imaging. *Chem. Commun.* **2018**, 54, 10758-10761.
- (522) Liu, H.; Audisio, D.; Plougastel, L.; Decuypere, E.; Buisson, D.-A.; Koniev, O.; Kolodych, S.; Wagner, A.; Elhabiri, M.; Krzyczmonik, A.et al. Ultrafast Click Chemistry with Fluorosydnones. *Angew. Chem., Int. Ed.* **2016**, 55, 12073-12077.
- (523) Richard, M.; Truillet, C.; Tran, V. L.; Liu, H.; Porte, K.; Audisio, D.; Roche, M.; Jego, B.; Cholet, S.; Fenaille, F.et al. New Fluorine-18 Pretargeting Pet Imaging by Bioorthogonal Chlorosydnone-Cycloalkyne Click Reaction. *Chem. Commun.* **2019**, 55, 10400-10403.
- (524) Hamberg, A.; Lundgren, S.; Wingstrand, E.; Moberg, C.; Hult, K. High-Throughput Synthesis and Analysis of Acylated Cyanohydrins. *Chemistry A European Journal* **2007**, 13, 4334-4341.
- (525) Friest, J. A.; Maezato, Y.; Broussy, S.; Blum, P.; Berkowitz, D. B. Use of a Robust Dehydrogenase from an Archael Hyperthermophile in Asymmetric Catalysis-Dynamic Reductive Kinetic Resolution Entry into (S)-Profens. *J. Am. Chem. Soc.* **2010**, 132, 5930-5931.
- (526) Bornscheuer, U. T.; Huisman, G. W.; Kazlauskas, R. J.; Lutz, S.; Moore, J. C.; Robins, K. Engineering the Third Wave of Biocatalysis. *Nature* **2012**, 485, 185-194.
- (527) Lutz, S. Reengineering Enzymes. *Science* **2010**, 329, 285-287.
- (528) Sun, Z.; Liu, Q.; Qu, G.; Feng, Y.; Reetz, M. T. Utility of B-Factors in Protein Science: Interpreting Rigidity, Flexibility, and Internal Motion and Engineering Thermostability. *Chem. Rev.* **2019**, 119, 1626-1665.
- (529) DeGrado, W. F. Introduction: Protein Design. Chem. Rev. 2001, 101, 3025-3026.
- (530) Cui, H.; Stadtmüller, T. H. J.; Jiang, Q.; Jaeger, K.-E.; Schwaneberg, U.; Davari, M. D. How to Engineer Organic Solvent Resistant Enzymes: Insights from Combined Molecular Dynamics and Directed Evolution Study. *ChemCatChem* **2020**, 12, 4073-4083.
- (531) Stepankova, V.; Bidmanova, S.; Koudelakova, T.; Prokop, Z.; Chaloupkova, R.; Damborsky, J. Strategies for Stabilization of Enzymes in Organic Solvents. *ACS Catalysis* **2013**, 3, 2823-2836.
- (532) Ogino, H.; Ishikawa, H. Enzymes Which Are Stable in the Presence of Organic Solvents. *Journal of Bioscience and Bioengineering* **2001**, 91, 109-116.
- (533) Tiwari, V. K.; Powell, D. R.; Broussy, S.; Berkowitz, D. B. Rapid Enantioselective and Diastereoconvergent Hybrid Organic/Biocatalytic Entry into the Oseltamivir Core. *J. Org. Chem.* **2021**, 86, 6494-6503.
- (534) Broussy, S.; Cheloha, R. W.; Berkowitz, D. B. Enantioselective, Ketoreductase-Based Entry into Pharmaceutical Building Blocks: Ethanol as Tunable Nicotinamide Reductant. *Org. Lett.* **2009**, 11, 305-308.
- (535) Kudalkar, G. P.; Tiwari, V. K.; Lee, J. D.; Berkowitz, D. B. A Hammett Study of Clostridium Acetobutylicum Alcohol Dehydrogenase (Caadh): An Enzyme with Remarkable Substrate Promiscuity and Utility for Organic Synthesis. *Synlett* **2020**, 31, 237-247.
- (536) Panigrahi, K.; Applegate, G. A.; Malik, G.; Berkowitz, D. B. Combining a Clostridial Enzyme Exhibiting Unusual Active Site Plasticity with a Remarkably Facile Sigmatropic Rearrangement: Rapid, Stereocontrolled Entry into Densely Functionalized Fluorinated Phosphonates for Chemical Biology. *J. Am. Chem. Soc.* **2015**, 137, 3600-3609.
- (537) Applegate, G. A.; Berkowitz, D. B. Exploiting Enzymatic Dynamic Reductive Kinetic Resolution (Dyrkr) in Stereocontrolled Synthesis. *Adv. Synth. Catal.* **2015**, 357, 1619-1632.

(538) Applegate, G. A.; Cheloha, R. W.; Nelson, D. L.; Berkowitz, D. B. A New Dehydrogenase from Clostridium Acetobutylicum for Asymmetric Synthesis: Dynamic Reductive Kinetic Resolution Entry into the Taxotere Side Chain. *Chemical Communications (Cambridge, United Kingdom)* **2011**, 47, 2420-2422.